Seismicity of the Austral Andes, Southernmost Patagonia

Seismicity of the Austral Andes, Southernmost Patagonia

Pedro Ignacio Guzmán Marín

Master of Science Thesis

IDEA League Joint Master in Applied Geophysics
Delft University of Technology
RWTH Aachen University
ETH Zürich

Supervisors:
Dr. Federica Lanza
Dr. Gerd Sielfeld

4th of September 2020

Abstract

Since December 2018, the first seismic network deployed around the Austral Andes and its Southern Patagonian Ice Field is recording passive seismicity at the western margin of Southern Patagonia, Southernmost South America. Here, active tectonics is dominated by the interplay between the Antarctic plate's subduction at the trench and the sinistral transform movement of the Scotia plate to the south.

This research shows the first catalogue of crustal seismicity located in this region, for almost a year of recording (from December 2018 to mid-November 2019). We finally localized 2685 seismic events, using an automatic event detection algorithm called REST, a new 1-D Minimum Velocity Model constrained with VELEST, and a probabilistic location approach using NonLinLoc.

We identified several seismicity clusters, from west to east: in the forearc, under the Reclus volcano, and in different sections of the fold and thrust belt. Additionally, seismic events aligned with the transform boundary to the south suggest a broader area of active deformation.

Keywords: Seismicity, Austral Andes, Patagonia, Chile, Argentina, South America, Active Tectonics, Reclus Volcano

Acknowledgements

The MSc studies of Pedro Guzmán Marín were funded by the Chilean National Agency for Research and Development (ANID) / Scholarship Program / MAGISTER BECAS CHILE / 2018 - 73191079.

Special thanks to María Paz, my parents, siblings, and friends for encouraged me to do this MSc.

Special thanks to Omar Rivera and David Naranjo, for showing me the gentle side of the geophysics and programming. I could not have done it without their help.

I would like to express thanks to Professor Hansruedi Maurer, who helped me since the beginning to find support to do this research.

Special recognition to Professor Douglas Wiens and Dr. Patrick Shore for accepting to share the seismic data of the 1P Network with me. I also thank ENAP for providing waveforms data from their seismic stations; special thanks to Rodrigo Rodrigo Adaros. Fundación Prisma Austral supported the logistics of the seismic deployment in the fjord region of Southern Chile.

Finally, I want to thank my supervisors for their infinite enthusiasm, guidance, and willingness to assist me through the long road of the thesis. I hope this text evolves into something else.

Contents

List of Figures

List of Tables

1. Introduction

To this day, the area located on the western margin of Southern Patagonia, in southernmost South America (southwards of 48°S), is one of the least explored areas of the World. Therefore, comparing it to the adjacent territories, the knowledge about tectonics in this region is still limited. This research is the first to characterize the local seismicity of this region, taking advantage of the first local seismic deployment in the Patagonian fjords zone.

The subduction of the Antarctic plate under the continent defines the Andean Austral subduction zone, with an active volcanic arc (49–54°S). The interplay between the subduction of the Antarctic oceanic slab with the northwestern tip of the sinistral transform margin between South America and Scotia plates determine the active tectonics in the southwestern margin of southernmost South America (50-53°S; yellow square in Figure 1).

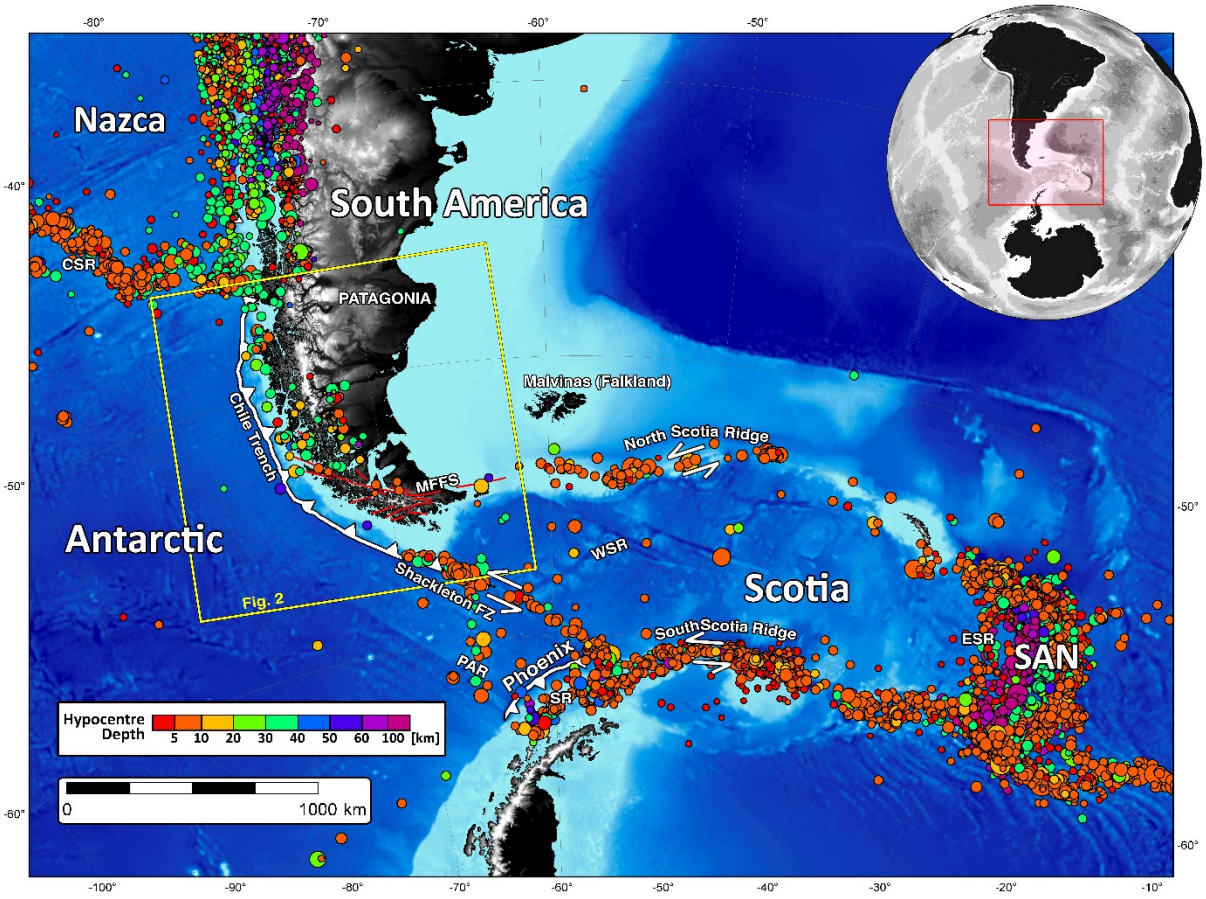

Figure 1. Present-day tectonic setting of southernmost South America and the Scotia Sea. Seismicity is from the Incorporated Research Institutions for Seismology (IRIS) database (period 1970-2019) and is coloured by depth. CSR: Chile Spreading Ridge (active); MFFS: Magnano–Fagnano Fault System (active transform boundary between Scotia and South America plates, red lines); SAN: South Sandwich Plate; WSR: West Scotia Ridge (extinct spreading centre); ESR: East Scotia Ridge (active spreading centre); PAR: Phoenix–Antarctic Ridge (extinct spreading centre); Shakleton FZ: fracture zone (active transpressive); SR: Shackleton Ridge (uplift from compressional deformation of oceanic crust after 8 Ma); NSR: North Scotia Ridge (tectonic front of the Cenozoic transpressive belt, north edge of Scotia Plate). Names based on Lagabrielle *et al.* (2009). The region of southernmost of South America (within a yellow square) has a lower seismicity amount than other nearby plate edges. Digital elevation model data from ETOPO1 (Amante and Eakins, 2009).

Figure 1 shows the distribution of the regional seismicity and the most important tectonic structures. It seems that the region of the southwestern margin of South America has a lower seismicity rate than the adjacent areas, or its distribution is diffuse, as Pelayo and Wiens (1989) suggested. Nevertheless, during the last century, two destructive earthquakes occurred along the transform boundary (Figure 2), with epicentres near the cities of Punta Arenas (Chile) and Ushuaia (Argentina). Furthermore, during the time window of analysis of this research, two events with moment magnitudes ≥ 5.0 were recorded, one in the fjord region (12th of December 2018) and another in the Andean fold and thrust belt (2nd of April 2019). Earthquakes with these magnitudes are not frequent in this area and have a long recurrence time.

The knowledge about the local seismicity along the Austral Andean subduction zone is scarce. Hence, this Master thesis aims to contribute to the understanding of the Austral Andes' crustal tectonics, through the analysis of the local seismicity recorded for almost one year by a temporary seismic and to establish a basic scientific knowledge for future studies in the area. Specific questions that we want to address are as follows:

- What are the primary sources of crustal seismicity in this region?
- What is the tectonic significance of the regional distribution of the seismicity?
- Is there any seismicity that could be related to volcanoes of the Austral Andean volcanic zone?
- How is the interplay between these three major tectonic plates?

1.1. Research Goals

- To compile a catalogue of the local seismicity taking advantage of the augmented seismic network and its increased azimuthal coverage and earthquake detection capabilities.
- To understand the velocity structure of the region, through the development of a new 1-D Velocity Model.
- To obtain first-order probabilistic locations for the detected seismic events.
- To compare the located seismicity with the geological structures of the region, and to discuss on which faults the active deformation is concentrated.

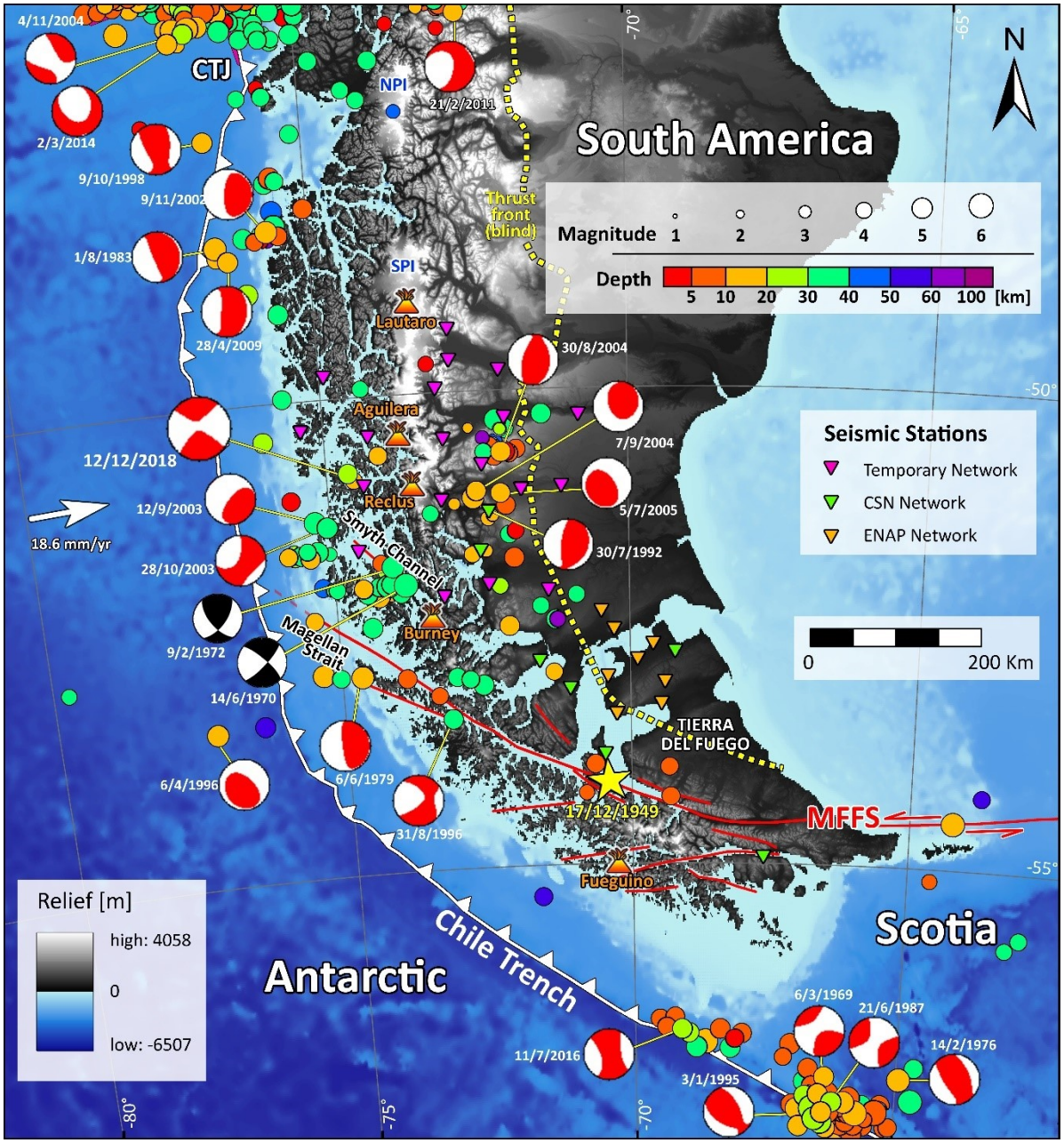

Figure 2. Epicentres of historical seismicity occurred in Southernmost Patagonia, compiled from IRIS catalogue (1970-2019) and Global Centroid Moment Tensor catalogue (gCMT, from 1976 to 2019; Red-white focal mechanisms; http://www.cmt.org/; Ekström *et al.*, 2012; Dziewonski *et al.*, 1981). Black-white focal mechanisms by Forsyth (1975). The slightly bigger red focal mechanism (centre-left) is from a catalogue event of the 12th of December 2018 (Table 1). White line with triangles: Chile trench. Red lines: transform boundary between Scotia and South America, known as Magallanes-Fagnano Fault System (MFFS), the trace is from Cunningham (1993). Yellow star: Epicentre of the Ms 7.5 earthquake of 17th of December 1949 (Castano, 1977). Volcano icons: active volcanoes from Austral Andean Volcanic Zone. Dashed yellow line: thrust front (blind), adapted from Ghiglione *et al.* (2019). Purple lines: Chile Ridge between Nazca and Antarctic plates. CTJ: Chilean Triple Junction. SPI: Southern Patagonian Ice Field. NPI: Northern Patagonian Ice Field. Digital elevation model data from ETOPO1 (Amante and Eakins, 2009).

2. Tectonic Setting

The current active tectonics of the Austral Andes is determined by interactions between South America, Antarctic, and Scotia plates, and until present-day is scarcely documented.

The oceanic crust of the Antarctic plate subducts under the South America continental plate at a rate of 18.64 mm/yr with an azimuth of 86.78° at the 51° latitude South, according to the MORVEL Model of DeMets *et al.* (2010). To the north, the subduction of the Chile Spreading Ridge (CSR), which limits the Nazca and Antarctic plates, has been related to a gap in the Andean volcanic arc and to a slab window which evolved during the Neogene and it is currently migrating northwards (Cande and Leslie, 1986; Breitsprecher and Thorkelson, 2009). Anomalous thermal gradient due to the subduction of the ridge, *a "young and warm oceanic plate, which could be too plastic or soft to allow rupture",* as well as the low slip rate between Antarctica and South America, has been suggested as potential causes of the lack of seismicity (Forsyth, 1975) for the Austral Andean region (Fig. 1). There is no historical earthquake documented for the Antarctica-South America subduction zone. Nevertheless, Piret et al. (2018), from a mega-turbidite triggered by an earthquake, provide the first evidence of paleoseismology south of the Chilean Triple Junction. Unfortunately, these authors did not provide estimates of the intensity and source of that earthquake. Recent seismicity is located in the forearc all along with the interface Antarctic-South American plates and within the Fold and Thrust Belt (south of 50°S).

The plate boundary between Scotia and South America is a 3000 km long transform fault system with left-lateral strike-slip kinematics (Klepeis, 1994). Of the entire transform margin, its section in eastern Tierra del Fuego (TdF) is probably the best studied. There, Smalley *et al.* (2003) obtained a slip rate of 6.6 ± 1.3 mm/yr with GPS measurements. In contrast, Mendoza *et al.* (2015) report a 5.9 ± 0.2 mm/yr slip rate with more GPS stations in the same region. Roy *et al.* (2019), using geomorphological markers and ^{10}Be cosmogenic nuclide depth profiles, obtained a left-lateral Late Pleistocene slip rate of 6.4 ± 0.9 mm/yr. Klepeis (1994) suggested a transtensive tectonic regime, with most of the slip in a horizontal direction (*ca.* 20-25 km) and less in the vertical (*ca.* 3 km). Adjacent faults are usually interpreted altogether in a left-lateral Riedel model (Cunninghamm, 1993; Klepeis, 1994; Lodolo *et al.*, 2003). From TdF to the east, the trace of the transform boundary is restricted to the North Scotia Ridge (NSR), a narrow strip with an E-W strike located at the north of the Scotia Sea, where this basin limits with the Malvinas (Falklands) plateau (Fig. 1). Whereas to its west tip, towards the Chile trench in the Pacific Ocean, the transform boundary bends to an NW-SE strike and is called as Magallanes-Fagnano Fault System (MFFS), and is described as a series of regional strike-slip fault zones and fractures arrays with an en echelon pattern (Lodolo *et al.*, 2003). The MFFS main trace is related to the Magellan Strait (Fig. 2), where usually a precise line of the tectonic

boundary is traced by most of the literature (following Fuenzalida, 1976). However, it is essential to emphasize that the western end of the transform margin has been suggested as a diffuse seismic zone (Pelayo and Wiens, 1989) and that many authors (Forsyth, 1975; Klepeis, 1994; Lodolo *et al.*, 2003) comment on the trace of the western section of this transform plate boundary, which is still unclear. An alternative is proposed by Cunningham (1993), who links the northern boundary of the Scotia Plate with the location of the Smyth Channel (52°S), northern of the Magellan Strait, based on long-term brittle deformation evidence and recent strike-slip seismicity (black-white focal mechanisms in Figure 2).

Two significant earthquakes are known along the MFFS. The first historical record was the 1st of February 1879, with a magnitude estimated from 7 to 7.5 (Martinic, 1988; Cisternas and Vera, 2008). Preceded by a strong foreshock some hours before, the second major earthquake happened on the 17th of December 1949, along the MFFS with a magnitude Ms 7.5, and its epicentre was likely in the fault trace (Lommitz, 1970; Castano 1977; Fig. 2). For this earthquake, Costa *et al.* (2006) estimated no more than 4 meters offset. However, Roy *et al.* (2019), estimated surface ruptures up to 6.5 meters along the MFFS for the 1949 earthquake.

2.1. Previous Seismic Studies

Few studies about the seismicity in southernmost South America has been carried out in the past years. First, Forsyth (1975) made a substantial contribution to the knowledge of the seismotectonic in the area; he mentioned the existence of a new tectonic plate (Scotia), due to the seismicity present along its margins. This author also located two strike-slip earthquakes (black-white focal mechanisms in Figure 2) northwards of the today conventional boundary between Scotia and South America plates (from Fuenzalida, 1976), in the Chilean fjord region. Pelayo and Wiens (1989) also worked mostly around the Scotia Sea and refined the state of the art of the region, providing more focal mechanisms they improved the knowledge about the kinematics and rates of movement of the plates boundaries using teleseismic data. The first study of local seismicity in Patagonia, conducted by Adaros (2003) with a temporary seismic network provided of four seismic stations located in the Andean foreland, detected 262 events with depths ranging between 0.15 and 135 km. Besides, he provided the first local 1-D velocity model for the region. Recently, Ammirati *et al.* (2020) presented new seismic data along the MFFS with a new velocity model based on inverted teleseismic receiver functions with Rayleigh-wave dispersion data.

Based on the gCMT catalogue solutions, we can recognize distinct regions that show different kinematics (red-white focal mechanisms in Fig. 2). Focal mechanisms reveal the occurrence of strike-slip earthquakes northwards of the Magellan Strait, with crustal depths

between 20 to 30 km. Concordantly, it suggests that the transform fault boundary could be extended to the north. In the same manner, the IRIS catalogue shows a greater number of earthquakes concentrated between the Magellan Strait and Smyth Channel faults (Fig. 2), outlining the diffuse seismic zone suggested by Pelayo and Wiens (1989). Reverse earthquakes occur in the South Patagonian Fold and Thrust Belt and along the forearc

Twelve earthquakes were detected by the Chilean Seismological Network (Centro Sismológico Nacional, CSN. http://www.sismologia.cl/) during our observation time window (from December 2018 to mid-November 2019). Four of these earthquakes were also detected by the National Earthquake Information Center (NEIC). Table 1 summarises the catalogue events detected during our observation time window.

Table 1. Seismic events registered by other seismological networks (CSN, NEIC and gCMT) during our observation time window. Symbols written before the date, define the same event. Magnitude: Mag.

Catalogue	Date (UTC)	Origin Time	Latitude [°]	Longitude [°]	Depth [km]	Mag.	Mag. Type
CSN	* 2018-12-12	00:31:03	-50.6300	-74.3230	37.6	5.2	Mw
	2018-12-14	13:28:37	-50.5530	-73.8760	36.3	4.0	M_L
	2019-01-18	18:02:47	-51.2000	-72.0490	7.8	3.3	M_L
	o 2019-02-09	02:37:41	-53.0860	-71.4930	25.0	4.1	M_L
	x 2019-02-17	10:26:50	-50.9560	-75.0350	19.3	4.8	Mw
	v 2019-04-02	13:17:38	-51.2240	-72.1960	2.9	5.0	Mw
	2019-04-03	01:49:09	-51.2280	-72.3250	7.7	3.5	M_L
	2019-04-09	11:41:55	-53.5340	-72.7000	15.0	3.0	M_L
	2019-04-26	22:13:18	-50.8980	-73.5260	30.4	3.7	M_L
	2019-04-29	08:09:53	-53.0840	-73.8400	27.5	3.8	M_L
	2019-06-28	01:16:00	-51.1760	-72.5380	7.5	2.9	M_L
	2019-08-22	22:16:59	-52.9800	-74.2020	25.7	3.3	M_L
NEIC (USGS)	* 2018-12-12	00:31:03	-50.6259	-74.1244	17.2	4.7	Mb
	o 2019-02-09	02:37:41	-52.8965	-71.2228	10.0	4.4	Mb
	x 2019-02-17	10:26:52	-50.8798	-74.6186	13.3	4.3	Mb
	v 2019-04-02	13:17:39	-51.2106	-72.0468	10.0	4.8	Mw
gCMT	* 2018-12-12	00:31:04.2	-50.7900	-74.6400	21.5	4.9	Mw

2.2. Morpho-structures of the Austral Andes

2.2.1. Basement domain

South of 46 °S, the basement of the Austral Andes is composed by a series of Palaeozoic metamorphic complexes, with very distinct structural and metamorphic histories, which emerge both to the west and east of the South Patagonian Batholith (SPB). To the west of the SPB, the basement of the coast is made up of the Madre de Dios Terrane (Forsythe and Mpodozis, 1983) and the Diego de Almagro Metamorphic Complex, both have been interpreted as subduction paleo prisms accreted to the western margin of Gondwana supercontinent (Willner *et al.*, 2004, 2009), and together define the Western Andean Metamorphic Complex (WMC). On the other hand, to the east of the SPB is the Eastern Andean Metamorphic Complex (EMC), which consists of a turbiditic succession, deposited in a passive margin (Hervé *et al.*, 2007, 2008). The SPB is the core of the basement domain and was formed during different stages of calk-alkaline arc magmatism from Late Jurassic until to the Neogene. Nevertheless, most of the volume of this unit has been assigned to a Cretaceous age (SERNAGEOMIN, 2003). Another unit that is part of the basement is made of Jurassic volcaniclastic sequences (Quemado Complex and Tobífera Fm.) related to the initial stage of Gondwana breakup (Calderón *et al.,* 2016), and locally known as Rocas Verdes Basin (RVB). In some areas of the RVB, high extension rates facilitated the creation of the oceanic crust, in the Sarmiento Ophiolitic Complex (Fig. 3).

The basement domain exhibits ductile deformation and is characterized by a thick-skinned style (Ghiglione *et al.*, 2019), encompassing the greatest width and volume of the Cordillera to the west. Willner *et al.* (2004) and Hervé *et al.* (2007) identified west-vergent thrust structures.

2.2.2 Austral Andean Volcanic Arc

Five Holocene stratovolcanoes (Lautaro, Aguilera, Reclus, Burney, Fueguino/Cook) have been recognized in the Austral Andean Volcanic Zone (Figure 2; Killian 1990). Only Lautaro volcano has historical eruptions. However, thick post-glacial tephra deposits of Burney, Reclus and Aguilera volcanoes have been recognized at the lee side of the Andes (Stern, 2008). Tephras assigned to Burney and Reclus volcanoes were also documented in the Malvinas (Falkland) Islands, *ca.* 1000 km to the east (Monteath *et al.*, 2009). Moreover, Hartman *et al.* (2019) found evidence of most recent tephra deposits from Relcus volcano (1459 C.E.) inside an ice core in the Antarctic. According to Stern and Killian (1996), all the volcanoes have erupted exclusively adakitic andesites and dacites, which magmas "require melting of a mixture of Middle Ocean Ridge Basalts and (MORB) and subducted sediment,

followed by interaction of this melt not only with the overlying mantle, but the crust as well". They argue that this could be related to the proximity of the slab window created by the subduction of the Chile Spreading Centre.

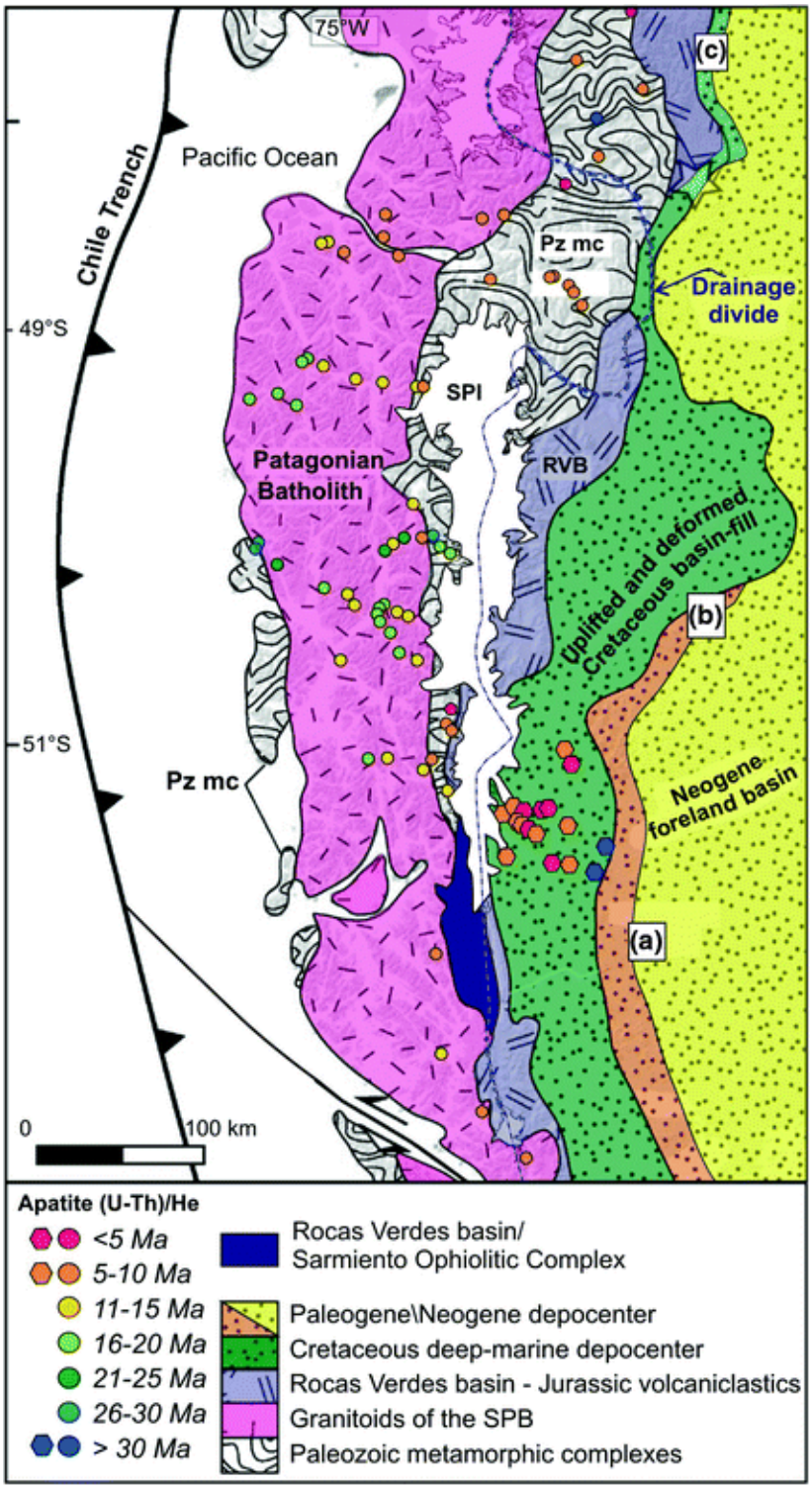

Figure 3. Simplified litho-tectonic units of the Austral Andes. Fission-track (U–Th)/He ages from Fosdick *et al.* (2013) (hexagons) and Thomson *et al.* (2010) (circles). SPI: Southern Patagonian Ice Field. Taken from Ghiglione *et al.* (2016), modified version from Fosdick *et al.* (2013).

2.2.3. South Patagonian Fold and Thrust Belt

The South Patagonian Fold and Thrust Belt (FTB; Figure 4) extends along the eastern side of the Cordillera. According to Ghiglione *et al.* (2019), southern of 48.5° S, there is a wide (100 to 120 km) FTB in the back-arc, which is a hybrid thin/thick-skinned system separated into two different domains (Figs. 5 and 6): 1) The western internal FTB with a hybrid structural style that accommodates most of the tectonic shortening. 2) An eastern external FTB, consisting of isolated inversion structures, blind thrusts and a frontal monocline along its margin. The boundary between the internal and external FTB domains is a back thrust conforming a triangle zone and a very continuous frontal monocline.

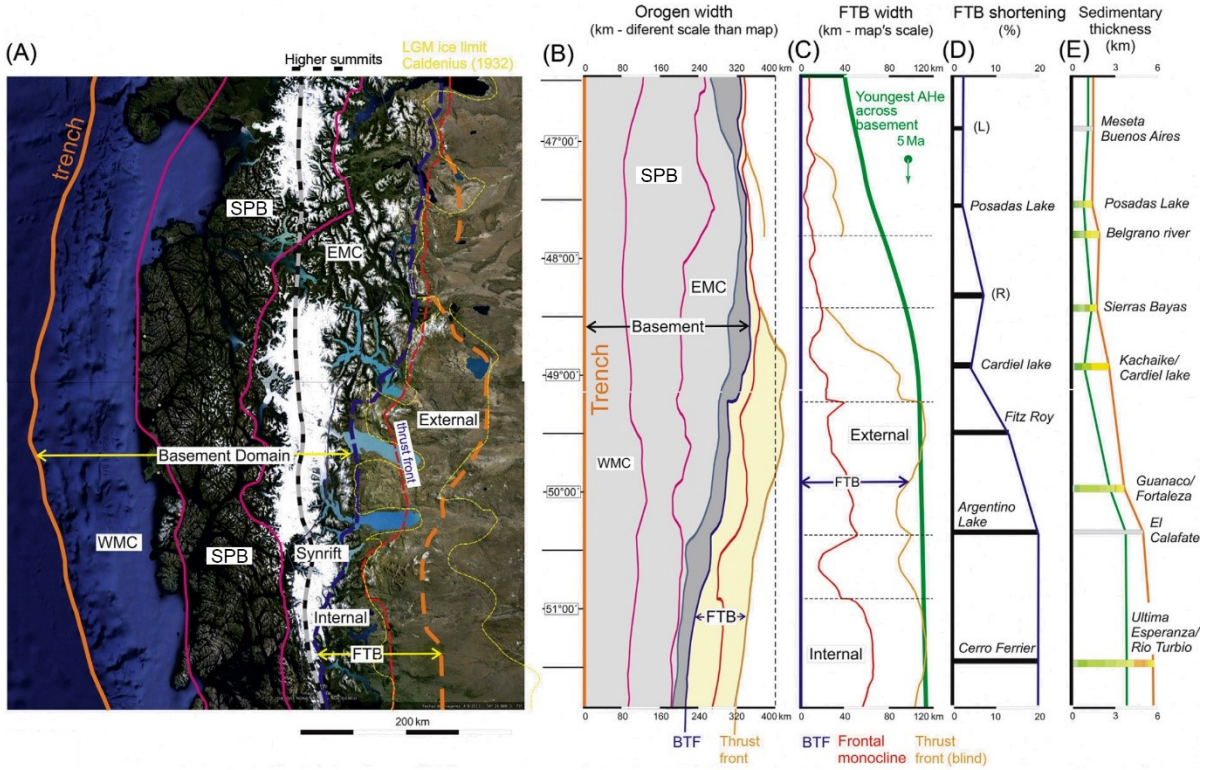

Figure 4. (A) Distribution of main structural domains of the orogen and their boundaries (Figure 3). Yellow dashed line indicates the Last Glacial Maximum ice front limit (Caldenius, 1932), and a dashed line indicates the joining higher summits. **(B)** Diagram showing orogen width constructed by unfolding the trench outline to an N-S datum. Longitudinal (W-E) vectors were used to unfold the trench and are the same as those applied on all the structural boundaries. Therefore, each line point was moved in a W-E direction remaining at the same latitude. Notice that W-E scale is ~40% of the map shown in (A). **(C)** FTB width calculated by unfolding the basement frontal thrust and restoring the outlines of the frontal monocline and thrust front in the same fashion as in (B). Vertical and horizontal scales are identical to the map scale. **(D)** N-S shortening parameters calculated subtracting the final length of the internal FTB to the line length of Río Mayer Formation from cross-sections in Fig. 4, and from sections (L): Lagabrielle *et al.* (2004) and (R): Ronda (2015) in Ghiglione *et al.* (2019). **(E)** Sedimentary thickness from columns (in colours) and from cross-section (in grey). Modified from Ghiglione *et al.* (2019).

Latitudinally, across the FTB, the amount of orogenic shortening increases southwards (Fig. 4D) as is suggested by Ghiglione *et al.* (2019). Northwards of Lago Viedma (*ca*. 49.3°S) in their "Fitz Roy- Puesto El Alamo" cross-section they calculated 10 km of shortening (13%); at the south of Lago Argentino, the estimated shortening along the geological cross-section (Fig. 6 A) is 8 km (20%), while at the area of Última Esperanza-Tapi Aike (Fig. 6 B) the

estimate is of 28 km (20%). Figure 5 shows a detailed geological map of the Lago Argentino and Última Esperanza-Tapi Aike areas, which are inside our study region. In Última Esperanza-Tapi Aike, a cluster of seismicity was detected related to the catalogue event of the 2nd of April 2019.

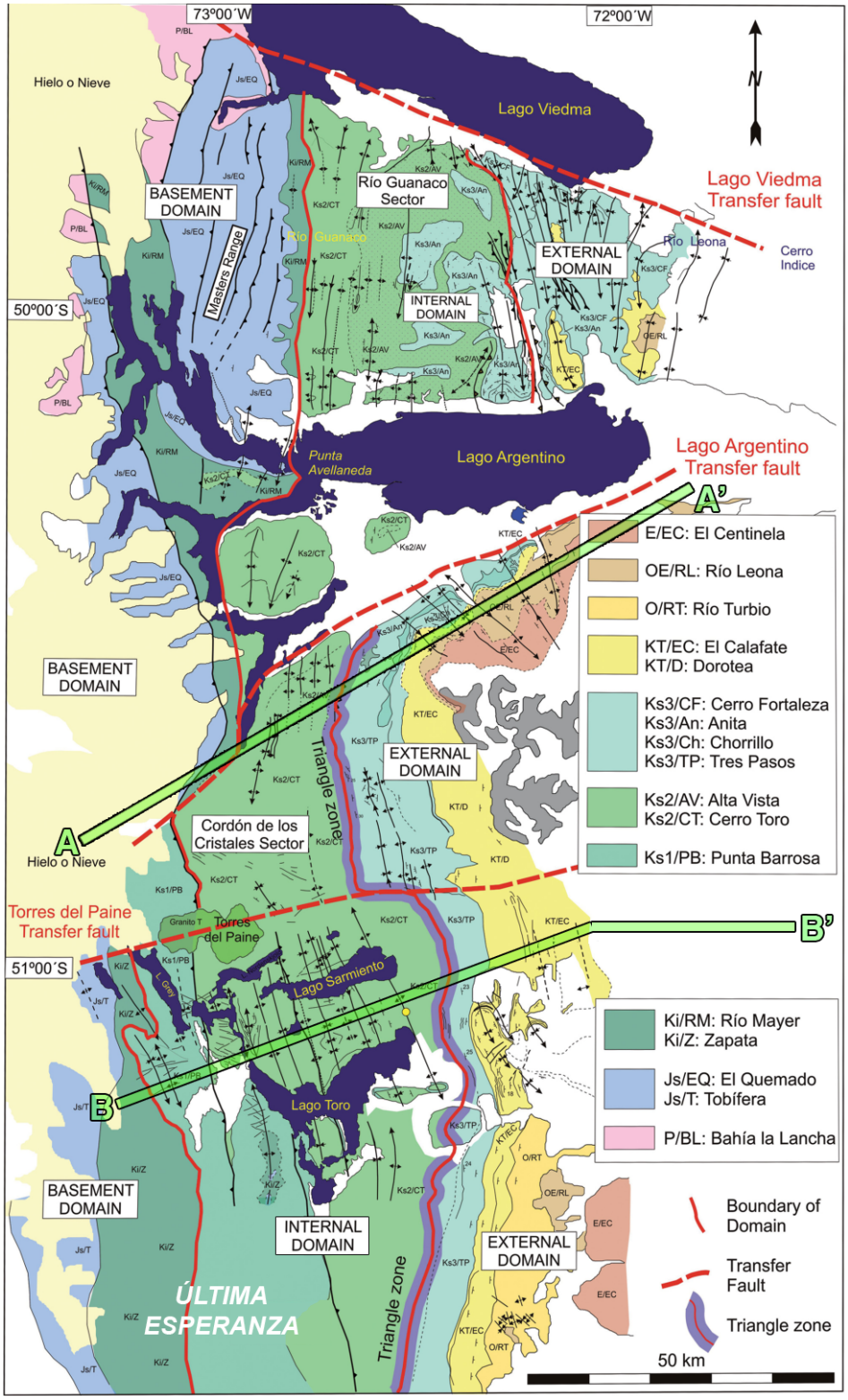

Figure 5. Geological map of the South Patagonian Fold and Thrust Belt between Lago Viedma and Última Esperanza regions. Modified from Ghiglione *et al.* (2009). Cross-sections denoted by green colour are shown in Figure 6.

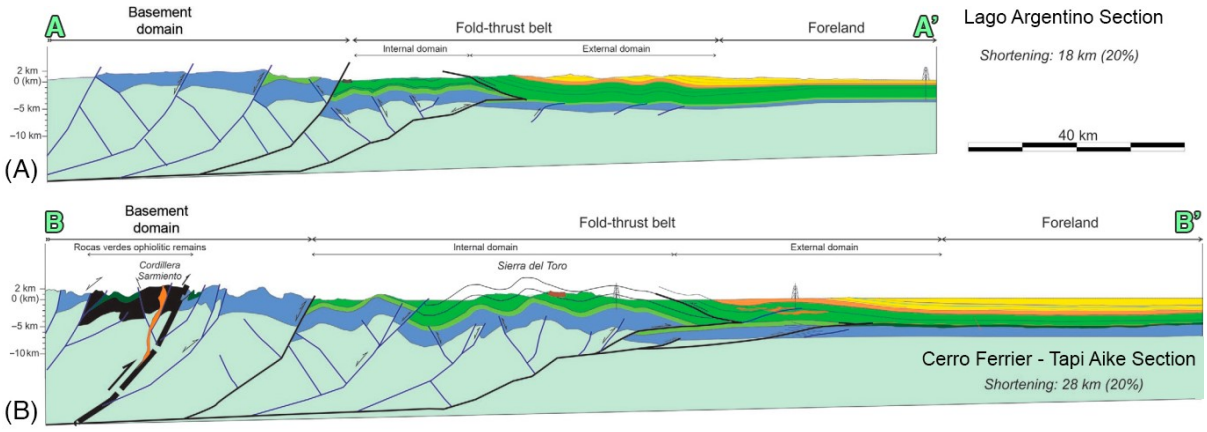

Figure 6. Geological cross-sections of the South Patagonian Fold and Thrust Belt at Lago Argentino and Última Esperanza regions. Modified from Ghiglione *et al.* (2019).

2.2.4. Margin-oblique Transfer Faults

The existence of abrupt latitudinal variations in the width of the FTB and the longitudinal position of its structural domains could be related to the reactivation of W-E oriented Late Jurassic rift accommodation zones (Ghiglione *et al.*, 2009 and 2019; Likerman *et al.*, 2013), which act now as transfer faults (Fig. 5). On the other hand, at the western slope of the Austral Andes, exist several morphological lineaments disposed obliquely to the current margin. Recent field studies suggest that these are faults with evidence of ductile deformation (G. Sielfeld, personal communication, 16th of June 2020).

2.2.5. Forearc Faults

In the forearc, specifically in the western coast at the Diego de Almagro Island (51.3°S 75°W) Lira (2016) reports left-lateral strike-with slip faults, oriented NW-SE, and right-lateral strike-slip faulting, oriented NNE-SSW. In line with this, to the west of the same zone, Polonia *et al.* (2007) in their seismic profiles show active normal faulting in the forearc basin, close to the coast.

3. Data

In this study, data from a total of 32 seismic stations (Figures 2 and 7) belonging to three different passive seismic networks (Table 2) were used during a time window of almost one year (from the 1st of December 2018 until the 19th of November 2019, Figure 8).

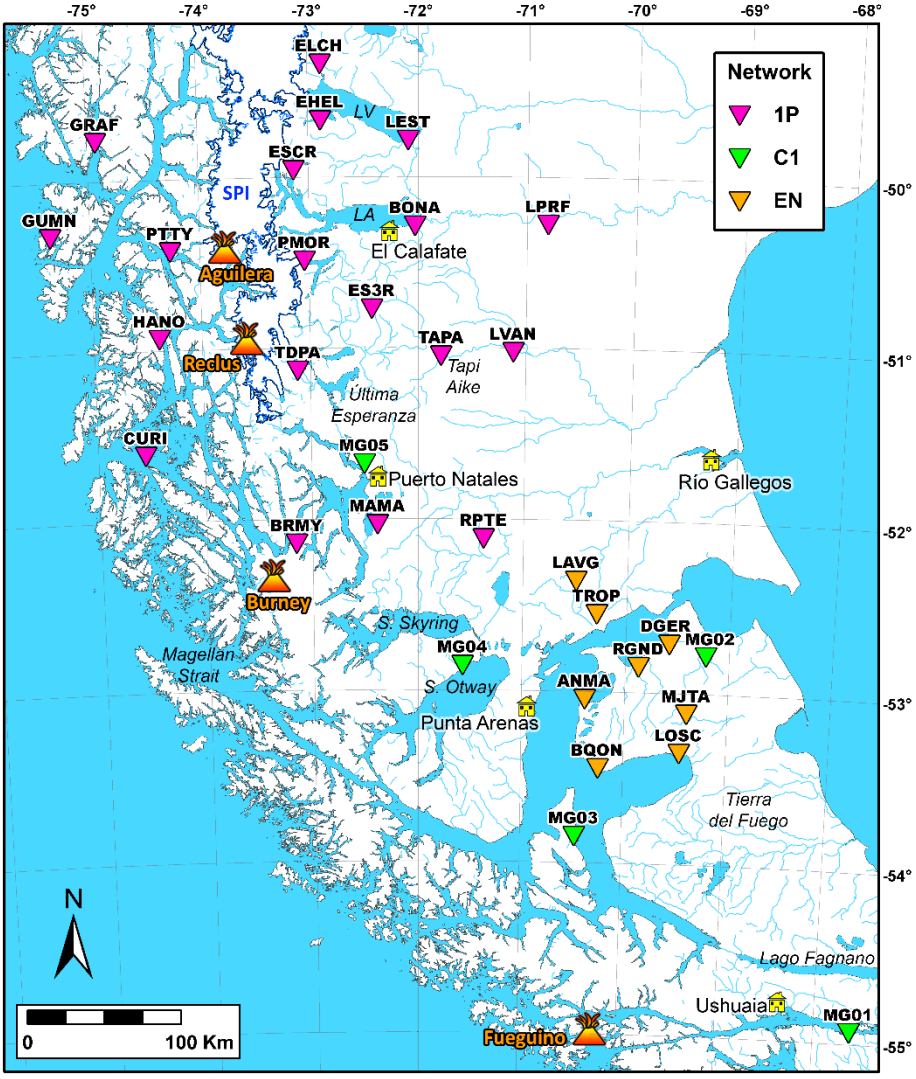

Figure 7. Seismic stations used in this research. Colour denotes the corresponding network. Active volcanoes, cities, names of provinces, and the Southern Patagonian Icefield (SPI) are also displayed. LA: Lago Argentino. LV: Lago Viedma.

Our primary source of data comes from 19 stations of a local temporary array (Network 1P; Wiens and Magnani, 2018) deployed around the Southern Patagonian Ice Field. All the 19 stations are equipped with broadband sensors Nanometrics Trillium 240. The local temporary seismic array was complemented with five permanent stations from the seismological network of Chile, (Network C1; Universidad de Chile, 2013) provided with broadband sensors Nanometrics Trillium 120P. Since April 2020, eight additional seismic stations equipped with broadband sensors Kinemetrics MBB-2 of a private network (EN), owned by ENAP (Chile), enhanced our array's azimuthal coverage. Most of the seismic stations were running in

continuous mode at a sample rate of 100 Hz. However, from November 2018 to middle March 2019, the land-based stations of the local temporary array were running at 200 Hz. The exact location of each of the stations is showed in the Supplementary Table 1.

Table 2. Details of seismic sensors of the three networks used in this study.

Network	Operator	N° of stations	Type of sensor	Brand and model	Period
1P	Wiens and Magnani	19	Broadband	Nanometrics Trillium	240 s
C1	CSN	5	Broadband	Nanometrics Trillium	120 s
EN	ENAP	8	Broadband	Kinemetrics MBB-2	120 s

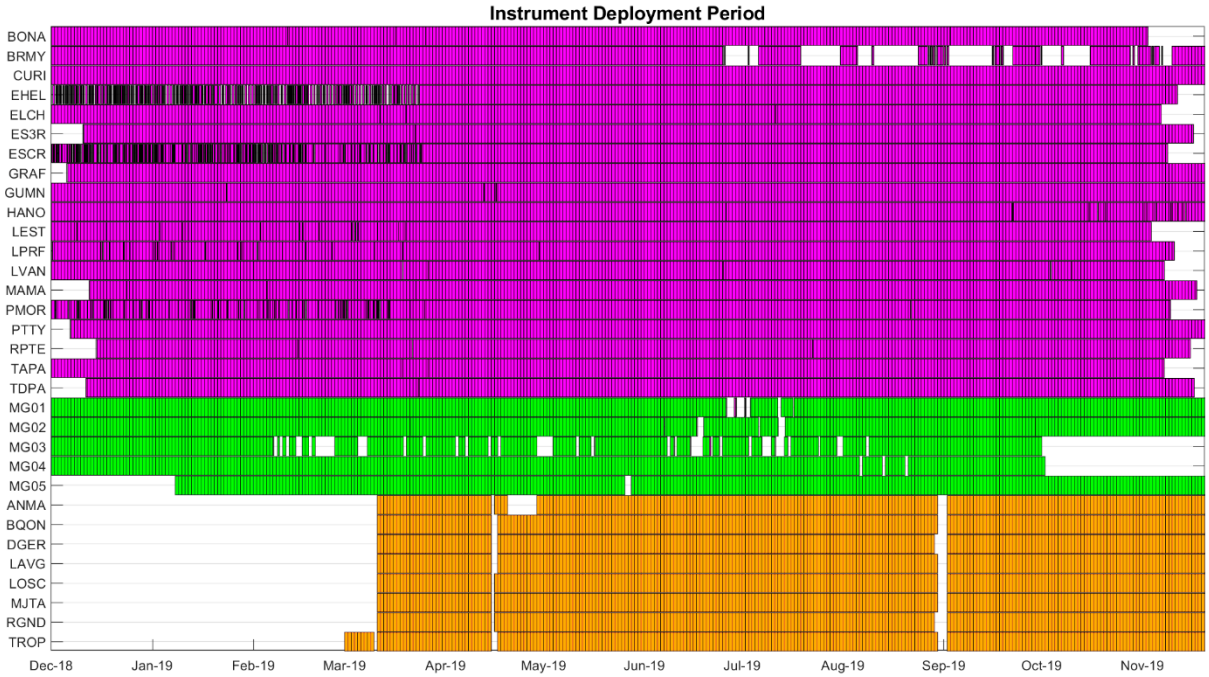

Figure 8. Available seismic records of stations from the networks used in this study. Purple: 1P, Green: C1, Orange: EN.

4. Methodology

4.1. Phase Picking and Event Detection

Automatic identification of phase arrival times was performed using REST (Regressive ESTimator), a package of programmes developed by Steven Roecker (Thurber *et al.*, 2017; Comte *et al.*, 2019; Lanza *et al.*, 2019) for automatic detection and catalogue generation of *P* and *S* wave arrival times and preliminary estimation of earthquake locations. The algorithms employed for earthquake detection and onset estimation are based on Pisarenko *et al.* (1987) and Kushnir *et al.* (1990). The detection algorithm compares the samples within a determined moving time window (in our case 420 seconds with 60 seconds of overlap) against a provided sample of noise and estimates how different is the signal in the sampled window from the background noise.

The next step seeks to collect the different sets of detections into seismic events. For this, we use 20 seconds as a maximum amount of time between detections to permit association. To constitute an event a minimum of 6 detections were needed, from which at least three must qualify as superior detection, therefore have a signal-to-noise ratio (SNR) superior to a user-defined threshold (in this case a SNR $\geq$ 2500). For all the possible events, the time series of each station were sectioned between -40 and 80 seconds before and after the detections, respectively. These constitute windows of data containing potential earthquakes. The next stage is to estimate the onsets of phases associated with each event, and its most probable location using a provided 1-D velocity model. We used the *Vp* velocity model of Adaros (2003) and approximate from this one a Vs using a ratio of 1.73 according to the average value for the crust in the region provided by Lawrence and Wiens (2004). Algorithms used for event location and travel time computation are from the tomoFD package of Roecker *et al.* (2006). The iterative refinement of the onset estimation is based on the nearest-neighbour similarity scheme of Rawles and Thurber (2015), combined with the auto-regressive approach of Kushnir *et al.* (1990). The estimation function of Kushnir *et al.* (1990) plays a crucial factor in obtaining a pick; in this manner, the uncertainties are assigned in relation to its fallout (Fig. 9), and its asymmetry serves as causality constraint (Lanza *et al.*, 2019). Furthermore, to achieve accurate identification of the different phase arrivals and to prevent inaccurate automatic picking of unclear arrivals, a preliminary calibration of different picking parameters was performed using the catalogue events detected by CSN. The parameters we tested for performance are the SNR threshold to be used for detections, which need to be calibrated according to the noisiness of the data, as well as the ratio between the amplitude before and after the *P* and *S* waves picks and the minimum contrast between the slopes of the estimation function before and after the maximum peak. A higher contrast will imply a more conservative constraint for the automatic picking, indispensable for an adequate estimation of the uncertainties. All waveforms were

bandpass filtered before picking, using a Bessel filter with a hi-pass of 1 Hz and a lo-pass of 25 Hz (0.5 *Nyquist*), which preserves the wave shape and phase.

The processing with REST yields a total of 2813 seismic events detected and preliminary located. Visual inspection of all the waveforms and the respective picks, with the aim of look for weak events, teleseismic events, quarry explosions and false detections (due to, e.g. spikes in the data), reduces the number of seismic events to 2685, with 37216 *P* and 15069 *S* arrival phases.

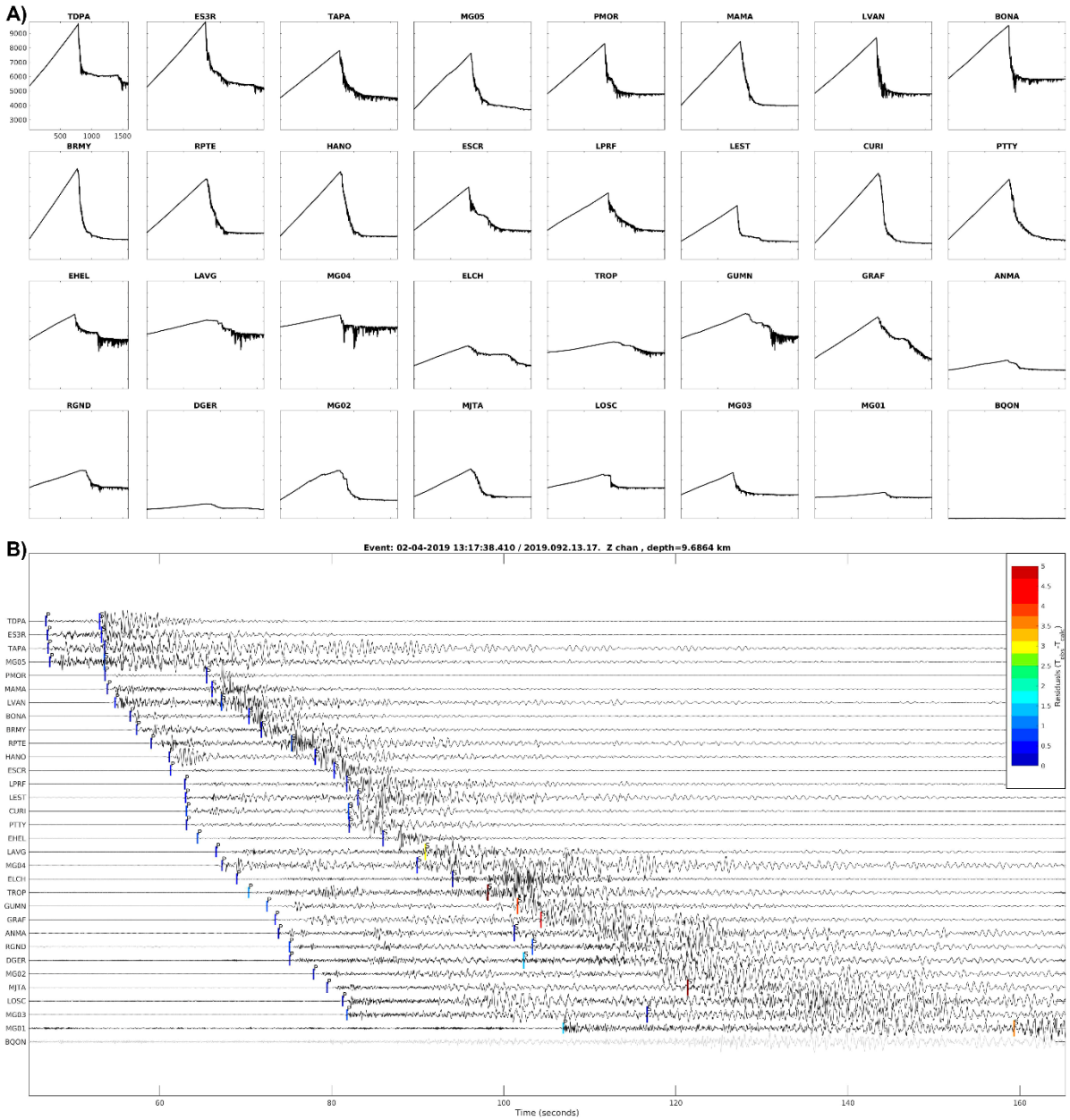

Figure 9. An example of automatic picking of seismic waveforms with REST for a catalogue earthquake of the 2nd of April 2019. A) Estimation function of Kushnir *et al.* (1990) for all stations with *P* wave detection. The uncertainties of the picks are related to the fallout of the estimation function (to the right). In this way, the station TDPA with a steep fallout of the estimation function has a *P* wave pick uncertainty of 0.020 seconds. In contrast, for the station MG04, the *P* wave picking uncertainty is 0.092 seconds. B) Waveforms of the catalogue earthquake of the 2nd of April 2019 with epicentre between the cities of El Calafate (Argentina) and Puerto Natales (Chile). To enhance the signal, we applied a Bessel filter with a hi-pass of 1 Hz and a lo-pass of 25 Hz (0.5 *Nyquist*).

4.3. Local Magnitudes

Local Magnitudes (M_L) were calculated for all the events in the catalogue by using the automated magnitude calculation Magcalc included in the REST software package, which generates Richter type estimates of earthquake magnitude using the following formula:

$$M_L = \log10(Amax) + 2.35*[\log10(dt)] - 2.92$$

Where *Amax* is the maximum amplitude of the *P*-wave coda from some set time before the onset to the minimum of 5 seconds and halfway to the *S*-wave arrival, and *dt* is the time difference between the *S* and *P* waves arrivals.

4.4. Velocity Model

The velocity structure of the Austral Andes is poorly known. The only available velocity model was from Adaros (2003), constructed for the foreland region, which we used for the initial location with REST. Hence, our goal is to produce a new velocity model, considering this is the first time a denser array has been in place for this area. We inverted for *P* and *S* arrival times of the newly detected events to constrain a new minimum one-dimensional (1-D) layered velocity model using *VELEST 4.5* (Kissling, 1988; Kissling *et al.*, 1994, 1995; Diehl *et al.*, 2017; Singer *et al.*, 2017). We solved simultaneously for the coupled hypocentre-velocity model problem. We followed the "recipe" to calculate a minimum 1-D model of Kissling *et al.* (1994, 1995) and based each step on Brill *et al.* (2018), Lange *et al.* (2007, 2012) and Husen *et al.* (1999).

The station TDPA was chosen as the reference station because of its location, approximately the closest to the centre of our array, and its high number of observations.

Following the criteria of Diehl *et al.* (2017), we classified the picks based on their absolute time uncertainty, resulting in 4 distinct classes: class 0 ≤ 0.025 s, class 1 ≤ 0.050 s, class 2 ≤ 0.100 s, class 3 ≤ 0.200 s and class 4 ≤ 0.400 s. Picks with higher uncertainties were discarded. The weighting scheme used then for the inversion is based on $1/(2^{class})$. Consequently, class 0 weights 100% (the best picks), class 1 weights 50%, class 3 weights 12.50% and class 4 weights 6.25% (the worst picks).

Due to the scarce a priori information about the crustal structure, in our first stage, we tested different thicknesses and number of layers to obtain the most suitable velocity structure. For this purpose, we used just P-wave arrivals of 624 high-quality, homogeneously distributed events located within our network (GAP ≤ 180°) and with at least 6 class 0 *P*-wave arrivals. In this first step, we created different crustal structure layer combinations, based on the refraction

profiles of Ludwig *et al.* (1965) and interpolating from three different velocity models (Adaros, 2003; Febrer *et al.*, 2000 and the velocity model from the station MILO of Lawrence and Wiens, 2004). The criteria to decide which is the most feasible layer structure was determined following the lowest root-mean-square (RMS) values for the three different input velocity models. Once, the most feasible layer structure was established, we tested a set of 3000 random *Vp* models to find the minimum 1-D *Vp* model, with the smallest RMS. Our best Minimum 1-D *Vp* Model has a RMS of 0.1397 seconds, a reduction of 84.48% with respect to the initial value of *ca.* 0.9 seconds (Supplementary Figure 1).

According to Husen *et al.* (1999), *S*-wave phases enhance the hypocentre location's accuracy, especially regarding the focal depth, and using an independent S-wave velocity field produces better results. We followed their approach to achieve a minimum 1-D Vs model. Using the best *Vp* model obtained from the random search and a set of 424 earthquakes within the network (GAP ≤ 180°) and with at least 10 class 0 *P*-wave and *S*-wave arrivals, we implemented 81 different models with *Vp/Vs* ratios ranging from 1.5 to 2.3. Our best minimum 1-D *Vp+Vs* model has a RMS of 0.158 seconds. Figure 10 summarises our velocity model search. It displays the best *Vp* and *Vs* models (thick black lines), as well as all the model space explored to obtain our Minimum 1-D *Vp+Vs* model, and the obtained *Vp/Vs* ratio. Table 3 shows the obtained velocities (*Vp* and *Vs*) and *Vp/Vs* ratio of our minimum 1-D velocity model. Reliable velocity data was achieved only for crustal depths (shallower than *ca.* 40 km) due to the lack of deep hypocentres (Supplementary Figure 2). Figures 11 to 12 show the distribution of the seismic rays used to constrain the Minimum 1-D *Vp* and *Vp+Vs* models, respectively. Figures 13 to 14 and Supplementary Table 1 show the stations corrections for our study area for *P* and *S* wave arrivals of our minimum *Vp+Vs* model.

Table 3. *P*-wave and *S*-wave velocities and resulting *Vp/Vs* ratio of the Minimum 1-D Velocity Model.

Z [km]	***Vp* [km/s]**	***Vs* [km/s]**	**Vp/Vs**
-5	3.47	1.65	2.10
0	5.43	2.02	2.69
3	5.60	2.85	1.96
6	5.85	3.54	1.65
15	5.89	3.54	1.66
20	6.61	3.74	1.77
25	6.62	3.83	1.73
30	6.65	3.83	1.74
35	7.48	4.13	1.81
40	7.91	4.13	1.92
50	7.92	4.13	1.92
60	7.92	4.13	1.92

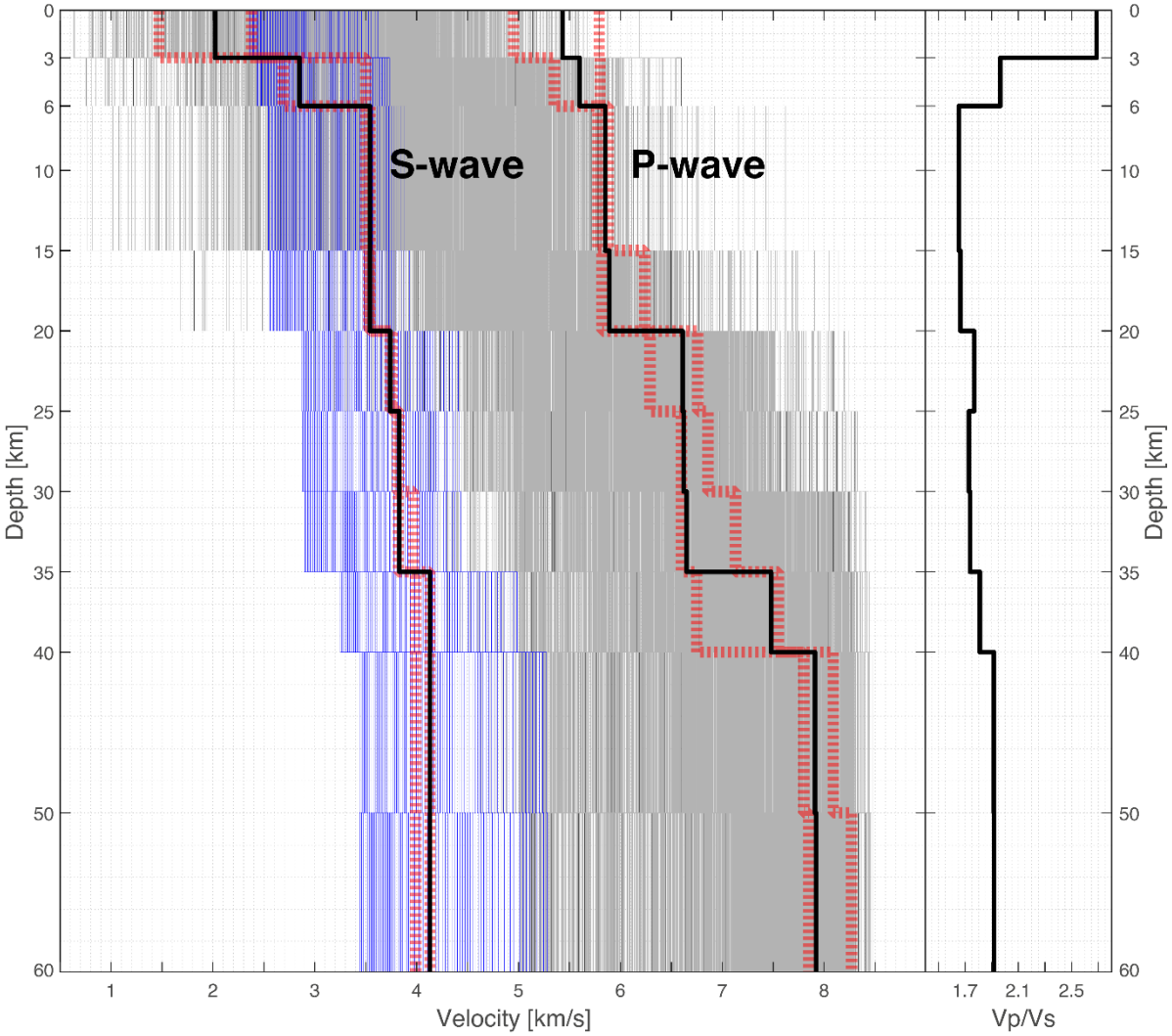

Figure 10. Minimum 1-D Velocity Models. Thick black lines are our best result for the Minimum *Vp* and *Vs* models. The explored model space is represented by grey lines for all the input *Vp* models (3000) and blue lines for all the input *Vs* models (81). Dashed red lines correspond to the best (lowest RMS) 5% obtained of each velocity model (4 *Vs* models and 150 *Vp* models). *Vp/Vs* ratios after 1-D inversion are displayed on the right.

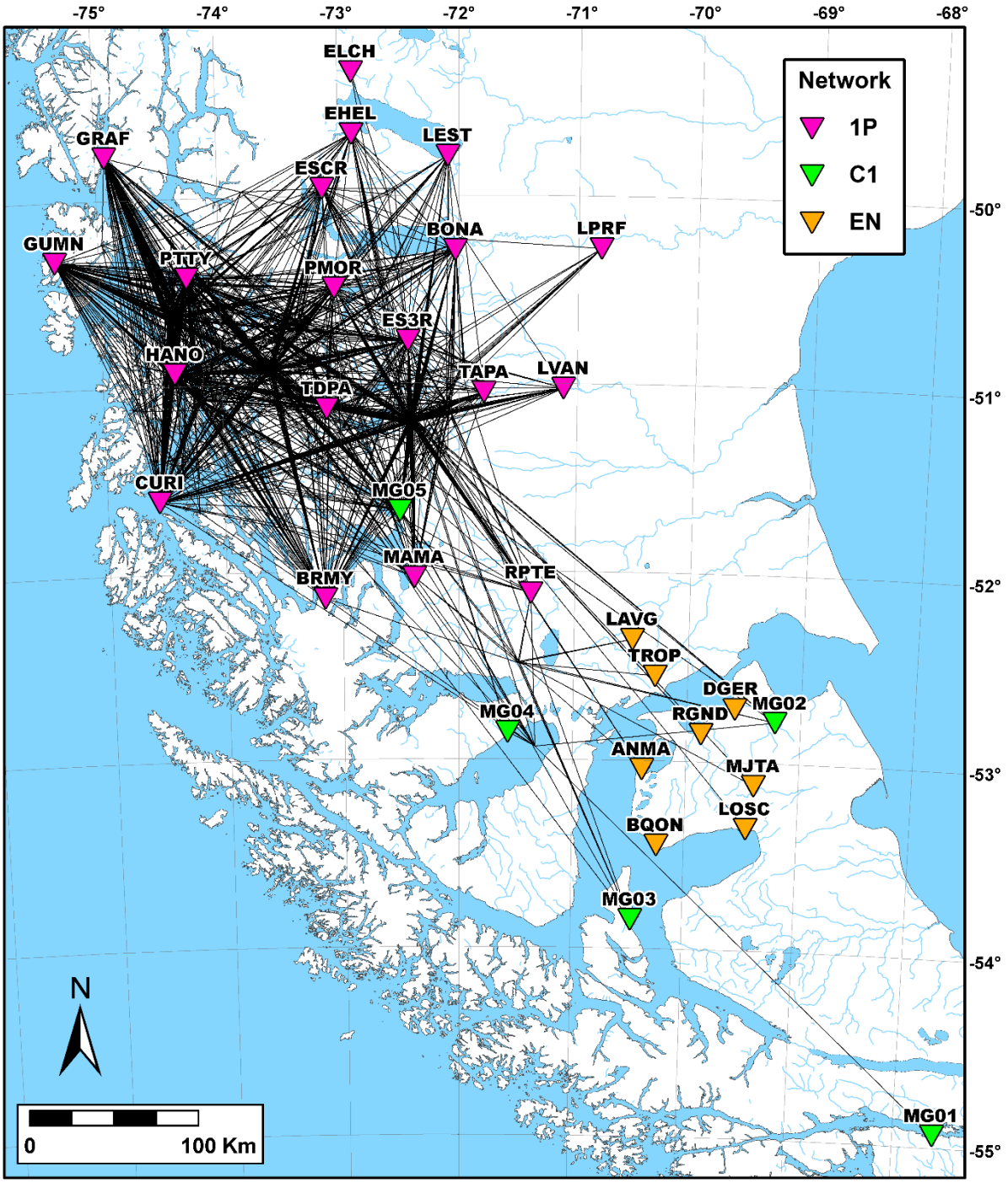

Figure 11. Ray paths used to generate the Minimum 1-D *Vp* Model. For this purpose, we used only class 0 *P*-wave arrivals (minimum 6 per earthquake), leading to 624 events located within our network (GAP ≤ 180°).

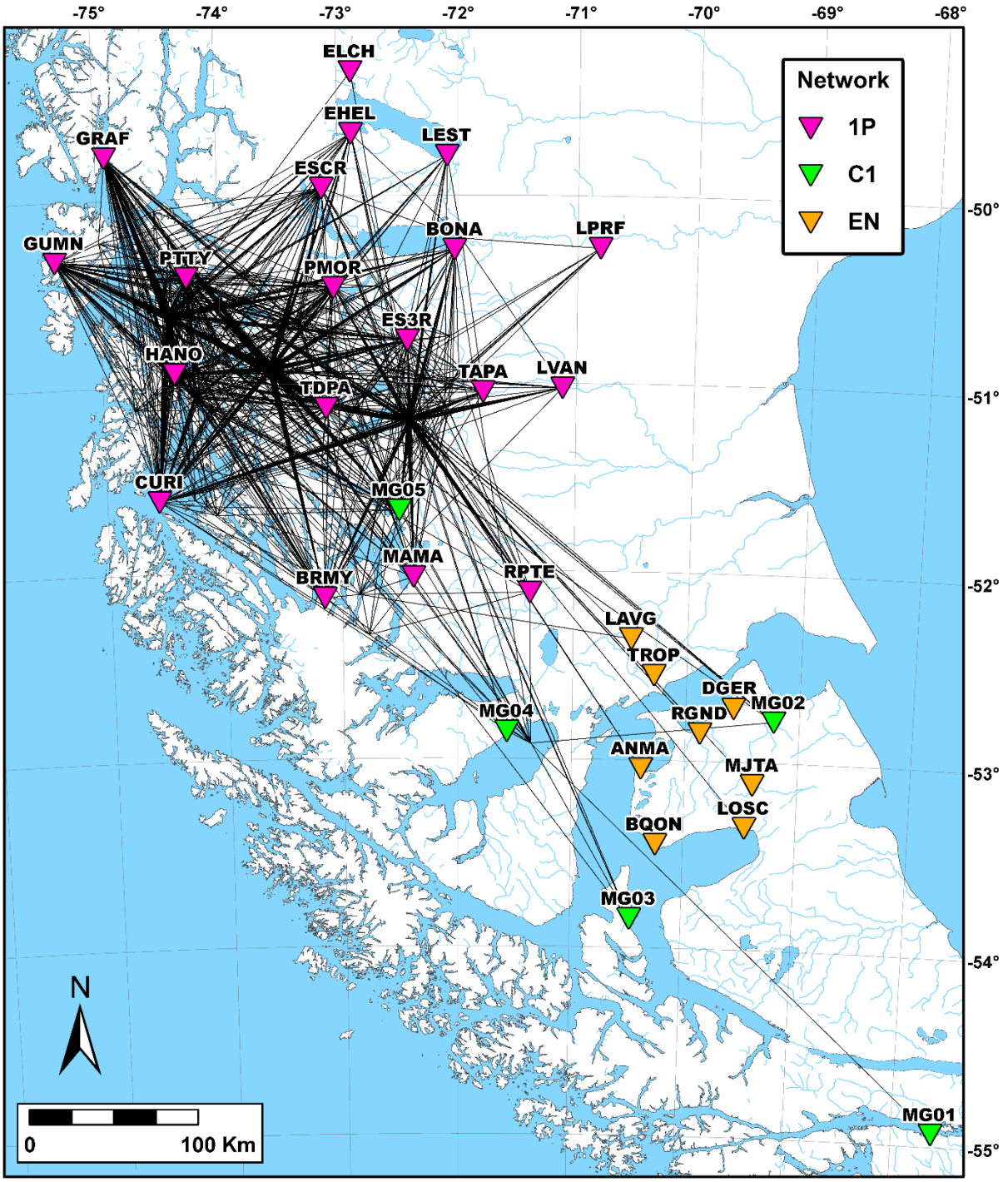

Figure 12. Ray paths used to generate the Minimum 1-D *Vp+Vs* Model. For this purpose, we used only class 0 *P*-wave and *S*-wave arrivals (combined, at least ten arrivals per earthquake) from to 424 events located within our network (GAP ≤ 180°).

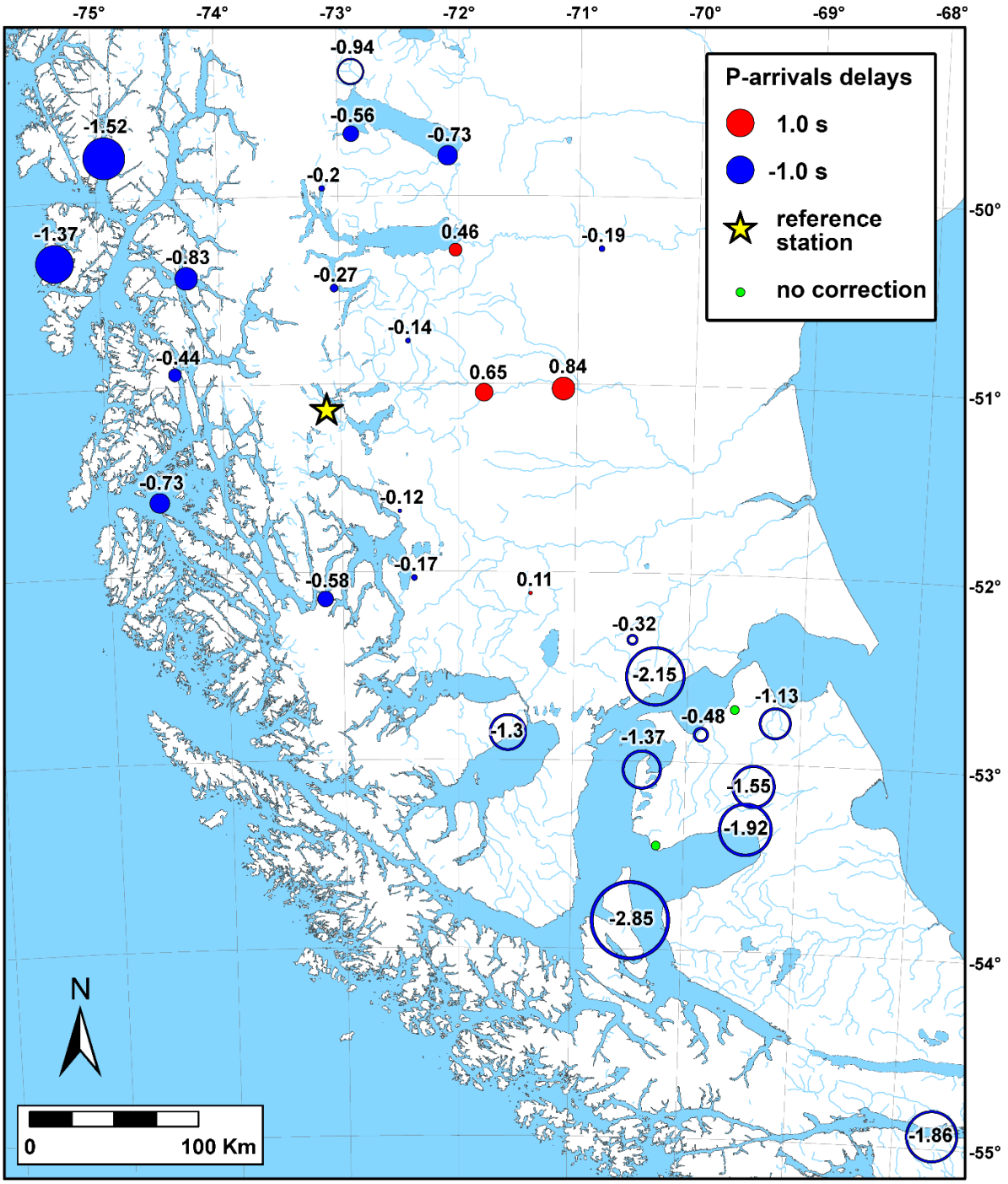

Figure 13. Station delays for *P*-wave arrivals of our Minimum 1-D *Vp+Vs* Model. Red circles indicate positive delays. Blue circles indicate negative delays. Delays symbols are scaled as indicated, and open circles denote stations with less than 9 *P* observations. Reference station TDPA (Torres del Paine) is marked by a yellow star. Green circles indicate no station corrections.

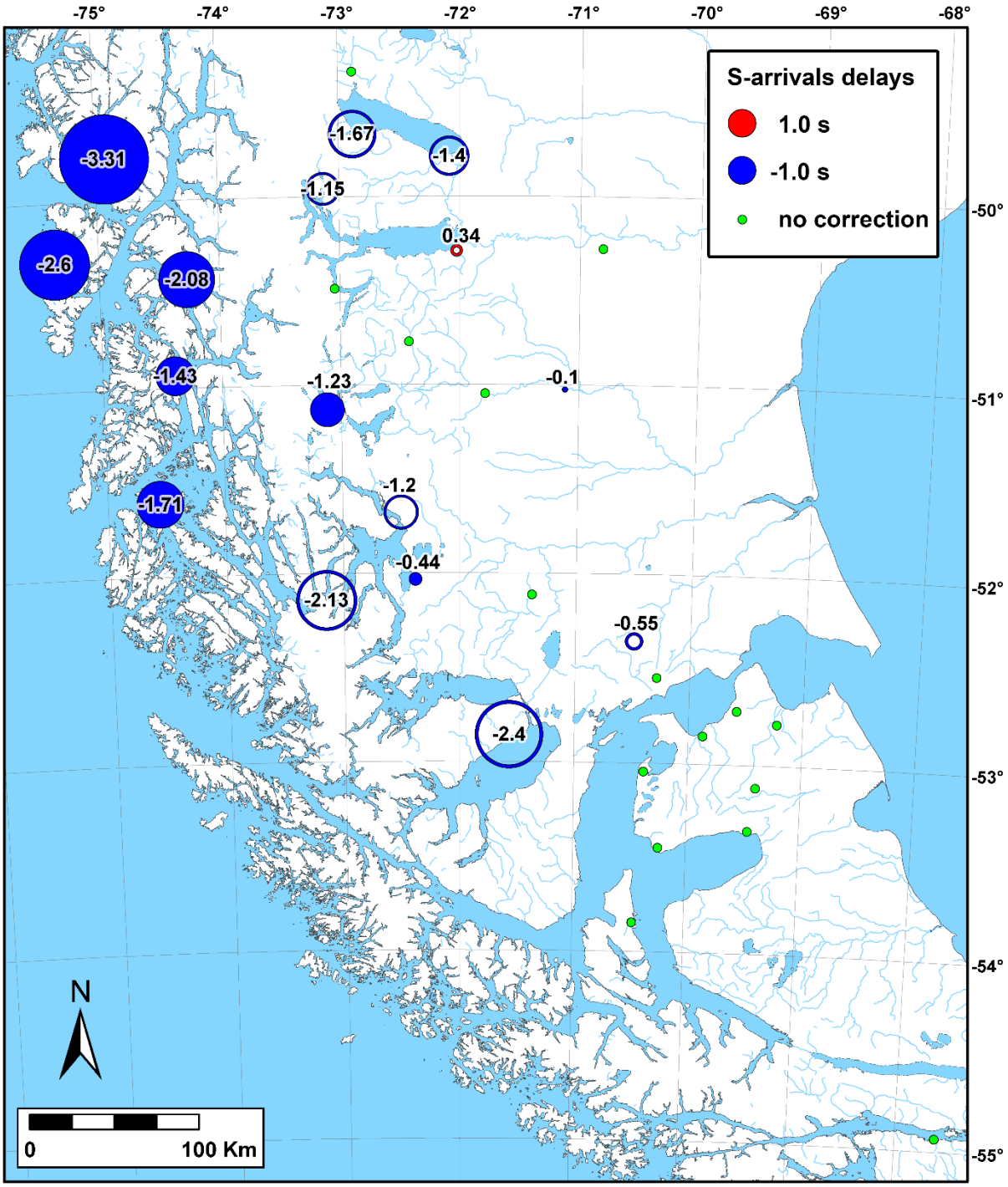

Figure 14. Station delays for *S*-wave arrivals of our Minimum 1-D *Vp+Vs* Model. Red circles indicate positive delays. Blue circles indicate negative delays. Delays symbols are scaled as indicated, and open circles denote stations with less than 9 *S* observations. Green circles indicate no station corrections.

4.5. Hypocentre Location

The final hypocentre location was performed using the software package *NonLinLoc* (Lomax *et al.*, 2000) and our Minimum 1-D *Vp+Vs* model. *NonLinLoc* uses a probabilistic approach based on a non-linear formulation of the earthquake location problem (unknown parameters: *x, y, z, t*), which comprises a complete description of location uncertainties, that are assumed to be Gaussian. It specifically integrates the a priori known uncertainties, such as those associated with the velocity model (travel time errors), and arrival time errors (uncertainties of the *P* and *S* wave arrivals) to estimate the maximum likelihood hypocentre (following Tarantola and Valette, 1982) in terms of probability density functions (PDF).

The programme uses a 3-D gridded volume to resolve for location. It was created using the coordinates 51.25°S 73° W as the origin point, and a Lambert transformation with the WGS84 reference ellipsoid. Using the reciprocity theorem, each station acts as an independent source, and the travel-times between that station and all the nodes (x,y,z) of the spatial grid are calculated using the Eikonal finite-difference scheme of Podvin and Lecomte (1991). Their scheme is based on the Huygen's principle in the finite difference approximation, which explicitly takes into account the existence of different propagation modes (transmitted and diffracted waves).

NonLinLoc has different search methods to compute the PDF: 1) A complete Grid Search algorithm through the volume, using a progressively finer grid, which returns excellent location results, but the computational time needed is high. 2) A Metropolis-Gibbs sampling algorithm, which performs a random walk within the volume to obtain a collection of samples that match the PDF, and is much faster but could be trapped in local minima, leading to missing some possible solutions (for PDFs with multiple minima). 3) An Oct-Tree Importance sampling algorithm. This search method starts with a bigger grid. When the cell of that grid with the highest probability of containing the hypocentre is identified, it divides the cell into new eight child cells. This generates a new finer grid inside this cell and starts the search process again. Then the same procedure is repeated many times. This algorithm converges fast to a solution and produces a more refined grid in the regions with higher probability. It is much faster than grid search (factor 1/100) and more stable and complete than Metropolis-Gibbs (Lomax and Curtis, 2001). To obtain the final locations, we used the Oct-Tree Importance sampling algorithm

The posterior PDF represents a complete, probabilistic solution to the location problem, including information on uncertainty and resolution (Lomax *et al.*, 2000). The density of points in the PDF scatter sample is directly proportional to the PDF value. Therefore, the zones with a greater density of points are the higher probability regions. Gaussian uncertainty information

for the final hypocentre is given in the form of a 68% spatial confidence ellipsoid, which is generated by Single Value Decomposition from the covariance matrix of the PDF scatter sample. The ellipsoid is an approximation to the PDF shape, truncated at the 68% confidence level. The centre of the ellipsoid is called the expectation hypocentre. Nevertheless, the optimal and final hypocentre is assigned to the point with the maximum likelihood (or minimum misfit) of the complete non-linear location PDF (Figs. 15 and 16).

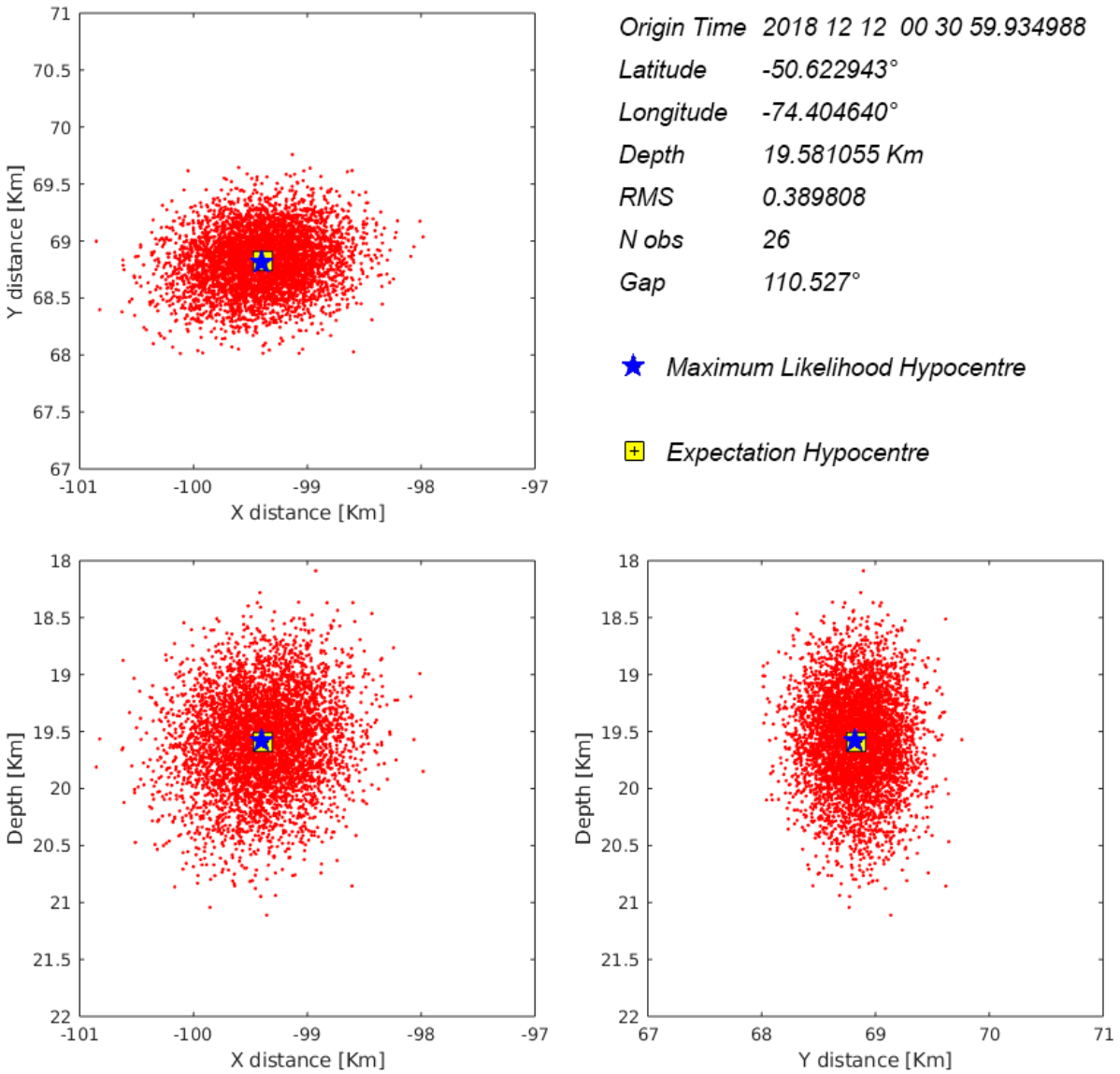

Figure 15. PDF scatter plots of the catalogue earthquake of 12th of December 2018 at 00:31. Note that expectation hypocentre and maximum likelihood hypocentre do not differ too much. Quality of NonLinLoc location is A.

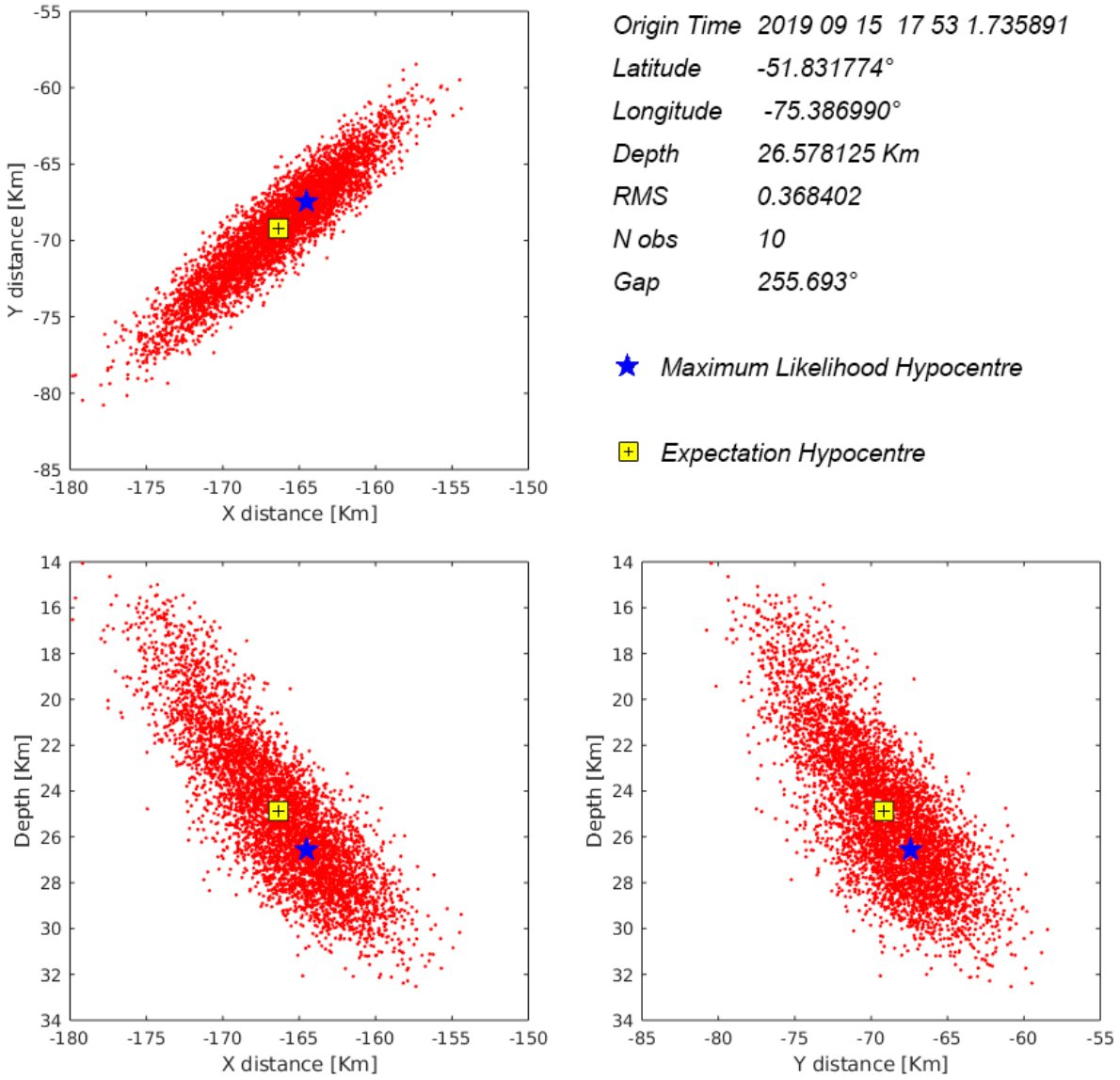

Figure 16. PDF scatter plots of an earthquake located at the offshore, which show the highest value of horizontal uncertainty in the location of our catalogue. Note that the maximum likelihood hypocentre is located deeper than the expectation hypocentre, and the location differs in kilometres. Quality of NonLinLoc location is C.

4.6. Earthquake Statistics

We use ZMAP7 (Reyes and Wiemer, 2020; Wiemer, 2001), a software package for MATLAB®, to calculate some statistical parameters of the earthquake catalogue. ZMAP allows us to evaluate and map the Minimum Magnitude of Completeness (Mc) of a catalogue. Furthermore, it has options to graph the cumulative moment release, plot a variety of histograms and create seismic swath cross-sections. The catalogue's Mc was calculated using the Maximum Curvature Method of Wiemer and Wyss (2000).

5. Results

5.1. Earthquake Catalogue Statistics

5.1.1 Rates of seismicity and seismic moment

A rate of *ca.* 1.5 seismic events per day (275 events in 182 days) were detected within December 2018 and end of May 2019, before the onset of the Reclus volcano seismic swarm. This value is considered as the background rate of seismicity within our study area. Some days have a higher occurrence of seismicity due to aftershock events related to the 12/12/2018 and 17/02/2019 and 02/04/2019 higher magnitude earthquakes. As of 1st of June 2019, with the beginning of the Reclus volcano swarm, the number of earthquakes per day increases dramatically. A total of 2410 seismic events were detected from this date until the end of our observation time window, reaching an overall rate of 14 seismic events per day. The difference can be seen clearly in Figure 17.

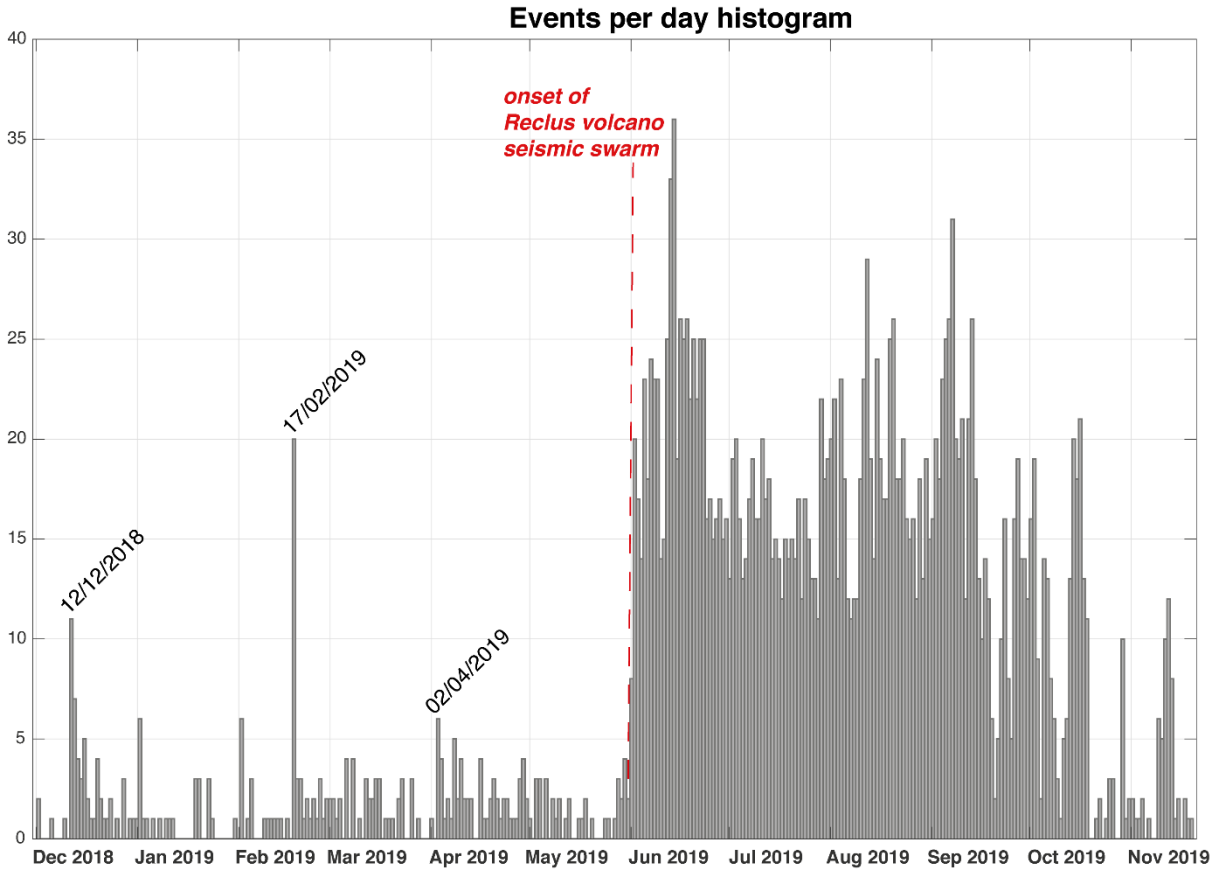

Figure 17. Histogram of seismic events per day. Highlighted dates denoted the three major catalogue events recorded by CSN during our analysis time window (Mw ≥4.8).

Figure 18 shows the cumulative seismic moment within our analysis time window. Analogue to the Events per day histogram, the cumulative moment rate jumps with the larger magnitude events, while the slope of the curve between those events is gentle. With the onset

of the Reclus volcano seismic swarm, there is a steepening of the slope, related to a greater release of energy in a diffuse way.

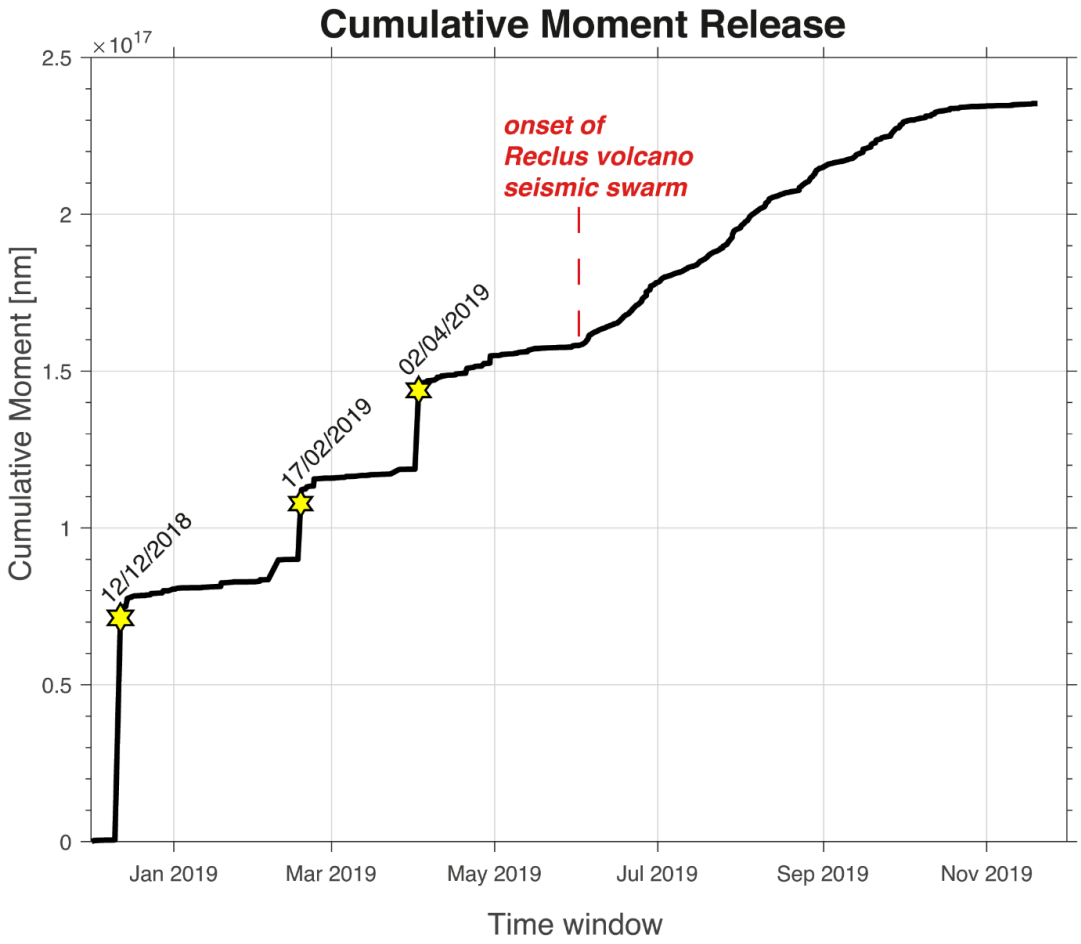

Figure 18. Cumulative Seismic Moment Release. Highlighted dates denoted the three major catalogue events recorded by CSN during our analysis time window (Mw ≥4.8). With the onset of the Reclus volcano seismic swarm, there is an increase in the momentum rate, denoted by a steeper slope.

5.1.2 Magnitude of completeness

Using ZMAP, we estimate the Magnitude of Completeness (Mc) and b-value distribution of our catalogue. Applying the Maximum Curvature method of Wiemer and Wyss (2002) to the Frequency-Magnitude distribution (FMD) leads to a Mc of 2.8 and an overall b-value of 1.63 ± 0.03 for the catalogue (Fig. 19).

Taking advantage of ZMAP utilities, we map the magnitude of complete recording (Fig. 20). The results show a lower Mc in the northern part of our study area, where the temporary seismic network (1P) is located. To the southwestern offshore and to the south, where the station coverage is sparser, the Mc has higher values.

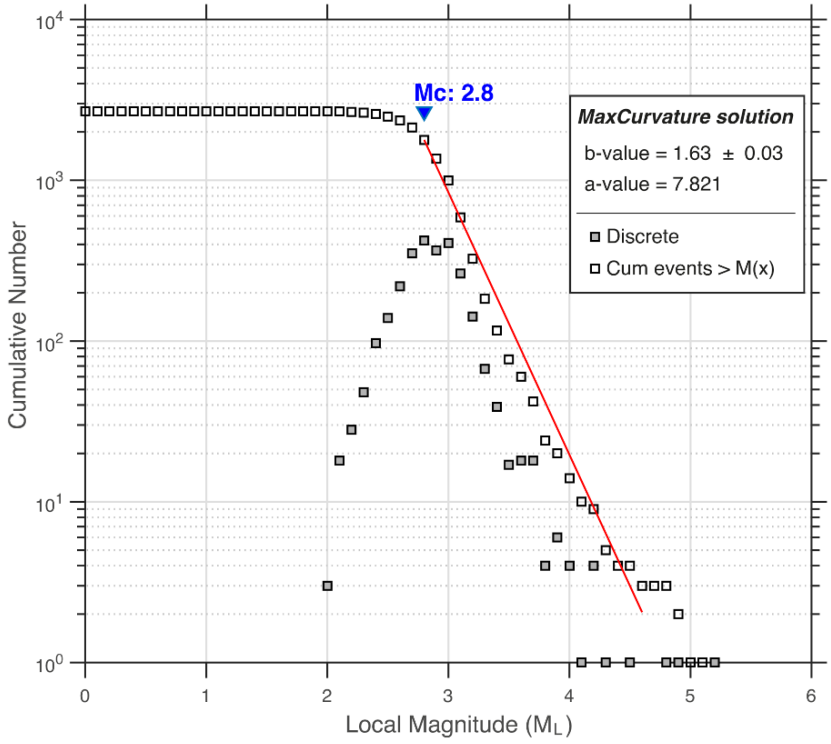

Figure 19. Frequency–magnitude distribution for all the events included in our catalogue (Appendix 2). The distribution of the non-cumulative (discrete) histogram has a pick at 2.8, which is assigned as a Magnitude of Completeness (Mc) following the Max. Curvature method of Wiemer and Wyss (2002). It coincides with the inflexion point of the cumulative distribution. The obtained b-value for the catalogue is of 1.63±0.03.

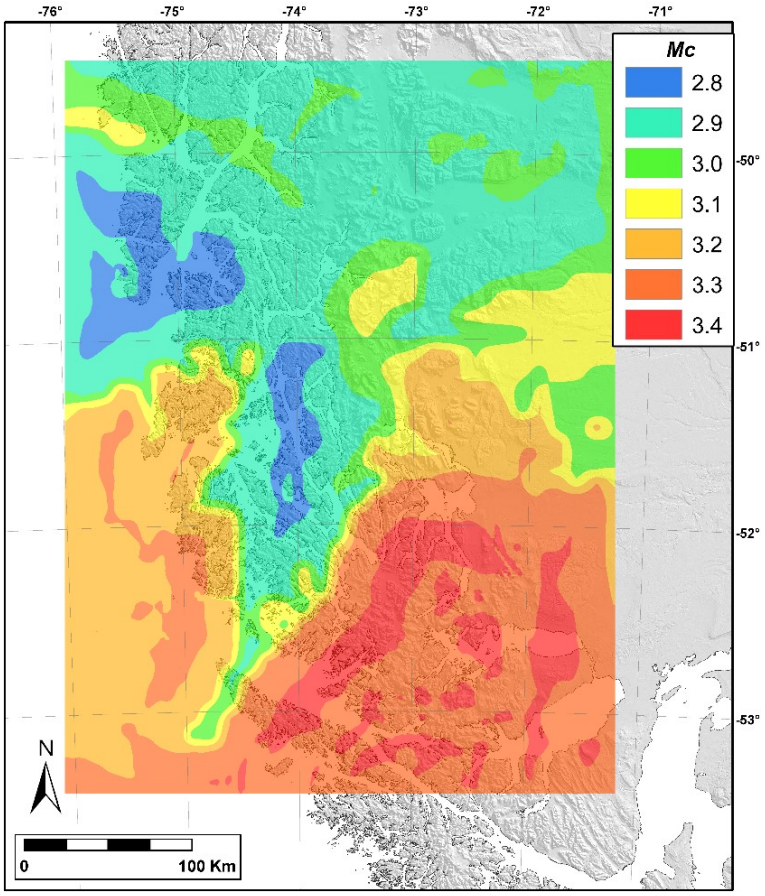

Figure 20. Map of our study area indicating the magnitude of complete reporting (Mc), computed using ZMAP7.

5.2. Location Errors

Non Lin Loc estimates the location error, taking into account the a priori identified uncertainties (e.g. travel/arrival time errors) of the data and location issues as the azimuthal gap. It produces an output of the error for x, y and z axis. The obtained location errors were averaged in 25 x 25 km cells (Figure 21). When comparing the axis's errors, our study area's west region has more significant errors for all the directions. The best performance is in the x-direction (longitude error); most of the regions have errors of hundreds of meters. The errors in the y-direction (latitude error) have good performance in the northern-central section with location errors of hundreds of meters, but it is slightly worse south of 52°S, where the location errors can be above 1000 meters. The vertical error (in-depth; z-direction) is bigger than the horizontal errors. In general terms, the values are higher in areas with worse azimuthal coverage (Figure 22). On the other hand, the spatial average of RMS of the locations is showed in Figure 23. The highest values are mostly in the southern region, while concentrated within the centre of the network, the RMS values are low.

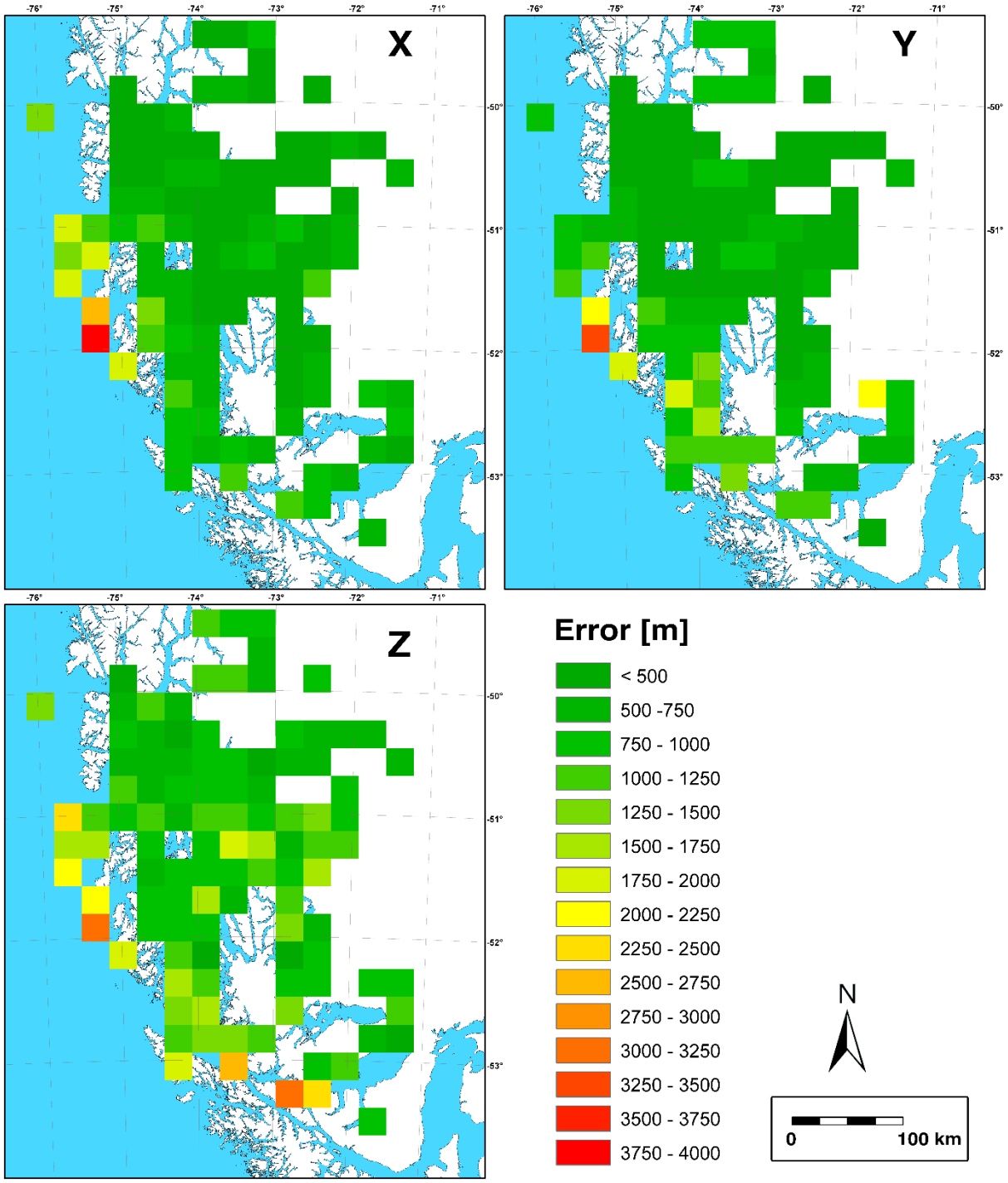

Figure 21. Map of average errors per area, in x, y and z directions. Each cell has 25x25 km.

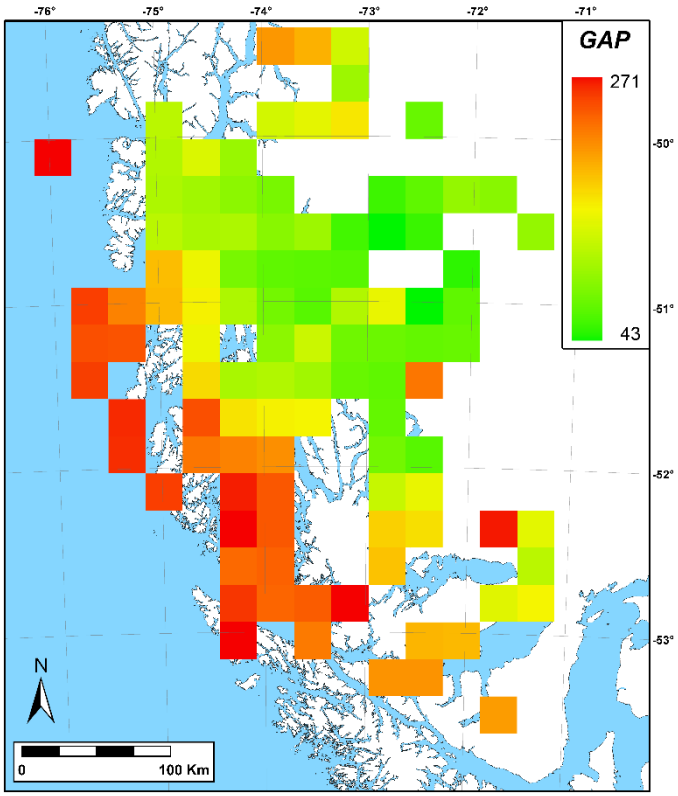

Figure 22. Map of average GAP per area. Each cell has 25x25 km.

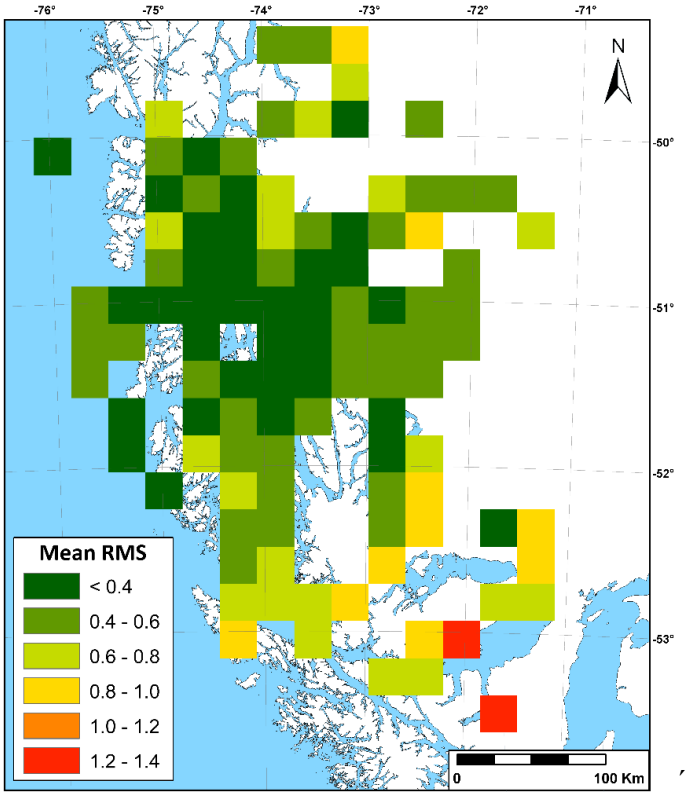

Figure 23. Map of average RMS per area. Each cell has 25x25 km.

5.3. Spatial Distribution of the Localised Crustal Seismicity

Most of the localized seismicity is in the area where we have the best coverage of seismic stations. We re-located 2685 earthquakes with *Non Lin Loc*, from which just 500 are located in different areas of our study region. The rest belongs to a seismic swarm under the Reclus volcano, which was very active from June 2019 until Mid October 2019.

In general terms, the seismicity that we locate follows several trends (Figure 24). In our study area centre, aligned epicentres into two different tendencies, form something like a cross. On one side, some align NE-SW along what has been described as the Lago Argentino Transfer Fault (Fig. 5; Ghiglione et al., 2009). In contrast, other epicentres are aligned into an NW-SE geomorphological lineament which dissects the Cordillera. Our three main hotspots, related to the two mainshocks (in the fjord region and the FTB, respectively) and under the Reclus volcano, are aligned into an NW-SE trend, just a bit south of this lineament (Fig. 24).

At the southwestern corner of our interest region, we found we found numerous crustal seismicity along the Smyth Channel (Fig. 25), concentrated in two different places along its passage. Figure 26 shows a cross-section of the seismicity distribution within the Smyth Channel group. Shallower hypocentres are located to the northeast, while deeper hypocentres are located towards the southwest.

At the western side of the centre of our study area, in the forearc of the Austral Andes, three seismic swarms were detected in different places. Two are related to the catalogue events on the 12th of December 2018 and the 17th of February 2019. Looking into the map and cross-sections (Figs. 27 and 28), it seems that the event on the 17th of February 2019 is faulting forearc at a depth range of 6 to 16 km, and the epicentres are aligned NE-SW. The event on the 12th of December 2018 is the better documented of our catalogue because it has a focal mechanism of gCMT (Fig. 2). Our locations show a trend of epicentres orthogonal to the margin with a WNW-ESE trend (Fig. 29). Cross-sections (Fig. 30) suggest that the hypocentres are concentrated along a fault which is dipping towards the northeast.

In the middle of our array, 2185 events are located under the Reclus volcano (Figs. 31 and 32), mostly at a depth range of 2 to 12 km.

At the eastern side of our study area, the earthquakes distribute almost homogeneously along the Austral Andes' thrust front. At the northern side (west of Viedma and Argentino lakes), we have shallow hypocentres under the Southern Patagonian Icefield. At the southern shore of Lago Argentino, earthquakes are aligned into a NE-SW tendency, along the Lago Argentino Transfer Fault and have depths from 3 up to 12 km (Fig. 33). Continuing south, the

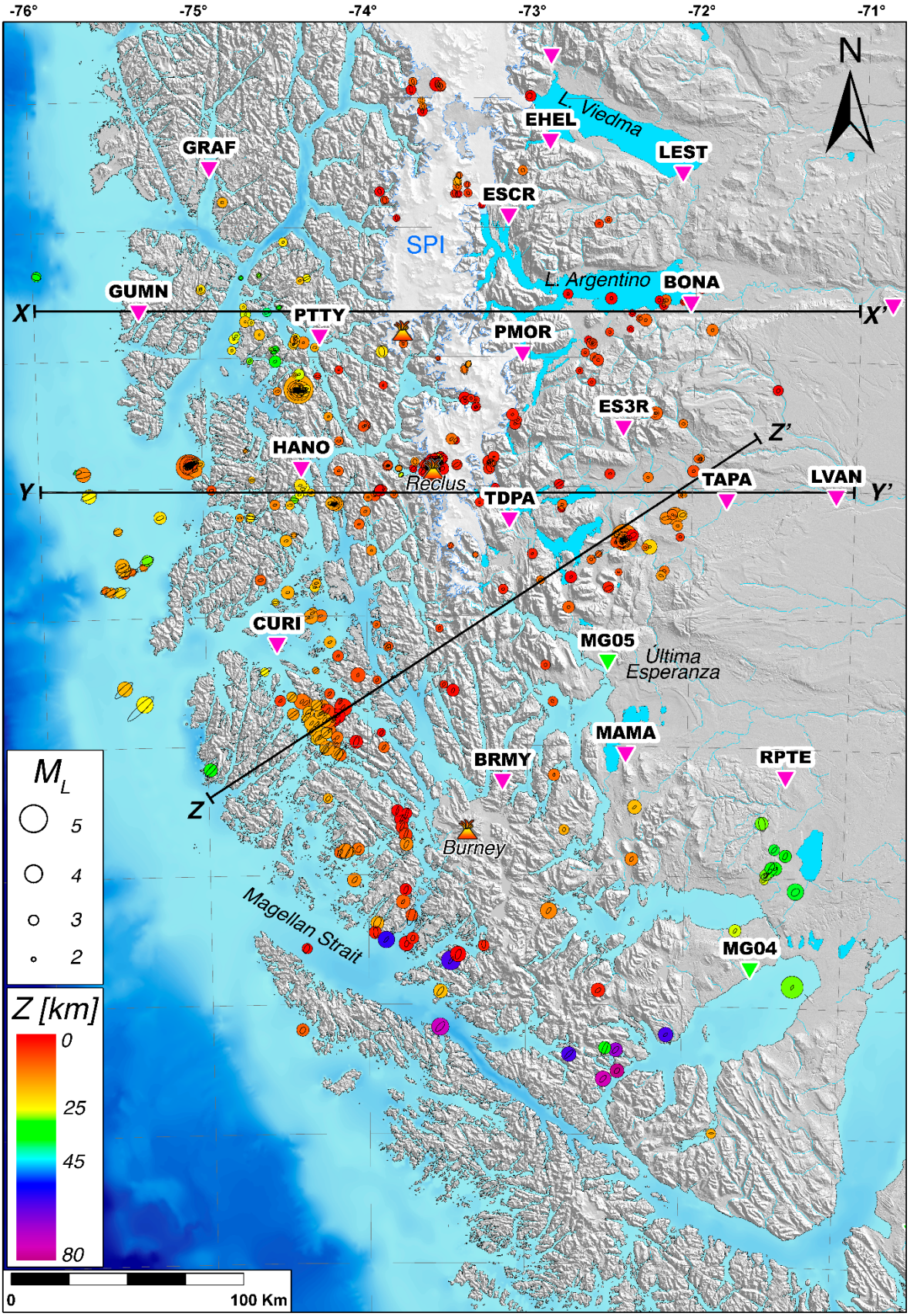

Figure 24. Seismicity map of the Austral Andes region. Earthquakes are displayed as circles, with size respect to the local magnitude and colour respect to the hypocentral depth. Black lines denoted regional seismic cross-sections. Each of those as a width (swath) of 50 km with the centre at the black line (25 km per each side). On land digital elevation model data from SRTM 1 Arc-Second Global (https://doi.org/10.5066/F7PR7TFT). Bathymetric data from GEBCO (Becker et al., 2009).

occurrence of seismicity in front of the FTB is common. In the Última Esperanza región, after the earthquake on the 2nd of April 2019, there is a seismic swarm around the hypocentre (Fig. 34). This happens at the triangle zone of the FTB, and the obtained depths range is mostly from 3 to 15 km.

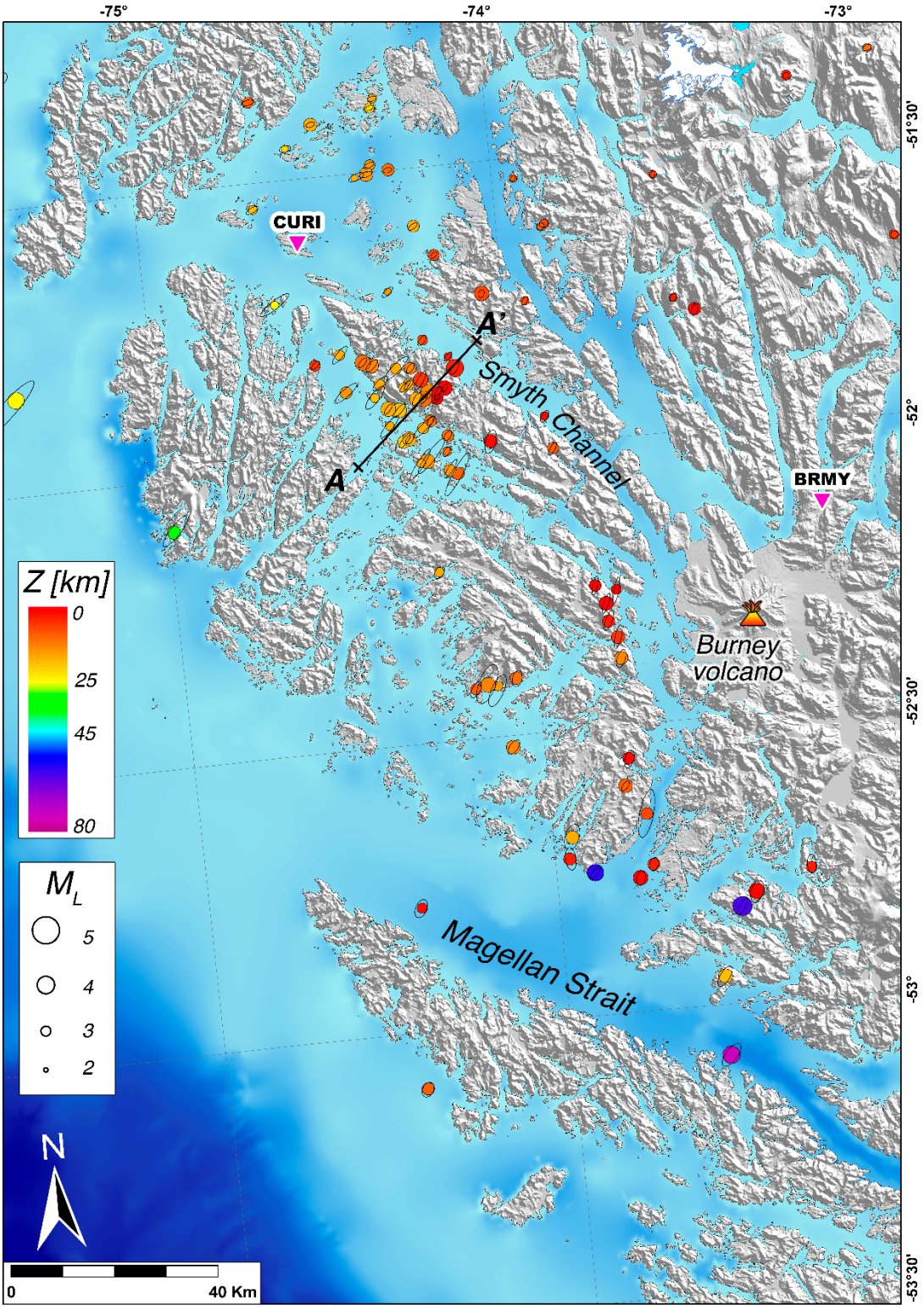

Figure 25. Southwestern corner of our study area. There is a cluster of seismicity along the Smyth Channel, starting from the Magellan Strait and continuing towards the northwest. A-A´ cross-section is displayed in Figure 26. Ellipsoids around the epicentres are a representation of the 68% confidence ellipsoid (section 4.5.).

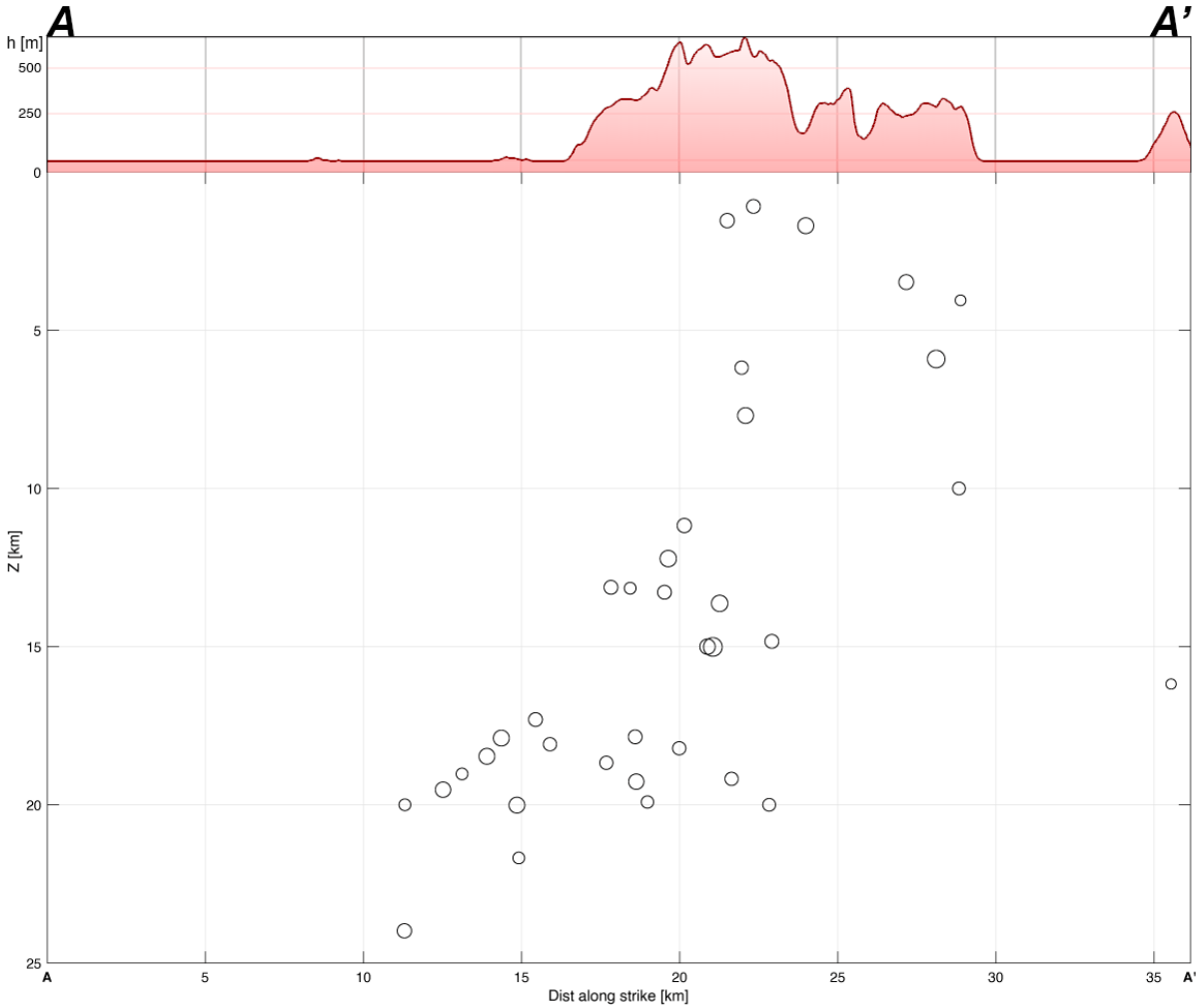

Figure 26. A-A' cross-section across the southwestern section of the Smyth Channel. Hypocentres are aligned dipping towards the southwest.

At the southern section of our study area, the obtained locations have a broader range of depth, from crustal events (*ca.* 5 km depth) up to 80 km depth earthquakes.

The seismicity that we located is mainly distributed at shallow depths (most of the hypocentres are at a depth ≤ 20 km). The figures 35 to 37 are regional cross-sections obtained with ZMAP7, and those traces are displayed in Fig. 24. Each of those has a width of 50 km (sections X-X', Y-Y' and Z-Z').

We also produce two cross-sections for the entire study area, which comprises all the dataset. One is oriented W-E (longitudinal cross-section, Figure 38) with the axis at the parallel 51.5°S. The other is oriented N-S (latitudinal cross-section, Figure 39) with the axis at the meridian 73.5°W. Both cross-sections have a sampling width of 500 km.

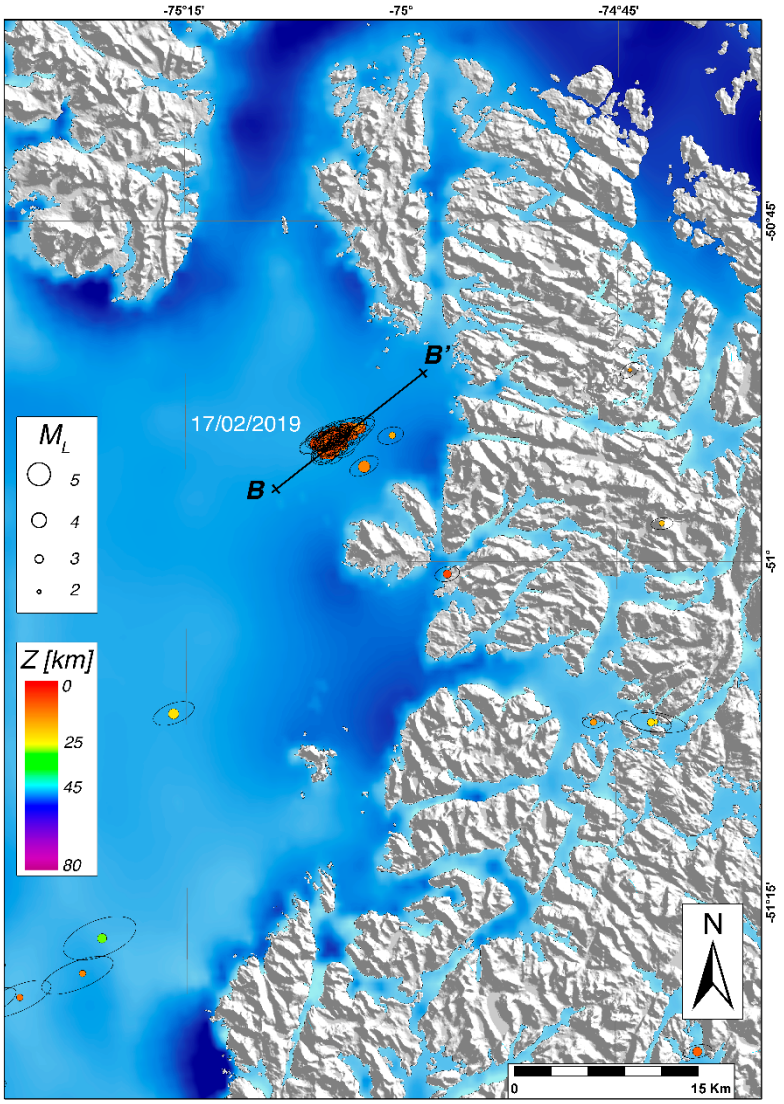

Figure 27.
Location of the seismic cluster on the 17th of February 2019. Almost all the events were on that day and are aftershocks of the Mw 4.8 earthquake from 10:26 am.

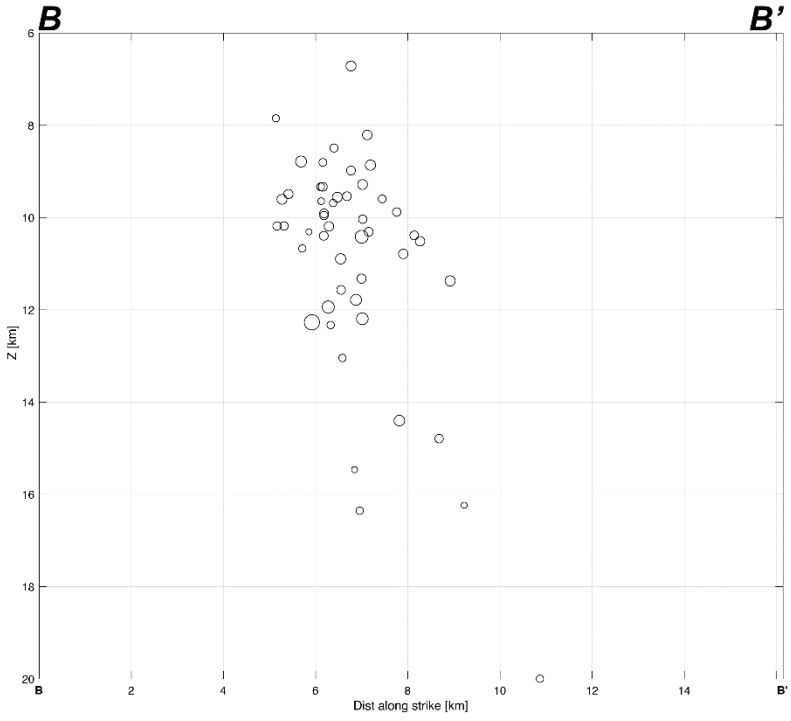

Figure 28.
Cross-section of the seismic swarm on the 17th of February 2018.

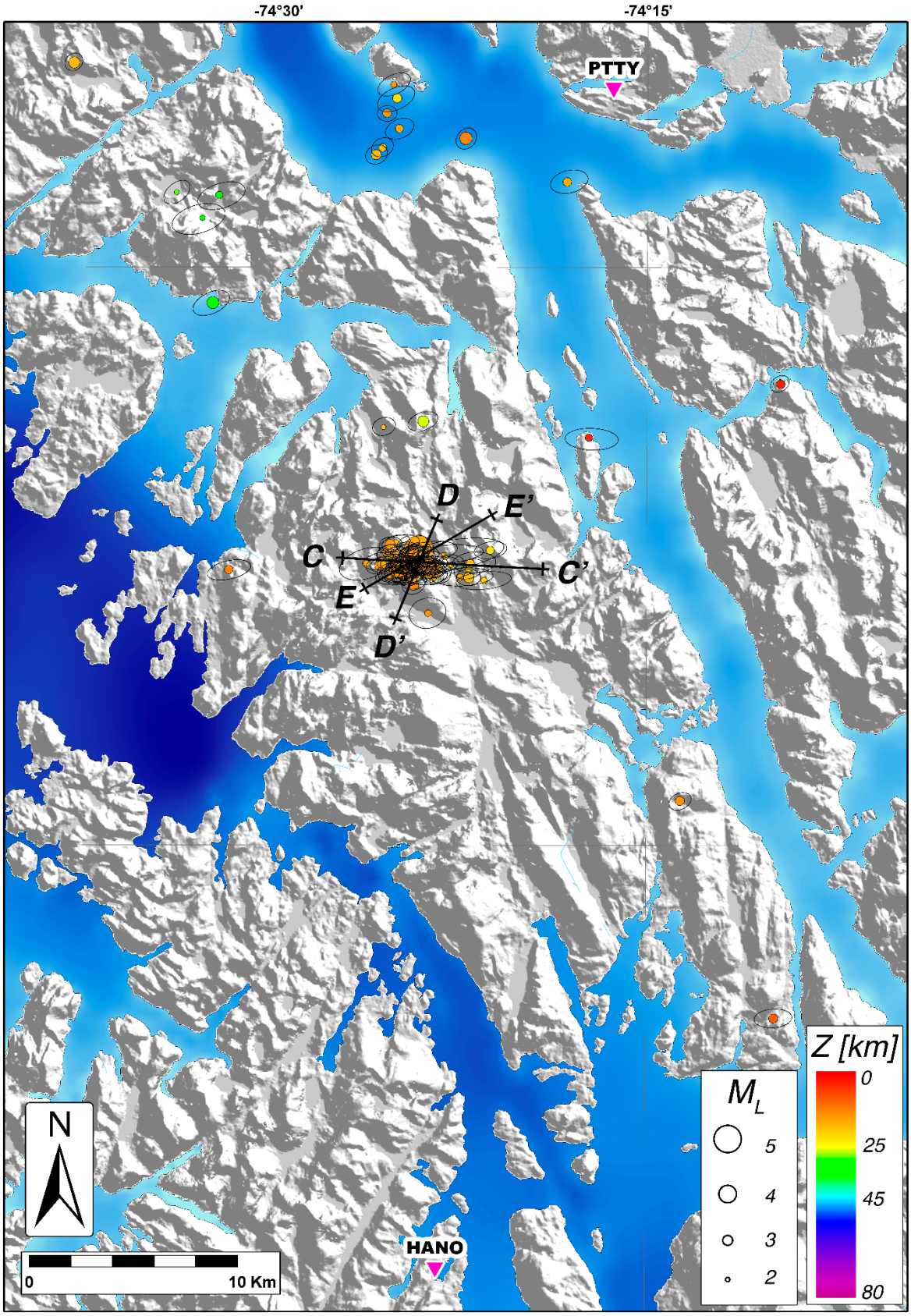

Figure 29. Location of the seismic cluster of 12th to 14th of December 2018. Ellipsoids around the epicentres are a representation of the 68% confidence ellipsoid (section 4.5.).

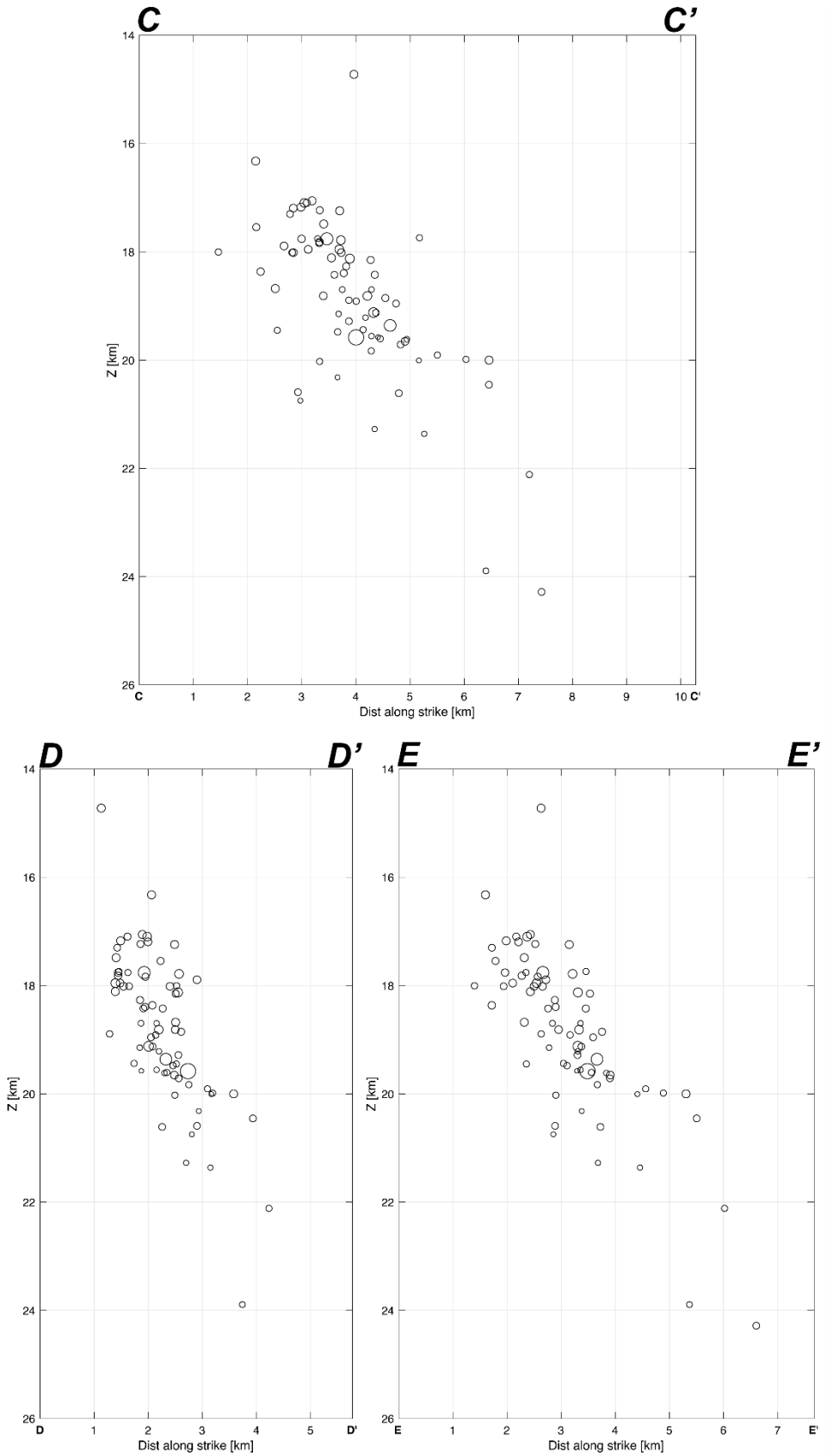

Figure 30. Cross-sections show the cluster of seismicity located in the area of the catalogue events of 12th and 14th of December 2018.

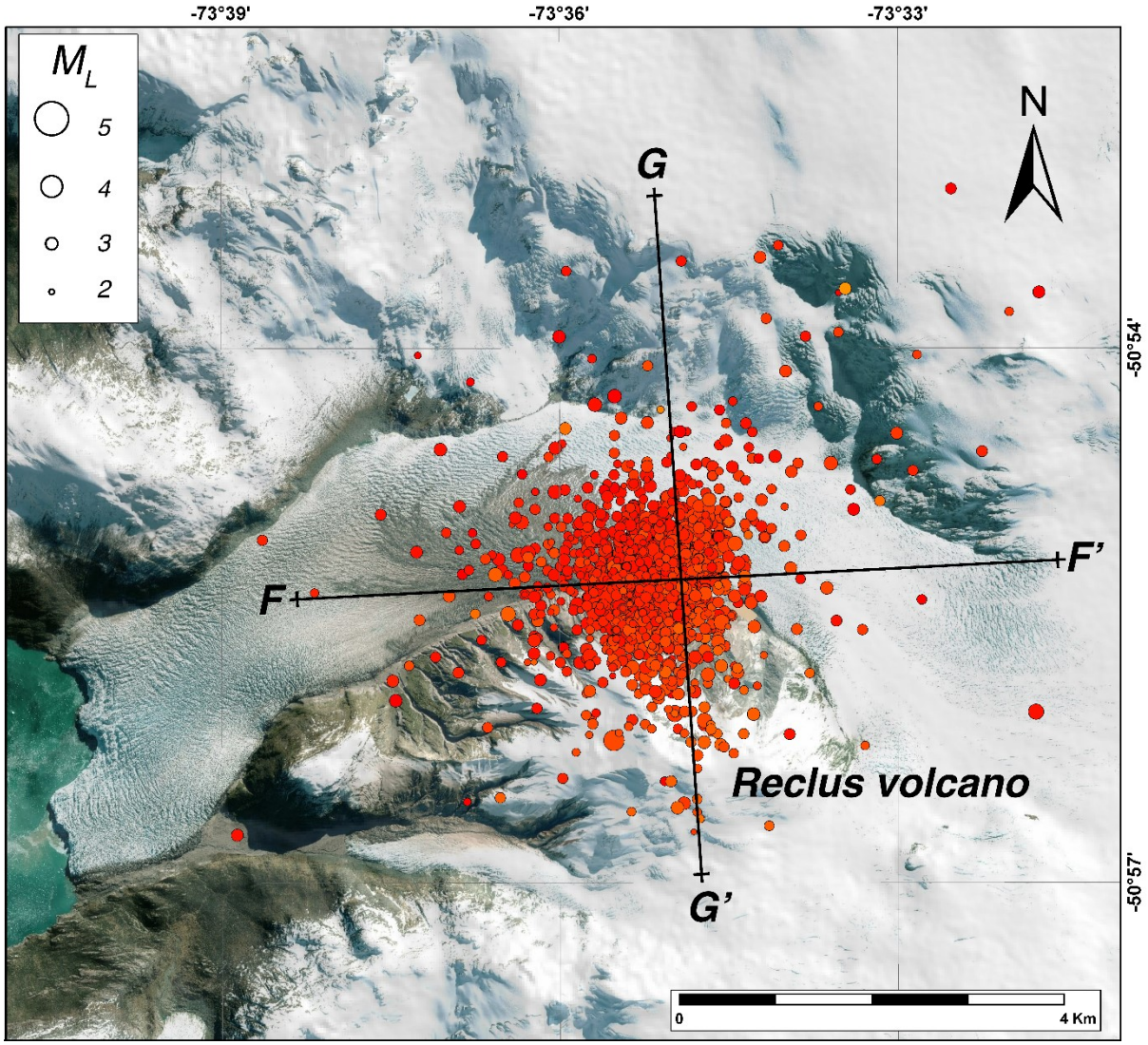

Figure 31. A cluster of seismicity located under the Reclus volcano (2185 events). Coloured depths are the same as the other figures.

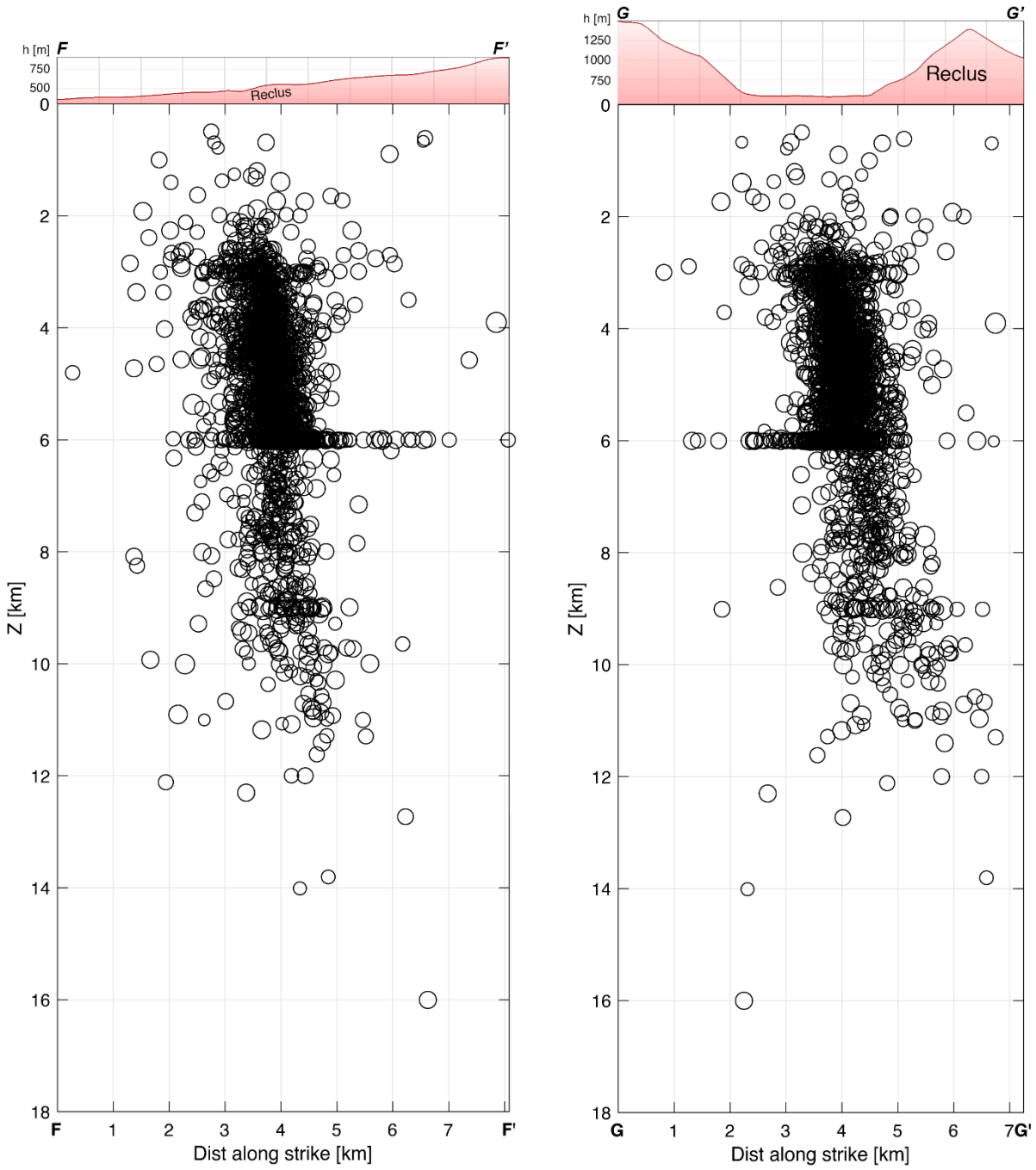

Figure 32. Cross-sections (traces in Fig. 31) show the distribution in depth of the seismicity under the Reclus volcano.

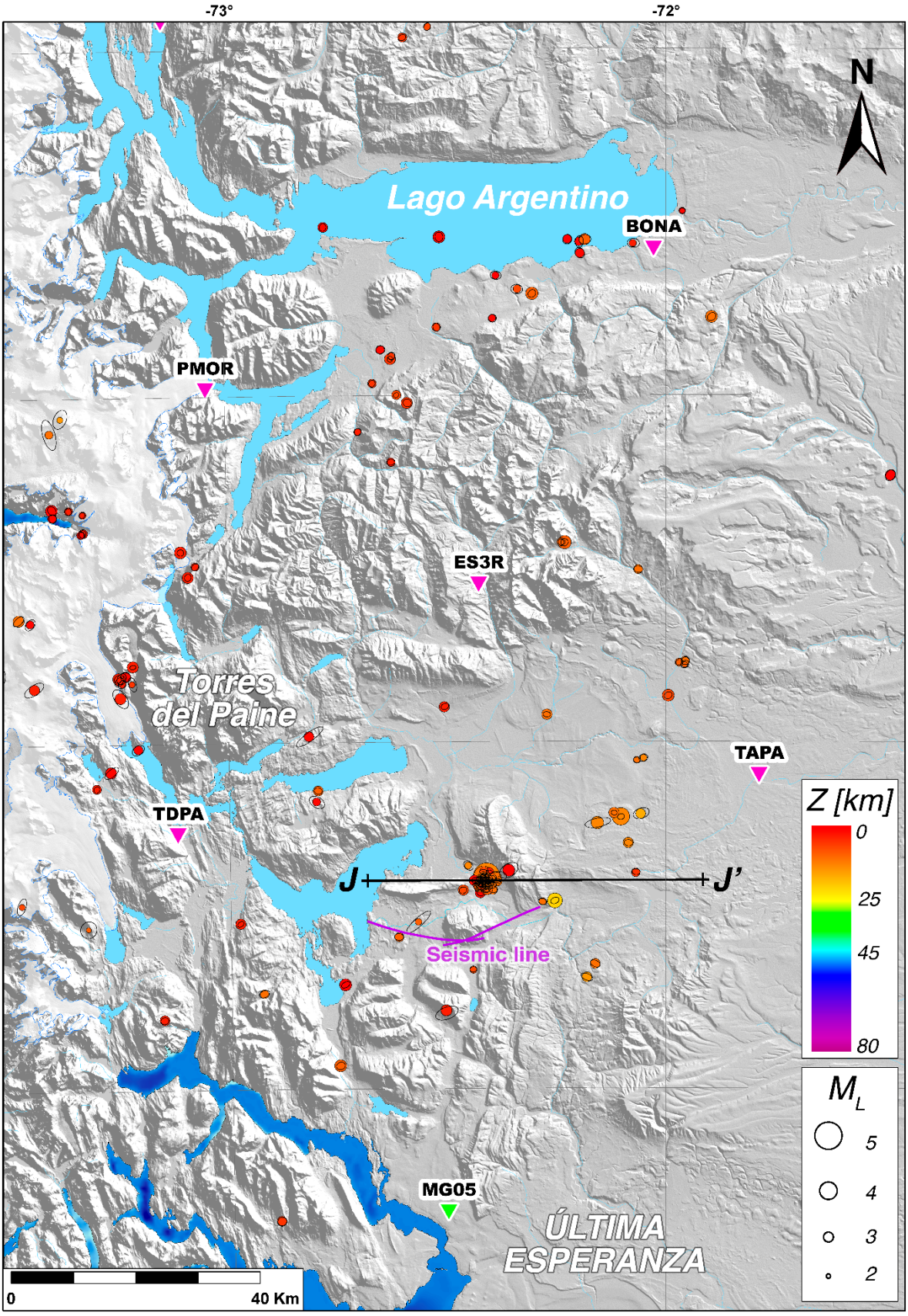

Figure 33. Map of the section of the FTB that is included within our study area. In the north, the epicentres are aligned at the southern shore of Lago Argentino along the transfer fault (Fig. 5). The events of the central-eastern section with depths up to 20 km represent the thrust front, which is blind. Within the J-J' cross-section is the seismic swarm associated with the catalogue event of the 2nd of April 2019. Seismic line from Fosdick *et al.* (2011) is shown in Fig. 40.

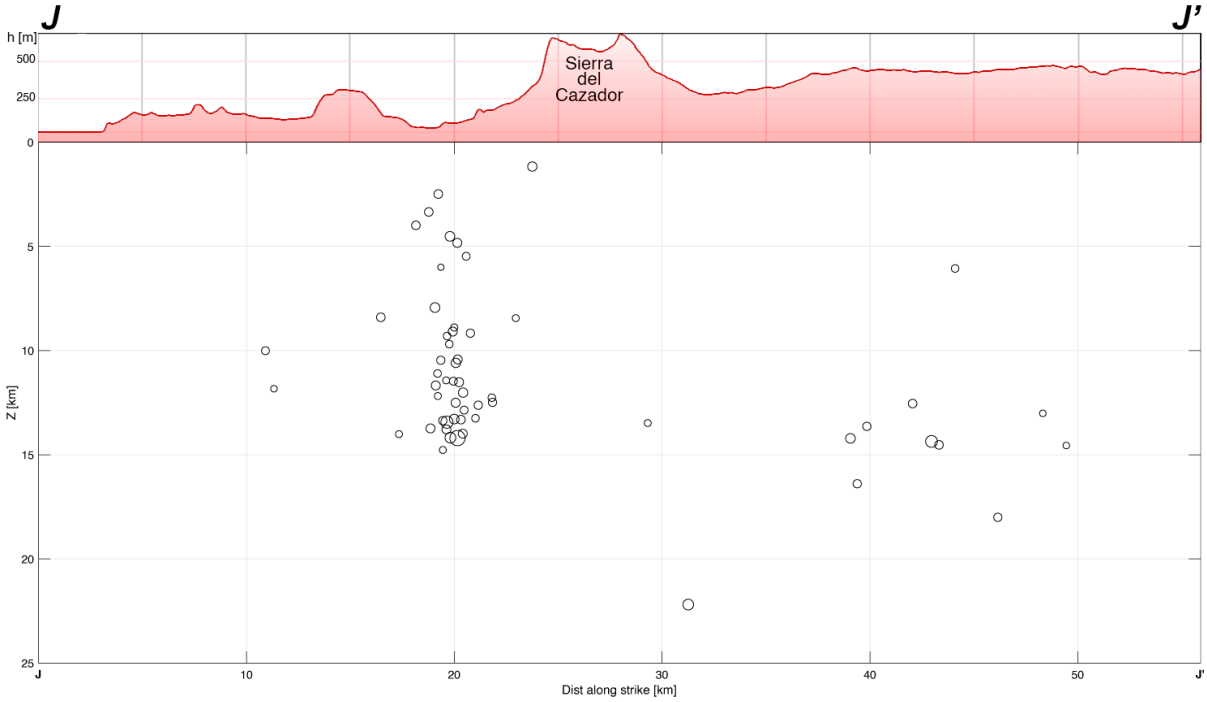

Figure 34. Cross-section of the seismic swarm in the triangle zone of the FTB (trace in Fig. 33).

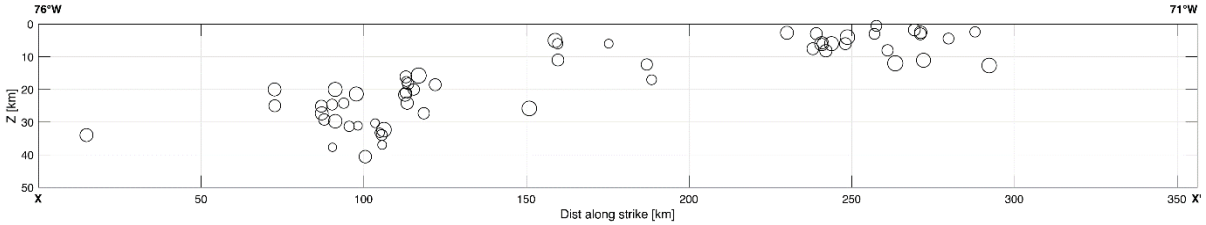

Figure 35. Regional seismic cross-section X-X', centred at 50.3°S. Orientation W-E.

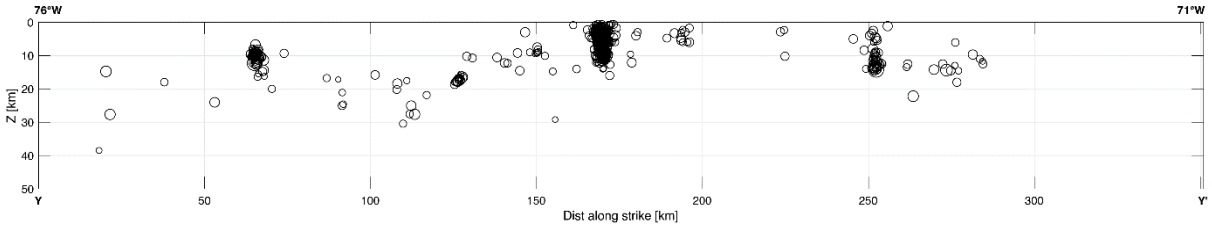

Figure 36. Regional seismic cross-section Y-Y', centred at 51°S. Orientation W-E.

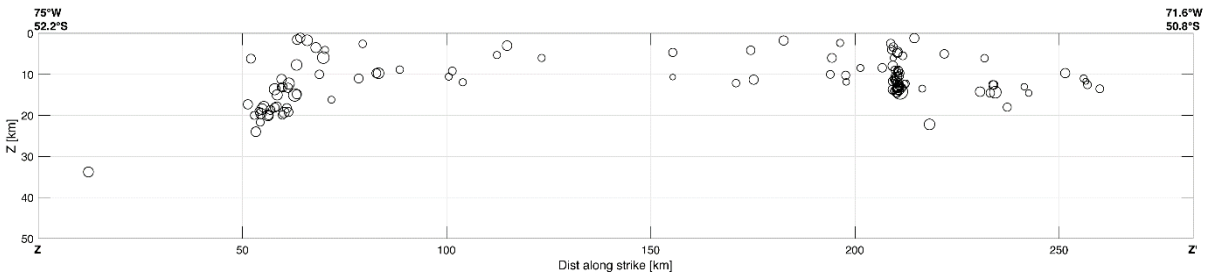

Figure 37. Regional seismic cross-section Z-Z', orientation SW-NE. From Smyth Channel towards Última Esperanza.

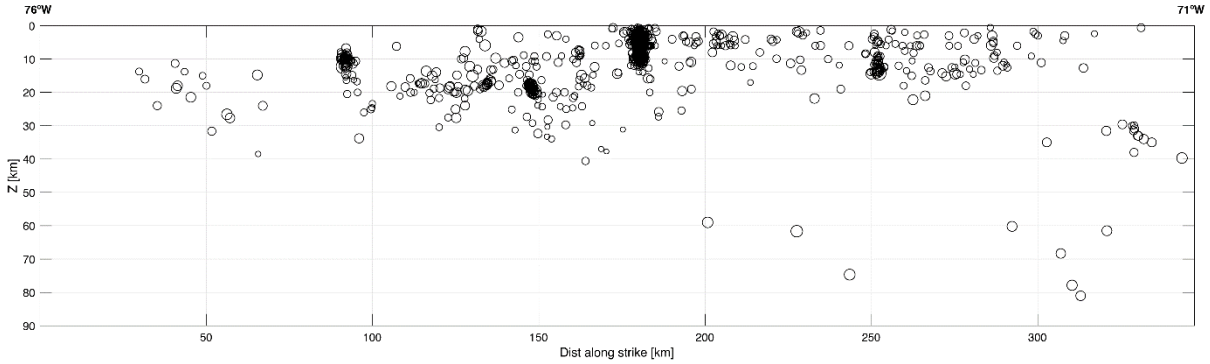

Figure 38. A longitudinal cross-section for the entire study area (all the catalogue). Orientation W-E, with the axis at the parallel 51.5°S. Sampling width of 500 km. It was produced with ZMAP7.

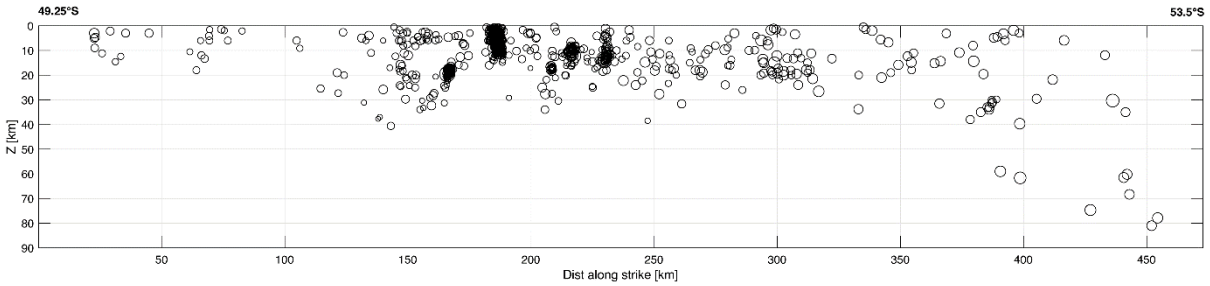

Figure 39. A latitudinal cross-section for the entire study area (all the catalogue). Orientation N-S, with the axis at the meridian 73.5°W. Sampling width of 500 km. It was produced with ZMAP7.

6. Discussion

6.1. 1-D Seismic Velocity Structure

6.1.1. Crustal Velocity Structure

The shallower velocity layer has a thickness of 3 km. This thickness is likely to be the Cenozoic sedimentary cover which overlies the Mesozoic sedimentary sequences at the Eastern side of the Cordillera. Through a seismic refraction survey, Ludwig *et al.* (1965) report equivalent thicknesses (from 1 to 4 km) of the Eocene-Miocene sequences in the northern area of Tierra del Fuego which also have slower seismic velocities compared with the Mesozoic sedimentary rocks. However, a considerable number of hypocentres are concentrated at 3 km depth below the Reclus Volcano, which can influence the layer thickness.

Two main factors could be related to a possible explanation of the seismic layer boundary at 6 km depth. First could be the large number of events that concentrate at this depth under the Reclus volcano. On the other hand, an overall sedimentary rock thickness of 5.8 km is described by Ghiglione *et al.* (2019; Figure 4) for the area of Última Esperanza - Río Turbio, close to our reference station TDPA. Several seismic refraction profiles from Ludwig *et al.* (1965) show the interface between the basement and the sedimentary rocks at depths ranging from 4 to 7 km. In comparison, Lawrence and Wiens (2004) sediment thickness results vary from 0.6 up to 4.3 km depth.

The third seismic layer has its top at 6 km depth and its bottom at 20 km. This layer is interpreted as the basement (SPB, RVB, EMC and/or WMC). We interpret that at 20 km depth is the brittle-ductile transition

6.1.2. Moho Depth

Our 1-D velocity structure results show that the Moho seismic discontinuity is located at a depth between 35 to 40 km, more likely at 35 km depth. This depth is slightly larger than the 30.4 km depth for the Moho obtained by Lawrence and Wiens (2004) about 60 kilometres southeast of our reference station. Moreover, Lawrence and Wiens (2004) and Ammirati *et al.* (2020), both studies using receiver functions, report shallower Moho depths ranging 25-30 km to the south. According to the first authors, there is an inverse relationship between the shallowest sediment thicknesses with respect to crustal thickness, which is in line with previous geological studies (e.g. Dalziel and Brown, 1989), which indicate that the Rocas Verdes Basin in western Patagonia was formed by crustal thinning, isostatic compensation and subsequent sedimentation. On the other hand, Ludwig *et al.* (1965), through seismic refraction profiles and Buffoni *et al*. (2019) through receiver functions, report deeper Moho depths analogue to our results (*ca.* 35 km) under the main mountain chain, and shallower Moho depths towards the foreland in Tierra del Fuego. We deduce that the 35 km we obtained for the Moho depth may

correspond to the depth of this under the Austral Andes at the latitude of the Reclus volcano, where most of the recorded seismic events are concentrated. In line with this, the results of Waldhauser *et al.* (1998) under the Alps show a variable Moho topography that responds to a complex tectonic history. For the Alpine instance, they detect dip of the Moho topography as well as abrupt changes in depth. The case of southernmost Patagonia may be similar due to the different collision and extension episodes during its geological history.

6.1.3. Implications of the spatial heterogeneity of the array in the Velocity model and the catalogue

Southwards of the 1P array (*ca.* 52.35° S, pink inverted triangles in Fig.), there is a lack of stations, which provide good azimuthal coverage. Therefore, fewer events were included to produce the velocity model (Figures 11 and 12), so this is less reliable for the area. The lack of an appropriate velocity model for that specific region added to a minor amount of stations, and higher gaps become evident in a general trend of higher RMS values for the located seismic events (Figure 23) in the south-eastern corner of our study area. Those high RMS values could also be related to a different Moho depth which distorts the velocity structure. Additionally, do not have many seismic stations in this area decreases the capacity of detections of smaller events, as is shown in the Magnitude of Completeness map (Figure 20).

6.1.4 Outlook for future studies

This work aimed to be an initial stage for future studies in the region. Our obtained Minimum Velocity Model is robust in the Austral Andes region northwards of the *ca.* 52°S. However, as was mentioned, it lacks reliability southwards. Additionally, the area of analysis is vast to be approximated in a 1-D model. We recommend as next step for seismic location in the region to follow the approach of Husen *et al.* (2011) and to subdivide the region of interest, creating simultaneously different local Minimum 1-D Velocity models. Those can be combined later into a 2-D model, as Lange et al. (2012) and Soto et al. (2018) performed, or into a 3-D model.

6.2. Major outcomes of the seismic catalogue

6.2.1. Seismicity close to the Triple Junction: Antarctic-South America-Scotia

In the Smyth Channel area, seismicity clusters are aligned with the channel (NW-SE) and dip towards the south (Figures 25 and 26). Although in this area, the location errors are bigger than 1000 m in a Z and Y directions (Fig. 21 and ellipsoids in Fig. 25) due to a high azimuthal

gap (Fig. 22), locations are still reliable because they indicate a clear trend. Furthermore, our locations are coherent with the previous data of geological faults and active seismicity (e.g. Cunningham, 1993). Constraining this sequence's focal mechanisms will help to elucidate one of our research questions about the interplay between the three major tectonic plates in the area. The Smyth Channel locates just northwards of the Magellan Strait, which is the main trace of the transform boundary between Scotia and South America, and within the zone of diffuse seismic zone proposed by Pelayo and Wiens (1989). There is a cluster of shallow earthquakes aligned *ca.* N-S, at the southern section of Smyth Channel east of Burney volcano. These two elements together suggest a possible transfer zone from the Magallanes Fault towards the north.

6.2.2. Reclus volcano seismic swarm

One of the biggest surprises during the analysis was the occurrence of a seismic swarm under the Reclus volcano, which was active for several months. This volcano was discovered very recently in 1987 (Harambour, 1988). Therefore, its knowledge is scarce and is not monitored. The closest cities are Puerto Natales (Chile) and El Calafate (Argentina), both located at *ca.* 110 km towards the southeast and northeast of the volcano, respectively. We found the highest concentration of earthquakes between 2 and 6 km in-depth and a lower concentration of hypocentres between 6 to 11 km in-depth (Figs. 31 and 32). However, because the coverage of stations on the volcano is not existent and the two closest stations (TDPA and HANO) are located at ca. 70 km away, these locations cannot be too accurate. Even so, it is important to communicate this phenomenon that may have repercussions for the Patagonian community

6.2.3. Seismicity in the Fold and Thrust Belt

The FTB (section 2.2.3) is very active. In the northern domain, where the deformation zone is restricted to the basement (Ghiglione *et al.*, 2019) and it has a thick-skinned structural style, we obtained a few hypocentres with depths of about 10 km, specifically in the northwestern sector of Lago Argentino (Brazo Upsala). Moving southwards, at the southern shore of Lago Argentino, there are many shallow events (3 to 7 km depth) which could be related to the Lago Argentino transfer fault (Ghiglione *et al.*, 2009; Fig. 5). Our seismicity locations are consistent with the "bending/widening" of the FTB, proposed by the cited authors, which it is assumed to be controlled by those transfer faults, orthogonal to the main Cordillera. A bit southwards, in the Torres del Paine/Última Esperanza region, the extension of the FTB is wider, and have undergone more shortening with respect to the north (Ghiglione *et al.,* 2019). Here, our re-located seismicity is concentrated both in the internal and external domains of the FTB, being the triangle zone (the boundary) an active locus of seismicity. We combined our J-J' cross-section with a seismic profile of Fosdick *et al.* (2011), which was obtained very close to the epicentral area (Fig. 40).

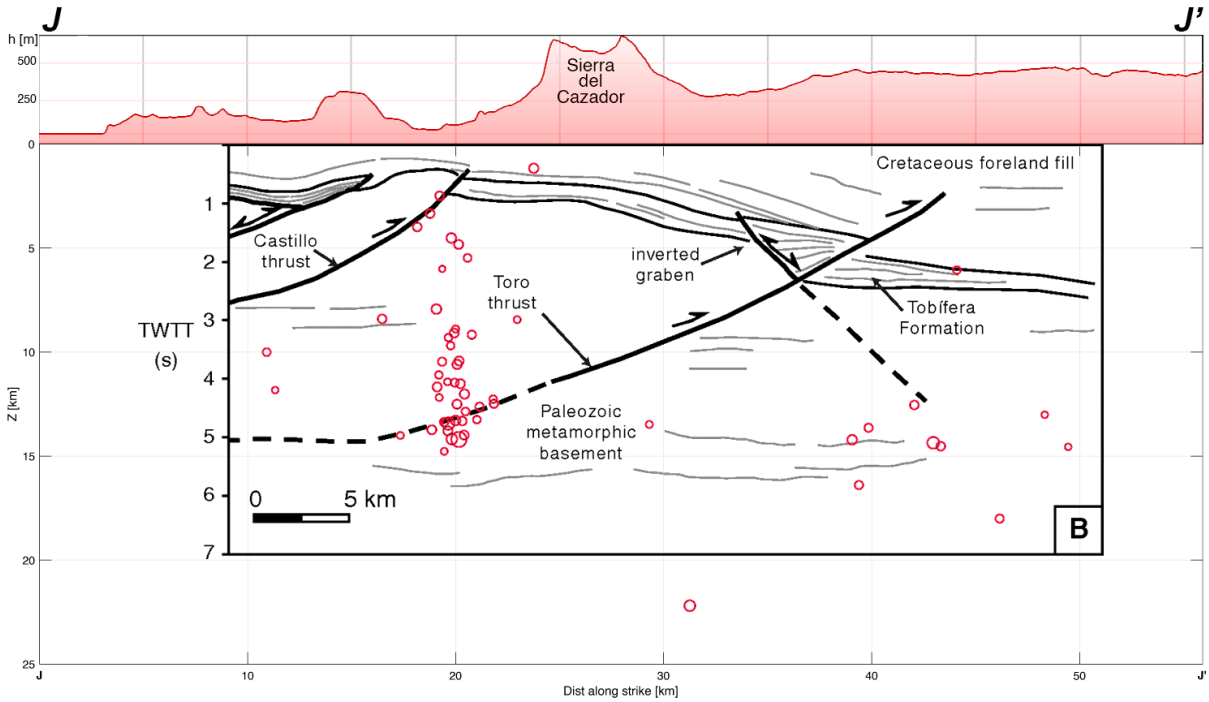

Figure 40. A combination between our final locations in the Última Esperanza seismic cluster and a seismic profile of Fosdick *et al.* (2011) obtained very close to the epicentral area (location in Fig. 33). The coincidence of the profile structures and the distribution of hypocenters is astonishing.

6.2.4. Fjord region

During our analysis time window, an exceptional Mw > 5.0 earthquake occurred in this region. gCMT reports a strike-slip focal mechanism. Due to the improved coverage of our array, many events were detected in the fjord area. To establish the kinematics of the seismic events, clustered in the fjord region, is crucial to reveal the active deformation pattern.

6.2.5. Foreland Tierra del Fuego, within ENAP Network

Our analysis time window has seven months of data from the ENAP Network (EN). During that period, no earthquakes were located inside or close to the network. One possible reason is that the orogenic front has not reached this sector of the foreland yet. However, future seismic events related to the oil/gas extraction cannot be excluded.

6.2.6. Summary

Z-Z' cross-section shows differences between the forearc and retro arc. In the forearc, active faulting is happening in the Smyth Channel represented by an NW-SE trend of the located events, with dip to the southwest. At the arc position, there is a lack of detected seismicity. On the other side of the Cordillera, in the Última Esperanza region, seismic clusters were identified in the Fold and Thrust Belt at the Castillo and Toro thrusts (from Fosdick et al., 2011; Fig. 29). Additionally, it is possible to map latitudinally the distribution of epicentres to the east (Fig. 24), which represents the active orogenic front.

7. Summary and Conclusions

Here we present the first results of seismicity for the Austral Andes region. With this, we began to fill a knowledge gap that existed between the Chilean Triple Junction and the Magallanes-Fagnano Fault System.

Our results show that most of the seismicity is located within specific areas, mostly related to geological structures.

The Fold and Thrust Belt is quite active, and the orogenic front can be visualized by the epicentre alignments.

We found an unexpected cluster of seismicity under the Reclus volcano, which comprises the majority of our events. This has social implications because the volcano is close to two cities and is not monitored.

Our Velocity Model is robust for the area within the Network 1P (temporary array). For the southern section of our study area, where we did not have too many input data (earthquakes), the velocities are not reliable.

8. References

Adaros, R. (2003). Sismicidad y Tectónica del extremo sur de Chile (Unpublished). *MSc Thesis, Facultad de Ciencias Físicas y Matemáticas, Universidad de Chile*.

Amante, C., & Eakins, B. W. (2009). ETOPO1 1 Arc-Minute Global Relief Model: Procedures, Data Sources and Analysis. *NOAA Technical Memorandum NESDIS NGDC-24. National Geophysical Data Center, NOAA.* doi:10.7289/V5C8276M

Ammirati, J.-B., Flores, M. C., & Ruiz, S. (2020). Seismicity along the Magallanes-Fagnano fault system. *Journal of South American Earth Sciences*, 102799. doi:https://doi.org/10.1016/j.jsames.2020.102799

Becker, J. J., Sandwell, D. T., Smith, W. H., Braud, J., Binder, B., Depner, J., *et al*. (2009). Global Bathymetry and Elevation Data at 30 Arc Seconds Resolution: SRTM30_{P}{L}{U}S. *Marine Geodesy, 32*, 355-371. doi:10.1080/01490410903297766

Brill, K. A., Waite, G. P., & Chigna, G. (2018). Foundations for Forecasting: Defining Baseline Seismicity at Fuego Volcano, Guatemala. *Frontiers in Earth Science, 6*, 87. doi:10.3389/feart.2018.00087

Buffoni, C., Schimmel, M., Sabbione, N. C., Rosa, M. L., & Connon, G. (2019). Crustal structure beneath Tierra del Fuego, Argentina, inferred from seismic P-wave receiver functions and ambient noise autocorrelations. *Tectonophysics, 751*, 41-53. doi:https://doi.org/10.1016/j.tecto.2018.12.013

Calderón, M., Hervé, F., Fuentes, F., Fosdick, J. C., Sepúlveda, F., & Galaz, G. (2016). Tectonic Evolution of Paleozoic and Mesozoic Andean Metamorphic Complexes and the Rocas Verdes Ophiolites in Southern Patagonia. En M. C. Ghiglione (Ed.), *Geodynamic Evolution of the Southernmost Andes: Connections with the Scotia Arc* (págs. 7–36). Cham: Springer International Publishing. doi:10.1007/978-3-319-39727-6_2

Cande, S. C., & Leslie, R. B. (1986). Late Cenozoic tectonics of the Southern Chile Trench. *Journal of Geophysical Research: Solid Earth, 91*, 471-496. doi:10.1029/JB091iB01p00471

Castano, J. C. (1977). *Zonificación sísmica de la República Argentina.* Instituto Nacional de Prevención Sísmica.

Cisternas, A., & Vera, E. (2008). Sismos Históricos y recientes en Magallanes. *Magallania (Punta Arenas), 36*, 43-51. Retrieved from https://scielo.conicyt.cl/scielo.php?script=sci_arttext&pid=S0718-22442008000100004&nrm=iso

Comte, D., Farias, M., Roecker, S., & Russo, R. (2019). The nature of the subduction wedge in an erosive margin: Insights from the analysis of aftershocks of the 2015 Mw 8.3 Illapel earthquake beneath the Chilean Coastal Range. *Earth and Planetary Science Letters, 520*, 50-62. doi:https://doi.org/10.1016/j.epsl.2019.05.033

Cunningham, W. D. (1993). Strike-slip faults in the southernmost andes and the development of the Patagonian orocline. *Tectonics, 12*, 169-186. doi:10.1029/92TC01790

Dalziel, I. W., & Brown, R. L. (8 de 1989). Tectonic denudation of the Darwin metamorphic core complex in the Andes of Tierra del Fuego, southernmost Chile: Implications for Cordilleran orogenesis. *Geology, 17*, 699-703. doi:10.1130/0091-7613(1989)017<0699:TDOTDM>2.3.CO;2

DeMets, C., Gordon, R. G., & Argus, D. F. (2010). Geologically current plate motions. *Geophysical Journal International, 181*, 1-80. doi:10.1111/j.1365-246X.2009.04491.x

Diehl, T., & Kissling, E. (2007). Users guide for consistent phase picking at local to regional scales. *Institute of Geophysics, ETH Zurich, Switzerland*.

Diehl, T., Singer, J., Hetényi, G., Grujic, D., Clinton, J., Giardini, D., & Kissling, E. (2017). Seismotectonics of Bhutan: Evidence for segmentation of the Eastern Himalayas and link to foreland deformation. *Earth and Planetary Science Letters, 471*, 54-64. doi:https://doi.org/10.1016/j.epsl.2017.04.038

Dziewonski, A. M., Chou, T.-A., & Woodhouse, J. H. (1981). Determination of earthquake source parameters from waveform data for studies of global and regional seismicity. *Journal of Geophysical Research: Solid Earth, 86*, 2825-2852. doi:10.1029/JB086iB04p02825

Ekström, G., Nettles, M., & Dziewoński, A. M. (2012). The global CMT project 2004–2010: Centroid-moment tensors for 13,017 earthquakes. *Physics of the Earth and Planetary Interiors, 200-201*, 1-9. doi:https://doi.org/10.1016/j.pepi.2012.04.002

Febrer, J. M., Plasencia, M. P., & Sabbione, N. C. (2000). Local and regional seismicity from Ushuaia broadband station observations (Tierra del Fuego). *Terra Antartica, 8*, 35–40.

Forsyth, D. W. (1975). Fault plane solutions and tectonics of the South Atlantic and Scotia Sea. *Journal of Geophysical Research (1896-1977), 80*, 1429-1443. doi:10.1029/JB080i011p01429

Forsythe, R., & Mpodozis, C. (1983). *Geología del basamento pre-Jurásico Superior en el archipiélago Madre de Dios, Magallanes, Chile.* Servico Nacional de Geología y Minería.

Fosdick, J. C., Grove, M., Hourigan, J. K., & Calderón, M. (2013). Retroarc deformation and exhumation near the end of the Andes, southern Patagonia. *Earth and Planetary Science Letters, 361*, 504-517. doi:https://doi.org/10.1016/j.epsl.2012.12.007

Fosdick, J. C., Romans, B. W., Fildani, A., Bernhardt, A., Calderón, M., & Graham, S. A. (9 de 2011). Kinematic evolution of the Patagonian retroarc fold-and-thrust belt and Magallanes foreland basin, Chile and Argentina, 51°30′S. *GSA Bulletin, 123*, 1679-1698. doi:10.1130/B30242.1

Fuenzalida, R. (1976). The Magellan fault zone. *Symposium on Andean and Antarctic Volcanology Problems. Int Association of Volcanology and Chemistry of the Earth's Interior, Napoli, Italy*, (págs. 373–391).

Ghiglione, M. C., Ramos, V. A., Cuitiño, J., & Barberón, V. (2016). Growth of the Southern Patagonian Andes (46–53\textdegreeS) and Their Relation to Subduction Processes. En A. Folguera, M. Naipauer, L. Sagripanti, M. C. Ghiglione, D. L. Orts, & L. Giambiagi (Edits.), *Growth of the Southern Andes* (págs. 201–240). Cham: Springer International Publishing. doi:10.1007/978-3-319-23060-3_10

Ghiglione, M. C., Ronda, G., Suárez, R. J., Aramendía, I., Barberón, V., Ramos, M. E., *et al*. (2019). Chapter 24 - Structure and tectonic evolution of the South Patagonian fold and thrust belt: Coupling between subduction dynamics, climate and tectonic deformation. En B. K. Horton, & A. Folguera (Edits.), *Andean Tectonics* (págs. 675-697). Elsevier. doi:https://doi.org/10.1016/B978-0-12-816009-1.00024-1

Ghiglione, M. C., Suarez, F., Ambrosio, A., Da Poian, G., Cristallini, E. O., Pizzio, M. F., & Reinoso, R. M. (2009). Structure and evolution of the Austral Basin fold-thrust belt, southern Patagonian Andes. *Revista de la Asociación Geológica Argentina, 65*, 215–226.

Harambour, S. M. (1988). Sobre el hallazgo del mítico Volcán Reclus, ex Mano del Diablo, Hielo Patagónico Sur, Magallanes, Chile. *Revista Geológica de Chile, 15*, 173-179. doi:http://dx.doi.org/10.5027/andgeoV15n2-a06

Hartman, L. H., Kurbatov, A. V., Winski, D. A., Cruz-Uribe, A. M., Davies, S. M., Dunbar, N. W., . . . Yates, M. G. (2019). Volcanic glass properties from 1459 C.E. volcanic event in South Pole ice core dismiss Kuwae caldera as a potential source. *Scientific Reports, 9*, 14437. doi:10.1038/s41598-019-50939-x

Hervé, F., Calderón, M., & Faúndez, V. (2008). The metamorphic complexes of the Patagonian and Fuegian Andes. *Geologica Acta, 6*, 43–53.

Hervé, F., Faundez, V., Calderón, M., Massonne, H.-J., & Willner, A. P. (1 de 2007). Metamorphic and plutonic basement complexes. In *The Geology of Chile.* Geological Society of London. doi:10.1144/GOCH.2

Husen, S., Kissling, E., & Clinton, J. F. (2011). Local and regional minimum 1D models for earthquake location and data quality assessment in complex tectonic regions: Application to Switzerland. *Swiss Journal of Geosciences, 104*, 455–469. doi:10.1007/s00015-011-0071-3

Husen, S., Kissling, E., Flueh, E., & Asch, G. (1999). Accurate hypocentre determination in the seismogenic zone of the subducting Nazca Plate in northern Chile using a combined on-/offshore network. *Geophysical Journal International, 138*, 687-701. doi:10.1046/j.1365-246x.1999.00893.x

Kilian, R. (1990). The Austral Andean Volcanic Zone (South Patagonia). *Intemational Symposium on Andean Geology (ISAG)*, *1*, págs. 301-304.

Kissling, E. (1988). Geotomography with local earthquake data. *Reviews of Geophysics, 26*, 659-698. doi:10.1029/RG026i004p00659

Kissling, E., Ellsworth, W. L., Eberhart-Phillips, D., & Kradolfer, U. (10 de 1994). Initial reference models in local earthquake tomography. *Journal of Geophysical Research: Solid Earth, 99*, 19635-19646. doi:10.1029/93JB03138

Kissling, E., Kradolfer, U., & Maurer, H. (1995). Program VELEST user's guide - Short Introduction. *Institute of Geophysics, ETH Zurich*.

Klepeis, K. A. (1994). The Magallanes and Deseado fault zones: Major segments of the South American-Scotia transform plate boundary in southernmost South America, Tierra del Fuego. *Journal of Geophysical Research: Solid Earth, 99*, 22001-22014. doi:10.1029/94JB01749

Kraemer, P. E., Ploszkiewicz, J. V., & Ramos, V. A. (2002). Estructura de la Cordillera Patagónica Austral entre los 46 y 52 S. En *Geología y Recursos Naturales de Santa Cruz* (Vol. 1, págs. 353–364). Relatorio del 15° Congreso Geológico Argentino. El Calafate Buenos Aires.

Lagabrielle, Y., Goddéris, Y., Donnadieu, Y., Malavieille, J., & Suarez, M. (2009). The tectonic history of Drake Passage and its possible impacts on global climate. *Earth and Planetary Science Letters, 279*, 197-211. doi:https://doi.org/10.1016/j.epsl.2008.12.037

Lange, D., Rietbrock, A., Haberland, C., Bataille, K., Dahm, T., Tilmann, F., & Flüh, E. R. (2007). Seismicity and geometry of the south Chilean subduction zone (41.5°S–43.5°S): Implications for controlling parameters. *Geophysical Research Letters, 34*. doi:10.1029/2006GL029190

Lange, D., Tilmann, F., Barrientos, S. E., Contreras-Reyes, E., Methe, P., Moreno, M., Beck, S. (2012). Aftershock seismicity of the 27 February 2010 Mw 8.8 Maule earthquake rupture zone. *Earth and Planetary Science Letters, 317-318*, 413-425. doi:https://doi.org/10.1016/j.epsl.2011.11.034

Lanza, F., Chamberlain, C. J., Jacobs, K., Warren-Smith, E., Godfrey, H. J., Kortink, M., Eberhart-Phillips, D. (2019). Crustal Fault Connectivity of the Mw 7.8 2016 Kaikōura Earthquake Constrained by Aftershock Relocations. *Geophysical Research Letters, 46*, 6487-6496. doi:10.1029/2019GL082780

Lawrence, J. F., & Wiens, D. A. (2004). Combined Receiver-Function and Surface Wave Phase-Velocity Inversion Using a Niching Genetic Algorithm: Application to Patagonia. *Bulletin of the Seismological Society of America, 94*, 977-987. doi:10.1785/0120030172

Likerman, J., Burlando, J. F., Cristallini, E. O., & Ghiglione, M. C. (2013). Along-strike structural variations in the Southern Patagonian Andes: Insights from physical modeling. *Tectonophysics, 590*, 106-120. doi:https://doi.org/10.1016/j.tecto.2013.01.018

Lira, M. P. (2016). Deformación Frágil del Sector Nororiental de la Isla Diego de Almagro, Archipiélagos Patagónicos, Región de Magallanes, Chile.(Unpublished). *Geologist (Diploma) Thesis, Departamento de Ciencias de la Tierra, Facultad de Ciencias Químicas, Universidad de Concepción*.

Lodolo, E., Menichetti, M., Bartole, R., Ben-Avraham, Z., Tassone, A., & Lippai, H. (2003). Magallanes-Fagnano continental transform fault (Tierra del Fuego, southernmost South America). *Tectonics, 22*. doi:10.1029/2003TC001500

Lomax, A., & Curtis, A. (2001). Fast probabilistic earthquake location in 3D models using Oct-Tree importance sampling. *Geophys. Res. Abstr., 3*.

Lomax, A., Michelini, A., & Curtis, A. (2014). Earthquake Location, Direct, Global-Search Methods. In R. A. Meyers (Ed.), *Encyclopedia of Complexity and Systems Science* (págs. 1–33). New, York, NY: Springer New York. doi:10.1007/978-3-642-27737-5_150-2

Lomax, A., Virieux, J., Volant, P., & Berge-Thierry, C. (2000). Probabilistic Earthquake Location in 3D and Layered Models. En C. H. Thurber, & N. Rabinowitz (Edits.), *Advances in Seismic Event Location* (págs. 101–134). Dordrecht: Springer Netherlands. doi:10.1007/978-94-015-9536-0_5

Lomnitz, C. (1970). Major earthquakes and tsunamis in Chile during the period 1535 to 1955. *Geologische Rundschau, 59*, 938–960. doi:10.1007/BF02042278

Ludwig, W. J., Ewing, J. I., & Ewing, M. (1965). Seismic-refraction measurements in the Magellan Straits. *Journal of Geophysical Research (1896-1977), 70*, 1855-1876. doi:10.1029/JZ070i008p01855

Martinic, M. (1988). Actividad volcánica histórica en la Región de Magallanes. *Revista Geológica de Chile, 15*, 181–186. doi:http://dx.doi.org/10.5027/andgeoV15n2-a07

Martinic, M. (1988). El gran temblor de tierra de 1879 en la Patagonia Austral. *Revista Patagónica*.

Mendoza, L., Richter, A., Fritsche, M., Hormaechea, J. L., Perdomo, R., & Dietrich, R. (2015). Block modeling of crustal deformation in Tierra del Fuego from GNSS velocities. *Tectonophysics, 651-652*, 58-65. doi:https://doi.org/10.1016/j.tecto.2015.03.013

Monteath, A. J., Hughes, P. D., & Wastegård, S. (2019). Evidence for distal transport of reworked Andean tephra: Extending the cryptotephra framework from the Austral volcanic zone. *Quaternary Geochronology, 51*, 64-71. doi:https://doi.org/10.1016/j.quageo.2019.01.003

Piret, L., Bertrand, S., Kissel, C., Pol-Holz, R. D., Hernando, A. T., & Daele, M. V. (2018). First evidence of a mid-Holocene earthquake-triggered megaturbidite south of the Chile Triple Junction. *Sedimentary Geology, 375*, 120-133. doi:https://doi.org/10.1016/j.sedgeo.2018.01.002

Pisarenko, V. F., Kushnir, A. F., & Savin, I. V. (1987). Statistical adaptive algorithms for estimation of onset moments of seismic phases. *Physics of the Earth and Planetary Interiors, 47*, 4-10. doi:https://doi.org/10.1016/0031-9201(87)90062-8

Podvin, P., & Lecomte, I. (1991). Finite difference computation of traveltimes in very contrasted velocity models: a massively parallel approach and its associated tools. *Geophysical Journal International, 105*, 271-284. doi:10.1111/j.1365-246X.1991.tb03461.x

Polonia, A., Torelli, L., Brancolini, G., & Loreto, M.-F. (2007). Tectonic accretion versus erosion along the southern Chile trench: Oblique subduction and margin segmentation. *Tectonics, 26*. doi:10.1029/2006TC001983

Rawles, C., & Thurber, C. (2015). A non-parametric method for automatic determination of P-wave and S-wave arrival times: application to local micro earthquakes. *Geophysical Journal International, 202*, 1164-1179. doi:10.1093/gji/ggv218

Reyes, C., & Wiemer, S. (2020). From ZMAP to ZMAP7: Fast-forwarding 25 years of software evolution. *EGU General Assembly Conference Abstracts*, (pág. 18878).

Roecker, S., Thurber, C., Roberts, K., & Powell, L. (2006). Refining the image of the San Andreas Fault near Parkfield, California using a finite difference travel time computation technique. *Tectonophysics, 426*, 189-205. doi:https://doi.org/10.1016/j.tecto.2006.02.026

Roy, S., Vassallo, R., Martinod, J., Ghiglione, M. C., Sue, C., & Allemand, P. (2019). Co-seismic deformation and post-glacial slip rate along the Magallanes-Fagnano fault, Tierra Del Fuego, Argentina. *Terra Nova, 32*, 1-10. doi:10.1111/ter.12430

SERNAGEOMIN. (2003). Mapa Geológico de Chile: versión digital. *Servicio Nacional de Geología y Minería, Publicación Geológica Digital, No. 4 (CD-Room, versión 1.0)*.

Sielfeld, G., Lange, D., & Cembrano, J. (2019). Intra-Arc Crustal Seismicity: Seismotectonic Implications for the Southern Andes Volcanic Zone, Chile. *Tectonics, 38*, 552-578. doi:10.1029/2018TC004985

Singer, J., Kissling, E., Diehl, T., & Hetényi, G. (2017). The underthrusting Indian crust and its role in collision dynamics of the Eastern Himalaya in Bhutan: Insights from receiver function imaging. *Journal of Geophysical Research: Solid Earth, 122*, 1152-1178. doi:10.1002/2016JB013337

Soto, H., Sippl, C., Schurr, B., Kummerow, J., Asch, G., Tilmann, F., Oncken, O. (2019). Probing the Northern Chile Megathrust With Seismicity: The 2014 M8.1 Iquique Earthquake Sequence. *Journal of Geophysical Research: Solid Earth, 124*, 12935-12954. doi:10.1029/2019JB017794

Stern, C. R. (2008). Holocene tephrochronology record of large explosive eruptions in the southernmost Patagonian Andes. *Bulletin of Volcanology, 70*, 435–454. doi:https://doi.org/10.1007/s00445-007-0148-z

Stern, C. R., & Kilian, R. (1996). Role of the subducted slab, mantle wedge and continental crust in the generation of adakites from the Andean Austral Volcanic Zone. *Contributions to Mineralogy and Petrology, 123*, 263–281. doi:https://doi.org/10.1007/s004100050155

Thomson, S. N., Brandon, M. T., Tomkin, J. H., Reiners, P. W., Vásquez, C., & Wilson, N. J. (2010). Glaciation as a destructive and constructive control on mountain building. *Nature, 467*, 313–317. doi:10.1038/nature09365

Thurber, C. H., Lanza, F., & Roecker, S. W. (2017). Application of a Hybrid Detection and Location Scheme to Volcanic Systems. *AGU Fall Meeting Abstracts*, *2017*, págs. S13B-0645.

Universidad De Chile. (2013). Red Sismologica Nacional. *Red Sismologica Nacional*. International Federation of Digital Seismograph Networks. doi:10.7914/SN/C1

Waldhauser, F., Kissling, E., Ansorge, J., & Mueller, S. (1998). Three-dimensional interface modelling with two-dimensional seismic data: the Alpine crust–mantle boundary. *Geophysical Journal International, 135*, 264-278. doi:10.1046/j.1365-246X.1998.00647.x

Wiemer, S. (2001). A Software Package to Analyze Seismicity: ZMAP. *Seismological Research Letters, 72*, 373-382. doi:10.1785/gssrl.72.3.373

Wiemer, S., & Wyss, M. (2002). Mapping spatial variability of the frequency-magnitude distribution of earthquakes. En R. Dmowska, & B. Saltzman (Edits.). Elsevier. doi:https://doi.org/10.1016/S0065-2687(02)80007-3

Wiens, D. A., & Magnani, M. B. (2018). Solid Earth response of the Patagonia Andes to post-Little Ice Age glacial retreat. *Solid Earth response of the Patagonia Andes to post-Little Ice Age glacial retreat*. International Federation of Digital Seismograph Networks. doi:10.7914/SN/1P_2018

Willner, A. P., Hervé, F., Thomson, S. N., & Massonne, H.-J. (2004). Converging PT paths of Mesozoic HP-LT metamorphic units (Diego de Almagro Island, Southern Chile): evidence for juxtaposition during late shortening of an active continental margin. *Mineralogy and Petrology, 81*, 43–84. doi:10.1007/s00710-004-0033-9

Willner, A. P., Sepúlveda, F. A., Hervé, F., Massonne, H.-J., & Sudo, M. (2009). Conditions and Timing of Pumpellyite–Actinolite-facies Metamorphism in the Early Mesozoic Frontal Accretionary Prism of the Madre de Dios Archipelago (Latitude 50°20′S; Southern Chile). *Journal of Petrology, 50*, 2127-2155. doi:10.1093/petrology/egp071

Appendix 1: Supplementary tables and figures

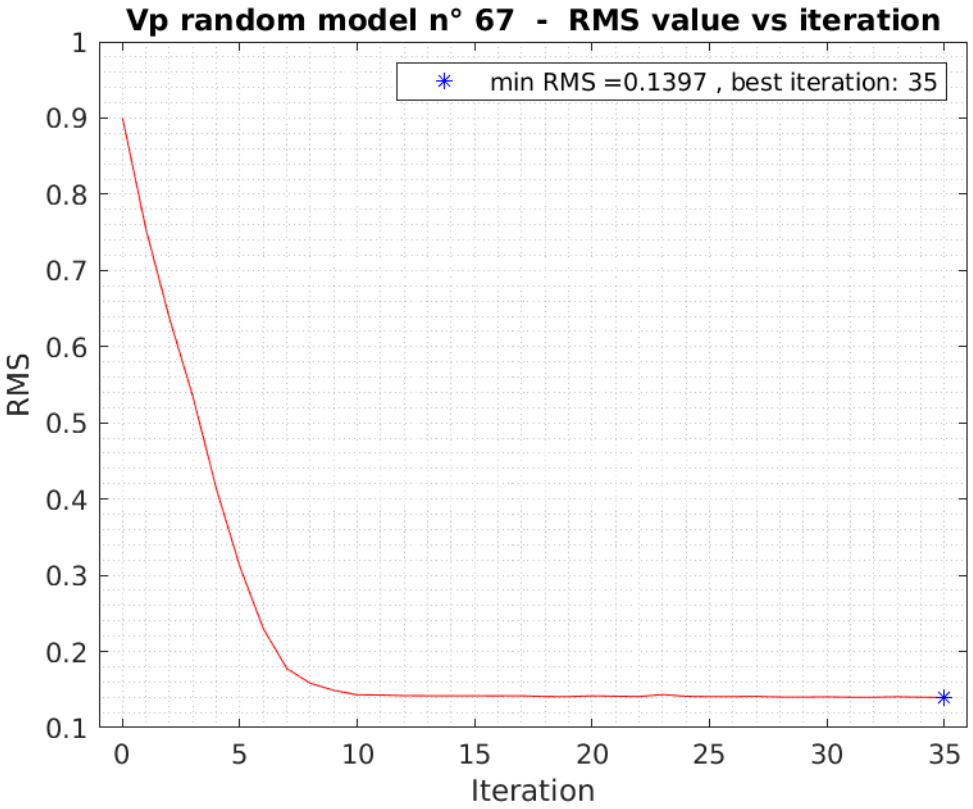

Supplementary Figure 1. The graph shows how a decrease in the RMS value as the VELEST software progresses in iterations. This case consists of the best obtained result (e.g. lowest RMS) in the *Vp* searching.

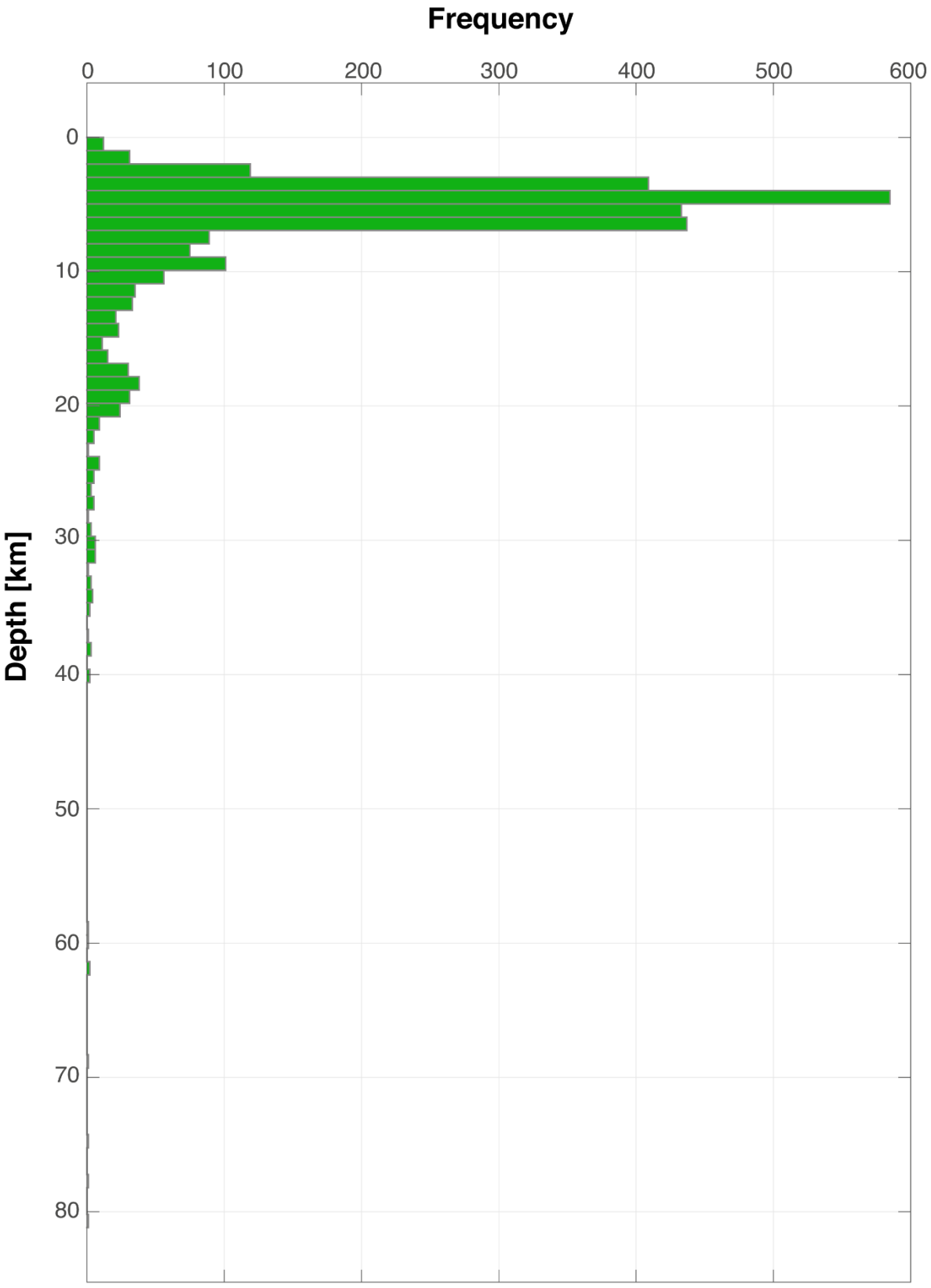

Supplementary Figure 2. In-depth distribution of the detected and localized seismicity.

Supplementary Table 1. Seismic Stations used in this study with the obtained corrections for *P* and *S* wave arrivals

Network	Station	Latitude [°]	Longitude [°]	Altitude [m]	P correction [s]	P readings	S correction [s]	S readings
1P	BONA	-50.2894	-72.0275	252	0.46	319	0.34	6
1P	BRMY	-52.1425	-73.1532	53	-0.58	257	-2.13	3
1P	CURI	-51.6131	-74.5560	51	-0.73	397	-1.71	45
1P	EHEL	-49.6686	-72.8857	299	-0.56	213	-1.67	4
1P	ELCH	-49.3389	-72.8834	428	-0.94	2	0.00	0
1P	ES3R	-50.7735	-72.4260	723	-0.14	351	0.00	0
1P	ESCR	-49.9588	-73.1319	215	-0.20	287	-1.15	3
1P	GRAF	-49.7702	-74.9223	62	-1.52	343	-3.31	75
1P	GUMN	-50.3199	-75.3644	52	-1.37	381	-2.60	34
1P	HANO	-50.9341	-74.3930	78	-0.44	420	-1.43	81
1P	LEST	-49.7877	-72.0906	299	-0.73	23	-1.40	1
1P	LPRF	-50.2791	-70.8098	490	-0.19	11	0.00	0
1P	LVAN	-51.0252	-71.1152	263	0.84	30	-0.10	2
1P	MAMA	-52.0337	-72.3827	184	-0.17	76	-0.44	10
1P	PMOR	-50.4904	-73.0428	222	-0.27	364	0.00	0
1P	PTTY	-50.4237	-74.2730	33	-0.83	413	-2.08	85
1P	RPTE	-52.1152	-71.3773	262	0.11	32	0.00	0
1P	TAPA	-51.0488	-71.7863	327	0.65	51	0.00	0
1P	TDPA	-51.1322	-73.1184	85	0.00	359	-1.23	9
C1	MG01	-54.9322	-67.6300	57	-1.86	1	0.00	0
C1	MG02	-52.7808	-69.2242	82	-1.13	8	0.00	0
C1	MG03	-53.8480	-70.4628	83	-2.85	5	0.00	0
C1	MG04	-52.8572	-71.5700	82	-1.30	6	-2.40	1
C1	MG05	-51.6784	-72.5032	99	-0.12	329	-1.20	6
EN	ANMA	-53.0461	-70.3836	49	-1.37	2	0.00	0
EN	BQON	-53.4487	-70.2434	450	0.00	0	0.00	0
EN	DGER	-52.7158	-69.5790	28	0.00	0	0.00	0
EN	LAVG	-52.3567	-70.4908	170	-0.32	1	-0.55	1
EN	LOSC	-53.3500	-69.4537	15	-1.92	1	0.00	0
EN	MJTA	-53.1199	-69.3939	257	-1.55	2	0.00	0
EN	RGND	-52.8517	-69.8704	27	-0.48	2	0.00	0
EN	TROP	-52.5481	-70.2857	330	-2.15	0	0.00	0

Appendix 2: Austral Andes Seismic Catalogue

ORIGIN TIME (UTC)						Latitude	Longitude	Depth	M_L	GAP	RMS	X error	Y error	Z error
yyyy	mm	dd	h	m	seconds	[°]	[°]	[Km]		[°]		[m]	[m]	[m]
2018	12	1	6	55	59.379	-50.66050	-73.39521	2.61	3.3	89	0.317	440.7	495.8	599.4
2018	12	2	5	51	27.057	-51.01028	-74.38591	27.62	3.6	127	0.574	710.6	425.3	551.9
2018	12	5	7	56	37.297	-50.27231	-72.51106	3.98	3.3	61	0.590	430.2	512.0	1042.0
2018	12	9	22	40	7.660	-50.90229	-73.23423	3.00	3.1	78	0.323	548.2	495.2	714.6
2018	12	12	0	31	2.263	-50.62274	-74.40415	19.58	5.2	110	0.390	374.6	252.3	415.8
2018	12	12	0	34	33.094	-50.62889	-74.41181	17.77	4.3	111	0.382	383.9	270.0	448.1
2018	12	12	0	42	2.958	-50.62905	-74.39831	19.61	2.5	110	0.172	550.6	267.0	774.5
2018	12	12	0	46	26.363	-50.62425	-74.40637	19.28	2.7	110	0.468	367.2	254.2	492.7
2018	12	12	0	51	29.610	-50.62402	-74.42566	18.68	3.1	111	0.364	365.9	258.2	475.4
2018	12	12	1	6	55.291	-50.62854	-74.44075	18.00	2.6	113	0.417	843.9	520.6	1092.6
2018	12	12	1	28	42.298	-50.57406	-74.28923	4.01	2.6	152	0.591	844.5	346.8	986.4
2018	12	12	1	41	22.734	-50.63143	-74.42202	18.01	2.7	112	0.319	543.4	259.5	525.2
2018	12	12	1	58	13.917	-50.62764	-74.43059	17.55	2.8	112	0.378	528.0	277.8	517.2
2018	12	12	4	2	57.080	-50.62837	-74.36983	20.46	2.7	108	0.425	684.5	333.8	1219.8
2018	12	12	4	7	40.987	-50.62924	-74.39976	18.42	2.8	110	0.432	470.5	261.4	488.4
2018	12	12	7	15	59.965	-50.63442	-74.37676	19.99	2.5	109	0.147	974.6	286.9	993.2
2018	12	12	10	10	7.492	-50.62947	-74.43113	16.32	3.1	112	0.522	456.8	264.3	561.5
2018	12	12	11	48	9.473	-50.62922	-74.40169	18.81	3.3	110	0.282	387.3	256.4	456.2
2018	12	12	19	11	36.630	-52.00943	-73.89760	11.00	3.2	207	0.474	549.4	742.4	717.2
2018	12	12	23	46	52.336	-50.62817	-74.42096	17.19	3.0	111	0.317	476.1	271.1	503.7
2018	12	13	0	5	43.035	-50.63078	-74.40753	18.27	2.8	111	0.359	379.1	256.9	480.5
2018	12	13	2	6	35.222	-50.62952	-74.41038	18.42	2.7	111	0.318	395.1	256.7	466.5
2018	12	13	8	1	35.524	-50.63316	-74.41435	17.82	2.9	111	0.274	399.2	319.6	546.4
2018	12	13	8	42	58.049	-50.63151	-74.41527	17.78	2.5	111	0.320	369.6	270.2	483.2
2018	12	13	15	9	52.169	-50.62932	-74.39301	19.71	2.7	110	0.172	678.8	276.4	886.9
2018	12	13	23	25	3.831	-50.63081	-74.37086	23.89	2.4	109	0.500	483.0	317.6	801.7
2018	12	14	13	28	33.827	-50.63051	-74.39594	19.36	4.2	110	0.328	376.7	240.9	433.2
2018	12	14	13	35	1.947	-50.63179	-74.40056	19.12	3.6	110	0.461	371.2	256.5	418.8
2018	12	14	16	54	8.023	-50.63309	-74.42014	17.74	2.9	112	0.357	565.6	257.7	527.9
2018	12	15	10	31	47.775	-52.28710	-73.78816	1.98	3.6	195	0.472	589.3	1247.3	467.1
2018	12	15	20	46	41.003	-50.62904	-74.41616	17.06	3.1	111	0.327	379.6	251.5	518.3
2018	12	15	21	25	27.075	-50.63362	-74.40954	18.01	3.0	111	0.386	384.1	254.6	471.3
2018	12	15	22	51	14.634	-50.62820	-74.41806	17.10	3.3	111	0.378	348.7	248.0	561.0
2018	12	16	5	39	14.233	-50.62382	-74.42517	19.45	2.5	111	0.148	423.9	265.5	693.9
2018	12	16	20	50	20.703	-51.83681	-74.38391	15.00	3.6	202	0.565	837.3	758.7	1486.1
2018	12	17	4	7	19.176	-51.04028	-73.27045	3.29	3.2	129	0.694	731.5	622.8	675.1
2018	12	17	22	31	4.694	-51.08562	-72.80065	2.34	2.7	154	0.274	804.0	665.5	1599.4
2018	12	18	14	45	3.881	-50.63400	-74.41245	18.11	3.1	111	0.334	504.2	262.2	527.4
2018	12	19	9	32	13.881	-50.63328	-74.40374	19.44	2.5	111	0.184	477.5	282.6	687.5
2018	12	19	13	38	27.601	-50.62449	-74.42085	18.01	3.0	111	0.350	331.1	247.3	465.6
2018	12	19	13	40	29.143	-50.62391	-74.40057	19.83	2.5	110	0.132	935.4	335.9	1152.7
2018	12	19	14	30	31.776	-50.62888	-74.42966	18.39	2.9	112	0.396	373.2	251.5	457.2
2018	12	20	13	8	46.560	-50.62488	-74.38806	20.01	2.1	160	0.190	1125.5	293.2	1227.2
2018	12	21	4	36	28.535	-50.63129	-74.39982	19.13	2.7	110	0.137	584.0	277.2	740.6
2018	12	21	18	50	54.678	-52.31840	-73.78621	5.58	3.4	224	0.844	685.0	1266.8	1151.1
2018	12	23	3	38	11.238	-49.55286	-73.64987	2.99	3.1	172	0.505	408.7	668.2	725.4
2018	12	23	11	31	53.505	-52.76782	-73.76141	3.27	3.7	216	0.524	582.4	909.1	834.6

ORIGIN TIME (UTC)						Latitude	Longitude	Depth	M_L	GAP	RMS	X error	Y error	Z error
yyyy	mm	dd	h	m	seconds	[°]	[°]	[Km]		[°]		[m]	[m]	[m]
2018	12	23	23	27	16.294	-51.09763	-74.00457	12.21	3.1	89	0.228	440.0	370.4	843.1
2018	12	25	8	45	2.249	-52.78477	-74.39356	3.00	3.1	252	0.694	850.0	1129.7	1074.9
2018	12	27	13	33	31.311	-50.38778	-71.89701	12.68	3.3	93	0.532	446.2	430.3	556.5
2018	12	27	19	19	16.711	-52.94377	-72.53734	5.91	3.6	189	0.844	790.5	725.7	811.1
2018	12	28	0	45	29.800	-53.19255	-72.71953	60.19	3.7	206	0.744	1188.1	1226.7	3002.5
2018	12	29	19	19	36.916	-50.63366	-74.42353	17.30	2.7	112	0.359	496.6	278.7	562.4
2018	12	30	11	5	57.921	-50.44464	-74.37317	15.75	3.4	95	0.331	327.3	332.0	396.9
2018	12	31	14	5	37.432	-51.23007	-72.25520	22.17	3.7	56	0.796	458.4	340.9	792.2
2019	1	1	12	35	26.599	-50.27936	-72.19640	2.99	2.8	101	0.487	416.5	618.5	618.9
2019	1	1	13	22	11.213	-50.29571	-72.19420	2.49	2.9	110	0.711	500.2	558.4	765.3
2019	1	1	13	43	58.939	-50.27681	-72.18207	11.12	3.2	99	0.429	643.4	495.1	845.4
2019	1	1	18	53	48.738	-50.63357	-74.41437	17.49	3.1	111	0.432	379.9	260.8	471.0
2019	1	2	4	56	20.664	-50.63268	-74.42013	17.17	3.1	112	0.479	464.9	308.1	513.0
2019	1	2	5	52	13.336	-50.63772	-74.40870	14.75	3.1	111	0.652	362.5	311.4	638.1
2019	1	2	8	10	19.730	-50.62948	-74.41424	17.23	2.8	111	0.383	424.4	267.9	534.6
2019	1	4	1	38	15.877	-51.60211	-74.22897	18.04	3.3	130	0.459	607.3	432.4	885.2
2019	1	5	11	17	57.778	-50.82495	-74.16243	10.73	2.9	75	0.268	598.9	301.4	1058.6
2019	1	7	9	32	33.454	-50.63147	-74.41816	17.10	2.8	111	0.388	495.6	457.4	708.7
2019	1	9	11	39	44.110	-50.32796	-72.38347	0.55	2.6	71	0.397	576.1	437.0	492.0
2019	1	11	4	49	59.393	-50.99156	-72.81661	2.89	3.0	212	0.414	1421.7	1054.9	718.1
2019	1	11	19	18	47.482	-51.34995	-72.73827	1.74	3.3	109	0.580	457.2	338.8	380.9
2019	1	18	12	46	12.405	-52.60615	-73.78077	10.87	3.6	210	0.769	519.3	589.8	787.8
2019	1	18	18	2	47.057	-51.10955	-72.10313	14.36	4.0	51	0.386	362.6	302.5	531.0
2019	1	19	2	25	20.383	-50.63584	-74.36040	22.10	2.5	117	0.127	883.8	293.5	1016.4
2019	1	19	21	17	53.851	-50.34754	-72.33575	8.08	2.7	110	0.341	632.4	478.7	1654.4
2019	1	19	23	20	42.069	-50.62866	-74.41422	17.84	2.8	111	0.317	407.7	276.8	502.5
2019	1	20	0	41	45.218	-50.32487	-74.58924	40.67	2.9	134	0.354	846.2	517.5	1014.9
2019	1	22	12	52	25.202	-51.11793	-72.15708	14.22	3.4	180	0.199	1350.2	537.7	902.1
2019	1	23	3	46	47.711	-50.62336	-74.41213	18.83	3.0	111	0.466	403.9	266.3	471.5
2019	1	23	5	21	58.133	-50.76014	-73.08840	4.02	3.2	48	0.483	360.2	373.9	694.0
2019	1	24	0	7	42.498	-50.63123	-74.53394	15.79	2.8	119	0.595	689.0	324.8	645.6
2019	1	31	3	44	9.051	-51.28170	-72.61343	10.01	2.9	64	0.384	487.9	353.1	1081.1
2019	2	2	1	51	23.709	-51.06426	-74.20347	17.78	3.5	113	0.352	445.5	309.5	625.2
2019	2	2	3	2	30.104	-51.07191	-74.21536	17.90	2.7	114	0.261	533.0	284.1	632.1
2019	2	2	3	29	10.667	-51.07124	-74.20073	17.29	2.7	124	0.212	618.6	345.9	937.8
2019	2	2	6	25	39.824	-51.06814	-74.18410	16.47	3.7	111	0.377	495.6	265.8	715.8
2019	2	2	6	49	13.887	-51.04955	-74.43722	30.52	2.7	182	0.348	1293.5	426.6	1380.1
2019	2	2	8	10	48.128	-51.06959	-74.20166	16.69	2.5	112	0.310	539.1	336.2	759.9
2019	2	3	11	30	12.402	-50.90453	-73.24249	2.17	2.5	61	0.237	487.1	586.9	977.6
2019	2	5	3	3	48.046	-49.87067	-73.45709	3.94	2.8	146	0.546	657.5	1122.7	1303.6
2019	2	5	5	53	56.203	-51.74980	-73.93791	8.83	2.8	160	0.357	448.5	533.8	1495.5
2019	2	5	7	4	12.129	-50.62463	-74.40927	19.48	2.6	110	0.319	410.5	274.6	542.4
2019	2	9	2	37	0.051	-52.91713	-71.29696	30.32	4.5	155	0.700	459.2	652.0	396.1
2019	2	9	11	57	24.776	-50.42114	-74.42148	17.62	2.4	118	0.052	518.1	368.6	585.9
2019	2	10	23	31	21.324	-50.41619	-73.77590	5.01	3.2	77	0.781	314.2	408.0	886.7
2019	2	11	16	39	30.103	-51.07130	-74.19489	16.69	2.8	112	0.235	661.1	299.0	736.3
2019	2	13	1	54	21.166	-50.63005	-74.40075	19.56	2.3	110	0.192	523.4	284.6	867.6

ORIGIN TIME (UTC)						Latitude	Longitude	Depth	M_L	GAP	RMS	X error	Y error	Z error
yyyy	mm	dd	h	m	seconds	[°]	[°]	[Km]		[°]		[m]	[m]	[m]
2019	2	13	22	58	44.651	-50.63270	-74.41820	17.96	3.0	112	0.390	443.0	260.1	467.0
2019	2	16	9	27	27.199	-51.07058	-74.20510	17.81	3.0	113	0.225	600.7	353.2	611.2
2019	2	17	10	26	49.315	-50.91771	-75.08214	12.27	4.8	188	0.498	467.6	301.3	502.4
2019	2	17	10	32	9.459	-50.90278	-75.04750	11.37	3.5	184	0.450	791.3	562.7	855.9
2019	2	17	10	39	12.813	-50.90964	-75.07595	11.78	3.7	187	0.384	809.1	526.0	771.3
2019	2	17	10	44	36.122	-50.90687	-75.08214	6.75	3.4	187	0.595	833.5	535.9	1431.7
2019	2	17	10	49	3.197	-50.90690	-75.06903	9.60	2.8	186	0.317	533.2	428.6	926.0
2019	2	17	11	9	30.695	-50.91160	-75.08089	9.56	3.4	187	0.471	824.3	541.5	848.6
2019	2	17	11	24	54.063	-50.90612	-75.07822	10.04	3.0	187	0.399	886.1	591.7	990.9
2019	2	17	11	45	18.597	-50.91532	-75.06698	11.32	3.2	186	0.805	888.7	590.4	874.7
2019	2	17	11	50	59.917	-50.92079	-75.09295	10.18	3.0	189	0.174	538.2	393.5	927.0
2019	2	17	13	41	24.736	-50.91310	-75.09989	9.49	3.2	189	0.322	865.6	580.7	880.1
2019	2	17	13	45	26.510	-50.90717	-75.07681	12.19	3.9	187	0.410	812.2	535.0	765.1
2019	2	17	15	26	38.491	-50.91252	-75.08627	9.65	2.5	188	0.122	675.2	423.9	1490.8
2019	2	17	15	35	23.305	-50.90800	-75.07588	10.42	4.2	187	0.571	765.3	483.1	727.4
2019	2	17	17	39	29.756	-50.90922	-75.08807	10.19	3.3	188	0.309	864.0	566.2	887.3
2019	2	17	18	46	40.037	-50.91473	-75.09996	9.61	3.4	189	0.442	836.5	537.0	850.8
2019	2	17	21	11	38.192	-50.90813	-75.01037	20.00	2.7	180	0.579	682.9	460.2	1442.8
2019	2	18	1	12	45.707	-50.90286	-75.06594	10.79	3.3	185	0.327	803.4	544.2	847.1
2019	2	18	2	26	53.287	-50.91220	-75.08140	8.49	2.9	187	0.356	865.3	596.1	1080.2
2019	2	18	7	42	46.424	-50.90915	-75.09195	9.33	2.8	188	0.333	867.8	594.9	970.0
2019	2	18	8	35	2.505	-50.91184	-75.07848	13.04	2.7	187	0.333	591.4	462.2	1204.8
2019	2	18	13	37	16.036	-50.91824	-75.07536	12.33	2.7	187	0.344	606.6	389.8	964.1
2019	2	18	15	43	20.705	-50.92347	-75.08045	10.67	2.7	188	0.189	604.0	399.4	1039.6
2019	2	19	6	43	43.441	-51.87922	-74.46254	17.30	3.3	216	0.580	1536.2	1161.4	959.0
2019	2	19	11	10	39.801	-50.90786	-75.07247	8.86	3.5	186	0.579	840.0	565.2	961.4
2019	2	19	16	47	35.215	-50.91992	-75.08466	8.79	3.7	188	0.468	834.5	553.6	906.8
2019	2	20	6	4	38.673	-50.90215	-75.06009	10.51	3.3	185	0.517	789.4	550.9	869.3
2019	2	20	10	54	4.911	-50.63443	-74.41053	17.96	3.3	111	0.368	419.2	265.3	480.7
2019	2	21	15	25	51.713	-52.25420	-73.81456	0.61	3.3	238	0.614	446.0	1190.2	455.4
2019	2	22	6	24	13.154	-50.91547	-75.08155	8.81	2.8	188	0.353	891.7	608.8	997.4
2019	2	22	10	45	2.343	-51.89559	-74.22952	15.01	4.2	213	0.535	446.5	526.5	900.2
2019	2	23	22	12	1.971	-50.91121	-75.07990	11.57	3.1	187	0.584	819.8	557.8	837.6
2019	2	23	23	51	23.845	-50.91218	-75.07121	16.37	2.7	186	0.528	644.4	472.2	1086.6
2019	2	24	13	51	20.739	-52.32590	-72.76559	19.01	3.1	175	0.563	458.6	566.3	830.6
2019	2	26	0	35	52.735	-52.55902	-73.76434	3.12	3.3	228	0.777	672.8	1122.0	748.0
2019	2	26	7	14	15.443	-50.90901	-73.24930	3.17	2.7	73	0.267	459.0	486.6	746.8
2019	2	26	7	21	56.863	-50.91251	-73.24107	5.99	2.6	73	0.420	416.5	442.9	701.6
2019	2	27	3	51	4.312	-50.43420	-72.64631	2.92	2.8	68	0.627	496.1	414.1	1163.6
2019	2	28	6	28	4.120	-51.23147	-72.28352	13.48	2.6	73	0.308	455.3	333.2	669.3
2019	2	28	6	56	7.948	-50.62082	-74.41977	20.75	2.1	111	0.161	638.6	315.0	1122.4
2019	2	28	22	59	34.998	-50.51276	-74.69852	31.28	2.5	118	0.418	452.4	380.5	664.9
2019	2	28	23	26	11.052	-51.01284	-73.89233	9.06	2.6	69	0.243	280.0	288.8	855.9
2019	3	1	23	23	28.400	-51.83364	-74.16743	4.05	2.7	195	0.402	505.7	579.0	608.2
2019	3	2	7	43	58.443	-50.91149	-75.08671	10.38	3.1	188	0.264	822.2	553.1	831.8
2019	3	2	13	17	31.964	-50.91167	-75.08818	9.29	3.1	188	0.382	869.8	567.6	1001.7
2019	3	3	17	13	46.682	-51.10490	-72.05790	18.00	3.0	70	0.717	845.1	591.5	1554.4

ORIGIN TIME (UTC)						Latitude	Longitude	Depth	M_L	GAP	RMS	X error	Y error	Z error
yyyy	mm	dd	h	m	seconds	[°]	[°]	[Km]		[°]		[m]	[m]	[m]
2019	3	4	8	57	30.121	-51.35964	-74.65371	10.62	3.2	169	0.398	765.5	369.2	1223.7
2019	3	5	20	15	15.584	-50.44041	-74.41821	18.27	2.7	96	0.264	450.0	333.5	497.4
2019	3	5	23	13	39.563	-51.48869	-74.33354	17.35	3.1	102	0.345	655.3	389.2	1040.2
2019	3	5	23	57	33.722	-51.53586	-73.94040	11.94	2.7	116	0.359	348.8	349.0	925.9
2019	3	6	10	15	42.822	-52.68736	-73.94526	19.59	3.5	252	0.367	1062.6	1582.1	2077.8
2019	3	7	11	53	5.964	-50.46914	-74.54022	33.97	2.6	105	0.162	728.3	450.6	689.8
2019	3	7	22	36	58.523	-50.64971	-74.39844	17.76	2.5	111	0.844	581.1	481.2	674.6
2019	3	8	0	48	51.995	-50.75211	-72.06258	13.50	2.9	57	0.554	467.5	353.0	582.2
2019	3	8	10	28	45.887	-49.91457	-73.29404	1.99	2.6	164	0.271	467.0	856.4	713.0
2019	3	9	15	16	46.868	-50.90228	-75.05233	14.79	3.0	184	0.555	552.8	464.2	957.6
2019	3	11	13	21	36.361	-50.91099	-75.08038	10.90	3.5	187	0.195	951.7	607.6	1162.8
2019	3	12	3	38	45.345	-51.26007	-72.56911	11.83	2.5	197	0.220	1287.3	1164.6	1773.6
2019	3	12	5	9	16.757	-51.32604	-75.48894	11.32	3.1	244	0.779	1868.9	1028.7	1195.6
2019	3	12	18	36	41.664	-51.30228	-75.37214	15.00	2.7	238	0.184	1925.0	1018.2	1671.6
2019	3	13	7	16	14.411	-51.23125	-73.48022	9.68	2.4	129	0.392	495.6	884.4	1832.9
2019	3	14	8	17	56.819	-50.74481	-73.07145	4.23	2.7	55	0.262	373.4	369.6	767.6
2019	3	14	10	58	9.684	-51.38805	-75.61001	13.75	2.8	251	0.578	1428.6	871.9	1698.7
2019	3	14	12	50	32.810	-51.39614	-75.57711	16.01	3.1	249	0.422	1907.0	1162.4	1610.3
2019	3	14	21	13	47.371	-51.31959	-75.44550	13.79	2.7	242	0.247	1896.2	1017.7	1428.0
2019	3	15	4	48	9.619	-50.66777	-73.32551	6.00	2.6	59	0.325	292.2	309.9	441.9
2019	3	15	12	29	41.993	-52.74640	-73.72061	4.46	3.3	214	0.870	582.8	842.3	847.2
2019	3	15	19	27	40.056	-50.27585	-72.22231	1.76	2.8	86	0.668	481.5	510.7	578.6
2019	3	16	1	58	14.408	-51.07298	-74.19006	17.64	2.7	111	0.247	457.2	311.4	590.9
2019	3	17	23	43	19.181	-50.90854	-75.09143	9.91	3.1	188	0.313	811.4	550.4	878.2
2019	3	19	7	46	7.599	-50.33201	-74.71987	29.73	3.1	112	0.393	387.0	401.3	843.0
2019	3	19	17	23	43.524	-51.19950	-72.41879	9.30	2.8	66	0.447	619.8	329.0	2509.6
2019	3	22	1	4	59.624	-49.46982	-73.71564	2.17	3.1	188	0.463	424.6	1162.6	892.9
2019	3	22	3	9	25.766	-49.43899	-73.70531	11.17	2.8	222	0.407	393.8	787.8	1296.7
2019	3	22	21	33	30.731	-51.03129	-74.40795	27.55	2.8	130	0.792	536.4	331.3	408.4
2019	3	22	22	10	41.029	-50.90449	-75.07815	10.31	3.1	187	0.552	788.4	526.2	918.0
2019	3	23	8	47	1.139	-52.11477	-72.83197	13.32	3.3	127	0.481	271.7	460.9	496.4
2019	3	25	19	29	26.940	-51.85466	-74.15113	5.90	4.0	190	0.579	596.3	735.7	732.6
2019	3	26	2	44	48.485	-50.62436	-74.40613	18.13	3.4	110	0.468	343.4	245.7	422.4
2019	3	26	9	5	10.538	-50.96142	-72.27213	12.56	3.1	48	0.451	395.1	277.8	770.3
2019	3	28	4	4	58.772	-51.32107	-72.16266	13.64	3.0	82	0.218	524.3	373.4	1019.6
2019	4	1	4	4	16.764	-49.49269	-73.00695	3.00	3.2	131	0.865	799.9	833.8	927.6
2019	4	2	13	17	38.455	-51.19445	-72.41177	14.20	4.9	51	0.494	229.2	191.0	359.5
2019	4	2	15	14	37.854	-51.20842	-72.40305	9.17	3.0	130	0.203	614.8	328.6	1146.1
2019	4	2	19	0	11.380	-51.20300	-72.42314	10.47	3.0	75	0.394	539.8	488.7	1494.6
2019	4	2	20	32	42.091	-51.19545	-72.38808	12.26	2.8	76	0.423	1035.5	582.6	1776.2
2019	4	3	1	49	8.921	-51.19306	-72.41912	13.44	4.1	51	0.489	252.2	245.0	487.7
2019	4	3	8	4	24.675	-51.19990	-72.41683	4.52	3.4	51	0.366	380.2	260.3	2080.1
2019	4	3	13	22	54.750	-51.20681	-72.40795	12.02	3.3	67	0.386	339.4	298.8	629.2
2019	4	3	19	45	18.046	-51.20083	-72.44026	3.99	3.1	65	0.426	499.8	300.8	2908.7
2019	4	3	22	40	9.482	-51.88776	-74.18494	1.69	3.7	187	0.674	396.0	507.7	274.9
2019	4	3	22	48	57.104	-51.20231	-72.40801	13.99	3.2	51	0.369	343.0	254.1	533.6
2019	4	5	9	39	43.603	-51.20152	-72.41388	13.29	3.4	56	0.357	321.7	259.8	648.1

ORIGIN TIME (UTC)						Latitude	Longitude	Depth	M_L	GAP	RMS	X error	Y error	Z error
yyyy	mm	dd	h	m	seconds	[°]	[°]	[Km]		[°]		[m]	[m]	[m]
2019	4	5	14	38	22.914	-50.93109	-75.04292	14.40	3.6	185	0.876	768.7	550.0	984.3
2019	4	5	17	44	16.860	-50.35410	-72.30256	12.00	3.4	56	0.657	402.8	404.1	665.3
2019	4	7	0	26	41.590	-51.20692	-72.43042	13.74	3.2	66	0.593	389.2	291.9	678.4
2019	4	7	12	37	54.745	-51.20478	-72.41286	10.59	3.3	56	0.480	312.8	235.7	710.6
2019	4	7	14	58	0.683	-51.21371	-72.39810	12.62	3.0	72	0.679	472.2	364.6	806.3
2019	4	8	7	45	46.744	-51.03882	-73.94490	9.23	3.1	76	0.365	265.4	264.1	857.8
2019	4	8	7	50	57.243	-50.61999	-74.42071	20.59	2.7	111	0.148	453.8	273.0	885.7
2019	4	8	10	47	49.441	-51.04338	-73.98684	12.27	2.8	81	0.300	345.7	301.3	835.2
2019	4	9	11	41	57.407	-53.28588	-72.49783	77.85	3.8	206	0.845	928.5	970.9	1463.6
2019	4	9	11	50	24.099	-53.25439	-72.40820	81.01	3.6	202	0.886	779.9	841.5	1409.5
2019	4	9	15	32	35.533	-51.18880	-72.40623	5.48	2.9	55	0.653	322.9	233.9	606.6
2019	4	10	4	32	35.338	-51.99777	-74.19654	13.15	2.9	226	0.399	496.1	582.7	827.0
2019	4	10	9	4	54.654	-51.21379	-72.41470	8.89	2.7	101	0.249	458.8	342.7	2035.3
2019	4	10	10	34	58.835	-51.20648	-72.42554	11.10	2.8	66	0.374	335.3	306.5	841.7
2019	4	10	23	47	49.700	-52.40213	-74.06252	12.34	3.4	267	0.774	679.2	978.4	1779.5
2019	4	11	1	0	57.532	-52.34637	-73.76267	6.75	3.5	255	0.433	610.2	1477.4	857.6
2019	4	11	17	5	19.555	-51.20179	-72.38751	12.49	3.0	67	0.496	409.5	312.8	689.4
2019	4	12	10	27	23.618	-51.20941	-74.49348	18.39	3.3	142	0.449	583.1	325.3	636.5
2019	4	13	3	12	40.194	-51.19948	-72.41488	9.09	3.2	66	0.372	423.4	314.5	2155.8
2019	4	13	12	35	51.073	-51.21835	-72.42637	2.49	3.1	75	0.428	388.1	332.2	429.6
2019	4	15	13	33	30.620	-51.20324	-72.43144	3.35	3.1	66	0.378	317.9	290.0	528.4
2019	4	16	8	49	50.468	-51.97422	-74.31463	23.98	3.4	233	0.275	794.4	889.8	1357.5
2019	4	16	9	29	43.353	-51.90438	-74.20993	1.53	3.4	191	0.548	473.4	596.1	300.3
2019	4	16	9	37	40.137	-51.20848	-72.41477	11.47	2.9	51	0.450	405.0	270.7	964.7
2019	4	17	4	45	38.625	-50.93441	-71.99483	9.69	3.3	51	0.480	428.3	368.6	644.6
2019	4	17	22	35	19.621	-51.19701	-72.41296	12.51	3.2	66	0.384	413.3	288.9	798.3
2019	4	18	21	26	56.010	-50.42747	-74.79250	27.33	3.0	113	0.304	396.1	389.1	1079.2
2019	4	18	22	30	25.015	-51.27656	-75.34928	31.64	3.2	234	0.671	1952.7	1166.7	1895.5
2019	4	19	22	27	10.535	-50.18246	-74.63564	31.13	2.2	160	0.248	530.2	452.1	1568.0
2019	4	20	4	8	55.618	-51.34043	-72.18190	16.39	3.0	82	0.453	638.4	402.0	751.6
2019	4	20	10	3	58.065	-53.08899	-73.54649	74.66	4.0	223	0.569	1291.8	1393.3	3043.9
2019	4	20	13	52	39.310	-51.89543	-74.20572	1.08	3.3	211	0.599	513.8	867.2	412.0
2019	4	20	14	34	36.364	-51.97011	-74.29812	19.52	3.6	205	0.373	569.1	614.8	796.1
2019	4	22	7	55	51.032	-53.17348	-72.41952	68.32	3.6	198	0.384	909.1	962.0	2161.5
2019	4	22	21	56	45.790	-50.40224	-72.51885	6.00	2.8	86	0.540	370.7	414.8	613.1
2019	4	23	0	29	54.250	-50.36112	-74.72260	20.00	3.2	100	0.637	313.7	320.9	851.1
2019	4	23	18	41	30.157	-51.02320	-75.69552	27.67	3.6	246	0.571	2342.9	1212.5	1924.1
2019	4	23	23	3	22.917	-49.89629	-73.87584	6.00	2.8	129	0.885	632.5	925.6	768.6
2019	4	24	22	57	55.150	-51.65559	-74.17961	9.71	3.2	152	0.420	416.4	401.3	852.3
2019	4	26	2	35	56.889	-51.11795	-74.70454	24.59	2.5	162	0.097	1907.9	595.6	2018.3
2019	4	26	22	13	17.296	-50.93672	-73.59201	9.00	3.9	54	0.534	269.6	317.8	528.6
2019	4	27	20	15	29.187	-49.86272	-73.90609	1.42	3.0	156	0.491	476.4	707.6	1361.7
2019	4	28	5	33	55.238	-51.19776	-72.39928	13.25	2.8	67	0.468	406.8	294.9	842.1
2019	4	28	8	0	8.834	-51.18804	-72.41796	9.69	2.8	66	0.393	420.5	257.3	2321.4
2019	4	28	20	18	57.755	-51.55061	-73.55000	6.00	2.7	106	0.230	387.6	420.8	759.0
2019	4	29	0	18	58.309	-51.36208	-72.92539	12.14	2.8	65	0.320	551.3	391.7	1128.1
2019	4	29	5	6	26.364	-51.21357	-72.41129	11.52	3.2	62	0.412	345.6	290.8	683.6

ORIGIN TIME (UTC)						Latitude	Longitude	Depth	M_L	GAP	RMS	X error	Y error	Z error
yyyy	mm	dd	h	m	seconds	[°]	[°]	[Km]		[°]		[m]	[m]	[m]
2019	4	29	8	9	58.774	-52.83289	-73.47743	61.64	4.2	233	0.883	745.7	992.4	1861.3
2019	4	29	15	19	47.378	-51.20560	-72.41188	4.83	3.2	56	0.571	361.9	255.8	1568.5
2019	4	30	4	5	32.983	-51.18988	-72.06935	6.06	2.8	80	0.308	426.0	309.6	1988.3
2019	4	30	15	46	47.906	-52.48981	-71.48337	30.98	3.2	99	0.771	529.5	646.0	585.9
2019	5	2	14	18	33.354	-50.62877	-74.40457	18.91	2.6	110	0.284	460.5	276.2	626.4
2019	5	3	11	4	5.011	-52.08999	-74.98537	33.79	3.5	248	0.376	1794.1	1852.5	1994.2
2019	5	3	11	51	11.213	-50.62682	-74.39680	18.85	2.8	110	0.489	374.5	250.7	512.5
2019	5	3	16	4	6.051	-50.62371	-74.40852	17.78	3.3	110	0.587	339.4	255.4	462.3
2019	5	3	23	53	6.396	-51.17921	-72.45419	14.01	2.6	96	0.485	508.7	484.8	1308.7
2019	5	4	2	2	49.544	-51.06351	-73.30369	4.77	2.9	59	0.404	313.6	334.7	631.5
2019	5	5	20	44	11.632	-51.94237	-74.23428	13.12	3.3	221	0.591	449.2	585.0	654.7
2019	5	6	7	58	3.245	-50.94996	-72.50642	5.01	3.1	43	0.496	401.2	324.1	1379.6
2019	5	6	11	8	25.463	-50.62976	-74.40798	18.40	2.8	111	0.486	440.8	271.1	522.7
2019	5	7	20	48	10.326	-50.05557	-74.48738	25.45	2.9	114	0.402	328.9	353.1	631.5
2019	5	8	6	17	44.313	-50.90492	-73.25025	4.69	3.2	51	0.266	410.8	393.9	1002.4
2019	5	9	7	9	29.324	-51.50029	-74.28374	13.93	3.4	103	0.411	546.1	327.6	843.2
2019	5	9	15	12	21.031	-51.07009	-74.19291	17.33	3.2	112	0.331	614.5	290.6	752.3
2019	5	10	3	25	43.899	-52.38402	-73.75930	15.82	3.5	246	0.227	673.1	1132.1	1121.2
2019	5	11	20	41	30.729	-50.72392	-73.10428	4.64	3.3	50	0.451	349.9	338.5	714.4
2019	5	13	5	18	57.209	-50.51572	-74.54463	32.33	3.3	109	0.151	576.3	398.3	793.3
2019	5	13	12	2	31.913	-51.30618	-75.49962	18.79	3.7	244	0.421	1751.4	1021.6	1553.6
2019	5	15	20	23	19.968	-51.82999	-74.40747	13.63	3.8	224	0.543	602.9	594.9	711.9
2019	5	17	14	0	16.450	-51.95359	-74.25643	18.08	3.2	225	0.331	1492.0	1250.1	1400.9
2019	5	18	1	16	35.674	-50.76548	-74.00227	7.17	3.1	61	0.526	286.6	269.2	838.6
2019	5	18	10	59	22.464	-50.76631	-74.00036	7.43	2.9	92	0.412	353.7	310.8	1027.2
2019	5	19	21	10	10.991	-50.63460	-74.37073	20.00	3.1	109	0.468	387.2	263.2	439.8
2019	5	24	1	10	6.263	-52.72446	-73.95919	4.88	3.4	271	0.309	677.4	1457.6	1620.7
2019	5	25	5	28	47.434	-50.77049	-74.01351	8.00	3.1	61	0.400	345.0	340.8	892.7
2019	5	27	10	39	27.607	-50.97221	-74.69774	21.10	2.5	154	0.278	590.3	316.4	807.2
2019	5	27	16	44	10.860	-51.20066	-72.40706	12.86	2.9	51	0.508	350.3	318.8	660.7
2019	5	27	23	49	54.722	-51.95246	-73.91334	2.56	2.8	197	0.469	556.4	730.2	530.2
2019	5	28	14	53	28.044	-51.39006	-74.31939	22.26	3.0	114	0.403	495.7	335.1	811.4
2019	5	29	4	49	11.057	-50.50746	-73.55607	6.00	2.2	120	0.611	261.4	732.7	846.7
2019	5	29	5	38	18.738	-52.41268	-74.11594	17.95	3.0	269	0.272	1255.8	1949.7	2267.8
2019	5	29	19	15	18.189	-50.91590	-75.08060	9.96	3.0	188	0.310	805.1	538.7	909.2
2019	5	29	22	46	42.311	-51.82686	-74.54253	6.18	3.2	229	0.885	542.5	471.6	650.6
2019	5	30	5	3	41.542	-52.95120	-73.54373	21.83	3.6	217	0.748	1000.5	1225.1	2144.9
2019	5	30	11	14	32.446	-50.19131	-74.74445	37.72	2.1	143	0.271	558.0	471.8	1218.8
2019	5	30	20	19	53.441	-51.19966	-72.41146	10.43	3.2	54	0.761	294.2	272.8	708.6
2019	5	31	6	53	3.896	-51.89326	-74.38366	21.68	2.9	230	0.377	1296.8	1373.3	1118.5
2019	6	1	7	33	37.213	-50.92091	-73.58429	5.92	2.7	54	0.129	341.5	388.7	924.6
2019	6	1	7	56	57.920	-50.93201	-73.57277	10.98	2.6	53	0.838	418.8	529.9	923.8
2019	6	1	8	19	40.205	-50.91898	-73.60125	3.12	2.6	54	0.258	383.6	466.3	1011.4
2019	6	1	9	29	32.136	-50.92049	-73.58622	4.77	2.6	54	0.140	363.2	408.1	1003.2
2019	6	1	10	40	24.848	-50.92457	-73.58821	3.78	2.6	53	0.127	406.4	470.7	1215.3
2019	6	1	11	52	49.548	-50.92455	-73.59210	4.32	2.6	58	0.120	442.0	521.1	1143.7
2019	6	1	13	3	27.524	-50.92136	-73.57555	6.00	2.6	53	0.358	378.3	449.4	717.9

ORIGIN TIME (UTC)						Latitude	Longitude	Depth	M_L	GAP	RMS	X error	Y error	Z error
yyyy	mm	dd	h	m	seconds	[°]	[°]	[Km]		[°]		[m]	[m]	[m]
2019	6	1	14	21	55.925	-50.92010	-73.58233	6.00	2.7	54	0.133	388.5	471.9	1020.2
2019	6	1	15	34	53.879	-50.92151	-73.58575	4.29	2.7	54	0.151	433.4	570.0	1379.2
2019	6	1	16	44	41.091	-50.91764	-73.58424	6.00	2.7	54	0.148	422.9	528.2	1014.3
2019	6	1	17	57	10.216	-50.92618	-73.59309	3.03	2.7	53	0.231	426.1	465.3	844.7
2019	6	1	20	4	44.428	-50.92112	-73.58283	4.35	2.6	54	0.158	469.4	542.4	1393.2
2019	6	1	21	18	56.479	-50.92091	-73.58429	3.52	2.7	57	0.195	399.0	486.4	988.4
2019	6	1	22	35	50.106	-50.92336	-73.58529	4.30	2.6	57	0.154	414.6	483.2	1165.9
2019	6	1	23	38	43.500	-50.92412	-73.59695	6.98	2.6	54	0.421	370.2	407.2	1062.0
2019	6	2	0	53	6.931	-50.89041	-73.56765	6.00	2.7	55	0.729	276.1	333.3	198.8
2019	6	2	4	23	38.807	-50.92088	-73.58914	3.80	2.7	57	0.242	455.2	509.8	955.0
2019	6	2	5	21	36.806	-50.92660	-73.59212	2.99	2.9	56	0.223	363.7	402.4	660.9
2019	6	2	6	7	24.372	-50.92626	-73.57756	6.00	2.7	56	0.249	392.3	414.6	668.0
2019	6	2	6	45	7.175	-50.92621	-73.58824	3.95	2.6	56	0.156	534.5	576.3	1200.0
2019	6	2	7	30	19.209	-50.92092	-73.58234	4.24	2.6	75	0.146	430.5	542.4	1221.0
2019	6	2	8	18	19.915	-50.92479	-73.58579	4.53	2.8	53	0.142	424.6	453.7	1195.1
2019	6	2	9	9	35.868	-50.92295	-73.58528	4.58	2.8	53	0.208	404.9	463.4	1141.1
2019	6	2	9	53	20.030	-50.92382	-73.57364	2.99	2.8	56	0.286	382.8	419.6	526.1
2019	6	2	12	11	1.199	-50.91719	-73.59200	2.90	2.8	57	0.216	393.7	414.0	592.8
2019	6	2	13	16	7.578	-50.92010	-73.58136	4.67	3.1	76	0.175	480.7	454.0	1223.9
2019	6	2	14	18	22.054	-50.92296	-73.58237	4.81	2.8	53	0.189	424.9	464.1	1242.1
2019	6	2	15	11	31.246	-50.91801	-73.59104	5.48	2.7	54	0.160	422.2	451.0	1173.2
2019	6	2	16	57	53.887	-50.92124	-73.59885	3.40	2.7	58	0.344	489.0	530.8	951.1
2019	6	2	17	45	48.016	-50.92700	-73.59213	5.59	2.8	53	0.142	455.3	483.9	1017.8
2019	6	2	20	55	26.060	-50.92355	-73.54646	0.61	2.7	53	0.841	370.5	463.7	416.6
2019	6	2	21	44	30.424	-50.91720	-73.58909	3.27	2.8	67	0.163	442.3	414.3	815.2
2019	6	2	22	40	35.372	-50.92050	-73.58331	4.73	2.8	54	0.199	409.5	429.6	1157.9
2019	6	2	23	41	48.682	-50.91764	-73.58424	5.96	2.9	54	0.173	365.9	396.3	1157.0
2019	6	3	0	45	49.106	-50.91926	-73.58718	6.00	2.7	54	0.243	413.7	420.2	762.5
2019	6	3	1	28	7.494	-50.92742	-73.59019	5.44	2.8	53	0.191	394.7	425.9	1042.0
2019	6	3	3	2	1.574	-50.91987	-73.58767	5.39	2.8	67	0.139	393.3	430.5	1109.5
2019	6	3	4	18	21.063	-50.92216	-73.57945	5.73	2.9	53	0.161	382.4	411.6	1085.3
2019	6	3	5	17	11.600	-50.92512	-73.55910	2.76	2.9	58	0.518	441.4	494.1	605.6
2019	6	3	6	15	29.016	-50.91970	-73.58136	5.28	2.9	68	0.122	444.3	507.7	1193.7
2019	6	3	7	20	49.658	-50.91196	-73.57350	6.00	2.9	69	0.552	431.4	484.5	819.1
2019	6	3	8	25	34.831	-50.92316	-73.58383	6.83	3.1	58	0.268	432.0	502.2	1419.9
2019	6	3	10	24	34.344	-50.92202	-73.60663	6.00	2.9	66	0.276	400.5	529.3	731.2
2019	6	3	11	25	1.964	-50.91335	-73.58176	4.29	3.0	68	0.420	427.3	468.2	876.7
2019	6	3	15	8	24.104	-51.46655	-72.75135	11.30	3.3	72	0.564	468.8	397.9	870.3
2019	6	3	15	38	25.871	-50.91988	-73.58573	3.94	3.1	54	0.155	377.3	404.1	800.8
2019	6	3	17	9	6.505	-50.92094	-73.57749	5.55	3.0	53	0.275	417.1	411.2	837.0
2019	6	3	18	30	25.737	-50.92626	-73.57659	6.00	3.2	67	0.255	430.3	433.9	994.7
2019	6	3	21	46	17.809	-50.92015	-73.57263	10.01	3.1	53	0.550	423.8	469.1	980.1
2019	6	3	22	29	22.538	-50.92292	-73.59014	4.44	3.1	54	0.173	401.4	446.9	1259.0
2019	6	4	1	23	4.963	-51.06487	-74.18304	16.67	3.2	111	0.380	467.3	313.9	770.7
2019	6	4	3	39	54.663	-50.91930	-73.57941	4.52	3.2	100	0.105	512.1	490.4	1200.1
2019	6	4	5	9	0.270	-50.92175	-73.57847	5.65	3.2	53	0.262	401.8	421.5	1284.3
2019	6	4	5	47	52.850	-50.92315	-73.58577	4.29	3.1	67	0.251	498.5	555.6	1406.3

ORIGIN TIME (UTC)						Latitude	Longitude	Depth	M_L	GAP	RMS	X error	Y error	Z error
yyyy	mm	dd	h	m	seconds	[°]	[°]	[Km]		[°]		[m]	[m]	[m]
2019	6	4	6	32	8.029	-50.91741	-73.58764	5.15	3.2	54	0.128	515.7	552.1	1720.9
2019	6	4	7	28	12.725	-50.91991	-73.57990	5.97	2.9	54	0.159	398.3	446.4	1037.8
2019	6	4	8	8	49.424	-50.91948	-73.58281	5.99	3.2	54	0.239	420.0	480.5	998.6
2019	6	4	9	41	40.067	-50.91825	-73.58377	4.25	3.2	57	0.151	534.2	564.4	1482.4
2019	6	4	12	5	10.920	-50.99537	-74.40103	25.05	3.4	128	0.277	515.3	295.1	444.4
2019	6	4	15	59	45.045	-50.91990	-73.58185	4.18	3.2	68	0.168	542.4	527.1	1301.1
2019	6	4	17	19	12.890	-50.91930	-73.57941	3.89	3.2	54	0.323	485.3	454.3	987.7
2019	6	4	18	53	42.451	-50.92093	-73.58040	5.40	3.3	53	0.164	433.0	454.1	1014.7
2019	6	4	19	29	57.210	-50.91967	-73.58621	4.26	3.3	67	0.172	541.0	490.1	1193.3
2019	6	4	21	21	25.294	-50.92212	-73.58721	5.14	3.2	67	0.183	412.8	444.0	973.0
2019	6	4	21	53	21.394	-50.91909	-73.57989	3.94	3.3	95	0.211	628.1	659.2	1460.8
2019	6	4	23	23	21.240	-50.92378	-73.58238	6.00	3.2	53	0.203	382.6	431.6	931.4
2019	6	5	0	29	57.173	-50.92054	-73.57651	5.40	3.1	53	0.183	369.3	402.7	862.3
2019	6	5	1	20	5.637	-50.91771	-73.56968	3.93	3.0	53	0.390	434.1	484.5	935.7
2019	6	5	2	5	3.700	-50.92093	-73.58040	4.69	3.0	53	0.118	449.1	457.6	1201.6
2019	6	5	2	46	0.291	-51.91876	-74.31846	20.01	3.7	226	0.340	866.0	827.3	680.6
2019	6	5	2	55	55.746	-50.91928	-73.58329	4.48	3.0	54	0.117	414.9	420.4	1232.3
2019	6	5	4	27	16.416	-50.92154	-73.57993	4.68	3.2	100	0.236	420.9	445.4	1067.5
2019	6	5	4	56	1.188	-50.41175	-74.63824	21.41	3.2	103	0.641	283.1	281.4	917.2
2019	6	5	5	16	45.999	-50.92213	-73.58527	5.40	3.0	54	0.219	380.4	420.6	1191.8
2019	6	5	6	0	18.285	-50.91909	-73.57989	4.88	3.0	80	0.087	534.1	549.7	1429.1
2019	6	5	6	48	36.157	-50.92135	-73.57750	5.44	3.1	68	0.181	425.2	449.6	973.9
2019	6	5	8	4	22.603	-50.92173	-73.58430	4.87	3.1	54	0.149	421.7	453.2	1152.4
2019	6	5	8	44	5.038	-50.91233	-73.58127	3.52	2.9	54	0.279	411.2	440.2	1042.0
2019	6	5	9	36	8.597	-50.91990	-73.58185	4.06	3.0	54	0.136	421.9	444.6	1129.5
2019	6	5	9	51	56.786	-50.25696	-72.77302	2.66	3.0	48	0.613	355.4	404.7	684.2
2019	6	5	10	21	15.480	-50.92505	-73.57463	6.00	2.9	75	0.255	496.9	522.8	792.2
2019	6	5	11	35	16.298	-50.91744	-73.58182	4.45	3.0	99	0.113	523.0	550.5	1489.6
2019	6	5	18	48	33.414	-50.92339	-73.57946	8.03	3.1	53	0.401	428.1	457.7	1768.9
2019	6	5	22	52	19.068	-50.91806	-73.58134	6.00	3.1	53	0.177	397.1	426.3	994.1
2019	6	6	0	2	49.260	-50.91969	-73.58233	5.87	3.0	54	0.206	405.8	435.0	1066.8
2019	6	6	0	57	10.139	-50.91559	-73.58422	4.83	3.1	54	0.356	402.3	434.1	884.0
2019	6	6	1	55	43.038	-50.92214	-73.58333	4.87	2.9	53	0.160	458.9	487.0	1325.3
2019	6	6	2	54	17.754	-50.92092	-73.58234	5.14	3.0	54	0.166	361.8	404.2	1063.5
2019	6	6	3	38	37.214	-50.92235	-73.58188	4.61	2.9	53	0.146	464.4	443.3	1175.4
2019	6	6	4	33	25.683	-50.92132	-73.58429	4.34	3.0	67	0.169	454.0	422.7	1092.5
2019	6	6	5	14	23.668	-50.91930	-73.57941	5.10	3.0	68	0.226	442.4	473.3	1426.9
2019	6	6	6	44	53.314	-50.92133	-73.58235	5.85	3.0	54	0.219	380.5	425.3	851.3
2019	6	6	7	18	54.597	-50.92476	-73.59162	4.41	2.8	59	0.207	430.6	447.7	1189.8
2019	6	6	8	21	48.856	-50.91761	-73.58910	7.90	2.8	54	0.248	400.2	438.5	1451.2
2019	6	6	9	14	33.370	-50.91764	-73.58327	5.77	3.0	54	0.168	409.1	484.2	1150.2
2019	6	6	10	6	23.439	-50.91067	-73.58707	8.62	2.8	54	0.403	396.8	464.7	1201.3
2019	6	6	11	7	35.348	-50.92012	-73.57845	7.55	2.8	54	0.430	404.7	442.4	1258.5
2019	6	6	11	46	16.226	-50.92463	-73.57559	7.51	2.8	68	0.611	431.6	457.3	1185.6
2019	6	6	13	27	21.226	-50.92051	-73.58234	6.00	2.8	54	0.153	394.2	458.0	989.4
2019	6	6	14	27	51.637	-50.92068	-73.58962	4.84	2.8	67	0.245	452.1	476.8	1743.7
2019	6	6	16	10	2.620	-50.92092	-73.58234	4.17	2.8	67	0.136	447.4	445.2	1117.3

ORIGIN TIME (UTC)						Latitude	Longitude	Depth	M_L	GAP	RMS	X error	Y error	Z error
yyyy	mm	dd	h	m	seconds	[°]	[°]	[Km]		[°]		[m]	[m]	[m]
2019	6	6	17	2	46.693	-50.92380	-73.57850	8.99	2.8	53	0.653	406.5	448.8	912.0
2019	6	6	19	26	19.077	-50.91763	-73.58619	6.98	3.1	76	0.202	394.8	448.3	1366.6
2019	6	6	20	35	21.412	-50.91439	-73.57935	6.00	2.7	54	0.290	377.8	433.2	880.0
2019	6	6	21	16	1.805	-50.91987	-73.58767	4.65	2.7	76	0.133	436.5	511.2	1289.3
2019	6	6	22	4	50.347	-50.92092	-73.58234	4.99	2.8	54	0.125	454.9	478.1	1311.9
2019	6	6	22	41	33.526	-50.91804	-73.58425	5.65	2.7	76	0.104	464.1	483.3	1405.7
2019	6	6	23	8	38.574	-50.62903	-74.38336	19.91	2.5	109	0.376	440.8	294.0	665.0
2019	6	6	23	37	58.808	-50.91888	-73.58135	5.92	2.7	76	0.138	389.9	455.3	1117.0
2019	6	7	0	38	50.235	-50.92051	-73.58234	5.61	2.8	54	0.163	382.6	420.0	1242.4
2019	6	7	1	27	54.937	-50.91764	-73.58327	5.53	2.8	59	0.231	435.2	460.0	1245.6
2019	6	7	2	6	12.115	-50.92112	-73.58283	4.90	2.8	95	0.159	553.3	621.8	1455.3
2019	6	7	2	44	3.323	-50.92193	-73.58478	5.02	2.7	54	0.148	433.8	471.5	1502.5
2019	6	7	3	24	37.096	-50.91321	-73.56866	6.00	2.7	76	0.280	401.8	437.8	813.3
2019	6	7	3	45	34.647	-52.41493	-74.17921	11.05	3.2	258	0.576	756.5	983.5	953.9
2019	6	7	4	8	21.221	-50.91804	-73.58425	6.00	2.8	58	0.151	411.5	482.0	1002.7
2019	6	7	5	45	5.186	-50.92251	-73.59013	5.87	2.9	54	0.282	399.9	461.0	995.7
2019	6	7	7	20	26.850	-50.91520	-73.58033	6.00	2.8	54	0.291	363.1	403.7	824.1
2019	6	7	8	48	46.999	-50.91887	-73.58329	5.71	2.7	54	0.167	369.3	420.1	1013.4
2019	6	7	9	33	57.873	-50.92071	-73.58380	4.33	2.7	54	0.149	423.8	507.2	1277.9
2019	6	7	10	14	9.590	-50.92091	-73.58331	4.17	2.6	75	0.150	403.2	465.3	1124.1
2019	6	7	10	59	59.496	-50.91643	-73.58035	5.12	2.6	76	0.180	411.4	461.6	1164.0
2019	6	7	12	47	7.529	-50.92092	-73.58234	5.61	2.6	54	0.176	421.2	474.0	1053.0
2019	6	7	15	8	24.207	-50.92173	-73.58430	5.10	2.7	57	0.154	412.0	470.2	1124.2
2019	6	7	16	7	22.708	-50.91627	-73.57112	5.99	2.6	54	0.284	382.4	426.8	911.4
2019	6	7	16	17	50.992	-50.30358	-74.73322	24.65	2.6	92	0.541	318.2	314.9	654.7
2019	6	7	17	35	12.729	-50.91989	-73.58379	4.06	2.6	54	0.173	364.4	409.7	934.9
2019	6	7	18	10	57.761	-50.91906	-73.58572	6.01	2.7	54	0.137	476.6	584.2	1260.5
2019	6	7	19	37	14.087	-50.91888	-73.58038	4.60	2.6	54	0.183	429.0	470.3	1123.9
2019	6	7	21	1	16.941	-50.92135	-73.57750	5.55	2.7	68	0.378	390.2	394.2	1076.9
2019	6	7	22	11	47.818	-50.91765	-73.58133	5.20	2.8	57	0.194	440.3	481.2	1079.0
2019	6	7	23	4	2.616	-50.91351	-73.59196	6.00	2.7	54	0.263	478.2	514.9	1004.6
2019	6	8	0	0	8.071	-50.92173	-73.58430	5.59	2.7	54	0.191	381.3	406.3	926.3
2019	6	8	0	55	5.348	-52.26441	-73.75576	1.59	3.1	237	0.457	562.5	1687.8	506.0
2019	6	8	1	21	29.329	-50.91238	-73.57253	5.26	2.7	54	0.358	353.3	401.2	839.3
2019	6	8	2	36	52.331	-50.91886	-73.58523	4.38	2.8	57	0.264	349.3	414.5	987.3
2019	6	8	3	24	8.950	-50.55085	-73.39814	12.38	2.7	196	0.872	759.7	1603.2	1577.8
2019	6	8	4	47	39.781	-50.91969	-73.58330	4.32	2.7	54	0.139	386.2	454.0	1094.1
2019	6	8	5	34	42.050	-50.92070	-73.58574	4.22	2.7	54	0.173	426.6	457.6	1139.2
2019	6	8	6	26	41.039	-50.91018	-73.60162	6.00	2.7	54	0.483	332.3	392.3	365.0
2019	6	8	7	35	5.288	-50.91841	-73.59299	7.33	2.8	54	0.301	400.9	451.0	1276.6
2019	6	8	9	12	39.904	-50.91928	-73.58329	4.48	2.8	54	0.263	354.8	381.7	1021.7
2019	6	8	10	5	34.703	-50.91436	-73.58420	6.00	2.7	76	0.173	399.1	473.8	980.4
2019	6	8	11	51	24.688	-50.92213	-73.58624	4.60	2.7	57	0.204	385.7	460.7	1107.2
2019	6	8	12	46	41.076	-51.97065	-74.18936	13.28	3.3	221	0.531	551.0	580.6	726.3
2019	6	8	13	12	45.178	-50.91767	-73.57745	6.00	2.8	54	0.289	384.4	414.9	760.0
2019	6	8	14	41	55.991	-50.92054	-73.57651	4.01	2.8	53	0.210	382.8	433.3	994.3
2019	6	8	15	52	59.971	-50.91948	-73.58281	4.43	2.8	54	0.302	396.4	421.7	1103.7

ORIGIN TIME (UTC)						Latitude	Longitude	Depth	M_L	GAP	RMS	X error	Y error	Z error
yyyy	mm	dd	h	m	seconds	[°]	[°]	[Km]		[°]		[m]	[m]	[m]
2019	6	8	16	42	58.043	-50.92048	-73.58816	5.51	2.8	54	0.173	451.9	462.6	1146.2
2019	6	8	18	6	3.643	-50.91764	-73.58230	5.65	2.8	54	0.388	377.5	392.7	807.2
2019	6	8	20	36	41.876	-50.91604	-73.57549	6.00	2.8	54	0.267	397.1	429.0	848.3
2019	6	8	21	37	56.621	-50.91844	-73.58620	5.38	2.7	54	0.187	423.0	419.1	1013.7
2019	6	8	22	33	25.895	-50.91771	-73.56968	6.00	2.7	53	0.330	423.3	453.3	853.6
2019	6	8	23	28	1.085	-50.92579	-73.59017	4.24	2.9	53	0.130	431.7	448.9	1136.6
2019	6	9	0	15	26.928	-50.92090	-73.58526	4.83	2.8	54	0.116	402.4	429.1	1088.5
2019	6	9	1	13	0.005	-50.91563	-73.57645	6.00	2.9	53	0.419	393.7	405.5	709.1
2019	6	9	2	4	26.600	-50.92296	-73.58334	4.87	2.7	53	0.135	435.9	473.6	1176.9
2019	6	9	3	1	33.200	-50.91968	-73.58427	4.34	2.7	54	0.142	403.1	441.1	1232.0
2019	6	9	3	54	9.951	-50.92155	-73.57798	5.39	2.8	53	0.281	413.6	459.0	1532.4
2019	6	9	4	45	15.875	-50.92050	-73.58428	4.58	2.9	54	0.303	400.5	443.0	974.9
2019	6	9	5	38	8.287	-50.91968	-73.58427	4.79	2.7	54	0.125	403.8	444.2	1259.9
2019	6	9	6	32	58.042	-50.92008	-73.58525	4.44	2.8	59	0.148	441.0	471.7	1289.6
2019	6	9	7	38	31.821	-50.91439	-73.57838	6.00	2.8	54	0.289	376.5	398.0	872.0
2019	6	9	8	35	43.656	-50.91599	-73.58519	5.38	2.7	54	0.338	391.4	443.9	1271.6
2019	6	9	9	37	56.875	-50.91522	-73.57645	6.00	2.9	59	0.277	418.2	461.3	1086.6
2019	6	9	10	30	9.228	-50.91604	-73.57549	6.00	2.8	54	0.517	407.5	421.7	1087.8
2019	6	9	11	45	48.315	-50.91684	-73.57938	6.00	2.7	54	0.273	375.6	378.1	874.3
2019	6	9	12	58	26.511	-50.91804	-73.58425	5.92	2.8	54	0.356	369.0	461.2	996.7
2019	6	9	14	11	23.821	-50.91642	-73.58229	6.00	2.8	54	0.281	395.7	401.7	953.1
2019	6	9	14	58	27.712	-50.92581	-73.58532	6.82	2.7	53	0.181	454.4	476.6	1279.0
2019	6	9	17	17	55.960	-50.90888	-75.06087	9.88	3.0	185	0.300	802.4	537.8	887.6
2019	6	9	17	32	10.163	-50.91604	-73.57646	6.00	2.7	54	0.280	395.0	441.9	926.7
2019	6	9	19	40	11.089	-50.91765	-73.58036	6.00	2.7	54	0.291	376.0	427.9	891.0
2019	6	9	20	35	32.110	-50.93129	-73.59364	4.61	2.8	53	0.308	468.3	514.5	1658.5
2019	6	9	21	33	17.105	-50.92046	-73.59108	3.85	2.7	54	0.226	438.8	514.5	1592.1
2019	6	10	0	41	36.676	-50.92049	-73.58525	4.71	2.8	54	0.140	453.6	473.4	1228.6
2019	6	10	3	17	20.220	-50.92072	-73.58186	4.53	2.8	75	0.108	489.4	581.3	1572.3
2019	6	10	5	7	8.782	-50.92176	-73.57750	4.89	2.8	53	0.177	377.3	430.0	1284.3
2019	6	10	6	1	0.516	-50.91559	-73.58422	2.99	3.0	54	0.372	383.3	470.3	591.2
2019	6	10	7	5	10.109	-50.92132	-73.58332	4.38	2.8	75	0.121	437.3	459.6	1323.9
2019	6	10	8	19	42.789	-50.91033	-73.57154	6.00	2.8	54	0.387	362.5	396.5	675.1
2019	6	10	9	6	4.859	-50.92315	-73.58577	4.80	2.9	53	0.123	472.6	493.8	1455.2
2019	6	10	9	59	12.761	-50.92320	-73.61635	9.93	3.0	94	0.762	514.4	489.1	963.2
2019	6	10	14	5	45.343	-50.92171	-73.58818	4.77	2.9	59	0.205	478.7	473.4	1158.5
2019	6	10	20	11	20.472	-50.91598	-73.58714	8.37	3.0	54	0.314	451.8	493.5	1383.0
2019	6	10	23	32	50.450	-50.91919	-73.60077	8.48	2.8	76	0.377	407.5	479.4	929.8
2019	6	11	1	6	2.407	-50.91929	-73.58038	7.74	2.9	54	0.323	397.0	448.1	1404.5
2019	6	11	2	8	8.637	-50.91326	-73.59923	3.32	2.9	77	0.333	395.4	450.7	970.5
2019	6	11	3	27	8.429	-50.92010	-73.58136	4.67	2.9	54	0.143	402.6	433.1	1077.8
2019	6	11	4	15	26.437	-50.91804	-73.58522	4.62	2.9	54	0.144	370.5	423.6	1184.3
2019	6	11	5	32	36.951	-50.92401	-73.57801	8.08	3.0	53	0.367	390.7	398.8	1272.9
2019	6	11	6	20	51.564	-50.92193	-73.58478	4.39	2.7	75	0.115	519.1	596.7	1640.0
2019	6	11	7	40	11.978	-50.92213	-73.58527	7.80	2.9	54	0.360	374.3	405.6	1327.6
2019	6	11	8	48	48.152	-50.91876	-73.60367	3.68	2.9	76	0.246	444.2	514.5	1448.3
2019	6	11	10	24	31.466	-50.92053	-73.57749	6.00	2.8	53	0.159	345.7	403.8	966.1

ORIGIN TIME (UTC)						Latitude	Longitude	Depth	M_L	GAP	RMS	X error	Y error	Z error
yyyy	mm	dd	h	m	seconds	[°]	[°]	[Km]		[°]		[m]	[m]	[m]
2019	6	11	11	20	53.131	-50.92110	-73.58672	4.27	2.9	54	0.268	365.3	401.4	995.7
2019	6	11	12	10	52.889	-50.92380	-73.57753	6.00	2.7	53	0.214	393.5	453.4	1051.6
2019	6	11	14	23	1.645	-50.91068	-73.58416	2.29	2.8	54	0.376	379.5	389.2	576.5
2019	6	11	15	20	26.905	-50.92010	-73.58136	4.79	2.8	54	0.146	402.1	441.9	1103.5
2019	6	11	16	20	50.981	-50.91724	-73.58230	3.05	2.8	54	0.213	384.5	445.6	812.4
2019	6	11	17	33	37.249	-50.91931	-73.57747	5.44	2.7	75	0.216	356.7	401.9	949.0
2019	6	11	18	43	58.496	-50.91848	-73.57940	5.38	2.7	54	0.154	400.0	438.0	1052.4
2019	6	11	19	24	38.066	-50.91559	-73.58519	5.46	2.7	54	0.205	436.1	427.5	1062.0
2019	6	11	19	57	33.666	-50.92172	-73.58527	5.10	2.7	54	0.232	404.5	408.2	1007.7
2019	6	11	20	47	33.468	-51.83074	-72.84342	9.89	3.0	81	0.382	425.5	435.0	1459.9
2019	6	11	21	19	46.671	-50.91991	-73.57990	5.97	2.9	75	0.148	384.5	431.0	934.4
2019	6	11	22	22	14.919	-50.92071	-73.58380	4.61	2.7	54	0.167	390.0	428.7	1108.7
2019	6	11	23	11	28.810	-50.91804	-73.58425	3.40	2.7	54	0.184	396.3	448.0	976.8
2019	6	12	0	4	51.998	-50.92193	-73.58478	3.92	2.8	54	0.147	396.4	437.1	1157.6
2019	6	12	0	44	43.272	-50.91042	-73.55310	3.50	2.7	54	0.462	437.8	485.0	1003.2
2019	6	12	1	35	10.711	-50.92255	-73.58236	6.00	2.8	53	0.176	375.4	415.0	953.4
2019	6	12	3	7	56.350	-50.92175	-73.58041	5.48	2.7	53	0.207	385.2	424.9	900.5
2019	6	12	4	37	41.304	-50.92542	-73.58143	8.54	2.6	53	0.594	446.0	461.6	1351.3
2019	6	12	5	19	45.469	-50.92216	-73.57848	5.48	2.7	68	0.227	395.9	392.0	846.4
2019	6	12	5	53	5.908	-50.92330	-73.59597	2.74	2.7	54	0.270	378.0	446.4	668.1
2019	6	12	6	28	30.580	-50.92585	-73.57658	4.36	2.6	67	0.198	441.0	453.0	1094.1
2019	6	12	7	52	26.156	-50.91969	-73.58233	4.01	2.7	54	0.281	381.8	390.4	906.8
2019	6	12	8	49	24.272	-50.92134	-73.57944	4.83	2.6	68	0.117	401.6	409.2	1119.2
2019	6	12	9	32	21.157	-50.91971	-73.57845	4.30	2.7	68	0.117	435.0	452.0	1191.8
2019	6	12	10	3	47.178	-50.92012	-73.57845	5.30	2.6	68	0.110	471.5	477.9	1229.0
2019	6	12	10	55	51.386	-50.92398	-73.58384	5.19	2.8	53	0.266	368.9	391.3	980.4
2019	6	12	11	42	18.991	-50.92052	-73.58040	5.22	2.7	54	0.169	411.2	441.8	1190.4
2019	6	12	13	2	28.175	-50.91848	-73.57843	4.89	2.6	68	0.118	389.3	409.9	1156.5
2019	6	12	13	28	25.029	-50.91579	-73.58568	5.97	2.6	68	0.174	474.8	505.2	1111.1
2019	6	12	16	21	31.737	-50.92011	-73.58039	6.00	2.6	54	0.142	370.6	395.7	903.4
2019	6	12	16	57	32.028	-50.92059	-73.56584	6.00	2.6	53	0.371	437.3	448.5	849.8
2019	6	12	17	50	30.158	-50.91636	-73.59394	2.17	2.8	54	0.253	351.3	397.2	595.2
2019	6	12	18	17	18.777	-50.92131	-73.58526	4.83	2.7	54	0.155	425.2	508.5	1380.0
2019	6	12	18	47	25.595	-50.91804	-73.58425	3.81	2.8	54	0.283	367.1	399.2	945.9
2019	6	12	20	3	36.417	-50.92254	-73.58528	4.73	2.7	54	0.274	350.8	383.8	893.4
2019	6	12	21	19	2.255	-50.92215	-73.58042	6.00	2.7	53	0.154	346.3	350.7	835.5
2019	6	12	22	3	36.957	-50.92007	-73.58913	3.52	2.8	54	0.273	326.5	359.5	664.1
2019	6	12	22	27	28.571	-50.47901	-74.55161	33.28	2.3	106	0.172	839.0	490.9	1260.3
2019	6	12	23	49	3.711	-50.90931	-73.57201	3.71	2.7	54	0.392	374.1	434.3	866.4
2019	6	13	0	26	21.529	-50.92500	-73.58337	6.00	2.8	53	0.248	363.9	413.6	660.1
2019	6	13	1	2	55.816	-50.91886	-73.58523	3.21	2.5	54	0.353	372.4	394.8	789.0
2019	6	13	2	11	58.774	-50.92380	-73.57947	6.00	2.7	53	0.147	355.1	391.4	898.6
2019	6	13	2	37	22.239	-50.92255	-73.58334	4.75	2.7	53	0.133	389.1	419.7	1169.8
2019	6	13	3	24	14.016	-50.92293	-73.58819	3.60	2.7	54	0.260	361.3	397.3	936.8
2019	6	13	4	14	6.187	-50.92049	-73.58622	3.17	2.7	54	0.297	350.7	395.4	692.2
2019	6	13	4	49	52.904	-50.92212	-73.58818	3.39	2.6	54	0.217	391.5	467.1	1079.3
2019	6	13	5	32	37.403	-50.92276	-73.58285	4.74	2.6	57	0.184	420.4	497.2	1144.9

ORIGIN TIME (UTC)						Latitude	Longitude	Depth	M_L	GAP	RMS	X error	Y error	Z error
yyyy	mm	dd	h	m	seconds	[°]	[°]	[Km]		[°]		[m]	[m]	[m]
2019	6	13	6	14	41.113	-50.92400	-73.57996	6.01	2.6	53	0.266	304.0	368.9	933.2
2019	6	13	6	36	44.389	-50.63036	-74.40848	18.72	2.4	111	0.167	434.3	263.8	565.6
2019	6	13	7	23	55.685	-50.92050	-73.58428	4.85	2.6	54	0.251	330.2	368.8	994.4
2019	6	13	8	5	1.537	-50.92560	-73.58580	2.85	2.5	53	0.172	381.8	440.9	822.8
2019	6	13	8	47	11.090	-50.92543	-73.58046	4.03	2.6	53	0.309	359.0	399.8	879.9
2019	6	13	9	32	0.601	-50.91558	-73.58616	3.19	2.7	54	0.220	343.2	412.4	830.9
2019	6	13	9	48	24.014	-49.80041	-73.42988	10.54	2.5	158	0.573	530.4	899.5	1873.4
2019	6	13	10	9	52.496	-50.92457	-73.58821	3.31	2.6	53	0.148	396.4	422.0	1017.1
2019	6	13	10	44	14.137	-50.92090	-73.58526	4.30	2.6	54	0.272	342.2	388.2	1020.1
2019	6	13	11	34	51.853	-50.91560	-73.58131	6.00	2.5	54	0.222	360.6	394.4	735.4
2019	6	13	12	53	8.857	-50.92132	-73.58429	5.79	2.7	54	0.177	357.2	372.4	879.1
2019	6	13	13	41	38.517	-50.92865	-73.59118	5.49	2.5	53	0.221	382.8	428.2	1044.5
2019	6	13	14	26	6.589	-51.19953	-72.42465	12.17	2.6	66	0.389	335.3	327.3	948.7
2019	6	13	14	42	5.700	-50.92174	-73.58138	3.46	2.6	53	0.264	366.8	432.5	906.0
2019	6	13	15	34	54.077	-50.91687	-73.57259	6.00	2.5	69	0.274	424.9	458.9	919.9
2019	6	13	16	12	46.687	-50.92010	-73.58233	4.65	2.6	54	0.133	425.9	448.9	1271.9
2019	6	13	16	56	23.185	-50.92050	-73.58331	5.20	2.5	54	0.197	361.2	438.8	993.6
2019	6	13	17	26	55.709	-50.92073	-73.57797	5.78	2.4	53	0.187	479.3	566.6	1245.3
2019	6	13	18	1	34.461	-50.92505	-73.57463	6.00	2.4	68	0.252	406.4	437.0	868.1
2019	6	13	18	39	3.679	-50.92092	-73.58137	5.46	2.4	54	0.177	391.8	479.8	992.2
2019	6	13	19	15	39.825	-50.92501	-73.58142	7.12	2.4	53	0.425	426.5	438.7	1281.8
2019	6	13	19	55	1.984	-50.92562	-73.58192	4.76	2.5	53	0.309	360.0	415.4	881.4
2019	6	13	20	42	25.890	-50.92094	-73.57846	6.00	2.4	53	0.349	366.9	397.6	657.8
2019	6	13	21	5	16.876	-50.92584	-73.58046	4.58	2.3	56	0.277	469.9	481.3	1368.1
2019	6	13	22	5	7.438	-50.91925	-73.58912	2.72	2.6	54	0.206	360.6	396.7	698.8
2019	6	13	22	38	29.538	-50.92151	-73.58575	3.94	2.5	67	0.233	410.9	427.2	947.7
2019	6	13	23	22	48.409	-50.92131	-73.58526	4.54	2.5	54	0.156	391.6	406.8	1031.9
2019	6	14	0	10	51.254	-50.93136	-73.58005	9.14	2.5	53	0.692	385.7	429.1	858.5
2019	6	14	0	54	51.778	-50.92619	-73.59212	3.01	3.3	53	0.242	372.5	419.2	788.0
2019	6	14	1	40	8.883	-50.90788	-73.57151	2.70	2.7	54	0.513	386.0	405.9	960.8
2019	6	14	2	24	10.546	-50.94054	-73.58453	2.00	2.6	54	0.696	374.3	412.1	602.9
2019	6	14	2	54	22.019	-50.92091	-73.58331	4.65	2.3	54	0.172	379.9	420.2	949.3
2019	6	14	4	25	5.144	-50.91887	-73.58232	3.78	2.4	54	0.229	360.2	420.9	944.2
2019	6	14	5	11	56.455	-50.92051	-73.58234	4.30	2.4	54	0.251	344.8	413.1	957.8
2019	6	14	5	37	22.282	-50.92380	-73.57850	5.90	2.4	56	0.336	403.1	463.6	823.3
2019	6	14	6	13	2.981	-50.92372	-73.59500	1.26	2.3	54	0.191	380.6	431.1	1374.3
2019	6	14	6	56	46.186	-50.92049	-73.58622	3.68	2.5	54	0.183	352.7	397.7	903.8
2019	6	14	7	38	25.884	-50.92070	-73.58574	3.55	2.4	54	0.153	393.9	435.6	1143.7
2019	6	14	8	24	22.213	-51.07330	-74.19884	16.73	2.7	112	0.348	436.4	273.1	792.2
2019	6	14	8	40	53.592	-50.92132	-73.58332	5.20	2.5	54	0.225	318.0	359.4	1057.8
2019	6	14	9	43	53.189	-51.94438	-74.34949	20.00	2.9	233	0.327	1262.5	1310.8	798.3
2019	6	14	9	59	44.989	-50.91969	-73.58330	3.95	2.5	54	0.251	343.3	385.3	921.1
2019	6	14	10	59	7.725	-50.91967	-73.58621	3.78	2.5	54	0.243	335.4	381.3	879.4
2019	6	14	12	8	14.476	-50.91847	-73.58134	4.87	2.4	54	0.168	352.8	430.2	977.9
2019	6	14	12	37	32.288	-50.93098	-73.57519	10.29	2.4	53	0.786	407.7	458.7	879.6
2019	6	14	13	37	21.830	-50.92006	-73.59010	3.78	2.4	54	0.217	377.3	438.7	1063.0
2019	6	14	14	4	37.885	-51.02438	-74.33477	21.84	2.7	123	0.734	517.3	400.0	538.2

ORIGIN TIME (UTC)						Latitude	Longitude	Depth	M_L	GAP	RMS	X error	Y error	Z error
yyyy	mm	dd	h	m	seconds	[°]	[°]	[Km]		[°]		[m]	[m]	[m]
2019	6	14	14	10	56.778	-50.92213	-73.58527	5.24	2.4	54	0.185	386.5	403.2	1079.1
2019	6	14	14	46	53.138	-50.91849	-73.57746	5.61	2.5	54	0.167	398.3	392.7	936.0
2019	6	14	15	33	22.687	-50.92909	-73.58342	3.25	2.4	101	0.190	468.6	535.8	972.1
2019	6	14	15	39	50.571	-50.88811	-73.21694	6.00	3.2	50	0.488	316.9	230.2	235.8
2019	6	14	16	34	26.422	-49.53468	-73.64539	12.40	2.6	211	0.359	379.1	685.7	1283.2
2019	6	14	16	40	56.110	-50.92295	-73.58431	4.64	2.5	53	0.147	365.1	383.6	1214.2
2019	6	14	17	49	26.608	-50.91974	-73.57262	4.11	2.6	53	0.280	379.2	401.5	931.3
2019	6	14	18	42	35.917	-50.91988	-73.58573	4.68	2.5	54	0.179	417.5	517.0	1359.1
2019	6	14	20	18	25.550	-50.93237	-73.58346	1.98	2.6	53	0.530	394.7	384.8	404.5
2019	6	14	21	14	1.200	-50.92070	-73.58574	3.71	2.7	54	0.268	352.4	382.8	772.9
2019	6	14	22	2	7.025	-50.91643	-73.58035	3.85	2.5	68	0.166	518.3	506.8	1136.8
2019	6	14	22	34	34.669	-50.91767	-73.57648	5.98	2.7	54	0.271	330.2	359.5	704.9
2019	6	14	23	20	11.351	-50.92170	-73.58915	3.01	2.6	54	0.401	501.9	561.5	884.7
2019	6	15	0	7	13.448	-50.92049	-73.58525	3.76	2.7	54	0.208	334.5	356.2	874.2
2019	6	15	1	38	42.831	-50.91928	-73.58232	7.29	2.7	53	0.353	340.1	379.4	1446.0
2019	6	15	3	25	39.105	-50.91602	-73.57937	3.03	2.8	54	0.212	337.6	374.4	767.9
2019	6	15	4	48	14.045	-50.92049	-73.58525	3.72	2.7	54	0.224	323.8	344.1	854.8
2019	6	15	5	49	59.872	-50.92090	-73.58526	4.07	2.6	54	0.253	346.2	379.2	935.1
2019	6	15	6	59	4.004	-50.91968	-73.58427	3.72	2.7	54	0.240	347.7	401.9	906.3
2019	6	15	8	11	5.947	-50.91967	-73.58621	3.54	2.6	54	0.255	338.2	354.3	783.2
2019	6	15	9	0	15.204	-50.92171	-73.58721	3.01	2.6	54	0.215	343.4	378.9	727.0
2019	6	15	12	2	17.530	-50.91638	-73.59005	2.27	2.6	54	0.277	342.4	387.2	515.7
2019	6	15	13	30	17.368	-50.91925	-73.58912	4.15	2.7	54	0.170	360.4	388.9	1043.4
2019	6	15	16	10	11.796	-50.92008	-73.58525	5.28	2.6	54	0.300	329.6	362.0	753.5
2019	6	15	17	30	24.984	-50.92214	-73.58236	5.38	2.6	53	0.160	364.7	401.1	1042.0
2019	6	15	17	53	23.908	-50.91438	-73.58032	4.62	2.5	54	0.228	414.1	503.1	1175.6
2019	6	15	18	27	38.356	-50.45168	-74.43393	21.63	3.0	98	0.422	348.1	306.8	582.7
2019	6	15	19	2	29.345	-50.91805	-73.58231	4.07	2.7	54	0.238	377.1	415.5	1177.8
2019	6	15	20	1	4.070	-50.91931	-73.57747	6.00	2.8	54	0.294	384.8	381.0	713.8
2019	6	15	21	17	4.476	-50.92162	-73.56439	3.59	2.7	53	0.373	374.4	428.2	813.5
2019	6	15	22	23	4.911	-50.92256	-73.58139	5.67	2.8	53	0.184	367.0	401.4	960.8
2019	6	15	23	14	50.189	-50.91885	-73.58717	4.67	2.9	54	0.301	378.2	472.9	1037.6
2019	6	16	0	5	59.398	-50.92251	-73.59013	3.17	3.2	54	0.185	386.4	435.8	941.3
2019	6	16	0	36	8.838	-50.91106	-73.58999	6.00	3.0	53	0.489	439.6	523.6	939.8
2019	6	16	1	35	57.144	-50.92007	-73.58816	2.90	3.0	54	0.248	361.0	414.8	720.8
2019	6	16	2	15	32.770	-50.92858	-73.60380	3.01	3.0	65	0.440	506.3	473.6	946.7
2019	6	16	2	53	15.310	-50.92071	-73.58380	5.27	2.7	54	0.245	339.2	390.3	1226.1
2019	6	16	4	15	58.095	-50.91575	-73.59344	1.95	2.8	54	0.235	339.6	413.3	393.8
2019	6	16	5	38	39.485	-50.92131	-73.58526	4.85	3.0	54	0.277	328.6	383.1	1353.7
2019	6	16	6	32	49.606	-50.92132	-73.58429	5.12	2.8	54	0.369	367.5	433.6	904.8
2019	6	16	7	49	21.160	-50.91596	-73.59102	2.90	2.9	54	0.246	369.1	375.9	721.0
2019	6	16	9	29	44.565	-50.19598	-74.34738	27.30	2.7	102	0.297	1045.2	595.2	901.1
2019	6	16	9	40	55.229	-50.20510	-74.38923	20.01	2.7	100	0.550	418.7	301.8	445.9
2019	6	16	11	33	48.583	-51.81286	-74.47029	20.00	3.1	226	0.496	1039.0	1048.1	521.2
2019	6	16	11	37	55.000	-50.91904	-73.58960	2.89	3.0	54	0.205	355.1	392.4	853.7
2019	6	16	12	14	39.963	-50.92338	-73.58043	4.89	3.0	80	0.243	468.5	486.1	1281.9
2019	6	16	13	7	4.748	-50.92175	-73.57847	5.63	2.9	53	0.158	379.6	415.1	1127.1

ORIGIN TIME (UTC)						Latitude	Longitude	Depth	M_L	GAP	RMS	X error	Y error	Z error
yyyy	mm	dd	h	m	seconds	[°]	[°]	[Km]		[°]		[m]	[m]	[m]
2019	6	16	14	13	1.017	-50.92463	-73.57657	3.05	3.1	53	0.323	345.6	348.4	595.8
2019	6	16	15	4	22.898	-50.92296	-73.58237	5.38	2.9	53	0.215	387.8	424.1	1047.9
2019	6	16	16	21	24.903	-50.92338	-73.58140	6.00	2.8	100	0.211	442.6	525.6	931.3
2019	6	16	16	52	32.648	-50.92234	-73.58382	3.63	2.9	53	0.199	336.3	353.7	814.2
2019	6	16	17	47	38.528	-50.92296	-73.58237	4.79	2.9	53	0.251	397.6	419.3	1174.2
2019	6	16	20	57	23.798	-50.91721	-73.58812	3.76	2.9	54	0.280	353.6	424.5	946.7
2019	6	16	22	7	19.433	-51.11212	-75.26489	24.02	3.4	216	0.394	1089.5	628.1	1083.4
2019	6	16	23	3	11.405	-50.92008	-73.58622	3.27	3.0	53	0.427	347.4	405.1	816.2
2019	6	17	0	9	5.562	-50.92478	-73.58773	5.47	3.0	53	0.434	361.9	389.0	1054.7
2019	6	17	1	20	24.098	-50.91926	-73.58718	2.70	3.0	54	0.234	336.3	378.4	640.7
2019	6	17	2	14	32.230	-50.92091	-73.58429	4.60	3.0	54	0.246	326.4	388.9	953.9
2019	6	17	3	0	27.648	-50.91848	-73.57940	4.09	2.8	54	0.335	387.7	454.0	882.9
2019	6	17	3	41	46.973	-50.92398	-73.58384	5.58	2.9	53	0.244	380.2	410.7	1180.3
2019	6	17	3	54	7.134	-51.39881	-73.15583	4.67	3.0	75	0.528	419.3	369.6	1080.4
2019	6	17	4	57	24.926	-50.91499	-73.58178	3.28	3.0	54	0.333	354.4	422.2	801.4
2019	6	17	6	11	54.911	-50.91906	-73.58572	4.65	2.9	54	0.217	332.9	359.3	907.3
2019	6	17	7	0	4.552	-50.92255	-73.58236	4.62	3.1	53	0.179	404.0	518.1	1153.0
2019	6	17	7	19	37.543	-50.92050	-73.58331	5.28	3.0	54	0.222	343.7	400.0	1009.6
2019	6	17	8	25	52.128	-50.91927	-73.58524	3.93	3.0	54	0.150	357.7	367.5	1009.6
2019	6	17	9	11	19.119	-50.92255	-73.58334	5.46	2.9	53	0.238	400.3	420.3	931.9
2019	6	17	10	10	6.377	-50.91194	-73.57738	3.56	2.9	54	0.311	417.5	470.5	924.2
2019	6	17	11	14	20.290	-50.91822	-73.58959	3.94	2.9	54	0.205	323.3	353.9	957.7
2019	6	17	12	20	43.706	-50.92622	-73.58532	2.60	3.0	53	0.383	352.9	382.6	630.1
2019	6	17	13	18	39.857	-50.92824	-73.59117	4.58	2.9	53	0.298	354.6	410.4	949.9
2019	6	17	14	1	57.947	-50.92373	-73.59209	3.91	2.9	54	0.211	397.9	414.9	1043.9
2019	6	17	14	36	34.461	-50.91071	-73.57833	5.94	2.7	54	0.220	403.0	495.7	1102.4
2019	6	17	15	58	30.514	-50.92173	-73.58430	5.89	2.9	54	0.350	331.5	361.4	826.3
2019	6	17	16	57	24.649	-50.92458	-73.58627	5.26	2.8	53	0.165	410.7	450.1	1219.7
2019	6	17	17	36	5.401	-50.92070	-73.58574	3.43	3.0	54	0.215	365.6	386.1	804.9
2019	6	17	19	20	17.244	-50.92131	-73.58623	4.50	3.0	54	0.155	347.5	375.2	1002.9
2019	6	17	19	55	36.268	-50.91765	-73.58133	4.99	2.9	57	0.212	412.1	435.3	991.4
2019	6	17	20	5	48.439	-50.62025	-74.42434	17.89	3.0	111	0.445	361.4	233.4	448.4
2019	6	17	20	52	8.493	-50.92174	-73.58235	5.83	3.0	53	0.183	350.9	375.1	959.4
2019	6	17	22	39	38.728	-50.92072	-73.58186	5.35	3.0	54	0.160	349.4	364.6	988.7
2019	6	17	23	22	30.049	-50.91923	-73.59300	5.26	2.9	100	0.305	390.2	473.6	918.3
2019	6	18	0	15	30.327	-50.92007	-73.58719	4.42	2.9	54	0.301	335.2	369.0	1107.4
2019	6	18	0	50	41.631	-50.92419	-73.58141	5.85	3.0	53	0.273	386.8	443.7	810.7
2019	6	18	1	52	27.468	-52.03791	-74.17125	11.25	3.4	230	0.624	1767.2	2620.4	1585.8
2019	6	18	2	3	11.739	-50.92172	-73.58527	4.56	2.9	54	0.226	336.2	356.5	1016.0
2019	6	18	3	1	48.027	-50.92743	-73.58825	4.44	2.8	53	0.246	401.8	438.1	928.4
2019	6	18	3	45	16.038	-50.91557	-73.58810	3.23	3.0	54	0.226	323.4	359.2	705.0
2019	6	18	4	30	55.430	-50.92108	-73.59060	3.10	3.0	54	0.232	340.2	406.5	735.3
2019	6	18	5	10	19.438	-50.92296	-73.58334	4.75	2.8	53	0.131	399.2	446.7	1205.2
2019	6	18	6	10	4.555	-50.92090	-73.58623	4.15	3.0	54	0.245	337.5	365.4	916.1
2019	6	18	6	41	2.518	-50.92255	-73.58334	5.38	2.8	53	0.144	365.7	387.6	1114.2
2019	6	18	7	35	39.653	-50.92214	-73.58333	5.16	3.0	53	0.196	357.9	384.6	989.8
2019	6	18	8	26	7.331	-50.91743	-73.58376	4.10	2.8	54	0.215	355.1	411.7	970.2

ORIGIN TIME (UTC)						Latitude	Longitude	Depth	M_L	GAP	RMS	X error	Y error	Z error
yyyy	mm	dd	h	m	seconds	[°]	[°]	[Km]		[°]		[m]	[m]	[m]
2019	6	18	8	59	40.979	-50.92215	-73.58139	4.93	2.8	53	0.187	369.6	378.2	1125.5
2019	6	18	10	28	14.440	-50.92091	-73.58331	4.50	2.9	54	0.269	349.9	381.3	1009.6
2019	6	18	11	15	30.056	-50.92129	-73.59012	4.40	2.9	54	0.295	366.2	428.4	1034.0
2019	6	18	13	14	37.943	-50.91928	-73.58232	6.00	2.9	54	0.351	358.2	397.6	944.0
2019	6	18	13	58	46.307	-50.92214	-73.58236	7.10	2.9	53	0.310	363.1	396.2	1202.0
2019	6	18	15	31	10.911	-50.91923	-73.59300	2.76	3.0	54	0.224	369.2	433.2	973.1
2019	6	18	16	12	28.812	-51.80085	-74.23437	10.00	3.1	195	0.494	564.2	642.6	739.9
2019	6	18	17	5	15.960	-50.92141	-73.60516	7.30	2.9	54	0.406	346.8	388.4	1458.2
2019	6	18	17	49	19.497	-50.89853	-73.55878	6.00	2.7	59	0.549	362.3	393.7	491.9
2019	6	18	18	15	15.882	-50.45143	-73.76783	11.00	2.8	91	0.810	318.6	431.9	604.6
2019	6	18	18	53	13.885	-50.92092	-73.58137	6.06	2.9	53	0.145	356.7	388.6	991.1
2019	6	18	20	39	0.112	-50.92071	-73.58380	4.80	2.8	54	0.253	351.6	384.0	1097.5
2019	6	18	21	24	51.858	-50.92562	-73.58192	6.05	2.8	53	0.255	398.9	453.6	1030.6
2019	6	18	22	23	59.955	-50.91689	-73.56870	6.00	2.8	53	0.306	378.9	450.0	892.1
2019	6	18	23	31	32.407	-50.92253	-73.58722	5.63	3.0	53	0.248	373.0	447.7	1128.5
2019	6	19	0	5	6.736	-51.26086	-72.97787	4.14	3.1	62	0.586	330.5	298.4	587.7
2019	6	19	0	34	43.389	-50.92172	-73.58624	4.54	2.9	54	0.156	388.1	463.7	1337.2
2019	6	19	1	20	20.000	-50.91805	-73.58328	8.99	2.6	54	0.389	393.8	396.7	1024.8
2019	6	19	2	31	36.128	-50.92049	-73.58525	5.10	2.7	54	0.207	350.2	417.9	1044.8
2019	6	19	4	13	34.078	-50.92165	-73.59983	2.99	2.7	54	0.200	372.6	385.9	932.9
2019	6	19	5	5	30.735	-50.91475	-73.58809	6.00	2.8	59	0.376	369.3	401.5	706.8
2019	6	19	6	53	34.541	-50.92295	-73.58528	5.77	2.8	95	0.268	388.2	447.3	1235.0
2019	6	19	7	41	36.396	-50.91643	-73.58035	6.00	2.9	54	0.371	370.4	406.9	845.4
2019	6	19	8	38	19.634	-50.91686	-73.57647	6.00	2.8	54	0.338	401.2	431.8	794.7
2019	6	19	11	6	47.816	-50.91842	-73.59008	5.22	2.8	54	0.174	370.0	424.8	1010.2
2019	6	19	13	38	18.786	-50.92338	-73.58140	6.00	2.9	56	0.259	362.4	401.0	788.0
2019	6	19	14	30	35.582	-50.91825	-73.58377	4.41	2.8	57	0.284	368.9	453.1	1143.4
2019	6	19	15	46	57.326	-50.92297	-73.58140	6.18	2.8	53	0.147	402.6	443.6	1083.3
2019	6	19	16	44	40.811	-50.91357	-73.57837	4.48	2.8	76	0.513	404.8	431.7	852.1
2019	6	19	18	52	9.919	-50.91887	-73.58232	6.00	3.0	54	0.335	382.7	455.0	825.9
2019	6	19	19	51	40.108	-50.92052	-73.58040	8.99	3.0	54	0.385	353.3	405.5	914.5
2019	6	19	20	35	49.362	-50.62443	-74.40879	17.24	3.1	110	0.505	353.3	259.0	621.2
2019	6	19	21	23	5.851	-50.92433	-73.59452	2.87	2.8	54	0.331	352.8	391.5	843.0
2019	6	19	22	17	8.864	-50.91904	-73.58960	3.00	2.9	54	0.338	374.8	384.3	681.4
2019	6	19	22	51	19.600	-50.62637	-74.40064	18.15	2.8	110	0.608	335.6	260.3	600.4
2019	6	19	23	12	56.439	-50.91625	-73.57501	4.04	3.1	99	0.142	619.2	577.1	1871.8
2019	6	20	1	4	44.600	-50.92050	-73.58428	3.58	2.8	54	0.271	344.7	366.6	793.6
2019	6	20	1	36	30.459	-50.92133	-73.58235	9.01	2.8	54	0.539	380.2	414.2	1144.6
2019	6	20	2	30	44.702	-50.92011	-73.58039	5.65	2.7	75	0.115	367.3	417.1	1154.5
2019	6	20	3	29	18.557	-50.92274	-73.58674	4.74	2.8	54	0.274	321.0	372.5	865.1
2019	6	20	5	48	19.353	-50.92092	-73.58234	5.67	2.9	54	0.127	368.6	390.9	1058.5
2019	6	20	6	37	35.615	-50.92050	-73.58428	5.01	3.0	54	0.204	351.3	386.6	947.5
2019	6	20	8	22	57.630	-50.91308	-73.59584	2.90	2.9	54	0.591	344.9	386.1	629.9
2019	6	20	9	9	13.107	-50.92705	-73.58242	8.89	3.0	53	0.504	348.2	408.4	926.2
2019	6	20	9	35	24.987	-50.67175	-73.39482	3.01	2.8	61	0.285	407.6	464.0	863.9
2019	6	20	10	0	14.452	-50.92415	-73.59015	4.19	3.0	54	0.166	350.5	366.9	952.7
2019	6	20	10	18	27.206	-51.03235	-73.82702	10.10	2.7	67	0.257	322.8	370.7	965.3

ORIGIN TIME (UTC)						Latitude	Longitude	Depth	M_L	GAP	RMS	X error	Y error	Z error
yyyy	mm	dd	h	m	seconds	[°]	[°]	[Km]		[°]		[m]	[m]	[m]
2019	6	20	11	13	8.593	-50.92088	-73.59011	2.98	3.4	76	0.247	477.2	452.4	1015.1
2019	6	20	11	48	54.118	-50.92316	-73.58383	4.25	3.0	53	0.173	351.3	399.1	980.3
2019	6	20	13	11	29.231	-50.91598	-73.58714	2.60	3.0	54	0.212	335.6	362.7	670.5
2019	6	20	13	58	1.534	-50.92213	-73.58624	4.54	2.9	54	0.090	394.3	447.0	1143.7
2019	6	20	15	2	56.019	-50.92379	-73.58044	6.96	3.0	53	0.418	349.3	383.6	936.1
2019	6	20	15	59	55.018	-50.92233	-73.58576	3.90	3.0	54	0.217	349.9	384.3	990.8
2019	6	20	17	35	28.151	-50.92318	-73.57995	7.73	3.0	53	0.416	339.7	359.0	1131.1
2019	6	20	18	53	0.238	-50.91723	-73.58424	3.07	3.0	54	0.232	334.7	403.6	770.8
2019	6	20	20	31	12.603	-50.91826	-73.58183	4.84	2.9	54	0.252	332.1	390.6	1041.3
2019	6	20	21	37	37.772	-50.91888	-73.58135	4.36	3.0	54	0.248	353.9	384.2	1051.5
2019	6	20	22	23	34.588	-50.92295	-73.58528	4.60	3.0	53	0.254	363.1	408.5	1056.8
2019	6	20	23	18	14.191	-50.92235	-73.58188	4.61	3.0	53	0.278	363.8	395.6	924.3
2019	6	21	0	41	14.044	-50.91619	-73.58665	2.79	3.1	54	0.226	342.4	390.4	885.1
2019	6	21	1	56	14.764	-50.92091	-73.58429	4.50	3.0	54	0.288	344.0	393.4	962.3
2019	6	21	3	37	55.881	-50.92297	-73.58140	7.35	3.0	53	0.378	325.9	350.1	1310.9
2019	6	21	5	7	47.149	-50.91725	-73.58036	4.93	3.1	54	0.300	303.9	402.7	939.6
2019	6	21	6	2	29.180	-50.92459	-73.58336	5.44	3.0	53	0.286	364.3	413.4	1220.7
2019	6	21	6	43	42.715	-50.91538	-73.58470	3.14	3.0	54	0.486	366.5	414.6	706.6
2019	6	21	7	45	23.874	-50.91967	-73.58621	3.31	3.0	54	0.233	337.8	359.6	743.5
2019	6	21	8	36	30.998	-50.94260	-73.58164	6.00	3.1	54	0.580	341.6	329.8	358.5
2019	6	21	9	39	41.285	-50.92297	-73.58043	5.48	3.0	53	0.251	405.0	388.4	812.3
2019	6	21	10	4	52.529	-52.43633	-72.33641	15.18	3.5	167	0.828	567.0	687.8	920.9
2019	6	21	10	48	36.534	-50.92257	-73.57848	5.59	3.0	53	0.156	329.4	345.6	878.5
2019	6	21	12	8	40.282	-50.92051	-73.58234	4.81	3.0	54	0.327	346.5	374.8	924.4
2019	6	21	12	43	41.134	-50.88511	-73.54213	0.67	2.9	58	0.777	381.4	412.4	464.8
2019	6	21	13	43	44.933	-50.92236	-73.57994	5.66	3.0	53	0.141	386.5	415.2	961.9
2019	6	21	14	16	27.591	-50.92049	-73.58622	3.60	3.0	54	0.195	342.9	381.2	800.8
2019	6	21	15	27	49.253	-50.91969	-73.58233	5.22	3.0	54	0.346	364.2	381.3	965.5
2019	6	21	16	32	24.678	-50.92214	-73.58236	5.98	2.9	53	0.199	372.6	418.5	875.2
2019	6	21	17	54	28.066	-50.92132	-73.58429	5.53	3.0	54	0.347	369.0	381.9	983.2
2019	6	21	19	21	40.969	-50.92132	-73.58429	6.00	3.0	54	0.375	333.9	347.1	930.0
2019	6	21	20	40	52.481	-50.91765	-73.58036	5.98	2.9	54	0.339	333.1	373.6	924.3
2019	6	21	22	1	34.595	-50.91929	-73.58135	5.08	3.0	54	0.254	346.4	392.6	1042.3
2019	6	21	23	4	9.031	-50.92215	-73.58042	6.00	2.9	53	0.303	340.5	379.7	807.8
2019	6	22	0	22	44.110	-50.92540	-73.58531	5.98	3.0	53	0.269	346.8	386.9	965.2
2019	6	22	2	4	58.931	-50.92233	-73.58576	4.76	3.1	54	0.258	336.9	383.7	1012.8
2019	6	22	2	49	58.084	-50.91803	-73.58619	3.89	2.9	54	0.271	340.1	409.2	876.0
2019	6	22	3	6	52.751	-50.91475	-73.58906	3.35	3.0	54	0.349	349.1	391.5	732.1
2019	6	22	4	18	22.658	-50.92707	-73.57854	10.22	3.0	53	0.658	343.8	373.4	821.6
2019	6	22	4	33	47.442	-50.92131	-73.58526	5.57	3.1	54	0.284	325.3	382.6	957.6
2019	6	22	5	23	31.858	-50.92050	-73.58331	6.00	2.9	54	0.199	374.1	436.6	866.8
2019	6	22	5	49	9.491	-50.92254	-73.58431	4.87	2.9	53	0.240	331.0	355.3	1000.3
2019	6	22	7	15	52.195	-50.91825	-73.58377	4.29	3.1	54	0.258	331.1	354.4	841.5
2019	6	22	8	10	35.469	-50.92458	-73.58627	4.91	3.1	53	0.272	339.9	413.9	1190.4
2019	6	22	8	47	8.275	-50.92317	-73.58189	5.27	2.9	53	0.293	402.4	467.2	1420.8
2019	6	22	9	55	43.468	-50.91638	-73.58908	3.19	3.1	54	0.290	339.2	378.6	736.9
2019	6	22	10	51	35.164	-50.92250	-73.59304	2.82	3.0	54	0.458	348.3	376.2	857.9

ORIGIN TIME (UTC)						Latitude	Longitude	Depth	M_L	GAP	RMS	X error	Y error	Z error
yyyy	mm	dd	h	m	seconds	[°]	[°]	[Km]		[°]		[m]	[m]	[m]
2019	6	22	11	34	49.226	-50.92091	-73.58331	4.56	2.9	54	0.125	403.2	482.7	1436.9
2019	6	22	11	52	28.415	-50.92210	-73.59110	2.76	3.0	54	0.126	380.3	438.3	1059.0
2019	6	22	12	51	45.213	-50.92742	-73.59116	2.43	3.0	53	0.444	325.1	373.4	479.5
2019	6	22	14	14	48.673	-50.91479	-73.58033	3.03	2.9	54	0.468	334.9	425.1	658.6
2019	6	22	15	6	5.771	-50.92091	-73.58429	7.21	2.9	54	0.410	379.7	427.3	1113.9
2019	6	22	16	6	9.232	-50.91663	-73.57986	5.78	3.0	54	0.236	363.2	394.9	872.5
2019	6	22	17	6	50.195	-50.91948	-73.58281	4.74	3.1	80	0.147	478.6	468.9	1541.6
2019	6	22	17	37	8.758	-50.92212	-73.58721	4.30	2.9	54	0.229	357.2	374.8	1102.1
2019	6	22	18	35	2.378	-50.91310	-73.59195	6.00	2.9	54	0.378	303.8	402.9	556.3
2019	6	22	19	36	15.641	-50.92051	-73.58234	5.59	3.0	54	0.189	393.0	407.5	993.1
2019	6	22	19	48	55.484	-50.92091	-73.58429	4.75	2.9	54	0.216	368.0	397.4	1203.8
2019	6	22	20	50	29.183	-50.91948	-73.58281	5.99	2.8	59	0.174	387.7	446.1	1055.4
2019	6	22	21	21	33.176	-50.92172	-73.58624	4.81	2.8	54	0.273	316.9	344.4	1487.9
2019	6	22	22	12	10.294	-50.92377	-73.58432	5.12	2.8	53	0.320	357.6	423.5	1178.3
2019	6	22	23	10	25.841	-50.91401	-73.57352	6.00	2.7	54	0.352	353.0	378.2	638.6
2019	6	22	23	36	30.439	-50.91990	-73.58185	4.68	2.8	54	0.255	331.8	380.6	1119.1
2019	6	23	0	38	33.822	-50.92582	-73.58338	4.87	2.8	53	0.302	342.3	393.4	1090.4
2019	6	23	1	52	0.141	-50.90500	-73.57438	2.99	2.6	54	0.518	432.3	492.4	684.9
2019	6	23	2	27	18.426	-50.92213	-73.58430	4.65	2.8	54	0.187	335.3	359.7	1067.0
2019	6	23	3	11	19.932	-50.92744	-73.58728	4.91	2.8	53	0.338	365.3	412.7	1006.6
2019	6	23	4	9	35.309	-50.93479	-73.58931	4.01	2.9	53	0.460	346.1	369.7	684.3
2019	6	23	4	50	33.864	-50.91889	-73.57941	3.50	2.7	68	0.267	476.6	510.1	968.6
2019	6	23	6	14	52.180	-50.92172	-73.58624	5.22	2.8	54	0.244	359.7	419.5	980.8
2019	6	23	7	27	47.731	-50.92458	-73.58530	4.36	2.8	53	0.311	363.3	436.3	1113.4
2019	6	23	8	35	10.862	-50.91905	-73.58766	3.12	2.9	54	0.268	350.8	391.8	729.2
2019	6	23	10	0	40.674	-50.92048	-73.58719	3.19	2.8	57	0.201	352.4	392.7	837.5
2019	6	23	10	58	50.183	-50.92213	-73.58430	5.38	2.8	54	0.278	377.3	376.0	882.2
2019	6	23	11	57	32.156	-50.92132	-73.58429	4.13	2.9	54	0.266	357.1	398.5	889.6
2019	6	23	13	25	38.215	-50.91767	-73.57745	5.38	2.9	54	0.348	332.9	390.6	908.4
2019	6	23	15	11	31.614	-50.92176	-73.57653	6.00	3.0	53	0.455	328.7	343.3	822.5
2019	6	23	16	14	32.652	-50.92052	-73.58040	4.65	3.0	54	0.266	354.5	371.4	990.5
2019	6	23	18	44	3.588	-50.92317	-73.58189	5.47	3.0	53	0.264	360.4	360.9	838.7
2019	6	23	19	40	3.913	-50.91768	-73.57551	4.30	3.1	99	0.291	399.3	435.8	878.2
2019	6	23	20	56	22.252	-50.91562	-73.57840	3.01	3.0	54	0.419	407.6	454.2	853.2
2019	6	23	21	32	3.941	-50.91015	-73.56814	2.26	3.1	54	0.698	399.9	451.8	594.8
2019	6	23	23	18	42.396	-50.91968	-73.58524	4.73	3.1	54	0.285	363.0	373.8	913.4
2019	6	24	1	10	33.345	-50.92009	-73.58330	4.93	3.1	54	0.360	330.4	373.7	910.7
2019	6	24	2	19	36.795	-50.91969	-73.58233	5.96	3.0	54	0.344	335.0	396.0	712.1
2019	6	24	4	8	4.255	-50.92091	-73.58429	4.71	3.3	54	0.256	327.5	371.4	983.0
2019	6	24	5	9	25.726	-50.92254	-73.58431	5.12	3.0	53	0.264	338.6	377.0	1024.7
2019	6	24	6	19	0.389	-50.92010	-73.58136	5.98	3.1	54	0.366	338.4	373.1	711.1
2019	6	24	7	52	55.778	-50.92375	-73.58820	3.97	3.0	53	0.263	351.5	381.5	1140.5
2019	6	24	9	16	0.243	-50.91114	-73.57446	3.11	3.0	54	0.496	335.9	379.3	666.5
2019	6	24	10	24	34.667	-50.92259	-73.57557	8.99	2.9	53	0.587	333.0	411.6	790.4
2019	6	24	13	19	57.074	-50.92458	-73.58530	6.00	3.1	53	0.410	352.2	368.0	698.9
2019	6	24	14	39	38.694	-50.91441	-73.57547	4.40	3.0	54	0.397	315.1	405.6	824.2
2019	6	24	16	7	22.262	-50.91888	-73.58135	6.24	3.0	54	0.374	350.8	418.6	1031.8

ORIGIN TIME (UTC)						Latitude	Longitude	Depth	M_L	GAP	RMS	X error	Y error	Z error
yyyy	mm	dd	h	m	seconds	[°]	[°]	[Km]		[°]		[m]	[m]	[m]
2019	6	24	17	12	29.651	-50.91889	-73.57844	6.00	3.0	100	0.204	400.5	456.2	966.6
2019	6	24	18	52	37.795	-50.92580	-73.58726	4.87	3.1	53	0.247	360.8	368.3	1071.0
2019	6	24	20	54	0.608	-50.92379	-73.58141	6.00	3.2	53	0.142	334.1	340.5	774.2
2019	6	24	22	51	3.450	-50.92213	-73.58624	4.32	3.5	54	0.265	355.7	405.6	876.7
2019	6	25	0	23	14.926	-52.03115	-74.19295	17.85	3.3	231	0.491	895.8	1122.8	1187.9
2019	6	25	0	28	15.838	-50.91970	-73.58039	5.79	3.2	54	0.328	338.3	369.3	825.4
2019	6	25	2	7	27.794	-50.91189	-73.58708	3.07	3.2	54	0.396	343.3	400.1	725.0
2019	6	25	2	31	29.541	-52.52131	-74.08953	14.37	3.6	228	0.583	786.3	880.7	1455.2
2019	6	25	3	39	31.473	-50.92053	-73.57749	6.00	3.1	53	0.308	357.6	419.8	833.4
2019	6	25	4	35	15.020	-51.21445	-72.46550	8.40	3.1	74	0.210	407.6	350.8	1772.5
2019	6	25	4	43	11.945	-50.91930	-73.57941	6.00	3.1	54	0.323	372.2	389.3	823.6
2019	6	25	6	24	20.900	-50.91768	-73.57551	6.00	3.3	54	0.319	361.5	379.1	722.4
2019	6	25	8	5	17.615	-50.92009	-73.58330	5.38	3.0	74	0.259	355.2	427.9	1283.3
2019	6	25	9	35	17.725	-50.92132	-73.58332	7.35	3.1	74	0.376	365.0	427.5	1372.4
2019	6	25	11	32	42.084	-50.91887	-73.58232	6.00	3.0	74	0.350	339.2	414.6	821.0
2019	6	25	12	58	12.157	-50.91112	-73.57737	5.34	3.0	120	0.424	430.4	551.6	1184.1
2019	6	25	14	44	14.391	-50.91866	-73.58474	5.17	3.1	74	0.265	364.2	464.1	1102.5
2019	6	25	16	45	32.431	-50.91498	-73.58373	4.18	3.1	54	0.400	379.5	421.3	863.8
2019	6	25	17	58	52.160	-50.92091	-73.58331	5.20	3.1	54	0.286	377.7	396.1	993.7
2019	6	25	19	20	24.232	-50.91684	-73.58035	5.83	3.1	54	0.374	396.3	454.8	1155.5
2019	6	25	20	50	58.471	-50.91805	-73.58231	5.98	3.3	74	0.341	364.4	412.2	921.5
2019	6	25	22	16	57.244	-50.91888	-73.58135	6.00	3.1	74	0.365	345.0	401.0	839.8
2019	6	26	0	56	28.044	-50.92830	-73.57855	9.01	3.1	75	0.383	340.6	395.2	869.0
2019	6	26	4	18	54.901	-50.91845	-73.58425	3.44	3.1	74	0.272	337.8	405.3	783.4
2019	6	26	5	38	56.666	-50.92050	-73.58331	4.64	3.1	74	0.260	344.1	451.1	1101.5
2019	6	26	7	13	19.355	-50.92745	-73.58437	9.03	3.1	74	0.642	316.8	351.5	893.9
2019	6	26	8	57	36.720	-50.91660	-73.58763	2.65	3.2	74	0.200	350.4	447.6	818.6
2019	6	26	10	55	27.016	-50.92091	-73.58429	4.58	3.0	74	0.268	327.2	418.1	1098.0
2019	6	26	12	15	35.912	-50.91966	-73.58912	3.83	2.9	74	0.243	346.9	357.6	704.2
2019	6	26	13	40	41.549	-50.92152	-73.58381	4.80	3.1	74	0.287	328.8	390.8	891.0
2019	6	26	15	24	20.137	-50.92153	-73.58187	5.90	2.9	74	0.343	350.5	413.8	1024.0
2019	6	26	16	15	6.473	-50.90939	-75.07837	8.98	3.1	187	0.367	822.5	592.8	926.9
2019	6	26	16	39	15.557	-50.91743	-73.58376	4.80	3.0	74	0.395	371.8	449.3	908.7
2019	6	26	16	41	55.293	-50.91114	-75.08378	11.90	4.0	188	0.448	840.8	532.2	698.9
2019	6	26	17	38	39.984	-50.92321	-73.57412	6.87	3.1	74	0.502	348.1	402.2	1014.6
2019	6	26	20	24	2.799	-50.91660	-73.58763	2.85	3.1	74	0.339	365.5	495.1	1529.3
2019	6	26	21	55	17.145	-50.92314	-73.58771	5.43	3.0	74	0.257	342.4	427.1	946.0
2019	6	26	23	1	44.670	-50.92049	-73.58525	5.44	2.9	74	0.310	343.8	395.6	852.4
2019	6	27	0	23	59.291	-50.91924	-73.59106	4.15	3.0	74	0.286	364.8	431.4	937.2
2019	6	27	1	40	45.388	-50.92459	-73.58433	6.45	2.9	73	0.235	356.0	389.0	1205.6
2019	6	27	5	10	10.473	-50.93811	-73.57965	9.64	2.9	75	0.764	348.1	415.0	907.4
2019	6	27	6	37	14.682	-50.91845	-73.58425	3.56	3.0	74	0.272	329.7	415.8	826.0
2019	6	27	7	55	40.937	-50.92498	-73.58725	5.08	3.1	74	0.230	352.7	413.1	912.5
2019	6	27	9	2	3.204	-50.93153	-73.58733	7.70	3.0	75	0.628	353.7	438.9	1185.8
2019	6	27	10	17	23.271	-50.92253	-73.58722	3.58	3.0	74	0.262	345.8	438.4	972.9
2019	6	27	12	23	21.763	-50.92337	-73.58237	4.81	3.0	74	0.251	345.5	471.5	1019.7
2019	6	27	13	22	15.020	-50.92174	-73.58235	5.96	2.9	74	0.159	381.5	469.7	1282.0

ORIGIN TIME (UTC)						Latitude	Longitude	Depth	M_L	GAP	RMS	X error	Y error	Z error
yyyy	mm	dd	h	m	seconds	[°]	[°]	[Km]		[°]		[m]	[m]	[m]
2019	6	27	14	44	1.438	-50.92750	-73.57563	7.86	2.9	74	0.369	370.1	414.3	982.9
2019	6	27	16	37	15.181	-50.92295	-73.58528	5.46	3.1	74	0.349	331.7	366.0	1120.6
2019	6	27	18	49	1.335	-50.91968	-73.58427	4.21	3.0	74	0.200	329.1	395.8	968.8
2019	6	27	20	6	5.369	-50.92395	-73.58966	4.49	3.0	74	0.331	355.7	430.9	936.4
2019	6	27	22	0	20.455	-50.92317	-73.58189	5.62	2.9	74	0.291	333.5	416.2	933.1
2019	6	27	22	53	38.239	-50.91931	-73.57553	6.00	2.9	74	0.209	329.9	424.3	759.2
2019	6	28	0	56	5.332	-50.91684	-73.57938	5.30	3.0	74	0.337	327.2	384.3	860.9
2019	6	28	1	16	2.364	-51.20368	-72.41654	14.18	3.7	65	0.713	261.4	225.1	465.9
2019	6	28	2	24	37.857	-50.92172	-73.58527	4.34	3.1	74	0.287	329.1	402.8	860.3
2019	6	28	5	16	21.483	-50.91722	-73.58521	3.09	3.0	74	0.210	332.7	406.6	903.9
2019	6	28	6	33	53.787	-50.92563	-73.57998	7.11	3.0	74	0.285	331.1	387.7	950.1
2019	6	28	7	27	1.646	-51.90277	-74.24658	12.21	3.8	194	0.467	507.8	584.1	845.6
2019	6	28	7	32	14.909	-50.92069	-73.58768	5.27	3.0	74	0.306	358.0	422.6	873.1
2019	6	28	8	53	47.118	-50.91948	-73.58281	4.82	3.0	74	0.249	339.4	412.7	1029.2
2019	6	28	10	36	15.843	-50.91866	-73.58474	3.92	3.0	74	0.321	326.5	426.9	824.5
2019	6	28	12	10	27.810	-50.92540	-73.58628	4.77	2.9	74	0.396	331.5	404.5	872.4
2019	6	28	13	59	27.315	-50.91597	-73.58908	3.48	3.0	74	0.227	339.3	403.7	787.5
2019	6	28	15	23	8.611	-50.91929	-73.58038	5.98	2.8	74	0.386	341.9	400.7	870.5
2019	6	28	17	26	59.258	-50.92007	-73.58719	6.00	2.9	74	0.225	377.0	483.4	1080.9
2019	6	28	19	34	23.589	-50.92151	-73.58575	4.25	2.8	74	0.234	353.4	448.9	1360.8
2019	6	28	20	52	7.984	-50.92374	-73.59112	4.32	2.9	74	0.354	367.4	462.4	1129.7
2019	6	28	22	33	8.151	-50.91948	-73.58281	5.99	3.0	74	0.286	376.0	470.1	1052.8
2019	6	28	23	40	26.850	-50.92274	-73.58674	5.99	2.9	74	0.224	382.5	465.4	879.6
2019	6	29	1	22	22.999	-50.91497	-73.58567	3.36	2.9	74	0.231	354.8	454.2	905.7
2019	6	29	2	54	21.125	-50.91990	-73.58185	5.23	2.8	74	0.191	379.2	495.8	1196.7
2019	6	29	4	34	42.566	-50.92008	-73.58622	3.70	2.9	74	0.205	340.9	422.3	948.1
2019	6	29	6	32	48.361	-50.92336	-73.58432	5.34	2.9	74	0.221	350.0	412.5	971.9
2019	6	29	8	23	37.310	-50.91884	-73.58814	3.91	3.0	74	0.222	337.3	390.8	892.6
2019	6	29	9	53	34.729	-50.92048	-73.58816	4.48	3.0	74	0.146	342.4	402.0	1040.6
2019	6	29	12	20	43.189	-50.91967	-73.58718	4.50	2.9	74	0.260	341.1	419.0	1038.6
2019	6	29	13	28	53.225	-50.91802	-73.58813	5.01	3.2	74	0.266	365.5	458.9	1019.3
2019	6	29	15	11	21.182	-50.91482	-73.61479	2.26	3.0	73	0.459	356.3	427.5	574.0
2019	6	29	16	4	9.103	-50.90817	-75.05502	10.39	3.1	185	0.310	831.0	601.4	880.8
2019	6	29	17	43	26.629	-50.91720	-73.58909	2.19	2.9	74	0.199	340.8	455.5	695.2
2019	6	29	19	44	1.227	-50.92461	-73.57948	8.48	2.9	74	0.479	329.0	379.3	980.2
2019	6	29	21	12	0.166	-50.92214	-73.58333	5.55	2.9	74	0.228	341.8	404.8	830.4
2019	6	29	22	55	47.505	-50.88457	-71.95613	12.53	2.9	55	0.484	413.2	399.0	945.4
2019	6	29	23	39	55.104	-50.93402	-73.58057	8.62	2.9	75	0.684	329.7	379.5	842.7
2019	6	30	0	59	29.207	-50.92089	-73.58720	4.30	3.0	74	0.266	326.1	385.8	869.1
2019	6	30	2	26	24.381	-50.92172	-73.58624	3.76	2.8	74	0.217	336.8	418.2	1026.4
2019	6	30	3	31	13.228	-51.84765	-74.27577	14.83	3.3	190	0.574	528.8	591.0	635.8
2019	6	30	4	52	32.832	-50.92153	-73.58187	4.68	3.0	74	0.393	325.9	414.2	1295.8
2019	6	30	5	6	5.530	-49.98398	-72.59061	6.00	2.9	75	0.502	379.4	329.6	621.5
2019	6	30	6	5	18.849	-50.92274	-73.58674	5.29	2.9	74	0.274	327.6	368.4	839.7
2019	6	30	8	26	16.842	-50.92233	-73.58576	4.68	2.9	74	0.216	335.6	421.5	1426.3
2019	6	30	9	14	43.612	-52.65782	-73.72671	8.02	3.3	239	0.806	1214.1	3005.4	2416.2
2019	6	30	10	45	59.427	-50.91925	-73.58815	3.48	3.0	74	0.239	327.9	406.0	867.3

ORIGIN TIME (UTC)						Latitude	Longitude	Depth	M_L	GAP	RMS	X error	Y error	Z error
yyyy	mm	dd	h	m	seconds	[°]	[°]	[Km]		[°]		[m]	[m]	[m]
2019	6	30	14	45	54.518	-50.91765	-73.58133	3.62	2.7	74	0.208	313.8	410.1	796.2
2019	6	30	16	42	55.371	-50.91925	-73.58912	4.13	2.7	74	0.277	354.4	497.2	953.2
2019	6	30	18	7	37.841	-50.92129	-73.58914	5.61	2.9	74	0.214	399.3	541.0	1142.2
2019	6	30	19	58	47.820	-50.92173	-73.58430	6.00	2.8	74	0.250	368.9	498.2	912.2
2019	6	30	21	36	55.586	-50.92911	-73.57953	6.00	2.8	73	0.221	428.2	482.4	990.8
2019	7	1	1	15	25.167	-50.92213	-73.58527	8.68	2.9	75	0.268	331.8	389.1	1562.0
2019	7	1	3	4	44.856	-50.92008	-73.58622	3.54	3.0	74	0.224	350.3	451.9	1011.7
2019	7	1	5	3	27.214	-50.91844	-73.58620	3.56	2.9	74	0.250	363.6	449.1	939.2
2019	7	1	6	14	51.265	-50.92151	-73.58575	5.74	2.8	74	0.204	380.0	450.2	970.3
2019	7	1	7	20	7.724	-50.92560	-73.58580	5.78	2.9	74	0.293	352.2	427.6	1019.8
2019	7	1	9	17	37.161	-50.91091	-73.57979	2.77	2.9	73	0.402	341.1	405.2	617.7
2019	7	1	11	7	19.929	-50.91480	-73.57936	6.00	3.0	74	0.479	334.5	423.8	604.3
2019	7	1	12	20	34.241	-50.92048	-73.58719	6.00	3.0	74	0.168	363.9	455.3	995.7
2019	7	1	14	39	1.370	-50.92007	-73.58719	4.38	3.1	74	0.233	348.9	420.9	1068.5
2019	7	1	16	3	48.162	-50.63097	-74.39210	19.65	3.0	110	0.409	323.6	273.8	673.9
2019	7	1	16	53	20.713	-50.92294	-73.58722	4.40	3.1	74	0.264	349.5	423.7	1033.6
2019	7	1	17	59	55.459	-50.91822	-73.58959	5.31	2.9	74	0.253	371.3	586.7	1589.3
2019	7	1	18	9	48.665	-49.84353	-73.44118	12.00	2.9	122	0.607	477.6	628.0	974.9
2019	7	1	19	25	36.896	-50.91824	-73.58571	3.71	3.1	74	0.330	337.0	442.2	845.9
2019	7	1	20	50	7.411	-50.91824	-73.58571	4.61	3.2	74	0.232	343.4	436.9	1169.6
2019	7	1	21	59	8.442	-50.92296	-73.58237	6.00	3.0	74	0.163	362.6	457.2	1188.5
2019	7	1	23	37	52.703	-50.94109	-74.16630	10.24	3.0	73	0.297	402.7	288.5	1137.6
2019	7	1	23	50	17.767	-50.91845	-73.58523	3.05	3.3	74	0.233	343.7	439.4	862.5
2019	7	2	1	30	45.623	-50.92009	-73.58428	4.46	3.1	74	0.262	333.8	397.7	934.2
2019	7	2	3	18	0.933	-50.91723	-73.58424	4.21	3.2	74	0.233	339.3	410.3	1009.4
2019	7	2	4	27	25.130	-50.92378	-73.58335	5.83	3.1	74	0.199	396.5	445.8	1001.5
2019	7	2	6	4	30.583	-50.91843	-73.58814	2.98	3.2	74	0.266	327.3	390.6	685.8
2019	7	2	8	27	56.338	-50.91843	-73.58911	3.01	3.1	74	0.242	333.5	422.1	846.5
2019	7	2	9	31	19.108	-50.92377	-73.58432	6.00	3.0	74	0.210	379.8	439.7	934.2
2019	7	2	11	28	33.031	-50.91907	-73.58378	4.68	3.1	74	0.250	320.7	388.7	917.0
2019	7	2	13	0	0.778	-50.91720	-73.58909	4.17	3.1	74	0.291	334.2	405.7	886.7
2019	7	2	14	38	14.686	-50.92045	-73.59302	2.99	3.1	74	0.305	354.4	416.7	695.3
2019	7	2	14	45	39.946	-50.69467	-73.32497	5.84	2.9	58	0.432	371.0	404.4	810.1
2019	7	2	16	34	40.089	-50.91927	-73.58524	3.35	2.9	74	0.209	348.0	389.5	851.6
2019	7	2	17	27	0.072	-50.92293	-73.58917	3.01	2.9	74	0.138	415.1	503.3	1128.2
2019	7	2	18	30	30.318	-50.90699	-73.58702	6.00	3.0	73	0.446	328.1	364.1	515.8
2019	7	2	19	27	41.186	-50.92009	-73.58330	5.03	2.9	74	0.182	470.6	518.3	1298.0
2019	7	2	20	42	46.539	-50.91948	-73.58281	4.27	3.0	74	0.254	346.8	426.2	992.9
2019	7	2	21	58	57.044	-50.92149	-73.58963	3.75	3.0	54	0.248	352.7	393.5	1046.8
2019	7	2	23	7	47.779	-50.91847	-73.58037	5.30	3.0	54	0.256	370.3	424.9	890.7
2019	7	3	1	2	10.549	-50.91561	-73.58034	3.13	2.9	54	0.243	331.3	352.7	700.7
2019	7	3	2	6	47.460	-50.92090	-73.58526	4.46	3.0	54	0.193	354.1	397.3	909.9
2019	7	3	2	52	2.281	-50.92376	-73.58626	4.24	2.9	53	0.231	333.7	369.2	977.1
2019	7	3	3	14	59.401	-51.06883	-74.19580	17.29	2.9	112	0.340	486.5	299.5	880.1
2019	7	3	5	9	5.457	-50.91866	-73.58474	3.77	3.0	74	0.268	334.3	420.7	927.7
2019	7	3	6	32	12.830	-50.92315	-73.58577	4.61	2.9	74	0.163	345.4	414.4	997.2
2019	7	3	8	3	37.385	-50.63451	-74.39534	18.95	2.7	110	0.445	350.7	238.3	469.4

ORIGIN TIME (UTC)						Latitude	Longitude	Depth	M_L	GAP	RMS	X error	Y error	Z error
yyyy	mm	dd	h	m	seconds	[°]	[°]	[Km]		[°]		[m]	[m]	[m]
2019	7	3	8	30	37.867	-50.92047	-73.58913	3.09	2.8	74	0.261	338.3	468.8	944.1
2019	7	3	9	19	6.327	-50.92256	-73.58139	4.87	2.7	82	0.119	390.1	492.1	1436.8
2019	7	3	11	1	13.388	-50.49954	-72.61023	8.17	2.9	39	0.683	276.3	265.9	762.2
2019	7	3	11	52	13.390	-50.91989	-73.58379	3.71	2.9	74	0.233	314.5	404.5	953.8
2019	7	3	14	9	32.084	-50.91475	-73.58906	2.60	2.8	74	0.191	338.8	437.2	808.0
2019	7	3	16	1	37.297	-50.92626	-73.57756	4.62	2.6	74	0.236	363.2	417.9	1034.1
2019	7	3	16	52	55.427	-50.92173	-73.58333	4.44	2.7	74	0.148	408.9	457.8	1174.6
2019	7	3	20	10	27.487	-50.91476	-73.58615	2.80	2.7	74	0.195	367.4	438.2	780.0
2019	7	3	21	4	35.940	-50.92011	-73.57942	5.57	2.7	74	0.174	368.9	433.7	964.8
2019	7	3	22	43	51.354	-50.91478	-73.58227	3.76	2.6	74	0.235	335.9	430.7	976.4
2019	7	4	1	30	27.422	-50.92051	-73.58137	5.18	2.6	74	0.160	348.0	410.1	1021.3
2019	7	4	2	49	16.628	-50.91640	-73.58520	3.15	2.7	74	0.214	345.6	433.5	915.5
2019	7	4	3	54	50.061	-50.91926	-73.58718	3.19	2.6	74	0.184	344.8	407.1	866.1
2019	7	4	5	50	14.087	-50.92498	-73.58725	4.05	2.8	74	0.286	332.1	395.6	1023.2
2019	7	4	7	24	12.359	-50.91948	-73.58281	8.81	2.8	74	0.428	344.8	404.7	1007.5
2019	7	4	8	38	55.539	-50.92295	-73.58431	4.01	2.7	74	0.329	338.6	411.2	875.4
2019	7	4	9	7	16.193	-50.73101	-74.22682	16.33	2.9	91	0.354	349.4	279.5	589.6
2019	7	4	10	39	30.956	-50.92171	-73.58721	3.91	2.8	74	0.261	329.4	400.8	932.1
2019	7	4	12	6	39.047	-50.91353	-73.58808	2.10	2.9	74	0.192	341.0	437.6	637.7
2019	7	4	13	44	43.383	-50.94471	-73.56904	11.30	2.7	90	0.562	358.0	419.6	808.4
2019	7	4	15	30	36.281	-50.91518	-73.58518	2.86	2.8	74	0.189	334.5	410.4	831.2
2019	7	4	15	49	47.983	-50.91178	-75.08236	9.68	2.7	188	0.323	850.8	612.9	960.0
2019	7	4	16	48	40.926	-50.91804	-73.58522	4.52	2.7	74	0.250	360.1	447.1	993.2
2019	7	4	18	56	59.877	-50.92173	-73.58430	6.96	2.8	74	0.356	337.9	419.5	955.7
2019	7	4	20	51	39.764	-50.92049	-73.58622	3.33	2.7	74	0.231	348.7	417.4	914.4
2019	7	4	21	56	24.978	-50.92256	-73.58139	5.87	2.6	74	0.170	347.7	420.5	890.0
2019	7	4	23	50	53.515	-50.91803	-73.58619	3.25	2.9	74	0.257	325.2	398.7	773.8
2019	7	5	1	15	40.348	-50.92497	-73.58919	3.60	2.7	74	0.306	380.7	494.3	908.3
2019	7	5	2	23	59.829	-50.92215	-73.58042	5.98	2.7	74	0.194	348.1	436.2	952.7
2019	7	5	4	12	29.413	-50.92211	-73.58915	3.60	2.9	74	0.337	361.0	412.9	858.1
2019	7	5	6	22	9.600	-50.92498	-73.58822	4.09	2.9	74	0.343	362.6	404.6	874.0
2019	7	5	8	13	28.612	-50.91966	-73.58815	2.56	2.8	74	0.265	359.0	472.5	979.4
2019	7	5	9	27	25.176	-50.91928	-73.58329	3.56	2.7	72	0.159	418.6	449.6	1066.7
2019	7	5	10	51	55.410	-50.91640	-73.58617	6.00	2.9	74	0.306	354.0	450.1	1105.7
2019	7	5	13	48	23.184	-50.92072	-73.58186	6.01	2.7	74	0.163	455.4	608.7	1323.7
2019	7	5	15	24	15.838	-50.91561	-73.58034	6.00	2.9	74	0.384	346.3	449.7	998.3
2019	7	5	17	11	16.329	-50.92213	-73.58527	5.34	2.8	74	0.158	413.6	499.6	1354.4
2019	7	5	19	2	0.337	-50.92193	-73.58478	5.17	2.8	74	0.121	432.9	494.0	1430.0
2019	7	5	19	59	29.878	-50.93721	-73.55487	9.65	2.6	85	0.341	685.7	720.1	1336.5
2019	7	5	22	3	28.047	-50.92129	-73.59012	4.09	2.9	74	0.222	355.7	462.0	1208.3
2019	7	6	0	3	22.731	-50.91805	-73.58328	6.00	2.9	74	0.238	352.1	457.2	973.9
2019	7	6	3	3	47.386	-50.92149	-73.58963	4.45	3.0	54	0.242	359.3	389.6	1158.4
2019	7	6	5	4	15.668	-50.92334	-73.58917	4.65	3.3	54	0.230	377.8	438.8	1274.7
2019	7	6	5	54	0.978	-50.91682	-73.58326	4.38	2.9	76	0.129	461.3	498.5	1249.5
2019	7	6	7	50	19.306	-50.91923	-73.59300	2.27	2.8	54	0.187	373.7	439.0	966.3
2019	7	6	10	10	10.351	-50.91274	-73.58224	4.44	2.8	59	0.232	412.0	398.1	1267.5
2019	7	6	12	4	45.258	-50.91987	-73.58767	4.45	2.8	57	0.160	400.7	436.6	1083.5

ORIGIN TIME (UTC)						Latitude	Longitude	Depth	M_L	GAP	RMS	X error	Y error	Z error
yyyy	mm	dd	h	m	seconds	[°]	[°]	[Km]		[°]		[m]	[m]	[m]
2019	7	6	13	37	14.216	-50.91804	-73.58425	5.98	2.8	54	0.341	375.4	417.1	790.4
2019	7	6	15	6	54.420	-50.92336	-73.58432	5.18	3.0	59	0.236	404.2	450.6	962.1
2019	7	6	16	24	30.045	-50.91602	-73.57937	6.00	2.8	54	0.283	438.1	458.9	948.9
2019	7	6	17	34	40.214	-50.91441	-73.57547	6.00	2.8	76	0.271	425.2	471.9	863.1
2019	7	6	18	56	44.801	-50.91597	-73.59005	5.85	3.0	54	0.319	378.5	423.7	1074.4
2019	7	6	20	18	11.519	-50.91477	-73.58518	4.09	2.7	54	0.338	353.2	395.8	860.4
2019	7	6	22	25	24.907	-50.44845	-74.42998	21.02	2.7	97	0.614	344.2	304.0	549.1
2019	7	6	23	16	51.969	-50.91970	-73.57942	5.98	2.7	75	0.153	397.5	452.3	1027.3
2019	7	7	1	3	7.671	-50.91968	-73.58524	4.40	2.8	54	0.243	333.7	375.0	1177.1
2019	7	7	2	43	34.437	-50.92047	-73.58913	2.99	3.0	54	0.222	347.9	367.5	800.4
2019	7	7	3	41	24.773	-50.92133	-73.58235	4.81	2.8	54	0.263	362.8	397.0	918.5
2019	7	7	5	22	58.201	-50.92336	-73.58432	5.08	2.9	53	0.211	331.7	376.1	1288.7
2019	7	7	6	41	10.994	-50.92112	-73.58283	4.66	2.8	54	0.235	351.1	385.6	1029.0
2019	7	7	8	6	11.816	-50.91967	-73.58718	3.27	2.8	54	0.206	355.6	367.8	874.2
2019	7	7	9	14	51.977	-50.92193	-73.58478	4.39	2.7	54	0.215	335.2	393.2	1135.5
2019	7	7	10	31	31.736	-50.93071	-73.58829	6.33	2.7	53	0.298	340.0	368.7	1040.0
2019	7	7	13	23	40.929	-50.92643	-73.58387	8.00	2.8	53	0.290	330.7	356.0	887.7
2019	7	7	14	23	51.825	-50.92170	-73.58915	3.33	2.8	54	0.274	378.7	452.8	875.1
2019	7	7	15	31	6.679	-50.91883	-73.59105	2.98	3.0	54	0.194	346.5	405.6	853.6
2019	7	7	16	39	1.885	-50.92110	-73.58672	3.49	3.0	54	0.180	343.1	384.2	917.1
2019	7	7	17	51	46.677	-50.91948	-73.58281	5.99	2.7	58	0.179	361.7	390.1	856.6
2019	7	7	19	12	24.700	-50.92451	-73.60084	8.07	2.9	54	0.556	348.3	361.3	1187.9
2019	7	7	22	55	51.851	-50.91927	-73.58524	4.19	2.7	54	0.230	345.2	391.9	1120.6
2019	7	8	0	23	54.967	-50.91966	-73.58912	3.39	2.7	57	0.222	342.8	420.3	992.1
2019	7	8	2	11	21.201	-50.90783	-73.58121	2.55	2.6	54	0.466	331.4	379.0	701.8
2019	7	8	3	4	57.840	-50.92336	-73.58529	4.50	2.6	53	0.191	354.2	380.6	968.0
2019	7	8	3	39	24.928	-50.43262	-73.76656	6.00	2.5	85	0.370	250.8	317.5	1184.2
2019	7	8	4	15	32.073	-50.90782	-73.58315	2.99	2.6	54	0.575	325.2	356.7	439.1
2019	7	8	5	40	21.088	-50.91926	-73.58718	3.09	2.5	54	0.209	335.2	390.6	858.6
2019	7	8	6	33	34.921	-50.92091	-73.58331	4.28	2.7	54	0.241	337.0	373.4	934.0
2019	7	8	8	5	57.740	-50.92540	-73.58531	6.88	2.8	53	0.228	327.2	368.1	1296.2
2019	7	8	9	28	7.289	-50.92088	-73.58914	3.35	2.7	57	0.201	338.0	420.9	878.0
2019	7	8	10	44	23.343	-50.92050	-73.58428	4.50	2.6	54	0.171	350.5	387.6	1110.5
2019	7	8	11	59	9.256	-50.91777	-75.06709	15.47	2.3	186	0.323	621.2	451.0	1573.6
2019	7	8	12	9	39.858	-50.92623	-73.58435	7.51	2.8	53	0.317	327.1	364.5	993.5
2019	7	8	13	12	55.135	-50.91803	-73.58716	3.01	2.7	54	0.204	352.2	377.4	845.6
2019	7	8	13	54	44.855	-50.62473	-74.40059	21.24	2.2	110	0.200	420.0	253.6	903.9
2019	7	8	15	3	55.141	-50.91904	-73.58960	3.32	2.7	54	0.188	352.0	420.7	993.5
2019	7	8	16	52	6.476	-50.91883	-73.59008	3.01	2.8	54	0.281	335.7	385.4	780.4
2019	7	8	17	47	26.814	-50.92046	-73.59108	2.99	2.7	54	0.225	375.8	438.0	903.8
2019	7	8	21	31	23.013	-50.92213	-73.58430	4.81	2.6	54	0.289	350.6	401.8	965.1
2019	7	8	23	56	8.695	-50.92255	-73.58236	6.37	2.8	53	0.309	325.0	381.2	1018.7
2019	7	9	1	6	57.728	-51.50861	-74.37935	19.99	2.6	105	0.259	987.7	537.3	1217.3
2019	7	9	1	16	55.178	-50.92274	-73.58674	4.20	2.6	54	0.206	322.7	359.2	1041.2
2019	7	9	2	12	13.640	-50.91885	-73.58620	3.74	2.7	57	0.269	345.4	403.1	864.7
2019	7	9	4	39	23.384	-50.92459	-73.58336	7.04	2.7	53	0.236	320.8	350.5	1184.2
2019	7	9	6	37	26.284	-50.92500	-73.58434	6.47	2.6	53	0.249	327.9	352.0	1063.4

ORIGIN TIME (UTC)						Latitude	Longitude	Depth	M_L	GAP	RMS	X error	Y error	Z error
yyyy	mm	dd	h	m	seconds	[°]	[°]	[Km]		[°]		[m]	[m]	[m]
2019	7	9	7	38	46.703	-50.92294	-73.58625	4.75	2.7	53	0.248	340.1	365.8	887.4
2019	7	9	9	31	15.452	-50.92337	-73.58335	5.06	2.7	53	0.269	319.8	353.5	1139.3
2019	7	9	10	56	0.164	-50.90908	-73.57637	3.87	2.8	54	0.463	311.3	352.3	704.4
2019	7	9	11	10	8.020	-51.87577	-74.28548	18.21	3.2	215	0.476	631.2	664.3	788.3
2019	7	9	12	0	12.889	-50.92254	-73.58528	4.11	2.6	54	0.353	329.2	369.9	818.4
2019	7	9	13	37	15.737	-50.91926	-73.58718	3.35	2.8	54	0.195	337.1	388.0	948.5
2019	7	9	15	3	28.869	-50.91926	-73.58621	4.71	2.8	54	0.290	334.9	368.0	897.1
2019	7	9	16	15	5.196	-50.92297	-73.58043	6.00	2.7	53	0.139	354.8	399.8	817.0
2019	7	9	17	46	46.241	-50.92053	-73.57749	5.55	2.8	53	0.256	345.9	402.2	834.2
2019	7	9	18	46	31.998	-50.92013	-73.57651	6.00	2.7	53	0.363	367.9	389.1	608.1
2019	7	9	20	39	27.070	-50.92133	-73.58235	4.26	2.8	54	0.204	340.1	362.9	964.2
2019	7	9	23	7	0.986	-50.91886	-73.58426	5.85	2.9	54	0.309	315.0	350.3	865.8
2019	7	10	1	13	10.418	-50.92070	-73.58574	4.84	2.9	54	0.291	326.3	359.8	1012.0
2019	7	10	2	38	9.964	-50.91905	-73.58766	3.90	2.9	54	0.189	330.9	385.3	912.2
2019	7	10	3	58	5.954	-50.92011	-73.57942	4.40	2.7	54	0.160	337.5	359.0	923.3
2019	7	10	5	41	26.213	-50.91926	-73.58718	2.68	2.9	54	0.255	338.8	375.5	888.2
2019	7	10	7	9	57.091	-50.91742	-73.58570	3.79	3.0	54	0.230	328.2	373.4	886.6
2019	7	10	7	49	54.835	-51.00985	-74.94667	9.33	3.0	180	0.355	656.3	413.9	919.0
2019	7	10	8	40	4.937	-50.91515	-73.59004	2.53	2.9	54	0.166	341.8	396.4	787.4
2019	7	10	9	44	56.242	-50.91986	-73.58961	2.89	2.9	54	0.208	356.3	387.7	724.5
2019	7	10	11	18	10.432	-50.92338	-73.58140	6.00	3.0	53	0.225	344.6	386.0	887.2
2019	7	10	12	53	32.292	-50.91681	-73.58521	3.39	3.0	54	0.354	323.2	366.8	758.6
2019	7	10	14	50	28.351	-50.92274	-73.58674	4.66	3.0	54	0.258	341.0	393.3	1220.7
2019	7	10	15	56	40.299	-50.92087	-73.59108	3.27	2.9	54	0.233	363.1	391.6	901.4
2019	7	10	17	29	0.633	-50.91763	-73.58522	4.87	2.8	54	0.379	351.5	399.0	894.9
2019	7	10	19	19	29.293	-50.92133	-73.58138	3.76	2.9	53	0.223	326.4	366.6	992.4
2019	7	10	20	2	54.337	-49.45006	-73.55014	5.21	3.1	186	0.462	417.8	710.8	835.3
2019	7	10	21	2	21.427	-50.92070	-73.58574	5.39	2.9	54	0.303	341.8	360.4	1036.0
2019	7	10	22	27	12.172	-50.92091	-73.58429	4.05	3.0	54	0.205	330.0	367.7	1045.5
2019	7	10	23	55	48.028	-50.91762	-73.58813	2.82	2.9	57	0.171	338.1	411.7	840.4
2019	7	11	1	23	26.228	-50.91802	-73.58910	2.86	2.9	54	0.161	340.8	398.3	851.9
2019	7	11	2	48	53.835	-50.92151	-73.58575	4.61	2.9	54	0.228	335.9	389.6	1044.2
2019	7	11	3	53	22.000	-50.92047	-73.58913	2.88	2.8	54	0.203	340.7	383.1	774.1
2019	7	11	5	43	47.647	-50.92744	-73.58631	6.00	3.0	53	0.309	317.6	331.9	649.5
2019	7	11	6	53	3.690	-50.92151	-73.58575	4.25	2.8	54	0.187	357.4	397.9	1033.5
2019	7	11	8	12	16.327	-50.92215	-73.58139	6.00	2.8	53	0.150	363.6	410.8	847.4
2019	7	11	8	49	12.259	-50.92708	-73.57660	8.09	2.9	53	0.251	320.5	339.5	803.2
2019	7	11	10	42	23.881	-50.92294	-73.58625	4.71	2.9	53	0.285	326.4	360.6	953.8
2019	7	11	11	34	33.304	-50.91885	-73.58717	3.58	2.8	54	0.245	332.2	374.9	888.5
2019	7	11	13	21	37.657	-50.92661	-73.59018	3.99	2.9	53	0.248	330.8	379.0	1009.3
2019	7	11	14	27	47.691	-50.93330	-73.70971	0.89	2.7	58	0.419	685.6	626.6	496.0
2019	7	11	14	35	49.840	-50.92149	-73.58963	3.82	2.9	54	0.292	355.4	385.7	1009.1
2019	7	11	16	17	27.235	-50.91966	-73.58815	3.91	2.9	54	0.201	332.8	395.4	913.7
2019	7	11	17	12	5.273	-50.91927	-73.58524	5.94	2.9	54	0.189	357.7	411.4	846.3
2019	7	11	18	55	14.136	-50.92210	-73.59110	3.13	2.8	54	0.184	331.8	363.5	785.5
2019	7	11	20	14	3.148	-50.91889	-73.57941	4.91	2.8	54	0.174	341.8	344.7	841.5
2019	7	11	21	22	47.796	-50.92112	-73.58283	5.60	2.8	54	0.266	364.2	367.7	857.9

ORIGIN TIME (UTC)						Latitude	Longitude	Depth	M_L	GAP	RMS	X error	Y error	Z error
yyyy	mm	dd	h	m	seconds	[°]	[°]	[Km]		[°]		[m]	[m]	[m]
2019	7	11	22	48	6.188	-50.92173	-73.58430	5.26	2.7	54	0.318	344.2	393.0	834.9
2019	7	12	0	26	57.051	-50.92056	-73.57263	4.07	2.9	53	0.434	328.0	339.1	1071.5
2019	7	12	0	49	54.216	-49.89880	-74.84695	19.01	3.1	121	0.648	471.4	372.9	368.2
2019	7	12	1	51	18.104	-50.91842	-73.59008	2.76	2.8	54	0.163	327.4	390.0	771.1
2019	7	12	3	5	1.950	-50.92276	-73.58285	5.45	2.8	53	0.164	352.5	390.3	910.6
2019	7	12	4	30	23.465	-50.92342	-73.57170	4.79	2.8	53	0.490	324.6	359.9	1109.7
2019	7	12	5	33	21.939	-50.90547	-73.56177	6.00	2.6	76	0.476	320.3	311.3	379.7
2019	7	12	6	58	0.972	-53.09845	-74.42814	11.91	3.4	264	0.884	800.7	915.7	1995.8
2019	7	12	7	28	20.392	-50.92746	-73.58243	7.99	2.9	53	0.414	324.7	343.5	872.9
2019	7	12	9	37	53.364	-50.92336	-73.58529	4.58	2.8	53	0.201	323.2	363.3	1191.0
2019	7	12	11	12	18.965	-50.90548	-73.58045	2.93	2.7	54	0.472	308.8	356.2	433.9
2019	7	12	12	9	28.514	-50.92150	-73.58769	4.18	2.7	54	0.162	352.7	365.6	917.2
2019	7	12	14	15	40.325	-50.91967	-73.58718	4.30	2.9	54	0.223	339.5	361.3	1126.4
2019	7	12	16	17	9.086	-50.92049	-73.58525	4.54	2.9	54	0.231	340.3	397.7	1107.9
2019	7	12	18	11	34.217	-50.92702	-73.58922	7.56	2.8	53	0.399	343.5	375.8	1394.8
2019	7	12	19	53	12.390	-50.92008	-73.58525	3.99	2.7	54	0.143	346.6	373.9	942.8
2019	7	12	21	7	41.424	-50.91926	-73.58718	4.13	2.7	54	0.154	356.3	360.8	969.9
2019	7	12	22	15	55.733	-51.10354	-72.11884	12.55	3.1	58	0.622	325.9	260.6	480.5
2019	7	12	22	43	36.891	-50.91866	-73.58474	4.39	2.9	54	0.221	333.5	386.6	1041.9
2019	7	13	0	0	19.666	-50.92336	-73.58432	5.67	2.7	57	0.204	337.8	394.3	1064.6
2019	7	13	1	31	36.913	-50.92009	-73.58330	4.71	2.6	54	0.136	348.9	385.5	1005.8
2019	7	13	2	17	45.975	-50.91682	-73.58423	3.60	2.5	54	0.219	350.7	439.2	989.9
2019	7	13	4	25	39.394	-50.91518	-73.58421	6.00	2.7	54	0.244	318.7	313.7	666.4
2019	7	13	6	12	56.234	-50.91884	-73.58911	2.99	2.7	54	0.263	332.5	389.9	748.1
2019	7	13	8	7	41.195	-50.92148	-73.59157	3.24	2.8	54	0.309	328.7	362.7	703.8
2019	7	13	9	53	13.039	-50.91967	-73.58621	3.35	2.5	54	0.202	336.1	380.3	935.3
2019	7	13	11	26	52.935	-50.92049	-73.58622	3.29	2.8	54	0.224	333.6	398.6	831.2
2019	7	13	12	33	0.553	-50.92006	-73.59010	2.92	2.7	54	0.256	363.7	399.1	774.2
2019	7	13	14	27	24.327	-50.91883	-73.59105	3.97	2.7	54	0.186	341.2	369.7	998.2
2019	7	13	14	52	49.280	-49.51150	-73.65592	14.58	2.6	213	0.390	382.5	705.6	864.6
2019	7	13	15	58	34.910	-50.92007	-73.58719	5.32	2.7	54	0.248	395.2	407.6	943.9
2019	7	13	17	15	18.730	-50.92335	-73.58626	3.58	2.8	53	0.194	346.4	391.8	1101.2
2019	7	13	19	12	48.621	-50.92213	-73.58624	4.69	2.7	54	0.313	331.5	372.0	1007.6
2019	7	13	20	56	53.131	-50.92333	-73.59014	3.01	2.6	54	0.241	342.8	398.0	853.8
2019	7	13	23	1	58.142	-50.92008	-73.58622	3.19	2.8	54	0.211	326.8	381.7	849.0
2019	7	14	1	1	30.146	-50.92172	-73.58527	3.64	2.7	54	0.227	329.8	379.5	941.5
2019	7	14	2	29	13.199	-50.91742	-73.58570	3.20	2.7	54	0.207	330.4	374.7	877.9
2019	7	14	3	41	35.007	-50.91969	-73.58330	4.42	2.7	54	0.241	347.6	379.8	958.3
2019	7	14	5	8	52.709	-50.91926	-73.58718	3.27	2.7	54	0.197	332.2	356.1	865.5
2019	7	14	7	25	38.682	-50.91968	-73.58427	7.60	2.8	54	0.302	328.3	362.6	1225.0
2019	7	14	9	37	1.989	-50.92210	-73.59110	3.64	2.9	54	0.335	321.9	359.0	748.2
2019	7	14	11	27	19.955	-50.92336	-73.58529	4.71	3.0	53	0.211	328.0	375.2	1208.3
2019	7	14	13	19	25.303	-50.92008	-73.58622	3.76	2.9	54	0.219	321.6	371.2	950.7
2019	7	14	15	8	10.233	-50.91803	-73.58619	2.86	2.8	54	0.182	344.1	382.8	835.4
2019	7	14	16	27	8.143	-50.92295	-73.58431	5.75	2.6	53	0.350	364.5	413.9	820.3
2019	7	14	16	54	9.521	-51.54613	-74.67079	20.49	2.9	206	0.441	815.3	462.8	507.6
2019	7	14	18	23	3.637	-50.92172	-73.58624	4.17	2.8	54	0.215	325.1	367.9	1101.5

ORIGIN TIME (UTC)						Latitude	Longitude	Depth	M_L	GAP	RMS	X error	Y error	Z error
yyyy	mm	dd	h	m	seconds	[°]	[°]	[Km]		[°]		[m]	[m]	[m]
2019	7	14	19	53	4.624	-50.92049	-73.58622	4.52	2.8	54	0.162	336.6	400.3	1054.6
2019	7	14	21	10	38.992	-50.92089	-73.58720	3.56	2.8	54	0.190	334.6	347.5	842.4
2019	7	14	21	55	49.788	-50.92193	-73.58478	4.55	2.8	54	0.228	345.9	399.1	1057.7
2019	7	15	0	25	40.322	-50.92582	-73.58435	6.74	2.9	53	0.200	323.9	358.9	1163.8
2019	7	15	1	49	46.684	-50.92375	-73.58918	3.21	2.7	54	0.295	335.9	356.2	730.9
2019	7	15	3	7	13.762	-50.91801	-73.59104	3.29	2.8	54	0.181	353.8	388.4	932.1
2019	7	15	3	33	5.629	-50.48294	-72.66518	7.55	2.8	38	0.597	334.5	349.3	775.0
2019	7	15	4	46	7.544	-50.92866	-73.58827	5.01	2.9	53	0.581	332.8	359.7	929.2
2019	7	15	6	10	14.365	-50.92010	-73.58136	5.87	2.7	54	0.206	356.4	400.9	876.0
2019	7	15	7	59	23.259	-50.91987	-73.58767	3.20	2.9	54	0.277	345.7	378.0	825.4
2019	7	15	9	17	23.600	-50.91602	-73.57937	5.36	3.1	54	0.182	379.5	413.2	1055.1
2019	7	15	10	37	17.243	-50.91887	-73.58329	5.18	2.9	54	0.128	381.3	420.5	1056.4
2019	7	15	11	43	48.558	-50.92130	-73.58720	5.53	2.9	54	0.222	372.6	416.5	1190.1
2019	7	15	12	40	45.445	-50.92012	-73.57748	3.35	2.8	58	0.192	437.9	457.0	847.5
2019	7	15	18	20	33.949	-51.14685	-72.08631	14.53	3.1	76	0.539	469.0	332.1	723.0
2019	7	15	18	57	31.241	-50.92398	-73.58384	5.27	3.2	53	0.265	387.7	417.5	1328.0
2019	7	15	21	18	15.859	-50.92335	-73.58626	6.00	3.3	53	0.158	433.1	448.9	1098.3
2019	7	15	23	17	52.989	-50.92048	-73.58816	3.76	3.2	54	0.131	440.8	436.7	1017.7
2019	7	16	1	29	10.014	-50.91970	-73.58039	5.67	3.2	54	0.171	414.4	447.7	1023.9
2019	7	16	3	12	10.465	-50.91825	-73.58377	4.88	3.2	54	0.157	447.4	475.7	1174.7
2019	7	16	4	56	35.828	-50.92459	-73.58433	5.16	3.2	53	0.420	455.1	479.8	1309.0
2019	7	16	6	41	49.238	-50.91516	-73.58907	3.89	3.2	54	0.283	405.3	450.9	1057.5
2019	7	16	9	8	59.287	-50.92259	-73.57557	9.01	3.1	53	0.556	382.2	374.8	837.3
2019	7	16	11	5	38.560	-50.92968	-73.58974	5.15	3.1	53	0.194	408.3	434.4	1213.6
2019	7	16	12	57	28.911	-50.44763	-72.62411	6.00	3.2	40	0.647	289.1	309.7	276.5
2019	7	16	13	26	33.495	-50.91783	-73.58667	4.20	3.1	54	0.295	370.5	406.3	929.7
2019	7	16	14	53	39.382	-50.92052	-73.58040	6.00	3.2	54	0.271	360.0	399.0	695.5
2019	7	16	16	44	19.049	-50.92009	-73.58330	4.23	3.1	54	0.110	380.8	410.7	1090.0
2019	7	16	18	32	24.860	-50.91929	-73.58135	6.00	3.1	54	0.159	354.6	379.8	843.5
2019	7	16	19	45	23.159	-50.92133	-73.58235	4.69	3.2	54	0.149	342.5	374.1	1060.9
2019	7	16	21	14	16.951	-50.92235	-73.58188	5.31	3.1	53	0.142	365.2	359.1	933.5
2019	7	16	23	25	32.948	-50.91662	-73.58375	3.28	3.1	54	0.218	342.9	394.8	989.0
2019	7	17	1	35	56.221	-50.90783	-73.58218	1.74	3.0	54	0.357	339.7	378.1	513.0
2019	7	17	4	27	11.735	-50.92132	-73.58429	6.78	3.1	54	0.233	324.9	359.5	1210.8
2019	7	17	6	57	46.092	-50.92112	-73.58283	5.37	2.9	54	0.227	326.0	359.0	1154.7
2019	7	17	8	41	9.162	-50.92254	-73.58431	3.72	3.0	53	0.230	379.8	447.2	1069.3
2019	7	17	11	38	24.683	-50.91989	-73.58379	4.53	2.9	54	0.211	318.5	351.9	1213.4
2019	7	17	13	22	3.658	-50.92088	-73.59011	7.74	2.9	54	0.482	326.1	359.5	1570.2
2019	7	17	15	12	4.762	-50.92007	-73.58913	2.92	3.0	54	0.189	336.0	405.0	842.6
2019	7	17	16	4	31.120	-50.91764	-73.58327	5.42	3.0	54	0.382	358.6	386.8	828.1
2019	7	17	17	52	50.486	-50.92049	-73.58622	5.73	3.0	54	0.184	348.5	377.8	951.4
2019	7	17	19	44	49.386	-50.92296	-73.58334	5.01	3.0	53	0.366	336.9	374.1	1047.8
2019	7	17	21	28	6.675	-50.92337	-73.58237	5.96	3.0	53	0.223	355.7	379.7	779.6
2019	7	17	22	25	31.479	-50.92254	-73.58431	4.81	3.0	53	0.230	345.2	360.4	877.0
2019	7	18	0	17	3.184	-50.92091	-73.58331	5.49	2.9	54	0.117	349.8	361.1	1038.6
2019	7	18	1	42	9.473	-50.91970	-73.58136	5.63	2.8	54	0.170	375.9	402.3	928.9
2019	7	18	2	46	48.591	-50.92069	-73.58768	3.20	3.0	54	0.231	332.5	386.0	820.5

ORIGIN TIME (UTC)						Latitude	Longitude	Depth	M_L	GAP	RMS	X error	Y error	Z error
yyyy	mm	dd	h	m	seconds	[°]	[°]	[Km]		[°]		[m]	[m]	[m]
2019	7	18	4	42	18.705	-50.92376	-73.58626	4.81	3.0	53	0.295	327.1	371.8	888.9
2019	7	18	6	52	43.741	-50.92579	-73.59017	4.62	3.0	53	0.252	353.0	383.6	978.5
2019	7	18	8	21	30.012	-50.91683	-73.58132	4.17	3.0	54	0.201	331.8	346.5	838.7
2019	7	18	9	49	24.895	-50.92380	-73.57753	5.18	2.8	53	0.174	413.9	464.5	1058.6
2019	7	18	10	34	18.233	-50.92461	-73.58045	6.00	3.0	53	0.245	381.6	394.7	818.3
2019	7	18	12	30	9.908	-50.92168	-73.59400	8.29	3.0	54	0.373	365.1	351.8	1321.9
2019	7	18	15	24	30.637	-50.92049	-73.58622	5.22	3.0	54	0.335	378.3	423.9	967.0
2019	7	18	17	3	25.037	-50.92011	-73.58039	4.64	3.1	54	0.346	343.8	365.0	860.8
2019	7	18	18	2	43.905	-50.92197	-73.57702	5.64	2.9	68	0.153	399.4	461.2	1111.6
2019	7	18	19	14	11.253	-50.92090	-73.58526	5.30	3.1	54	0.296	359.4	405.6	885.7
2019	7	18	20	38	47.785	-50.91927	-73.58524	4.40	3.0	54	0.233	382.9	422.4	1131.2
2019	7	18	21	26	48.279	-50.92274	-73.58674	5.76	3.0	58	0.163	425.9	461.7	1009.9
2019	7	18	23	28	0.694	-50.92579	-73.59017	5.32	3.2	74	0.300	376.7	470.3	1338.1
2019	7	19	1	28	2.707	-50.92171	-73.58721	4.83	3.0	74	0.226	357.2	444.9	1393.3
2019	7	19	4	15	37.230	-50.91969	-73.58233	4.44	3.1	74	0.242	390.3	549.2	1229.5
2019	7	19	6	24	44.925	-50.92377	-73.58529	5.46	3.1	74	0.278	374.9	463.0	1126.8
2019	7	19	8	22	56.438	-50.92152	-73.58381	4.80	3.2	74	0.201	378.4	431.2	1095.1
2019	7	19	9	36	15.557	-50.91676	-73.59588	2.45	3.0	82	0.411	428.1	490.3	556.1
2019	7	19	11	43	58.257	-50.91799	-73.59590	5.63	3.2	74	0.355	368.1	440.8	1235.9
2019	7	19	14	32	42.699	-50.92295	-73.58431	4.46	3.2	74	0.261	370.9	432.5	1249.0
2019	7	19	16	11	1.447	-50.92662	-73.58630	6.00	3.2	74	0.216	370.6	468.5	1032.4
2019	7	19	16	37	32.998	-51.20895	-72.42746	7.94	3.4	66	0.294	364.3	306.4	1327.1
2019	7	19	18	27	50.884	-50.92193	-73.58478	4.08	3.1	74	0.173	359.2	403.7	1197.3
2019	7	19	20	22	29.341	-50.92335	-73.58723	3.93	3.2	74	0.244	366.9	427.7	1008.3
2019	7	19	22	31	23.641	-50.91967	-73.58621	3.62	3.1	74	0.234	359.2	422.2	1042.2
2019	7	19	23	40	34.308	-50.92457	-73.58724	6.00	2.9	74	0.221	407.6	477.1	1098.8
2019	7	20	1	10	40.801	-50.91886	-73.58523	4.65	3.0	74	0.247	333.1	415.3	989.4
2019	7	20	2	38	19.337	-50.91842	-73.59105	2.82	3.1	74	0.211	347.8	434.4	719.1
2019	7	20	3	27	6.488	-50.91971	-73.57748	6.00	3.1	74	0.198	358.8	424.7	862.3
2019	7	20	4	40	39.589	-50.92046	-73.59205	2.39	3.1	74	0.252	326.7	421.1	542.9
2019	7	20	7	46	22.055	-50.92254	-73.58528	5.51	3.0	74	0.141	373.4	443.7	1102.6
2019	7	20	9	36	20.649	-50.91968	-73.58524	3.66	3.0	74	0.239	351.9	437.1	1036.1
2019	7	20	11	6	18.287	-50.91824	-73.58571	3.94	3.0	74	0.216	350.2	427.1	1095.6
2019	7	20	11	26	36.286	-51.19643	-72.41932	13.79	3.2	66	0.343	308.4	317.8	644.2
2019	7	20	12	34	13.228	-50.92255	-73.58334	5.90	3.1	74	0.255	331.3	385.0	915.6
2019	7	20	16	5	39.635	-50.91848	-73.57940	4.89	3.1	82	0.304	313.6	456.3	1157.7
2019	7	20	17	38	28.756	-50.92790	-73.57661	9.42	3.0	79	0.662	344.8	437.8	925.2
2019	7	20	18	52	31.759	-50.92233	-73.58576	6.01	3.0	95	0.160	448.4	742.7	1174.3
2019	7	20	20	5	44.001	-50.92459	-73.58433	4.67	3.1	74	0.199	353.3	401.8	1207.9
2019	7	20	21	51	37.128	-50.93072	-73.58441	9.38	3.0	75	0.517	354.5	410.3	912.3
2019	7	20	23	14	13.326	-50.91931	-73.57747	6.00	3.0	74	0.276	352.9	407.6	667.6
2019	7	21	0	55	0.710	-50.92295	-73.58431	4.85	3.0	74	0.280	345.8	380.0	1101.2
2019	7	21	2	47	29.375	-50.91639	-73.58811	3.58	3.0	74	0.304	352.2	416.2	897.7
2019	7	21	5	0	34.899	-50.91760	-73.59104	2.62	3.0	74	0.211	355.2	453.9	856.6
2019	7	21	6	30	14.986	-50.92805	-73.58777	7.57	3.0	74	0.282	351.7	433.8	1429.6
2019	7	21	9	0	11.934	-50.92088	-73.58914	4.87	3.0	74	0.232	354.3	442.7	1067.5
2019	7	21	11	1	55.256	-50.91660	-73.58763	4.06	3.0	74	0.265	351.1	440.8	1101.4

ORIGIN TIME (UTC)						Latitude	Longitude	Depth	M_L	GAP	RMS	X error	Y error	Z error
yyyy	mm	dd	h	m	seconds	[°]	[°]	[Km]		[°]		[m]	[m]	[m]
2019	7	21	12	24	20.121	-50.92256	-73.58042	6.00	2.8	82	0.154	388.6	536.3	1185.8
2019	7	21	12	44	47.383	-50.92071	-73.58380	4.92	2.9	74	0.152	362.3	415.8	1002.6
2019	7	21	14	4	12.159	-50.93277	-73.58541	9.15	3.0	75	0.452	360.8	432.2	1095.0
2019	7	21	16	6	37.695	-50.92252	-73.58916	4.50	3.0	72	0.321	371.2	447.4	956.8
2019	7	21	18	14	58.619	-50.93114	-73.58247	6.53	2.9	75	0.370	365.7	434.9	896.4
2019	7	21	19	12	59.094	-50.92911	-73.58050	7.39	3.0	94	0.255	394.8	516.6	1257.8
2019	7	21	20	14	52.319	-50.92409	-73.60277	3.56	2.9	74	0.254	364.9	467.7	1549.5
2019	7	21	21	16	51.854	-50.92558	-73.58968	5.54	2.8	82	0.142	460.7	585.2	1667.1
2019	7	21	22	14	48.468	-50.92293	-73.58917	4.48	2.7	82	0.239	359.8	500.6	1584.1
2019	7	21	23	4	5.807	-50.92297	-73.58140	6.00	2.8	75	0.166	363.6	479.5	1122.1
2019	7	22	0	20	58.188	-50.91763	-73.58619	4.24	2.9	74	0.242	357.6	447.9	1112.2
2019	7	22	1	33	16.898	-50.91800	-73.59396	4.28	2.9	74	0.262	369.2	490.3	1254.8
2019	7	22	3	33	17.861	-50.91967	-73.58718	3.64	2.8	74	0.233	349.4	483.7	1117.4
2019	7	22	4	46	50.338	-50.92564	-73.57803	7.93	2.8	75	0.281	396.0	570.5	1298.6
2019	7	22	6	21	11.941	-50.92581	-73.58532	5.51	2.9	74	0.267	360.5	363.2	1098.5
2019	7	22	8	18	16.915	-50.92416	-73.58821	5.26	2.7	74	0.235	339.7	397.8	899.5
2019	7	22	9	33	26.023	-50.93610	-73.57282	10.92	2.8	79	0.630	434.3	479.0	880.3
2019	7	22	10	31	8.913	-50.91946	-73.58669	4.66	2.8	74	0.218	377.7	479.6	1220.3
2019	7	22	12	27	20.907	-50.91831	-73.61240	2.78	2.7	74	0.190	415.4	496.9	1123.9
2019	7	22	14	19	37.318	-50.91599	-73.58519	6.00	2.9	74	0.330	361.5	456.0	854.4
2019	7	22	16	25	34.074	-50.91725	-73.58036	4.64	2.9	74	0.133	356.5	412.0	748.3
2019	7	22	21	38	5.536	-50.94026	-73.59958	5.50	2.8	83	0.328	379.4	484.4	1133.1
2019	7	22	23	32	30.039	-50.91351	-73.59099	2.99	3.0	72	0.543	377.2	424.5	667.7
2019	7	23	1	15	45.545	-50.91886	-73.58426	4.40	3.0	74	0.262	389.3	462.6	1409.0
2019	7	23	2	38	0.887	-50.91970	-73.58136	6.00	2.9	74	0.147	357.7	451.7	1045.7
2019	7	23	4	30	18.611	-50.92310	-73.59548	5.19	3.0	74	0.245	367.4	420.9	1419.1
2019	7	23	6	42	45.886	-50.92093	-73.57943	6.00	2.9	82	0.145	367.0	479.2	1000.9
2019	7	23	9	0	22.446	-50.92420	-73.57947	6.00	3.0	74	0.166	389.5	452.4	1142.8
2019	7	23	10	57	13.021	-50.92133	-73.58138	8.85	3.0	74	0.449	356.0	457.4	1181.6
2019	7	23	12	25	35.843	-50.92337	-73.58237	6.00	3.1	82	0.144	399.8	507.4	1199.1
2019	7	23	13	20	10.555	-50.91904	-73.58960	4.80	3.0	74	0.290	361.3	500.4	1101.2
2019	7	23	15	12	38.347	-50.92314	-73.58771	5.78	2.9	74	0.237	361.6	442.6	1181.2
2019	7	23	16	30	31.735	-50.91561	-73.57937	6.00	3.0	74	0.283	370.6	431.3	693.2
2019	7	23	18	31	35.467	-50.92006	-73.59010	3.01	2.9	74	0.208	346.1	427.6	868.4
2019	7	23	19	29	12.860	-50.92075	-73.57409	4.88	2.7	94	0.198	467.0	613.1	1860.8
2019	7	23	20	44	7.786	-50.93237	-73.58249	9.21	3.0	75	0.522	337.8	422.2	851.7
2019	7	23	22	45	0.442	-50.92008	-73.58622	3.52	2.9	74	0.283	358.2	440.3	889.0
2019	7	23	23	42	55.497	-50.92457	-73.58821	9.58	2.9	74	0.356	396.1	507.4	1263.6
2019	7	24	1	39	58.860	-50.92254	-73.58431	4.11	3.0	74	0.235	348.1	419.3	1139.8
2019	7	24	2	37	16.253	-50.92372	-73.59403	5.51	2.9	74	0.291	345.7	419.5	1107.3
2019	7	24	3	16	19.043	-50.82414	-73.44939	2.98	2.7	107	0.768	538.7	593.0	1186.5
2019	7	24	4	53	27.171	-50.91886	-73.58426	5.83	2.9	121	0.264	370.1	491.8	953.6
2019	7	24	6	48	24.995	-50.92049	-73.58525	4.65	3.0	74	0.311	345.4	412.8	1025.7
2019	7	24	8	12	52.548	-50.92173	-73.58333	5.98	2.9	74	0.201	364.3	424.1	867.5
2019	7	24	9	9	26.851	-50.89892	-73.56363	2.86	2.8	117	0.502	425.6	601.2	797.2
2019	7	24	9	45	34.827	-51.06733	-74.20307	17.57	3.5	113	0.275	464.3	296.0	666.8
2019	7	24	10	36	4.766	-50.92235	-73.58188	5.86	3.1	74	0.175	398.5	490.4	1303.8

ORIGIN TIME (UTC)						Latitude	Longitude	Depth	M_L	GAP	RMS	X error	Y error	Z error
yyyy	mm	dd	h	m	seconds	[°]	[°]	[Km]		[°]		[m]	[m]	[m]
2019	7	24	13	56	12.192	-50.92212	-73.58818	6.00	2.7	74	0.159	401.0	493.1	1278.7
2019	7	24	16	13	48.011	-50.92011	-73.58039	6.00	2.8	74	0.307	381.1	465.5	948.7
2019	7	24	17	53	2.258	-50.91886	-73.58426	5.75	2.8	74	0.375	387.8	527.0	1131.8
2019	7	24	20	3	16.046	-50.92459	-73.58336	4.83	2.8	74	0.255	433.8	414.8	1301.4
2019	7	24	21	24	20.279	-50.92251	-73.59110	3.72	2.7	74	0.221	368.7	456.7	1070.4
2019	7	24	22	47	47.938	-50.92485	-73.61249	12.12	2.7	74	0.777	434.5	525.7	1310.5
2019	7	25	0	31	49.321	-50.92419	-73.58239	5.69	2.7	74	0.194	357.2	426.0	904.2
2019	7	25	1	49	5.216	-50.90581	-73.57633	1.65	2.8	73	0.574	371.4	431.9	755.6
2019	7	25	3	35	52.529	-50.93370	-73.60338	3.90	2.8	75	0.369	383.7	443.3	947.2
2019	7	25	4	37	15.119	-50.92214	-73.58236	5.92	2.8	74	0.158	386.1	446.7	1056.3
2019	7	25	5	10	26.326	-50.92459	-73.58433	5.18	2.9	74	0.255	364.0	448.4	1299.8
2019	7	25	7	16	9.346	-50.92007	-73.58719	3.40	2.9	74	0.231	362.8	441.6	993.7
2019	7	25	8	37	38.292	-53.11199	-72.09974	61.49	3.7	186	1.374	638.1	542.0	1089.4
2019	7	25	8	49	23.848	-50.91513	-73.59489	6.00	2.8	74	0.397	318.2	413.3	520.9
2019	7	25	10	36	39.062	-50.91883	-73.59008	3.01	3.0	74	0.328	358.3	469.9	828.6
2019	7	25	12	2	50.170	-50.92134	-73.58041	6.00	2.8	73	0.214	444.4	441.6	896.0
2019	7	25	15	30	53.506	-50.92383	-73.57170	6.00	3.1	74	0.368	352.9	392.6	486.0
2019	7	25	16	51	20.222	-50.91884	-73.58911	5.12	3.0	74	0.349	365.6	406.8	988.2
2019	7	25	18	6	37.409	-50.91480	-73.57839	6.00	2.9	81	0.329	421.2	517.2	940.3
2019	7	25	18	57	43.469	-50.92254	-73.58431	6.00	3.1	74	0.363	368.8	411.2	849.7
2019	7	25	20	24	10.455	-50.92213	-73.58527	5.26	3.0	74	0.241	332.1	392.0	1079.1
2019	7	25	22	19	23.284	-50.91987	-73.58767	3.36	3.0	74	0.211	353.2	432.7	1017.3
2019	7	25	23	37	39.959	-50.92255	-73.58236	6.00	2.8	121	0.210	451.2	540.1	1242.9
2019	7	26	0	41	55.833	-50.91886	-73.58426	5.73	3.0	74	0.313	347.1	457.5	821.8
2019	7	26	2	51	6.324	-50.93711	-73.57623	11.40	3.0	75	0.695	344.2	419.7	680.1
2019	7	26	4	58	23.641	-50.92004	-73.59398	4.62	3.0	74	0.327	359.1	389.8	907.0
2019	7	26	6	35	50.547	-50.91907	-73.58378	4.61	3.0	72	0.266	355.4	436.4	970.7
2019	7	26	7	42	59.633	-50.92087	-73.59205	4.05	2.9	82	0.219	362.9	512.8	1318.9
2019	7	26	11	21	41.972	-50.91976	-73.60903	4.57	2.9	74	0.278	408.5	477.0	1229.5
2019	7	26	13	57	55.798	-50.92051	-73.58234	6.00	3.1	74	0.264	393.0	442.2	794.0
2019	7	26	17	57	21.986	-51.06617	-74.21618	18.60	3.1	114	0.202	788.2	544.4	675.7
2019	7	26	19	29	37.582	-50.91726	-73.57842	6.00	3.0	74	0.341	379.8	389.0	777.1
2019	7	26	20	51	46.201	-50.92150	-73.58769	5.50	3.0	74	0.275	358.6	420.1	982.5
2019	7	26	21	57	59.670	-51.40871	-74.48721	18.15	3.5	140	0.452	561.8	336.9	645.0
2019	7	26	22	13	9.656	-50.91971	-73.57748	6.00	2.9	74	0.226	368.8	495.2	935.2
2019	7	27	1	14	44.556	-50.92543	-73.58046	7.64	3.1	74	0.448	336.5	432.7	1088.1
2019	7	27	2	20	46.571	-50.92970	-73.58391	7.03	3.3	83	0.385	359.2	486.9	1045.1
2019	7	27	4	13	41.710	-50.91597	-73.59005	4.85	3.3	74	0.315	404.2	547.3	976.9
2019	7	27	6	28	58.777	-50.91988	-73.58573	6.01	3.1	74	0.148	423.5	496.9	1294.1
2019	7	27	7	53	13.274	-50.91970	-73.57942	6.00	3.3	74	0.238	386.6	537.1	1083.2
2019	7	27	10	7	47.868	-50.92007	-73.58913	4.97	3.4	76	0.275	377.0	458.9	1547.7
2019	7	27	11	37	25.324	-50.93421	-73.58300	7.71	3.5	79	0.467	456.1	591.7	1259.3
2019	7	27	14	4	41.657	-50.91986	-73.58961	4.45	3.2	82	0.255	390.1	582.2	1500.4
2019	7	27	16	15	13.165	-50.91967	-73.58621	5.81	3.2	94	0.382	387.5	529.9	1124.8
2019	7	27	19	55	59.767	-50.92050	-73.58428	6.28	3.4	74	0.246	411.3	481.3	1252.4
2019	7	27	22	23	49.515	-50.92170	-73.59012	3.99	3.2	74	0.213	368.1	465.3	1190.8
2019	7	28	0	11	5.204	-50.92331	-73.59402	4.89	3.2	74	0.224	380.0	512.2	1046.0

ORIGIN TIME (UTC)						Latitude	Longitude	Depth	M_L	GAP	RMS	X error	Y error	Z error
yyyy	mm	dd	h	m	seconds	[°]	[°]	[Km]		[°]		[m]	[m]	[m]
2019	7	28	1	33	27.792	-50.92212	-73.58721	4.23	3.2	82	0.316	399.5	538.1	1155.8
2019	7	28	3	13	32.902	-50.91924	-73.59106	4.23	3.3	74	0.241	375.2	422.0	1079.4
2019	7	28	6	59	43.778	-50.92538	-73.58920	5.32	3.3	74	0.226	369.1	405.7	1341.5
2019	7	28	8	27	48.708	-50.92488	-73.60764	10.01	3.3	74	0.518	372.2	461.2	934.9
2019	7	28	10	35	33.712	-50.92620	-73.58921	4.15	3.2	74	0.216	381.9	521.6	1247.5
2019	7	28	12	0	29.338	-50.92169	-73.59109	3.52	3.2	74	0.245	401.6	479.4	1068.2
2019	7	28	14	27	35.672	-50.91598	-73.58714	6.00	3.3	74	0.351	381.1	454.1	946.0
2019	7	28	15	58	40.247	-50.91799	-73.59493	3.05	3.4	74	0.238	423.6	510.9	1238.3
2019	7	28	19	4	51.932	-50.92071	-73.58380	5.82	3.3	74	0.374	358.0	420.0	802.4
2019	7	28	20	16	42.595	-50.91967	-73.58621	3.80	3.3	74	0.254	391.4	486.3	1103.6
2019	7	28	22	15	3.301	-52.63911	-72.85820	14.37	3.9	182	0.967	685.0	877.8	1276.1
2019	7	28	22	40	55.565	-50.92314	-73.58771	5.07	3.2	74	0.208	330.0	410.1	1193.3
2019	7	28	23	41	4.684	-50.92214	-73.58333	6.00	3.1	74	0.155	406.9	485.0	1224.5
2019	7	29	0	35	52.908	-50.92208	-73.59595	4.11	3.3	74	0.327	355.3	462.8	1261.7
2019	7	29	1	57	44.779	-50.92250	-73.59207	2.55	3.2	74	0.265	350.7	454.6	710.7
2019	7	29	2	24	52.429	-50.92008	-73.58622	5.65	3.1	74	0.114	390.6	460.0	1162.6
2019	7	29	3	42	29.655	-50.92213	-73.58527	4.46	3.2	74	0.244	339.5	433.6	1033.6
2019	7	29	5	0	43.845	-50.91803	-73.58619	3.56	3.2	74	0.204	336.2	426.6	926.1
2019	7	29	5	39	52.241	-50.92337	-73.58335	6.00	3.1	74	0.194	394.7	496.1	1077.6
2019	7	29	6	52	59.723	-50.91966	-73.58815	3.09	3.2	74	0.225	339.5	410.1	821.7
2019	7	29	7	29	38.587	-50.92377	-73.58432	5.98	3.0	82	0.181	360.1	425.8	882.7
2019	7	29	8	5	46.126	-52.23503	-72.32243	21.00	3.6	147	0.995	529.5	502.4	962.1
2019	7	29	8	21	16.004	-50.92005	-73.59204	4.52	3.1	74	0.254	345.6	406.8	1094.5
2019	7	29	9	12	41.208	-50.92174	-73.58138	5.87	3.0	74	0.136	352.3	423.3	1043.9
2019	7	29	11	30	51.197	-50.92254	-73.58431	5.40	3.1	74	0.193	324.2	405.7	1018.3
2019	7	29	12	48	24.294	-50.92294	-73.58722	3.68	3.2	74	0.297	337.9	412.3	824.1
2019	7	29	14	0	24.818	-50.92418	-73.58433	5.98	3.0	82	0.226	367.6	472.3	904.7
2019	7	29	15	8	49.649	-50.92213	-73.58430	5.26	3.1	74	0.192	324.3	400.6	1181.9
2019	7	29	16	30	32.726	-50.92089	-73.58817	4.36	3.1	74	0.184	336.0	422.6	979.8
2019	7	29	17	4	59.507	-50.92255	-73.58236	5.55	2.9	74	0.151	375.0	445.0	1075.0
2019	7	29	18	54	13.111	-50.91761	-73.58910	3.39	3.0	74	0.226	342.9	409.3	844.8
2019	7	29	20	18	54.982	-50.92049	-73.58622	3.93	3.0	74	0.184	325.1	392.3	931.3
2019	7	29	21	31	35.420	-50.92255	-73.58236	5.14	2.9	82	0.172	358.7	432.6	947.9
2019	7	29	23	1	5.073	-50.92378	-73.58335	5.20	2.9	74	0.177	329.5	426.6	1274.8
2019	7	30	0	34	59.271	-50.92213	-73.58527	4.89	3.0	74	0.254	323.1	404.4	954.8
2019	7	30	1	34	15.219	-50.91078	-73.56475	6.00	2.8	73	0.439	331.3	377.9	409.7
2019	7	30	2	45	10.154	-50.92457	-73.58821	4.21	3.0	74	0.211	336.0	409.0	1118.0
2019	7	30	4	27	52.331	-50.92131	-73.58526	4.11	2.8	82	0.215	328.0	442.5	1276.4
2019	7	30	5	41	47.649	-50.92173	-73.58430	4.60	2.7	82	0.232	339.0	414.6	1071.6
2019	7	30	6	56	42.245	-50.92744	-73.58728	0.69	2.9	74	0.731	349.8	429.9	929.9
2019	7	30	8	39	13.385	-50.92725	-73.58388	7.42	2.8	82	0.304	345.3	438.7	1134.4
2019	7	30	9	35	33.673	-50.93195	-73.58442	9.30	3.0	83	0.505	358.4	448.1	1170.7
2019	7	30	10	35	55.545	-50.92418	-73.58433	5.46	2.8	82	0.179	338.7	438.7	1344.6
2019	7	30	12	40	37.036	-50.93155	-73.58345	7.82	2.9	79	0.410	338.0	439.1	1007.2
2019	7	30	13	48	35.297	-50.91967	-73.58621	5.14	2.7	82	0.314	344.7	401.8	1011.6
2019	7	30	15	9	41.135	-50.92132	-73.58332	6.00	3.0	82	0.239	330.6	460.1	1021.7
2019	7	30	16	2	39.940	-50.92375	-73.58820	5.24	2.9	74	0.165	344.3	457.1	1457.7

ORIGIN TIME (UTC)						Latitude	Longitude	Depth	M_L	GAP	RMS	X error	Y error	Z error
yyyy	mm	dd	h	m	seconds	[°]	[°]	[Km]		[°]		[m]	[m]	[m]
2019	7	30	17	55	10.286	-50.92212	-73.58721	3.91	2.7	74	0.271	326.2	426.8	895.6
2019	7	30	19	50	18.947	-50.91680	-73.58812	2.99	2.7	74	0.232	331.5	409.4	715.0
2019	7	30	21	25	8.533	-50.91905	-73.58766	3.00	2.8	74	0.195	337.8	408.2	765.1
2019	7	30	22	46	37.010	-50.91883	-73.59008	1.33	2.7	82	0.130	362.8	451.9	862.5
2019	7	30	23	41	5.776	-50.92441	-73.57899	6.85	2.9	74	0.224	326.5	380.5	973.3
2019	7	31	1	4	49.864	-50.94055	-73.58356	10.71	2.9	75	0.693	345.1	432.0	709.1
2019	7	31	2	38	9.719	-50.92623	-73.58338	6.41	2.8	74	0.234	360.5	446.0	1207.1
2019	7	31	3	49	21.680	-50.92151	-73.58575	4.45	2.7	82	0.216	356.5	517.7	1289.3
2019	7	31	4	50	45.109	-50.92214	-73.58236	4.44	2.8	57	0.175	319.9	392.2	1096.8
2019	7	31	6	10	45.450	-50.91966	-73.58815	2.94	2.9	57	0.205	326.8	404.2	802.9
2019	7	31	7	40	17.961	-50.92499	-73.58531	4.85	2.7	56	0.356	386.1	414.0	877.0
2019	7	31	9	5	21.570	-50.92501	-73.58142	6.37	2.9	56	0.158	341.4	377.7	1000.1
2019	7	31	10	12	42.285	-50.92010	-73.58233	5.98	2.6	57	0.156	366.6	400.0	864.0
2019	7	31	11	4	24.987	-50.92092	-73.58234	5.51	2.9	57	0.190	335.7	359.7	907.9
2019	7	31	12	27	45.080	-50.92129	-73.59012	3.81	2.8	57	0.178	343.0	395.6	975.4
2019	7	31	13	30	10.033	-50.92496	-73.59113	4.19	2.7	56	0.180	378.3	450.5	999.7
2019	7	31	14	24	30.993	-50.92253	-73.58625	4.56	2.9	57	0.196	345.0	421.4	1063.6
2019	7	31	15	42	31.107	-50.92232	-73.58770	3.82	2.9	57	0.223	344.3	406.3	1017.7
2019	7	31	17	16	37.096	-50.91766	-73.57842	6.00	2.8	57	0.268	362.6	425.8	696.1
2019	7	31	17	56	30.744	-50.92211	-73.58915	4.32	2.9	57	0.189	333.3	387.2	1017.5
2019	7	31	19	25	47.014	-50.92622	-73.58532	7.35	2.9	56	0.447	334.7	398.4	1462.9
2019	7	31	20	47	39.382	-50.92091	-73.58331	5.44	2.8	57	0.189	372.5	429.5	1007.9
2019	7	31	21	44	58.829	-50.92089	-73.58817	4.30	3.0	57	0.248	348.7	401.4	1019.2
2019	7	31	22	46	39.578	-50.92171	-73.58818	2.99	2.7	57	0.131	438.0	460.9	920.0
2019	7	31	23	47	43.467	-50.92541	-73.58337	5.67	2.9	56	0.237	321.9	377.6	1030.6
2019	8	1	0	24	58.005	-51.91473	-74.34910	18.46	3.7	220	0.500	568.1	620.7	660.2
2019	8	1	1	22	29.545	-50.92253	-73.58722	4.46	3.0	54	0.208	327.7	362.9	1099.4
2019	8	1	2	24	54.061	-50.92905	-73.59216	4.42	3.0	53	0.347	341.4	384.5	861.8
2019	8	1	3	17	59.867	-50.92495	-73.59404	4.36	3.0	54	0.233	343.1	386.5	1029.3
2019	8	1	4	36	56.196	-50.92050	-73.58331	5.28	2.9	54	0.182	349.8	395.0	965.7
2019	8	1	5	42	45.247	-50.91991	-73.57990	4.65	3.0	54	0.190	415.9	399.0	951.5
2019	8	1	6	46	27.396	-50.92213	-73.58527	4.67	3.0	54	0.293	332.8	388.9	1123.9
2019	8	1	7	30	14.174	-50.91724	-73.58230	4.56	3.0	54	0.137	425.8	466.4	1201.3
2019	8	1	7	56	52.884	-50.91543	-75.07233	9.54	3.1	187	0.319	781.4	536.8	830.3
2019	8	1	9	25	29.655	-50.92540	-73.58531	7.12	3.0	53	0.481	344.2	353.9	1057.7
2019	8	1	10	26	8.373	-50.92050	-73.58331	5.69	3.0	54	0.294	428.9	415.6	850.5
2019	8	1	11	34	39.854	-50.92007	-73.58913	3.39	3.1	54	0.261	351.9	389.9	793.6
2019	8	1	13	2	46.479	-50.92250	-73.59304	4.26	3.1	54	0.243	376.8	414.1	1321.7
2019	8	1	15	27	56.367	-50.91559	-73.58519	5.75	3.0	54	0.331	348.2	422.1	1122.4
2019	8	1	18	3	33.781	-50.91802	-73.58910	6.00	3.1	54	0.361	362.6	389.3	883.2
2019	8	1	19	38	10.925	-50.92539	-73.58725	4.62	3.2	53	0.267	418.6	419.1	1002.0
2019	8	1	21	28	38.406	-50.92456	-73.59016	4.21	3.1	53	0.248	369.8	418.1	931.2
2019	8	1	22	27	46.541	-50.92396	-73.58772	4.68	3.0	53	0.084	517.5	497.3	1452.9
2019	8	2	0	8	22.728	-50.91844	-73.58717	4.77	3.0	54	0.278	336.0	354.3	1035.0
2019	8	2	1	44	2.184	-50.92294	-73.58722	5.61	3.1	54	0.156	349.6	389.7	908.0
2019	8	2	2	59	23.123	-50.91886	-73.58426	3.68	2.9	54	0.237	433.2	421.6	925.0
2019	8	2	3	48	35.758	-50.92172	-73.58624	4.38	3.1	54	0.218	332.3	382.7	1050.9

ORIGIN TIME (UTC)						Latitude	Longitude	Depth	M_L	GAP	RMS	X error	Y error	Z error
yyyy	mm	dd	h	m	seconds	[°]	[°]	[Km]		[°]		[m]	[m]	[m]
2019	8	2	4	55	45.638	-50.92974	-73.57614	10.78	3.1	53	0.635	576.2	512.5	1179.5
2019	8	2	5	20	32.452	-50.92540	-73.58531	5.42	2.9	53	0.261	357.3	388.1	1285.9
2019	8	2	6	47	19.758	-50.92031	-73.58088	5.09	3.0	54	0.167	395.0	393.0	1070.6
2019	8	2	7	26	17.983	-50.92172	-73.58527	3.91	3.0	54	0.224	346.6	377.7	956.9
2019	8	2	8	48	1.655	-50.91644	-73.57743	4.81	2.9	54	0.184	413.8	403.5	1102.7
2019	8	2	8	58	33.800	-50.92172	-73.58527	5.44	3.0	57	0.307	334.6	396.1	800.2
2019	8	2	10	22	34.234	-50.92294	-73.58625	4.50	3.0	53	0.248	435.0	411.2	1071.6
2019	8	2	11	11	21.362	-50.92214	-73.58333	5.18	3.1	53	0.256	349.9	357.3	891.6
2019	8	2	12	25	49.942	-50.92943	-73.59701	3.03	3.1	53	0.297	412.0	408.6	676.5
2019	8	2	13	15	14.556	-50.42730	-74.41974	24.17	2.9	95	0.146	594.1	408.3	801.0
2019	8	2	13	29	46.678	-50.92483	-73.57802	8.32	3.1	53	0.490	467.7	472.5	1393.5
2019	8	2	14	15	50.737	-50.91159	-73.56573	7.15	3.0	54	0.471	314.7	379.5	925.0
2019	8	2	15	37	58.936	-50.91884	-73.58814	6.92	2.9	54	0.236	462.0	481.9	1266.7
2019	8	2	16	13	44.677	-50.92254	-73.58528	4.13	3.0	54	0.208	348.5	425.4	1215.0
2019	8	2	17	40	33.585	-50.92252	-73.58819	3.91	3.1	54	0.232	353.5	398.7	1083.9
2019	8	2	20	7	0.621	-50.92256	-73.58139	4.83	3.0	53	0.149	395.8	398.2	1194.2
2019	8	2	21	29	36.717	-50.92496	-73.59113	7.58	3.1	53	0.347	409.6	451.8	1621.1
2019	8	2	22	53	15.168	-50.90754	-73.59916	12.30	3.0	54	0.534	418.6	495.0	1154.8
2019	8	3	0	40	56.974	-50.92397	-73.58578	6.29	2.9	53	0.219	438.0	449.6	1247.5
2019	8	3	2	36	13.450	-50.91292	-73.58661	3.02	3.1	76	0.292	438.6	448.8	852.0
2019	8	3	4	24	30.912	-50.92059	-73.56584	8.99	3.0	75	0.637	454.8	493.0	1228.8
2019	8	3	6	52	10.637	-50.92052	-73.57943	6.00	3.1	75	0.136	414.7	461.6	1010.9
2019	8	3	8	12	20.905	-50.92232	-73.58770	4.80	3.1	54	0.176	487.9	469.1	1555.2
2019	8	3	10	56	2.830	-50.90868	-73.57540	5.96	3.1	69	0.324	458.1	404.6	868.5
2019	8	3	14	8	0.005	-50.91965	-73.59009	5.65	3.2	54	0.253	389.6	458.9	973.8
2019	8	3	15	19	9.150	-50.91806	-73.58134	5.71	3.3	54	0.513	368.3	408.5	1028.4
2019	8	3	16	28	14.448	-50.92014	-73.57360	5.18	3.2	55	0.322	396.7	423.6	1208.2
2019	8	3	17	56	42.485	-50.92376	-73.58723	7.55	3.2	53	0.426	364.6	393.5	1575.3
2019	8	3	18	55	21.150	-50.91270	-73.58904	4.24	3.3	54	0.421	374.4	469.8	966.8
2019	8	3	20	22	44.669	-50.92741	-73.59311	4.58	3.1	53	0.141	418.7	461.4	1548.2
2019	8	3	21	40	52.213	-50.92579	-73.58920	5.48	3.1	53	0.201	384.7	410.4	1046.4
2019	8	3	23	9	26.284	-50.92072	-73.58186	5.78	3.1	54	0.187	375.7	396.6	919.1
2019	8	4	0	21	14.246	-50.92110	-73.58672	5.99	3.1	54	0.192	349.7	356.5	838.8
2019	8	4	1	20	36.067	-50.48180	-73.89768	25.82	3.3	120	0.801	846.8	1379.8	1391.2
2019	8	4	2	14	56.051	-50.92256	-73.58139	6.00	3.2	53	0.180	437.9	474.0	1131.8
2019	8	4	3	58	11.166	-50.92171	-73.58818	4.73	3.2	54	0.228	341.9	380.5	1018.7
2019	8	4	4	54	52.826	-50.92399	-73.58190	5.27	3.0	53	0.137	442.8	456.0	1246.9
2019	8	4	5	13	56.573	-50.92419	-73.58141	6.00	3.2	100	0.216	382.5	407.8	842.4
2019	8	4	6	40	44.478	-51.14761	-74.04370	10.57	3.1	99	0.339	354.1	269.4	881.9
2019	8	4	6	42	14.790	-50.91986	-73.58961	3.82	3.1	54	0.195	363.0	386.4	1118.0
2019	8	4	7	40	26.594	-50.92988	-73.58925	8.99	3.2	53	0.563	397.5	430.2	1011.6
2019	8	4	8	28	24.234	-50.91807	-73.57843	6.00	3.0	54	0.182	382.6	386.0	873.8
2019	8	4	9	3	35.400	-50.92542	-73.58240	6.00	3.1	53	0.227	385.9	412.1	895.5
2019	8	4	11	11	25.006	-50.92293	-73.58917	1.88	3.2	54	0.177	400.4	428.0	766.7
2019	8	4	12	17	46.954	-50.91890	-73.57649	9.65	3.1	54	0.650	429.2	437.4	970.8
2019	8	4	13	5	20.919	-50.92255	-73.58334	6.00	2.9	53	0.183	522.2	489.6	1012.5
2019	8	4	14	0	16.957	-50.93218	-73.58006	4.37	3.1	56	0.319	362.9	464.0	1167.1

ORIGIN TIME (UTC)						Latitude	Longitude	Depth	M_L	GAP	RMS	X error	Y error	Z error
yyyy	mm	dd	h	m	seconds	[°]	[°]	[Km]		[°]		[m]	[m]	[m]
2019	8	4	15	16	35.917	-50.92214	-73.58333	5.24	3.0	53	0.258	376.8	410.0	1183.6
2019	8	4	16	4	36.270	-51.07169	-74.46615	20.19	2.9	136	0.187	724.1	345.6	531.7
2019	8	4	16	55	33.445	-50.92336	-73.58529	4.50	3.1	53	0.212	361.5	369.6	1027.6
2019	8	4	17	55	23.970	-50.92622	-73.58629	6.37	3.0	53	0.285	375.1	414.9	1130.1
2019	8	4	18	38	27.482	-50.92276	-73.58285	5.99	2.9	53	0.182	425.8	461.7	1087.7
2019	8	4	19	54	33.404	-50.92090	-73.58526	3.91	3.1	54	0.244	341.9	376.9	862.7
2019	8	4	21	8	41.252	-50.93525	-73.57864	5.01	3.0	53	0.542	337.3	367.5	689.0
2019	8	4	21	45	24.842	-50.92068	-73.58962	4.41	2.9	54	0.164	458.1	482.5	1365.7
2019	8	4	22	59	54.185	-50.91842	-73.59105	3.15	3.0	54	0.487	344.3	377.6	723.9
2019	8	4	23	52	3.282	-50.92543	-73.58046	9.01	3.0	53	0.456	374.0	403.5	1036.6
2019	8	5	0	46	58.653	-50.92293	-73.58917	5.79	3.0	54	0.212	355.5	391.1	1057.3
2019	8	5	3	5	42.529	-50.92541	-73.58434	6.00	3.0	53	0.308	324.0	340.4	675.6
2019	8	5	4	34	8.178	-50.92560	-73.58580	5.74	3.0	53	0.284	332.5	372.7	836.0
2019	8	5	6	19	51.727	-50.92089	-73.58720	4.07	3.0	54	0.227	346.2	398.8	1004.4
2019	8	5	6	59	41.987	-50.92480	-73.58385	6.01	2.9	53	0.207	417.8	524.3	1171.7
2019	8	5	7	41	24.351	-50.92090	-73.58526	5.22	2.9	54	0.257	352.3	399.8	1043.9
2019	8	5	9	14	3.737	-50.92087	-73.59108	3.54	2.9	54	0.280	346.5	406.2	915.8
2019	8	5	11	14	20.177	-50.92741	-73.59213	5.79	3.0	74	0.344	358.4	423.9	1019.6
2019	8	5	12	44	38.521	-50.91764	-73.58230	6.00	3.0	74	0.334	344.2	396.7	812.5
2019	8	5	14	19	13.369	-50.92272	-73.59062	5.99	3.1	74	0.236	385.2	468.4	929.6
2019	8	5	16	16	6.946	-50.92418	-73.58530	6.00	3.0	74	0.189	354.9	439.2	1120.9
2019	8	5	18	7	33.958	-50.91845	-73.58523	5.38	3.0	72	0.195	377.7	450.4	940.8
2019	8	5	19	32	8.568	-50.91966	-73.58815	6.00	3.2	82	0.351	449.1	564.1	1104.2
2019	8	5	21	56	27.691	-50.92005	-73.59204	3.97	3.1	74	0.217	375.0	436.1	1393.8
2019	8	6	0	1	26.999	-50.92823	-73.59214	5.20	3.1	74	0.283	370.0	451.8	1057.0
2019	8	6	2	28	19.407	-50.92395	-73.58966	6.64	3.0	74	0.288	420.9	511.0	1625.8
2019	8	6	3	52	17.246	-50.93689	-73.57866	10.83	3.1	73	0.822	364.8	439.6	814.0
2019	8	6	6	11	41.947	-50.92151	-73.58575	4.80	3.1	74	0.239	370.0	466.0	1150.4
2019	8	6	7	47	7.691	-50.92253	-73.58625	5.46	3.2	74	0.260	371.3	448.7	1362.6
2019	8	6	9	18	6.465	-50.92807	-73.58389	4.88	3.1	74	0.327	419.6	532.8	1689.5
2019	8	6	10	28	23.430	-50.92703	-73.58630	7.62	3.1	74	0.252	405.1	490.3	1235.7
2019	8	6	12	9	50.354	-50.91396	-73.58323	4.13	3.1	72	0.396	368.2	436.2	890.5
2019	8	6	16	7	44.968	-50.91644	-73.57841	6.00	3.2	74	0.273	420.2	476.5	970.5
2019	8	6	18	4	51.052	-50.92552	-73.60328	8.00	3.0	82	0.231	481.7	615.9	1847.8
2019	8	6	20	9	13.490	-50.92542	-73.58240	8.99	3.3	74	0.442	388.3	495.8	909.6
2019	8	6	23	32	47.124	-50.92558	-73.59163	7.69	3.1	74	0.303	441.6	530.2	1943.5
2019	8	7	1	28	19.244	-50.92051	-73.58234	6.00	3.1	74	0.207	355.9	427.3	1140.6
2019	8	7	3	3	33.619	-50.91583	-73.57791	6.01	3.0	82	0.279	368.7	516.5	850.5
2019	8	7	5	5	36.489	-50.92749	-73.57660	8.99	3.2	82	0.344	372.7	466.4	924.7
2019	8	7	7	31	22.261	-50.92093	-73.58040	6.00	3.0	74	0.126	345.5	448.2	994.2
2019	8	7	9	39	28.523	-50.91438	-73.58032	6.00	3.0	81	0.369	389.9	473.6	761.5
2019	8	7	11	38	37.765	-51.20956	-72.42697	11.68	3.2	66	0.262	574.3	367.0	1119.0
2019	8	7	12	26	7.502	-50.91346	-73.60069	3.01	3.2	81	0.272	353.6	493.1	927.5
2019	8	7	16	31	58.844	-50.92561	-73.58386	7.77	3.2	74	0.209	461.4	551.4	1399.4
2019	8	7	18	9	41.026	-50.91886	-73.58426	6.00	3.2	94	0.312	399.3	523.6	942.9
2019	8	7	20	9	45.904	-50.92745	-73.58534	6.90	3.0	74	0.193	421.9	490.9	1145.7
2019	8	7	22	32	56.524	-50.93427	-73.57134	10.29	3.1	75	0.659	364.9	466.3	814.6

ORIGIN TIME (UTC)						Latitude	Longitude	Depth	M_L	GAP	RMS	X error	Y error	Z error
yyyy	mm	dd	h	m	seconds	[°]	[°]	[Km]		[°]		[m]	[m]	[m]
2019	8	8	0	21	7.106	-50.92219	-73.57265	8.99	3.2	74	0.532	401.7	463.7	949.2
2019	8	8	2	33	52.010	-50.92069	-73.58768	4.41	3.2	74	0.199	375.7	469.0	1062.3
2019	8	8	4	0	19.866	-50.92394	-73.59160	5.50	3.0	141	0.236	588.9	742.2	1518.8
2019	8	8	5	23	5.148	-50.91738	-73.59346	3.98	3.1	74	0.248	387.0	433.5	1004.1
2019	8	8	7	55	52.706	-50.92048	-73.58816	4.23	3.0	74	0.200	375.9	480.1	1317.5
2019	8	8	9	54	50.770	-50.92458	-73.58627	4.91	3.0	74	0.198	370.5	491.7	1575.1
2019	8	8	11	39	47.642	-50.91593	-73.59878	2.60	2.8	81	0.227	390.9	534.9	933.3
2019	8	8	13	32	32.813	-50.93297	-73.62425	1.92	3.1	74	0.585	445.1	551.8	594.0
2019	8	8	16	7	26.122	-50.91807	-73.57940	6.00	3.0	74	0.292	408.8	530.1	819.3
2019	8	8	17	43	50.717	-50.91501	-73.57790	5.66	2.9	120	0.271	462.1	673.0	1615.2
2019	8	8	19	35	45.276	-50.92479	-73.58579	7.89	3.0	73	0.219	445.8	540.9	1442.7
2019	8	8	21	19	18.530	-50.89281	-73.59897	2.89	2.7	80	0.451	484.0	689.8	1461.5
2019	8	8	23	44	24.913	-50.92969	-73.58585	5.23	2.8	83	0.176	440.2	566.4	1625.0
2019	8	9	1	54	13.821	-50.92622	-73.58629	6.00	3.0	74	0.282	401.7	449.8	905.1
2019	8	9	3	33	6.666	-50.92313	-73.58965	5.62	3.0	74	0.174	452.8	509.8	1469.3
2019	8	9	6	11	15.892	-50.61560	-71.49044	0.59	3.1	99	0.627	525.3	583.3	643.9
2019	8	9	7	16	9.632	-50.92315	-73.58577	6.17	3.1	74	0.154	390.0	480.2	1110.9
2019	8	9	9	30	49.936	-50.93114	-73.58344	7.99	2.8	73	0.258	386.9	460.5	1098.7
2019	8	9	11	34	58.095	-50.92336	-73.58529	5.98	2.9	74	0.104	410.6	489.9	1230.6
2019	8	9	13	35	51.454	-50.92952	-73.58051	6.00	2.8	130	0.501	379.0	624.7	1121.2
2019	8	9	15	30	46.315	-50.92295	-73.58431	6.00	3.0	74	0.152	355.2	365.4	925.4
2019	8	9	17	20	22.851	-50.91519	-73.58227	5.51	3.0	74	0.299	385.1	411.1	993.0
2019	8	9	19	26	50.108	-50.92865	-73.59118	4.77	3.1	73	0.312	409.3	485.7	1498.9
2019	8	9	20	50	20.566	-50.92395	-73.58966	4.33	3.0	53	0.301	389.6	445.1	917.7
2019	8	9	22	30	45.832	-50.92260	-73.57266	5.01	3.0	53	0.195	406.4	424.5	1362.9
2019	8	9	23	53	42.717	-50.92583	-73.58143	8.64	3.4	53	0.257	402.6	481.6	1201.2
2019	8	10	0	53	57.332	-50.92704	-73.58533	6.00	3.3	56	0.222	358.6	393.1	828.7
2019	8	10	2	3	15.161	-50.91722	-73.58618	5.28	3.1	54	0.264	417.2	538.8	1175.8
2019	8	10	2	28	13.286	-50.92335	-73.58626	5.30	3.1	53	0.170	359.1	411.5	1454.5
2019	8	10	3	24	34.157	-50.91809	-73.57551	3.60	3.0	59	0.178	483.1	520.0	1156.0
2019	8	10	4	4	44.557	-50.92435	-73.59064	5.29	3.2	54	0.270	361.3	412.1	1159.0
2019	8	10	6	15	58.221	-50.91480	-73.57936	6.00	3.1	68	0.313	478.1	514.6	1143.2
2019	8	10	7	13	28.745	-50.92335	-73.58626	4.34	3.2	53	0.257	346.1	353.1	889.9
2019	8	10	7	38	51.459	-51.86940	-74.25012	7.69	3.7	210	0.442	797.3	1131.8	1885.7
2019	8	10	8	21	12.115	-50.92012	-73.57748	6.84	3.0	75	0.401	384.4	458.3	1074.0
2019	8	10	8	52	33.883	-50.93484	-73.57863	9.85	3.3	53	0.774	357.8	400.6	831.8
2019	8	10	10	35	42.082	-50.92663	-73.58533	5.55	3.0	74	0.199	352.8	360.4	786.5
2019	8	10	16	2	51.929	-50.92110	-73.58672	4.12	3.1	82	0.174	337.5	481.5	1193.4
2019	8	10	17	14	10.618	-50.93071	-73.58732	9.52	3.1	83	0.357	433.2	496.7	1183.7
2019	8	10	17	33	27.272	-50.92624	-73.58144	8.01	3.2	73	0.549	343.9	391.0	981.4
2019	8	10	20	51	17.308	-50.93104	-73.60286	3.64	3.0	82	0.536	383.1	539.5	952.4
2019	8	10	21	45	38.044	-50.92891	-73.58002	5.43	3.1	83	0.250	383.9	493.5	1252.0
2019	8	10	22	34	28.259	-50.92539	-73.58823	6.00	3.0	74	0.160	369.5	462.6	920.1
2019	8	11	0	10	1.834	-50.92439	-73.58287	5.29	3.0	74	0.173	325.5	409.7	1255.5
2019	8	11	1	2	21.822	-50.92295	-73.58431	5.26	3.0	82	0.223	379.3	484.5	1015.4
2019	8	11	2	2	22.633	-50.92540	-73.58628	5.20	3.1	74	0.218	331.8	384.2	931.6
2019	8	11	2	59	58.536	-50.92970	-73.58391	7.18	3.0	73	0.252	415.6	511.9	1464.7

ORIGIN TIME (UTC)						Latitude	Longitude	Depth	M_L	GAP	RMS	X error	Y error	Z error
yyyy	mm	dd	h	m	seconds	[°]	[°]	[Km]		[°]		[m]	[m]	[m]
2019	8	11	3	41	58.860	-50.92315	-73.58577	4.29	2.9	74	0.183	338.8	410.6	1112.4
2019	8	11	5	15	46.072	-50.92333	-73.59014	3.85	3.0	74	0.206	337.7	422.0	1127.3
2019	8	11	6	30	28.658	-50.92337	-73.58237	5.40	2.9	82	0.155	343.2	451.1	1157.2
2019	8	11	7	18	22.244	-50.92417	-73.58724	4.67	3.0	74	0.231	338.8	422.3	1074.2
2019	8	11	8	26	21.285	-50.91681	-73.58521	3.78	3.1	72	0.326	327.5	375.4	774.5
2019	8	11	9	3	36.149	-50.92174	-73.58138	5.38	3.0	74	0.122	389.7	439.6	1138.1
2019	8	11	10	33	22.684	-52.47233	-71.45986	32.99	3.4	103	0.969	690.5	656.9	545.7
2019	8	11	10	42	1.650	-50.92234	-73.58382	4.68	3.0	74	0.196	333.1	409.9	1061.7
2019	8	11	12	36	38.048	-50.92078	-73.60855	2.64	3.0	74	0.345	338.7	431.9	856.5
2019	8	11	13	16	57.494	-50.94220	-73.57970	10.57	2.7	79	0.554	413.2	560.9	920.3
2019	8	11	13	37	43.131	-51.90255	-74.26740	19.23	3.6	230	0.493	616.7	758.4	683.4
2019	8	11	14	17	47.578	-50.92576	-73.59600	2.84	3.0	74	0.279	350.6	377.7	577.4
2019	8	11	15	27	18.958	-50.92296	-73.58334	5.01	3.0	82	0.181	427.3	619.9	1198.5
2019	8	11	16	29	21.967	-50.91908	-73.62115	3.37	3.0	74	0.236	353.3	410.3	842.3
2019	8	11	17	11	9.582	-50.92622	-73.58629	5.94	3.1	82	0.174	393.1	495.8	984.0
2019	8	11	18	14	15.513	-50.92009	-73.58428	5.14	2.7	74	0.321	349.2	397.4	1032.9
2019	8	11	19	22	11.688	-50.91762	-73.58813	3.97	2.8	74	0.305	420.6	605.0	1168.6
2019	8	11	20	18	48.930	-50.92891	-73.61837	2.39	2.8	74	0.481	357.7	444.0	677.9
2019	8	11	21	24	45.330	-50.92459	-73.58336	5.83	2.8	74	0.158	361.0	455.2	1129.8
2019	8	11	21	32	23.015	-50.66205	-73.35805	5.34	2.7	60	0.374	310.0	372.3	802.1
2019	8	11	23	14	42.093	-50.92642	-73.58581	5.31	2.6	82	0.140	430.1	616.4	1460.6
2019	8	12	0	1	15.729	-50.92211	-73.58915	4.09	2.9	74	0.188	337.8	400.9	955.0
2019	8	12	1	13	49.691	-50.91781	-73.59056	3.02	2.9	74	0.227	349.7	423.6	825.3
2019	8	12	2	3	45.685	-50.92890	-73.58196	7.26	2.7	75	0.273	404.8	578.4	1432.9
2019	8	12	2	42	14.989	-50.92276	-73.58285	5.21	2.8	74	0.199	344.7	407.6	972.7
2019	8	12	4	3	19.326	-50.92541	-73.58434	4.26	2.7	74	0.280	337.1	418.5	1173.6
2019	8	12	4	37	47.038	-50.92908	-73.58536	4.73	2.6	83	0.148	329.6	520.5	1547.7
2019	8	12	5	43	50.375	-50.92502	-73.57948	7.12	2.8	74	0.223	336.1	401.4	1025.7
2019	8	12	6	44	5.882	-50.92480	-73.58385	5.97	2.6	82	0.156	381.2	501.2	1143.2
2019	8	12	7	40	16.686	-50.93033	-73.58246	8.05	2.7	75	0.497	345.4	434.0	967.4
2019	8	12	8	22	20.847	-50.92990	-73.58634	5.90	2.6	75	0.209	412.3	481.8	1304.7
2019	8	12	8	49	31.097	-51.94641	-72.27516	15.01	3.0	68	0.638	476.2	429.1	580.2
2019	8	12	9	16	3.871	-50.92908	-73.58633	7.23	2.7	75	0.226	330.4	393.4	1333.9
2019	8	12	10	12	34.821	-50.92376	-73.58723	4.46	2.7	74	0.150	364.5	462.2	1015.3
2019	8	12	10	55	40.961	-50.92131	-73.58526	4.40	2.7	74	0.162	336.2	411.7	1131.0
2019	8	12	11	42	57.897	-50.92662	-73.58630	4.28	2.6	74	0.166	410.8	520.5	1145.0
2019	8	12	12	45	36.933	-50.92903	-73.59604	3.31	2.8	73	0.491	343.3	437.9	872.2
2019	8	12	13	29	39.911	-50.92213	-73.58624	4.09	2.6	74	0.169	416.2	528.1	1110.5
2019	8	12	14	23	30.003	-50.92067	-73.59156	4.76	2.7	141	0.121	624.4	897.3	1852.9
2019	8	12	14	35	40.012	-50.92336	-73.58529	4.67	2.8	74	0.201	337.2	429.0	1037.5
2019	8	12	15	16	16.549	-50.92439	-73.58287	5.45	2.8	82	0.200	427.3	576.2	1680.1
2019	8	12	16	23	43.854	-50.92334	-73.58820	4.21	2.7	74	0.353	342.8	444.7	955.4
2019	8	12	17	9	33.721	-50.92582	-73.58435	6.00	2.6	82	0.188	396.7	476.8	1069.1
2019	8	12	18	7	32.788	-50.92048	-73.58719	4.64	2.8	74	0.234	341.6	439.1	1391.1
2019	8	12	18	50	45.290	-50.91888	-73.58135	4.71	2.7	72	0.346	384.1	504.8	989.0
2019	8	12	19	58	15.366	-50.92396	-73.58772	4.80	2.6	74	0.186	340.9	482.1	1366.6
2019	8	12	21	51	2.778	-50.92151	-73.58575	5.07	2.7	74	0.365	336.1	417.8	875.5

ORIGIN TIME (UTC)						Latitude	Longitude	Depth	M_L	GAP	RMS	X error	Y error	Z error
yyyy	mm	dd	h	m	seconds	[°]	[°]	[Km]		[°]		[m]	[m]	[m]
2019	8	12	23	6	8.659	-50.92418	-73.58530	5.16	2.8	74	0.351	333.1	389.8	735.9
2019	8	13	0	12	31.031	-50.93793	-73.57430	9.80	2.7	75	0.783	376.3	449.8	844.2
2019	8	13	0	50	3.688	-50.92131	-73.58623	3.54	2.8	74	0.208	362.9	462.7	1014.7
2019	8	13	2	36	50.895	-50.47103	-74.80665	25.12	2.8	120	0.678	342.4	376.9	592.8
2019	8	13	2	53	3.413	-50.92579	-73.59017	3.01	2.8	82	0.561	344.7	422.2	620.5
2019	8	13	4	5	31.270	-50.91194	-73.57738	6.00	2.7	73	0.424	360.4	435.8	504.3
2019	8	13	4	39	4.019	-50.92334	-73.58917	5.34	2.6	72	0.238	337.5	435.9	1073.0
2019	8	13	6	20	20.186	-50.36504	-74.68605	24.22	2.5	99	0.434	309.3	333.4	678.7
2019	8	13	6	24	52.366	-50.92828	-73.58244	6.10	2.9	75	0.323	319.3	325.5	677.4
2019	8	13	8	20	35.708	-50.92254	-73.58431	5.51	2.7	74	0.234	336.8	398.9	821.7
2019	8	13	9	17	0.291	-50.92112	-73.58283	5.29	2.5	74	0.169	369.3	455.5	1036.1
2019	8	13	9	58	51.129	-50.91847	-73.58134	4.38	2.7	74	0.187	355.7	532.3	1308.2
2019	8	13	11	27	27.793	-50.91804	-73.58522	3.81	2.7	74	0.138	354.3	455.0	1072.4
2019	8	13	12	37	14.323	-50.92499	-73.58531	5.26	2.6	95	0.142	391.4	558.9	1299.3
2019	8	13	14	7	25.721	-50.91987	-73.58767	4.10	2.8	74	0.224	346.7	444.4	1014.4
2019	8	13	16	13	57.483	-50.91844	-73.58717	3.31	2.9	74	0.239	336.7	449.4	1123.8
2019	8	13	18	7	53.987	-50.92049	-73.58622	4.30	2.6	74	0.211	333.8	406.8	1076.6
2019	8	13	19	48	59.702	-50.92458	-73.58530	5.16	2.8	74	0.192	367.9	462.9	1084.6
2019	8	13	21	49	6.443	-50.92049	-73.58622	3.58	2.7	74	0.218	353.0	408.5	980.8
2019	8	13	23	3	58.955	-50.91843	-73.58911	3.19	2.7	74	0.268	366.2	470.0	890.2
2019	8	14	0	53	33.982	-50.91824	-73.58571	3.55	2.8	74	0.244	346.7	451.1	929.0
2019	8	14	2	46	24.851	-50.92172	-73.58527	4.19	2.9	74	0.224	333.9	432.3	1168.8
2019	8	14	4	19	44.743	-50.92333	-73.59014	7.41	2.7	74	0.320	359.5	395.9	1599.8
2019	8	14	7	19	41.563	-50.92293	-73.58819	3.91	2.8	74	0.208	340.7	409.5	1028.6
2019	8	14	9	2	49.255	-50.92416	-73.58821	4.62	2.7	74	0.230	348.0	400.7	1060.2
2019	8	14	10	42	35.753	-50.92379	-73.58044	6.12	2.6	74	0.308	360.1	437.9	1079.4
2019	8	14	10	56	37.311	-50.91925	-73.58815	3.01	2.8	74	0.330	329.8	418.6	718.1
2019	8	14	12	49	3.671	-50.89725	-73.56944	6.00	2.8	73	0.643	322.8	334.5	253.8
2019	8	14	14	45	37.370	-50.91929	-73.58038	7.37	2.8	74	0.463	335.3	405.5	1019.2
2019	8	14	16	21	48.154	-50.91968	-73.58427	6.00	2.8	74	0.326	343.6	412.0	816.7
2019	8	14	18	5	18.417	-50.92744	-73.58631	7.15	2.9	74	0.251	342.0	432.1	1382.2
2019	8	14	19	35	3.677	-50.93521	-73.58738	8.97	2.7	79	0.338	347.2	429.9	887.0
2019	8	14	21	40	32.490	-50.92362	-73.87169	9.30	2.7	79	0.132	320.8	313.7	1153.3
2019	8	14	21	48	40.462	-50.92339	-73.57849	3.95	2.7	74	0.525	337.5	410.8	1077.4
2019	8	14	21	55	9.464	-50.92207	-73.86001	8.81	2.4	66	0.272	356.3	315.7	1187.9
2019	8	14	23	49	6.257	-50.92992	-73.58149	7.78	2.8	75	0.286	323.6	411.4	932.4
2019	8	15	1	24	21.162	-50.92418	-73.58433	5.98	2.8	74	0.309	338.3	394.7	917.3
2019	8	15	2	24	48.614	-50.92421	-73.57753	8.99	2.6	82	0.403	364.5	458.5	1117.7
2019	8	15	2	41	0.772	-49.96595	-73.80575	2.12	2.6	119	0.274	393.0	629.1	937.7
2019	8	15	3	11	49.419	-50.92009	-73.58330	4.36	2.8	74	0.366	320.8	407.7	808.4
2019	8	15	4	23	15.973	-52.39003	-71.43716	38.00	3.2	132	0.673	801.0	903.2	1320.9
2019	8	15	5	5	29.749	-50.92209	-73.59304	3.37	2.8	74	0.255	338.5	430.6	882.8
2019	8	15	6	42	7.359	-50.92129	-73.58914	3.01	2.8	74	0.523	329.0	399.6	594.7
2019	8	15	7	47	49.290	-50.92215	-73.58139	5.36	2.6	74	0.134	372.6	446.4	1131.0
2019	8	15	8	26	42.268	-50.92174	-73.58235	6.00	2.7	74	0.215	342.6	391.8	836.9
2019	8	15	9	21	1.656	-51.20727	-72.41967	11.43	2.6	100	0.424	406.4	351.5	1204.4
2019	8	15	9	40	6.196	-50.91847	-73.58134	6.00	2.6	74	0.283	356.2	361.5	601.2

ORIGIN TIME (UTC)						Latitude	Longitude	Depth	M_L	GAP	RMS	X error	Y error	Z error
yyyy	mm	dd	h	m	seconds	[°]	[°]	[Km]		[°]		[m]	[m]	[m]
2019	8	15	9	41	9.776	-50.92037	-73.86775	9.28	2.6	70	0.344	285.6	279.0	987.1
2019	8	15	10	18	40.436	-50.92707	-73.57951	6.69	2.6	74	0.159	339.7	410.1	842.5
2019	8	15	11	29	32.360	-50.92245	-73.86390	9.07	2.5	97	0.286	350.6	319.3	1202.9
2019	8	15	12	6	0.391	-50.92070	-73.58574	4.10	2.8	74	0.233	323.1	423.7	972.3
2019	8	15	13	59	55.083	-50.92252	-73.58819	5.08	2.8	82	0.223	330.0	447.4	1114.8
2019	8	15	15	18	28.155	-50.93526	-73.57767	10.87	2.6	79	0.541	473.4	550.4	916.9
2019	8	15	17	29	9.970	-50.91395	-73.58420	3.01	3.1	74	0.377	323.8	392.2	574.0
2019	8	15	18	47	40.950	-50.91944	-73.59058	4.66	2.7	74	0.152	371.1	433.7	1096.5
2019	8	15	19	26	42.025	-50.90101	-73.59520	3.71	2.6	80	0.569	398.1	570.1	1100.4
2019	8	15	20	20	44.716	-50.92294	-73.58625	4.40	2.8	74	0.361	343.1	431.4	882.6
2019	8	15	23	22	48.578	-50.91843	-73.58911	5.67	2.8	74	0.274	334.8	432.0	908.8
2019	8	16	0	56	23.172	-50.92623	-73.58338	6.26	2.8	74	0.152	355.1	469.1	1155.8
2019	8	16	2	5	43.776	-50.89661	-73.53353	6.00	2.6	80	0.699	378.3	525.4	355.5
2019	8	16	2	41	19.430	-50.91716	-73.59686	3.01	2.7	74	0.247	332.6	443.8	779.6
2019	8	16	4	3	52.765	-50.92039	-73.60467	1.63	2.8	74	0.398	339.1	443.4	782.9
2019	8	16	4	52	59.894	-50.92251	-73.59013	7.74	2.6	74	0.380	353.2	424.9	1186.8
2019	8	16	6	18	27.871	-50.91906	-73.58572	3.82	2.9	74	0.245	324.3	418.4	973.9
2019	8	16	7	45	9.269	-50.92052	-73.57943	9.32	2.8	74	0.444	329.9	419.3	929.8
2019	8	16	9	3	27.347	-50.92256	-73.58139	5.49	2.7	74	0.137	370.2	468.7	1087.5
2019	8	16	9	38	27.771	-50.92643	-73.58387	6.60	2.8	73	0.191	328.8	377.3	1029.0
2019	8	16	11	8	7.196	-50.92255	-73.58334	6.00	2.6	82	0.157	385.1	519.5	1145.7
2019	8	16	11	35	20.337	-50.91722	-73.58618	3.40	2.7	74	0.219	332.8	436.6	1016.3
2019	8	16	12	59	47.858	-50.91310	-73.59195	1.20	2.9	120	0.662	409.3	603.1	592.4
2019	8	16	14	10	46.726	-50.91836	-73.60173	6.00	2.7	74	0.513	435.7	497.3	744.1
2019	8	16	15	0	38.738	-50.92171	-73.58721	4.42	2.8	74	0.256	335.4	443.2	1101.3
2019	8	16	16	26	4.397	-50.92047	-73.58913	3.62	2.8	74	0.193	343.0	439.6	1222.2
2019	8	16	17	43	1.937	-50.92108	-73.59060	4.04	2.7	82	0.178	391.1	502.0	1083.3
2019	8	16	20	53	0.345	-50.92661	-73.58921	5.10	2.8	74	0.220	339.5	390.0	1122.2
2019	8	16	22	20	58.189	-50.92703	-73.58728	4.32	2.8	74	0.226	333.5	408.4	1132.5
2019	8	17	0	27	1.790	-50.91683	-73.58229	4.38	2.7	74	0.229	332.5	417.8	995.9
2019	8	17	1	48	56.965	-50.92703	-73.58728	7.45	2.7	73	0.336	337.5	407.3	1342.8
2019	8	17	4	15	48.801	-51.87055	-74.36711	18.67	3.2	232	0.521	988.9	833.5	1066.7
2019	8	17	4	42	50.661	-50.92581	-73.58532	7.25	2.7	74	0.445	342.3	383.6	948.5
2019	8	17	5	55	14.110	-50.92253	-73.58625	5.14	2.5	74	0.139	377.0	433.1	1031.2
2019	8	17	7	6	58.949	-50.92126	-73.59594	2.23	2.8	74	0.640	343.5	415.8	657.4
2019	8	17	7	47	45.598	-50.93137	-73.57811	9.57	2.7	75	0.468	368.3	442.9	1310.4
2019	8	17	8	24	11.901	-50.91845	-73.58523	3.60	2.7	72	0.252	340.4	413.5	860.1
2019	8	17	9	46	33.683	-50.92764	-73.58680	5.68	2.7	82	0.137	409.3	565.4	1460.4
2019	8	17	10	44	40.629	-50.92292	-73.59014	3.39	2.7	74	0.229	341.8	454.0	893.3
2019	8	17	12	10	16.495	-50.92562	-73.58192	3.82	2.8	74	0.340	344.8	441.5	877.0
2019	8	17	14	21	23.030	-50.92049	-73.58622	4.05	2.9	74	0.199	336.1	414.1	1025.2
2019	8	17	15	36	58.296	-50.93234	-73.58831	8.76	2.7	75	0.415	353.6	463.0	1118.0
2019	8	17	17	27	25.792	-50.91968	-73.58427	4.21	2.8	74	0.224	346.5	422.8	921.6
2019	8	17	18	57	36.312	-50.91804	-73.58522	4.32	2.7	74	0.209	337.3	392.1	972.2
2019	8	17	20	46	2.505	-50.91589	-73.60655	2.29	2.6	81	0.323	365.4	472.3	705.8
2019	8	17	22	14	6.275	-50.92089	-73.58817	4.60	2.6	82	0.202	341.4	469.4	1284.9
2019	8	17	23	23	46.171	-50.63342	-74.39217	19.62	2.3	110	0.406	407.2	281.0	732.2

ORIGIN TIME (UTC)						Latitude	Longitude	Depth	M_L	GAP	RMS	X error	Y error	Z error
yyyy	mm	dd	h	m	seconds	[°]	[°]	[Km]		[°]		[m]	[m]	[m]
2019	8	17	23	50	49.229	-50.92256	-73.58042	4.21	2.7	82	0.293	335.7	464.2	1779.8
2019	8	18	0	59	54.655	-50.92153	-73.58187	4.88	2.4	74	0.167	390.5	482.3	1259.2
2019	8	18	1	6	20.994	-50.91766	-73.57939	6.00	2.6	74	0.283	363.1	448.3	672.4
2019	8	18	2	41	37.454	-52.48977	-71.49593	30.04	2.8	153	0.855	792.8	804.1	880.6
2019	8	18	2	47	48.518	-50.92622	-73.58629	5.10	2.7	74	0.266	330.7	400.7	1236.4
2019	8	18	4	14	57.129	-50.92070	-73.58574	3.90	2.6	74	0.215	327.0	409.0	1020.7
2019	8	18	5	50	54.307	-50.92940	-73.60381	11.00	2.2	82	0.517	398.9	519.4	813.9
2019	8	18	7	9	17.884	-50.92462	-73.57851	4.21	2.3	74	0.197	401.6	484.1	1180.2
2019	8	18	7	22	28.348	-50.92417	-73.58627	5.87	2.5	74	0.269	355.6	463.4	1064.7
2019	8	18	8	57	35.963	-50.91495	-73.58955	2.18	2.1	81	0.410	408.9	521.3	1213.1
2019	8	18	12	12	34.043	-50.92067	-73.59156	4.14	2.5	74	0.254	327.7	429.1	889.7
2019	8	18	13	12	48.676	-51.06889	-74.18996	15.61	2.4	111	0.299	415.4	294.5	712.9
2019	8	18	16	20	22.362	-51.00768	-73.20704	1.74	2.9	119	0.193	652.2	552.6	956.7
2019	8	18	17	3	24.626	-50.92132	-73.58429	5.77	2.7	74	0.211	344.5	413.7	1171.1
2019	8	18	19	31	36.971	-50.92233	-73.58576	5.39	2.5	82	0.125	449.5	559.5	1378.3
2019	8	18	19	47	41.472	-50.92392	-73.59549	5.54	2.4	74	0.226	346.3	445.1	906.4
2019	8	18	20	41	48.881	-50.92090	-73.58526	4.28	2.4	82	0.160	421.7	534.1	1203.2
2019	8	18	21	58	59.054	-50.91887	-73.58232	6.28	2.7	74	0.329	344.3	436.3	1064.9
2019	8	18	23	51	6.029	-50.92173	-73.58333	6.55	2.6	74	0.313	328.5	391.9	967.3
2019	8	19	0	27	55.029	-50.93113	-73.58441	6.00	2.4	83	0.220	445.7	639.4	1252.2
2019	8	19	1	2	46.924	-50.91885	-73.58717	5.75	2.6	74	0.319	351.8	466.1	916.4
2019	8	19	3	11	45.472	-50.92294	-73.58722	4.79	2.9	74	0.242	338.0	441.0	1138.2
2019	8	19	4	16	16.551	-50.93476	-73.59514	7.99	2.4	79	0.326	380.4	559.2	1710.2
2019	8	19	5	42	42.615	-50.92397	-73.58578	4.92	2.4	82	0.149	465.2	615.9	1738.8
2019	8	19	6	59	45.694	-50.92416	-73.58821	4.52	2.5	74	0.251	349.8	415.9	1600.8
2019	8	19	7	58	27.288	-50.62012	-74.41010	20.32	2.1	110	0.239	482.8	300.4	913.4
2019	8	19	8	0	9.430	-50.92053	-73.57749	4.24	2.3	74	0.370	366.2	474.0	924.9
2019	8	19	8	23	13.499	-50.92704	-73.58533	6.63	2.5	74	0.133	339.5	413.6	1205.2
2019	8	19	9	15	46.824	-50.92316	-73.58383	6.01	2.4	74	0.206	401.1	488.4	1252.5
2019	8	19	9	45	37.366	-50.91842	-73.59105	2.82	2.5	74	0.172	339.5	420.7	999.7
2019	8	19	10	46	31.245	-52.20559	-74.25154	20.00	3.0	260	0.722	676.1	750.7	1073.0
2019	8	19	11	24	28.597	-50.92827	-73.58535	6.84	2.5	74	0.168	355.7	451.3	1160.8
2019	8	19	12	11	38.089	-50.90926	-73.58171	6.01	2.4	140	0.427	722.0	991.7	1099.3
2019	8	19	12	40	1.071	-50.93161	-73.57083	6.63	2.5	75	0.554	489.4	626.0	1041.3
2019	8	19	13	37	45.249	-50.91154	-73.57640	6.00	2.5	81	0.387	349.7	438.8	703.3
2019	8	19	14	40	21.948	-50.91650	-73.60704	5.97	2.2	81	0.345	476.8	683.5	1198.6
2019	8	19	16	7	54.486	-50.91889	-73.57844	6.00	2.7	74	0.273	342.8	390.0	664.3
2019	8	19	17	4	25.521	-50.92614	-73.60086	5.90	2.4	82	0.242	383.7	513.6	927.5
2019	8	19	18	36	13.774	-50.91801	-73.59104	5.55	2.7	74	0.310	331.9	403.0	852.6
2019	8	19	19	32	56.738	-50.91809	-73.57551	6.00	2.1	94	0.283	404.2	535.7	1098.9
2019	8	19	20	0	42.860	-50.92255	-73.58334	6.00	2.5	95	0.280	386.4	506.5	789.5
2019	8	19	21	4	45.138	-50.92376	-73.58626	4.81	2.3	74	0.221	371.7	474.8	1053.9
2019	8	19	22	19	40.194	-50.92478	-73.58773	6.83	2.7	74	0.179	326.6	435.4	1307.5
2019	8	19	22	38	35.216	-50.92274	-73.58674	5.29	2.2	95	0.111	466.0	705.6	1685.5
2019	8	19	23	33	41.267	-50.92503	-73.57851	5.30	2.6	74	0.238	336.0	416.9	960.4
2019	8	20	0	23	37.473	-52.50838	-71.49580	29.87	2.8	138	0.924	674.4	575.4	1107.4
2019	8	20	0	28	16.472	-50.92825	-73.58923	6.49	2.2	82	0.280	386.9	495.3	1154.6

ORIGIN TIME (UTC)						Latitude	Longitude	Depth	M_L	GAP	RMS	X error	Y error	Z error
yyyy	mm	dd	h	m	seconds	[°]	[°]	[Km]		[°]		[m]	[m]	[m]
2019	8	20	1	25	24.179	-50.92210	-73.59110	5.28	2.5	74	0.234	351.5	431.8	1304.1
2019	8	20	2	32	2.622	-50.92782	-73.59311	7.10	2.3	78	0.289	351.1	442.4	1134.3
2019	8	20	3	47	16.291	-50.94244	-73.61369	0.69	2.4	75	0.813	398.1	561.0	413.2
2019	8	20	5	5	49.473	-50.92048	-73.58719	4.77	2.4	74	0.240	340.4	419.9	1011.1
2019	8	20	6	13	39.143	-50.91409	-73.59730	3.00	2.4	72	0.329	332.6	394.3	633.4
2019	8	20	8	19	55.056	-50.92376	-73.58626	7.17	2.5	74	0.255	347.0	398.2	1169.6
2019	8	20	9	31	32.646	-50.92939	-73.60478	6.74	2.3	74	0.273	386.0	464.4	1236.5
2019	8	20	10	3	38.304	-50.92886	-73.58973	5.70	2.2	74	0.178	480.0	593.7	1607.6
2019	8	20	10	38	20.677	-50.91783	-73.58667	3.96	2.4	74	0.190	333.2	435.1	1150.4
2019	8	20	11	21	39.150	-50.92638	-73.59358	4.57	2.1	96	0.217	558.3	806.3	1573.3
2019	8	20	12	3	57.936	-50.92214	-73.58236	5.98	2.3	74	0.215	346.4	430.2	742.3
2019	8	20	12	52	51.711	-50.92072	-73.58186	5.39	2.1	94	0.194	498.9	697.7	1514.0
2019	8	20	13	8	9.826	-50.91883	-73.59008	4.42	2.5	74	0.215	357.8	440.7	1024.8
2019	8	20	13	50	50.772	-51.16243	-75.52502	18.00	2.8	239	0.487	1330.7	788.4	1622.7
2019	8	20	14	33	10.653	-51.19624	-72.42176	14.77	2.6	65	0.460	260.2	309.0	530.1
2019	8	20	15	26	27.527	-50.91683	-73.58229	6.00	2.4	74	0.267	349.7	411.9	816.3
2019	8	20	16	39	46.829	-50.91965	-73.59107	5.77	2.3	74	0.383	370.5	453.7	843.7
2019	8	20	17	47	26.101	-50.92289	-73.63625	4.80	2.6	74	0.434	435.4	521.1	1717.7
2019	8	20	19	28	54.947	-50.92252	-73.58819	4.73	2.4	74	0.176	367.3	413.4	1253.4
2019	8	20	20	37	27.247	-50.92068	-73.58962	3.94	2.3	74	0.145	370.4	459.3	1144.6
2019	8	20	21	14	38.407	-50.23507	-71.96344	2.39	2.5	104	0.326	323.3	279.3	319.9
2019	8	20	22	3	38.058	-50.92171	-73.58721	4.71	2.4	74	0.170	363.8	447.6	1337.9
2019	8	21	0	21	41.125	-51.21056	-72.42354	6.00	2.4	93	0.236	436.5	393.9	1558.7
2019	8	21	0	46	10.995	-50.92499	-73.58628	7.23	2.4	82	0.312	368.6	516.5	1687.9
2019	8	21	2	41	33.768	-50.91886	-73.58523	3.97	2.4	74	0.221	352.2	438.5	1132.7
2019	8	21	3	36	2.465	-50.93380	-73.58396	10.00	2.5	75	0.546	365.2	442.2	857.4
2019	8	21	5	6	6.631	-50.92869	-73.58147	8.76	2.5	75	0.343	353.9	435.8	1013.6
2019	8	21	6	23	53.121	-50.92120	-73.60759	2.12	2.6	82	0.239	348.9	436.0	460.2
2019	8	21	7	11	10.825	-50.93197	-73.58054	9.01	2.4	83	0.537	483.4	513.4	1143.7
2019	8	21	8	35	4.879	-50.92008	-73.58525	4.52	2.5	82	0.207	337.2	446.0	1087.6
2019	8	21	9	43	26.897	-50.92411	-73.59792	4.77	2.6	82	0.291	360.3	478.1	1408.8
2019	8	21	11	9	25.083	-50.92047	-73.58913	2.51	2.5	82	0.160	381.2	451.6	1028.7
2019	8	21	12	37	33.370	-50.91808	-73.57746	4.58	2.5	82	0.237	387.8	484.9	1160.2
2019	8	21	14	15	59.540	-50.91436	-73.58420	6.61	2.9	93	0.362	361.3	491.7	1273.5
2019	8	21	15	37	2.572	-50.92336	-73.58529	5.51	2.8	82	0.118	390.6	480.0	1215.9
2019	8	21	18	43	47.564	-50.92088	-73.59011	4.36	2.5	74	0.116	398.8	463.7	1494.7
2019	8	21	19	55	43.041	-50.91883	-73.59105	3.99	2.7	74	0.261	347.6	434.2	985.1
2019	8	21	22	30	32.802	-50.92461	-73.57948	8.64	2.6	74	0.437	355.0	430.4	936.9
2019	8	21	23	35	36.666	-50.92126	-73.59497	3.01	2.7	74	0.172	368.7	437.8	773.9
2019	8	22	0	55	28.967	-50.91617	-73.59054	3.34	2.6	74	0.204	339.6	434.4	966.5
2019	8	22	2	35	3.787	-50.91905	-73.58766	3.75	2.7	74	0.242	339.6	407.1	903.6
2019	8	22	5	0	55.888	-50.92069	-73.58768	3.59	2.6	74	0.247	327.7	366.9	721.2
2019	8	22	6	21	40.469	-50.92559	-73.58774	7.69	2.8	74	0.319	351.7	428.8	1300.0
2019	8	22	6	45	18.152	-50.63035	-74.40944	19.15	2.3	111	0.160	467.6	269.1	648.7
2019	8	22	7	47	7.364	-50.91884	-73.58911	3.58	2.7	74	0.228	366.8	470.3	1068.1
2019	8	22	8	57	18.690	-50.92376	-73.58723	5.46	2.6	74	0.185	373.7	425.5	973.2
2019	8	22	10	9	18.661	-50.92010	-73.58136	6.00	2.7	74	0.191	377.7	434.3	922.8

ORIGIN TIME (UTC)						Latitude	Longitude	Depth	M_L	GAP	RMS	X error	Y error	Z error
yyyy	mm	dd	h	m	seconds	[°]	[°]	[Km]		[°]		[m]	[m]	[m]
2019	8	22	12	29	53.302	-50.91758	-73.59589	2.60	2.7	74	0.175	361.8	457.7	772.2
2019	8	22	13	47	40.515	-50.91675	-73.59685	4.03	2.8	74	0.241	399.7	507.4	1152.2
2019	8	22	15	36	1.587	-50.30763	-74.51727	36.99	2.2	152	0.176	885.6	513.9	1153.7
2019	8	22	15	59	6.530	-50.91317	-73.57642	6.00	2.8	74	0.450	392.4	460.3	1034.8
2019	8	22	17	39	0.519	-50.91967	-73.58621	4.44	2.8	74	0.241	341.7	427.7	1108.3
2019	8	22	18	24	17.275	-49.82491	-73.44148	18.00	2.8	179	0.684	781.0	1248.5	1184.6
2019	8	22	18	55	12.022	-50.91779	-73.59444	3.02	2.8	74	0.210	373.9	480.6	1081.6
2019	8	22	20	15	47.195	-50.69650	-73.33030	3.70	2.7	58	0.432	328.3	349.3	685.5
2019	8	22	20	34	55.743	-50.93564	-73.58253	4.52	2.7	83	0.493	387.2	499.6	1423.8
2019	8	22	21	14	24.626	-50.92376	-73.58723	5.30	2.8	74	0.160	374.0	438.2	1153.1
2019	8	22	22	17	4.513	-52.75200	-73.88903	58.98	3.9	219	0.844	704.8	798.2	2141.6
2019	8	22	22	48	46.018	-50.92211	-73.58915	4.13	2.8	74	0.283	332.7	403.4	903.4
2019	8	23	0	21	48.084	-50.92826	-73.58729	2.00	2.8	74	0.472	340.4	385.0	431.7
2019	8	23	1	52	17.546	-50.92090	-73.58623	4.28	2.9	74	0.236	361.0	429.7	983.2
2019	8	23	3	34	33.887	-50.92131	-73.58526	4.64	2.9	74	0.216	339.2	409.8	1133.9
2019	8	23	5	5	3.206	-50.92418	-73.58433	6.73	2.9	78	0.220	388.4	503.0	1346.4
2019	8	23	6	28	4.069	-50.91825	-73.58377	3.63	2.8	82	0.219	360.8	466.9	1297.0
2019	8	23	7	51	17.634	-50.92336	-73.58432	6.18	3.0	73	0.141	369.2	494.5	1227.4
2019	8	23	9	33	25.123	-50.94301	-73.58262	10.96	3.1	74	0.727	329.9	396.0	660.5
2019	8	23	11	7	37.554	-50.92152	-73.58381	4.37	2.9	74	0.226	354.7	421.0	1161.8
2019	8	23	12	31	55.525	-50.92784	-73.58826	7.68	3.1	74	0.309	360.0	425.0	1606.0
2019	8	23	13	57	28.975	-50.92782	-73.59214	8.11	3.0	74	0.474	382.0	481.2	1790.2
2019	8	23	15	20	1.007	-50.92120	-73.86582	7.45	3.1	70	0.321	285.7	281.0	1054.7
2019	8	23	15	23	28.527	-50.92164	-73.86292	8.25	2.8	97	0.288	393.3	330.1	1234.3
2019	8	23	15	31	26.642	-50.92581	-73.58629	7.66	3.1	74	0.396	390.5	513.3	1853.9
2019	8	23	16	51	28.615	-50.92799	-73.59942	6.40	2.9	74	0.525	378.1	433.6	1024.8
2019	8	23	18	10	11.053	-50.93055	-73.57810	8.63	3.1	122	0.399	446.2	570.8	1399.0
2019	8	23	19	50	47.572	-50.92110	-73.58672	5.45	3.0	74	0.116	355.3	420.4	1008.2
2019	8	23	21	34	54.653	-50.92130	-73.58720	4.48	3.0	74	0.264	402.9	482.9	1165.3
2019	8	23	22	50	34.821	-50.92639	-73.59164	7.85	2.8	74	0.374	392.7	487.0	1918.1
2019	8	23	23	0	0.998	-51.20620	-72.40943	13.32	3.1	65	0.500	289.0	288.7	567.4
2019	8	24	0	19	50.375	-50.92132	-73.58332	3.76	3.0	74	0.276	350.1	420.4	858.8
2019	8	24	2	26	10.640	-50.91639	-73.58714	3.33	3.0	74	0.220	345.6	431.2	955.7
2019	8	24	3	40	26.922	-50.91842	-73.59008	5.63	2.9	54	0.164	392.5	413.5	988.1
2019	8	24	4	43	39.413	-52.48782	-71.48746	31.49	3.2	100	0.798	581.4	693.9	668.1
2019	8	24	5	15	49.856	-50.92417	-73.58724	4.24	3.0	53	0.224	378.8	395.9	1106.7
2019	8	24	6	52	7.749	-50.92211	-73.58915	4.52	3.0	54	0.490	370.0	431.3	1045.5
2019	8	24	9	51	3.089	-50.93236	-73.58540	9.79	3.1	53	0.730	348.4	407.2	906.5
2019	8	24	11	33	28.598	-50.92621	-73.58824	5.12	3.0	53	0.237	358.1	389.7	1069.1
2019	8	24	13	4	11.399	-50.92048	-73.58719	5.63	3.2	54	0.338	366.4	384.6	976.2
2019	8	24	14	48	52.454	-50.91930	-73.57941	6.00	3.1	54	0.266	373.5	412.1	839.8
2019	8	24	17	17	29.539	-50.92069	-73.58768	4.68	3.1	54	0.256	369.7	402.9	1696.3
2019	8	24	18	48	41.278	-50.92662	-73.58727	8.72	3.0	53	0.459	367.6	410.6	1180.1
2019	8	24	20	24	17.432	-50.92543	-73.57949	9.15	3.2	53	0.464	319.8	378.7	1509.9
2019	8	24	21	48	18.742	-50.90451	-73.59184	1.39	3.2	54	0.505	372.4	383.7	432.1
2019	8	24	23	4	57.832	-50.92495	-73.59307	5.22	3.0	54	0.268	378.2	409.1	1136.5
2019	8	25	0	36	7.424	-50.90949	-73.61763	2.87	3.1	77	0.695	423.5	448.4	599.2

ORIGIN TIME (UTC)						Latitude	Longitude	Depth	M_L	GAP	RMS	X error	Y error	Z error
yyyy	mm	dd	h	m	seconds	[°]	[°]	[Km]		[°]		[m]	[m]	[m]
2019	8	25	2	17	27.750	-50.92091	-73.58331	6.00	3.0	54	0.241	336.9	360.0	1031.8
2019	8	25	4	10	45.695	-50.92084	-73.59691	3.95	2.9	54	0.355	362.1	412.5	979.3
2019	8	25	5	41	18.199	-50.92008	-73.58622	5.98	2.9	54	0.332	368.8	388.7	854.9
2019	8	25	7	9	44.061	-50.91968	-73.58427	4.07	2.9	54	0.262	353.3	409.7	971.8
2019	8	25	8	38	50.705	-50.92416	-73.58918	4.44	3.0	53	0.277	354.9	391.6	970.5
2019	8	25	9	47	48.649	-50.92169	-73.59109	4.17	2.9	54	0.263	377.8	397.7	993.0
2019	8	25	11	56	33.514	-50.91802	-73.58910	3.40	2.9	54	0.237	349.2	401.8	903.6
2019	8	25	13	51	12.933	-50.92293	-73.58819	4.19	2.9	54	0.250	357.6	421.7	1037.3
2019	8	25	15	42	15.832	-50.92233	-73.58576	4.65	2.9	54	0.211	352.4	392.9	1129.8
2019	8	25	17	14	6.057	-50.92335	-73.58626	5.98	2.9	53	0.193	378.1	398.0	901.4
2019	8	25	18	47	16.141	-50.92130	-73.58817	4.15	2.8	54	0.197	353.9	377.8	1058.7
2019	8	25	20	12	49.577	-50.92293	-73.58819	5.71	2.9	54	0.192	376.0	415.4	893.2
2019	8	25	21	42	33.264	-50.92296	-73.58237	4.60	2.9	53	0.377	375.5	382.0	1759.6
2019	8	25	23	18	18.877	-50.92254	-73.58528	4.54	3.0	54	0.266	360.3	402.3	1510.3
2019	8	26	1	28	25.163	-50.92089	-73.58817	3.76	2.8	54	0.224	377.2	399.4	1098.5
2019	8	26	3	7	53.288	-50.92332	-73.59305	4.26	2.8	54	0.244	372.1	425.0	1083.9
2019	8	26	4	29	27.827	-50.92257	-73.57848	5.98	2.9	53	0.178	379.2	428.3	945.3
2019	8	26	5	55	47.625	-50.92381	-73.57656	6.00	2.9	53	0.185	421.4	443.2	905.8
2019	8	26	6	59	40.458	-50.91599	-73.58519	3.91	3.1	99	0.298	413.0	497.5	1010.6
2019	8	26	8	37	47.604	-50.93037	-73.57372	9.01	3.1	53	0.458	324.5	397.7	859.0
2019	8	26	9	48	21.842	-50.92256	-73.58139	5.77	3.0	100	0.195	374.2	505.1	1045.7
2019	8	26	11	33	54.726	-50.91767	-73.57648	6.00	3.1	54	0.299	379.7	420.0	843.4
2019	8	26	13	15	22.413	-50.91724	-73.58133	6.00	3.2	54	0.337	426.8	481.3	947.5
2019	8	26	14	45	38.912	-50.91080	-73.55989	6.00	3.2	98	0.542	422.1	475.4	459.9
2019	8	26	16	32	45.054	-50.91850	-73.57552	6.33	3.4	54	0.385	391.6	442.3	964.0
2019	8	26	18	3	30.762	-50.91683	-73.58132	6.00	3.2	54	0.307	422.6	447.6	809.1
2019	8	26	19	10	35.896	-50.92148	-73.59157	6.01	3.4	88	0.188	561.2	585.7	1396.5
2019	8	26	21	3	56.542	-50.92291	-73.59305	9.42	3.2	53	0.353	433.4	429.0	922.6
2019	8	26	22	32	30.884	-50.92706	-73.58145	6.00	3.4	74	0.229	452.7	504.7	1126.8
2019	8	26	23	33	42.819	-50.91976	-73.60903	2.93	3.1	130	0.189	521.1	718.5	1526.7
2019	8	27	1	14	28.859	-50.91971	-73.57845	6.00	3.1	74	0.301	392.8	455.5	936.2
2019	8	27	2	22	41.076	-50.92338	-73.58043	6.00	3.1	74	0.137	412.1	453.9	1138.9
2019	8	27	3	32	42.320	-50.92046	-73.59205	8.89	3.1	74	0.329	445.3	510.7	1420.3
2019	8	27	4	50	51.436	-50.92119	-73.60953	10.96	3.2	74	0.645	394.1	477.5	1036.5
2019	8	27	6	22	48.678	-50.91805	-73.58328	5.42	3.1	74	0.254	427.7	491.2	1216.5
2019	8	27	7	58	15.936	-50.92174	-73.58235	6.00	3.1	67	0.167	449.2	432.4	909.4
2019	8	27	10	10	50.905	-50.81913	-73.47549	12.12	3.2	104	0.709	563.7	530.7	1276.3
2019	8	27	11	34	25.760	-50.91848	-73.57940	5.69	3.2	68	0.146	438.2	460.8	1146.3
2019	8	27	15	2	10.935	-50.92704	-73.58533	6.00	3.3	74	0.270	485.1	544.6	1104.3
2019	8	27	20	51	42.587	-50.92686	-73.58096	6.34	3.3	53	0.209	440.2	439.4	1122.0
2019	8	27	22	37	52.332	-50.92213	-73.58430	4.42	3.3	54	0.243	391.3	431.8	1162.9
2019	8	28	0	3	21.376	-50.92009	-73.58428	4.81	3.4	54	0.199	373.4	355.2	1212.8
2019	8	28	1	23	6.721	-50.91802	-73.58813	4.44	3.2	54	0.254	370.7	408.8	973.0
2019	8	28	2	43	15.406	-50.92458	-73.58530	5.55	3.1	53	0.360	372.0	401.7	1269.8
2019	8	28	4	11	48.939	-50.92069	-73.58768	4.65	3.1	54	0.266	355.7	402.5	1009.4
2019	8	28	5	25	46.241	-50.91630	-73.60558	4.56	3.2	66	0.369	431.7	420.5	965.0
2019	8	28	6	51	33.892	-50.92008	-73.58622	4.40	3.1	54	0.184	373.9	405.2	1000.6

ORIGIN TIME (UTC)						Latitude	Longitude	Depth	M_L	GAP	RMS	X error	Y error	Z error
yyyy	mm	dd	h	m	seconds	[°]	[°]	[Km]		[°]		[m]	[m]	[m]
2019	8	28	8	8	4.501	-50.93336	-73.24604	5.43	3.2	156	0.559	825.1	1002.1	1028.9
2019	8	28	9	50	29.077	-50.92295	-73.58528	5.98	3.0	74	0.132	391.8	473.2	1287.9
2019	8	28	11	9	36.191	-50.92480	-73.58385	7.03	3.0	82	0.151	425.5	629.9	1726.1
2019	8	28	12	52	10.855	-50.92395	-73.58966	7.38	3.0	72	0.289	377.1	592.2	1548.6
2019	8	28	15	27	52.845	-50.91764	-73.58230	5.34	3.0	54	0.335	381.4	437.3	1029.8
2019	8	28	16	24	29.374	-50.92391	-73.59743	3.36	3.1	88	0.081	540.4	572.4	1791.5
2019	8	28	17	20	6.092	-50.91741	-73.58764	5.07	3.0	54	0.146	625.8	620.6	1610.2
2019	8	28	17	45	0.381	-49.45542	-73.54172	4.68	3.2	184	0.345	519.9	844.7	1094.2
2019	8	28	19	18	11.782	-50.92458	-73.58627	5.06	3.0	53	0.140	397.3	416.0	1105.4
2019	8	28	19	40	11.216	-52.01170	-74.25408	17.89	3.7	233	0.543	1892.6	2094.7	1910.6
2019	8	28	21	35	0.160	-50.92246	-73.56052	10.00	3.1	53	0.810	353.7	433.7	851.0
2019	8	29	0	13	9.462	-50.92173	-73.58430	5.46	3.1	54	0.123	399.7	421.7	1390.4
2019	8	29	1	37	6.621	-50.91518	-73.58421	5.51	3.2	99	0.265	425.8	504.2	970.0
2019	8	29	3	27	17.614	-50.91925	-73.58912	4.87	3.1	54	0.255	383.9	454.8	1427.2
2019	8	29	3	52	57.235	-51.50429	-74.34628	17.26	3.6	128	0.194	807.0	368.0	832.6
2019	8	29	5	4	42.241	-50.91644	-73.57841	4.01	3.2	76	0.311	353.1	481.8	1321.3
2019	8	29	6	37	54.592	-50.91928	-73.58232	5.32	3.1	54	0.151	394.4	449.1	1096.4
2019	8	29	8	25	0.026	-50.92296	-73.58237	5.42	3.1	74	0.121	403.4	437.3	1127.9
2019	8	29	9	54	42.446	-50.91931	-73.57747	4.13	3.0	74	0.338	344.7	462.6	2209.8
2019	8	29	12	55	58.491	-50.91501	-73.57790	6.01	3.0	74	0.353	507.5	606.0	1217.2
2019	8	29	15	31	7.764	-50.91558	-73.62644	2.85	2.9	77	0.574	515.4	584.9	1601.6
2019	8	29	17	57	55.254	-50.90531	-73.59477	3.23	3.2	54	0.452	397.6	449.7	904.9
2019	8	29	18	42	55.541	-50.92285	-73.60470	6.12	3.0	88	0.332	473.9	622.3	1107.2
2019	8	29	20	17	13.851	-50.91766	-73.57842	6.00	3.0	54	0.288	408.7	427.8	938.0
2019	8	29	21	30	39.755	-50.92249	-73.59498	5.61	3.0	54	0.171	424.2	441.9	1155.5
2019	8	29	23	13	23.406	-50.92317	-73.58189	5.62	3.0	53	0.226	363.6	394.0	995.3
2019	8	30	0	52	37.289	-50.92054	-73.57651	6.00	3.0	53	0.244	412.1	425.1	800.9
2019	8	30	1	58	53.042	-50.90167	-73.58696	9.01	2.8	57	0.666	386.1	403.3	1237.4
2019	8	30	3	33	17.602	-49.78053	-73.05011	13.31	3.0	104	0.666	483.5	572.6	686.2
2019	8	30	4	18	42.510	-50.91988	-73.58573	4.25	3.0	54	0.246	344.1	368.8	1002.9
2019	8	30	5	4	18.376	-51.37402	-74.30864	18.85	2.9	114	0.315	614.5	331.7	871.0
2019	8	30	5	15	45.435	-50.91843	-73.58814	4.77	2.9	54	0.230	363.3	403.8	1211.6
2019	8	30	6	11	56.715	-50.23528	-74.98719	20.01	3.0	114	0.515	365.9	338.0	497.2
2019	8	30	7	8	39.722	-50.91471	-73.59586	3.72	2.9	54	0.366	377.3	403.0	966.8
2019	8	30	9	0	54.436	-50.92049	-73.58622	4.15	2.9	54	0.228	355.2	430.5	1169.1
2019	8	30	9	50	23.105	-50.91925	-73.58815	3.56	2.8	54	0.165	426.7	482.9	1012.4
2019	8	30	11	21	51.334	-50.92231	-73.58964	4.22	2.9	54	0.214	366.8	430.0	1328.0
2019	8	30	11	30	6.149	-50.23037	-74.98698	25.01	2.8	115	0.465	417.9	365.7	739.2
2019	8	30	12	26	3.624	-50.92694	-73.60378	3.25	2.8	54	0.245	387.3	499.5	1182.2
2019	8	30	15	8	55.232	-50.91835	-73.56435	7.77	2.8	75	0.307	421.4	513.5	1169.5
2019	8	30	18	53	39.152	-50.92293	-73.58917	6.00	2.8	54	0.149	386.6	435.7	986.9
2019	8	30	19	49	14.377	-50.91446	-73.60604	5.45	2.7	54	0.394	445.4	572.2	1705.9
2019	8	30	22	3	29.154	-50.92498	-73.58822	6.14	2.7	56	0.143	409.2	470.7	1226.0
2019	8	30	23	29	17.598	-50.92580	-73.58726	6.00	2.8	53	0.204	399.1	454.7	900.3
2019	8	31	0	59	39.351	-50.91946	-73.58669	5.99	2.8	54	0.177	413.7	499.2	1112.9
2019	8	31	1	49	5.667	-50.92071	-73.58380	5.11	2.7	54	0.134	440.6	461.9	1327.1
2019	8	31	3	0	39.324	-50.92213	-73.58527	6.00	2.6	54	0.134	384.3	441.8	970.2

ORIGIN TIME (UTC)						Latitude	Longitude	Depth	M_L	GAP	RMS	X error	Y error	Z error
yyyy	mm	dd	h	m	seconds	[°]	[°]	[Km]		[°]		[m]	[m]	[m]
2019	8	31	4	34	0.943	-50.91805	-73.58328	6.00	2.7	54	0.278	377.7	391.8	756.0
2019	8	31	7	14	21.222	-50.93613	-73.56603	2.62	2.9	54	0.615	414.7	437.6	687.9
2019	8	31	8	54	19.751	-50.92375	-73.58918	5.55	2.8	54	0.126	373.4	392.3	1174.8
2019	8	31	10	14	15.093	-50.92130	-73.58817	3.25	2.8	54	0.232	363.0	406.3	787.1
2019	8	31	11	51	43.064	-50.92724	-73.58582	5.54	2.9	67	0.160	471.3	470.3	1120.8
2019	8	31	13	2	45.978	-50.91763	-73.58522	6.00	2.7	54	0.284	385.5	405.7	839.6
2019	8	31	14	40	9.188	-50.92663	-73.58436	6.00	2.9	53	0.108	428.8	449.3	1170.0
2019	8	31	15	42	11.874	-50.92249	-73.59401	5.05	2.9	54	0.156	417.0	423.8	1224.0
2019	8	31	17	10	46.736	-50.92632	-73.56494	9.73	2.9	82	0.553	400.4	472.8	831.8
2019	8	31	18	44	12.809	-50.91431	-73.55266	12.73	2.8	74	0.796	435.5	522.5	896.9
2019	8	31	20	1	41.665	-50.92295	-73.58528	5.71	2.6	82	0.115	410.8	489.1	1297.6
2019	8	31	21	3	54.165	-50.92082	-73.60176	4.23	2.8	82	0.166	419.6	551.6	1314.9
2019	8	31	23	9	18.743	-50.91765	-73.58036	8.58	2.9	82	0.502	383.3	455.8	1111.2
2019	9	1	0	54	36.184	-50.92378	-73.58335	6.00	2.8	53	0.151	336.0	389.8	814.5
2019	9	1	1	37	2.580	-52.70598	-71.67182	29.58	3.4	143	0.704	512.1	671.1	517.3
2019	9	1	3	35	38.382	-50.92013	-73.57651	7.58	2.9	59	0.208	397.6	435.5	1379.5
2019	9	1	4	54	43.506	-50.92173	-73.58333	6.00	2.9	54	0.188	397.9	416.3	1013.7
2019	9	1	6	34	59.992	-50.92171	-73.58721	6.00	2.9	54	0.173	375.0	436.1	899.5
2019	9	1	7	38	10.453	-50.92413	-73.59403	5.90	2.9	54	0.156	385.8	426.4	1157.0
2019	9	1	9	12	56.535	-50.91681	-73.58521	5.96	3.0	99	0.361	409.0	467.1	1119.4
2019	9	1	10	19	39.599	-50.91508	-73.60363	4.95	2.8	54	0.403	432.1	456.6	914.4
2019	9	1	11	32	58.914	-50.91726	-73.61676	4.65	2.7	74	0.397	449.8	587.6	1627.5
2019	9	1	14	22	50.388	-50.92746	-73.58243	8.29	2.8	74	0.431	370.0	429.4	1084.9
2019	9	1	15	30	24.538	-50.93517	-73.59515	8.19	2.8	97	0.365	409.1	584.4	1331.4
2019	9	1	18	9	3.062	-50.92293	-73.58819	8.58	3.0	82	0.552	424.8	497.4	1043.5
2019	9	1	19	25	44.557	-50.91684	-73.58035	6.00	2.8	57	0.290	410.5	449.3	895.1
2019	9	1	20	31	37.460	-50.92399	-73.58190	8.24	2.9	53	0.467	400.6	457.3	1055.1
2019	9	1	21	47	27.603	-50.91395	-73.58420	6.00	2.8	54	0.441	385.1	434.8	1088.0
2019	9	1	21	50	26.788	-51.39781	-75.51932	23.96	3.2	247	0.378	2443.8	1398.6	2934.5
2019	9	1	23	11	42.144	-50.91192	-73.58223	3.01	3.0	54	0.481	359.0	378.3	647.7
2019	9	2	0	0	44.853	-50.92715	-73.60330	3.00	2.8	54	0.319	449.7	518.9	1180.3
2019	9	2	0	39	49.928	-50.92375	-73.58918	5.44	2.9	54	0.191	360.6	386.6	931.6
2019	9	2	2	13	32.667	-50.92131	-73.58623	3.95	2.8	54	0.165	370.0	403.2	1030.5
2019	9	2	3	22	27.594	-50.92123	-73.60079	3.85	3.0	54	0.164	364.9	413.0	933.3
2019	9	2	4	42	45.094	-50.92072	-73.58186	3.75	2.7	163	0.075	608.6	642.6	1303.0
2019	9	2	5	18	12.800	-50.91838	-73.59881	3.99	2.7	54	0.245	400.1	425.3	958.0
2019	9	2	5	47	33.914	-50.28173	-72.07472	4.44	2.6	91	0.396	646.1	476.3	756.9
2019	9	2	6	50	45.838	-50.92213	-73.58527	5.36	2.8	54	0.117	367.6	413.4	1159.0
2019	9	2	7	53	13.710	-50.92071	-73.58380	5.66	2.8	54	0.122	390.0	441.9	1102.0
2019	9	2	10	20	36.645	-50.92452	-73.59792	3.39	2.8	54	0.306	435.0	538.6	1368.6
2019	9	2	11	50	16.969	-50.91655	-73.59734	2.57	2.8	94	0.178	377.8	562.9	1084.8
2019	9	2	12	48	7.070	-50.91717	-73.59589	4.21	3.2	82	0.446	433.3	535.9	1023.1
2019	9	2	13	22	0.421	-50.91963	-73.59495	5.63	2.7	82	0.237	447.0	541.4	1271.1
2019	9	2	15	0	9.349	-50.92106	-73.59448	4.43	3.0	95	0.073	581.2	727.0	2051.3
2019	9	2	18	12	0.011	-50.92937	-73.60867	2.60	2.7	82	0.372	405.9	463.6	665.4
2019	9	2	19	21	49.488	-50.92591	-73.60619	3.81	2.9	82	0.281	410.1	496.1	1218.3
2019	9	2	20	49	8.757	-50.92439	-73.58287	5.37	2.8	82	0.111	406.1	451.7	1230.9

ORIGIN TIME (UTC)						Latitude	Longitude	Depth	M_L	GAP	RMS	X error	Y error	Z error
yyyy	mm	dd	h	m	seconds	[°]	[°]	[Km]		[°]		[m]	[m]	[m]
2019	9	2	21	36	13.150	-50.92306	-73.60324	7.11	2.8	92	0.454	443.0	612.6	1157.7
2019	9	2	23	42	3.140	-50.59654	-72.62389	5.46	2.8	53	0.574	390.6	325.3	598.9
2019	9	3	0	21	48.174	-50.93934	-73.57966	9.01	2.6	73	0.725	421.0	495.6	928.3
2019	9	3	3	9	27.643	-50.90317	-73.61318	1.37	2.5	71	0.475	411.3	438.7	563.1
2019	9	3	4	37	9.477	-50.92397	-73.58578	8.75	2.7	73	0.452	394.1	451.9	1072.0
2019	9	3	5	49	24.086	-50.92455	-73.59113	5.24	2.5	82	0.166	390.3	476.4	1126.0
2019	9	3	7	35	23.087	-50.93415	-73.59465	2.16	2.6	75	0.401	355.6	314.5	326.2
2019	9	3	8	22	16.480	-50.92731	-73.61155	2.66	2.7	74	0.286	421.1	498.4	1572.3
2019	9	3	9	6	41.648	-50.92369	-73.59985	2.92	2.5	74	0.278	422.4	506.6	1054.0
2019	9	3	9	58	30.906	-50.92045	-73.59399	3.37	2.8	74	0.208	350.8	413.5	871.6
2019	9	3	12	3	3.703	-50.92090	-73.58526	5.14	2.8	74	0.139	352.0	434.1	1073.7
2019	9	3	13	56	57.220	-50.91847	-73.58134	5.75	2.8	74	0.174	360.2	426.7	1203.6
2019	9	3	14	57	33.665	-50.91761	-73.58910	5.98	2.6	74	0.259	385.0	431.3	995.9
2019	9	3	16	23	18.961	-50.91476	-73.58615	3.91	2.9	81	0.358	376.1	476.3	974.5
2019	9	3	17	20	2.887	-50.93036	-73.61499	4.02	2.9	83	0.720	582.7	592.7	1124.3
2019	9	3	17	27	26.489	-50.62901	-74.40217	19.22	2.3	110	0.322	365.6	270.8	585.1
2019	9	3	18	24	14.188	-50.91763	-73.58619	5.24	2.4	91	0.296	422.3	613.9	1055.5
2019	9	3	20	40	42.079	-50.91781	-73.59056	4.51	2.5	74	0.164	481.5	610.5	1604.0
2019	9	3	21	49	31.775	-50.96580	-73.60428	11.94	2.6	85	0.811	385.2	427.8	710.8
2019	9	4	1	0	21.208	-50.94343	-73.57971	9.01	2.6	132	0.436	392.8	621.4	1013.3
2019	9	4	4	4	35.992	-50.91185	-73.59485	2.58	2.5	81	0.549	333.3	436.8	518.4
2019	9	4	4	46	21.070	-50.91817	-73.59930	3.67	2.9	141	0.153	668.6	834.3	2203.4
2019	9	4	5	47	11.589	-50.92805	-73.58777	6.36	2.7	74	0.328	340.8	417.8	1028.4
2019	9	4	6	16	35.945	-50.92397	-73.58578	4.06	2.4	82	0.166	489.9	584.8	1559.1
2019	9	4	6	47	38.797	-50.91268	-73.59292	2.99	2.6	73	0.296	350.1	419.1	730.4
2019	9	4	7	27	40.911	-50.92723	-73.58776	5.66	2.4	82	0.145	425.3	564.9	1428.3
2019	9	4	8	7	25.541	-50.92558	-73.59163	7.38	2.5	72	0.250	480.4	584.7	1618.3
2019	9	4	8	47	27.790	-50.93230	-73.59608	9.36	2.6	75	0.517	350.9	411.2	778.2
2019	9	4	9	22	56.766	-50.92213	-73.58527	6.00	2.5	74	0.226	392.9	373.7	999.6
2019	9	4	10	3	12.252	-50.91926	-73.58718	3.50	2.6	82	0.223	350.2	480.6	1056.6
2019	9	4	10	56	29.177	-50.91946	-73.58669	3.26	2.4	74	0.153	424.5	498.8	1461.0
2019	9	4	12	7	55.236	-50.91623	-73.57889	5.99	2.7	78	0.296	379.7	553.3	791.0
2019	9	4	13	19	12.727	-50.91891	-73.61484	2.97	2.6	74	0.243	385.9	488.2	928.0
2019	9	4	14	37	58.993	-50.92307	-73.60130	6.56	2.6	74	0.336	423.3	636.6	1475.4
2019	9	4	14	52	48.280	-50.63374	-74.39990	19.58	2.0	133	0.127	672.5	292.8	920.0
2019	9	4	15	23	31.912	-50.92234	-73.58382	4.22	2.7	74	0.276	347.5	435.8	916.6
2019	9	4	16	18	34.776	-50.92599	-73.59066	4.27	2.9	80	0.370	580.9	662.1	1730.1
2019	9	4	16	40	15.488	-50.92112	-73.58283	5.99	2.6	74	0.130	371.4	436.9	1048.3
2019	9	4	18	45	38.641	-50.91990	-73.58185	4.57	2.5	74	0.132	374.9	424.2	1078.9
2019	9	4	20	2	8.809	-50.92215	-73.58139	4.56	2.6	74	0.195	363.4	402.1	944.4
2019	9	4	21	21	19.778	-50.92478	-73.58773	5.97	2.6	74	0.160	353.4	415.6	988.8
2019	9	4	22	14	53.669	-50.92246	-73.60178	2.98	2.7	74	0.298	369.0	486.8	771.3
2019	9	4	23	7	45.270	-50.92478	-73.58773	5.58	2.3	82	0.159	436.1	717.2	1569.8
2019	9	5	1	24	21.621	-50.92053	-73.57846	6.00	2.4	82	0.363	397.7	453.1	1188.7
2019	9	5	2	17	47.137	-50.92545	-73.57560	3.80	2.7	74	0.335	350.9	410.4	830.7
2019	9	5	3	3	13.053	-50.91756	-73.59880	2.99	2.6	82	0.218	377.6	483.2	944.1
2019	9	5	3	39	4.302	-50.92661	-73.58921	6.00	2.3	82	0.251	424.9	619.1	1200.7

ORIGIN TIME (UTC)						Latitude	Longitude	Depth	M_L	GAP	RMS	X error	Y error	Z error
yyyy	mm	dd	h	m	seconds	[°]	[°]	[Km]		[°]		[m]	[m]	[m]
2019	9	5	4	18	39.201	-50.91920	-73.59785	4.42	2.6	74	0.259	354.9	451.4	1161.8
2019	9	5	5	30	19.668	-50.92811	-73.57612	8.75	2.5	75	0.425	364.4	441.2	1246.3
2019	9	5	6	16	37.658	-50.92474	-73.59550	4.72	2.4	96	0.178	436.1	603.5	1545.8
2019	9	5	7	25	48.697	-50.92132	-73.58429	3.89	2.5	74	0.199	350.6	439.7	1161.7
2019	9	5	8	10	55.601	-50.93782	-73.59761	9.80	2.5	75	0.505	359.4	448.6	872.8
2019	9	5	9	25	2.567	-50.91660	-73.58763	5.00	2.5	74	0.197	566.1	695.7	1665.9
2019	9	5	10	3	38.188	-50.92290	-73.59402	7.78	2.6	74	0.289	375.7	481.3	1419.4
2019	9	5	10	28	13.301	-50.92070	-73.58574	4.92	2.3	74	0.151	427.3	581.5	1503.3
2019	9	5	11	10	22.776	-50.91967	-73.58621	7.76	2.6	74	0.379	359.9	437.3	1383.8
2019	9	5	13	4	32.548	-50.92539	-73.58725	4.77	2.7	74	0.229	351.4	440.5	1473.1
2019	9	5	13	51	45.513	-50.92247	-73.59887	2.90	2.6	74	0.308	405.6	473.2	752.1
2019	9	5	14	48	35.961	-50.91990	-73.58185	4.57	2.2	74	0.146	431.8	514.7	1432.8
2019	9	5	15	4	12.711	-50.61124	-73.89025	4.49	2.8	66	0.414	257.0	282.5	551.7
2019	9	5	16	29	26.376	-50.91433	-73.59100	2.88	2.6	74	0.204	351.3	428.3	738.4
2019	9	5	17	3	46.152	-50.91986	-73.58961	3.00	2.3	95	0.111	462.3	769.5	1903.6
2019	9	5	18	23	20.280	-50.91926	-73.58621	3.66	2.6	74	0.242	360.8	423.0	1119.2
2019	9	5	19	28	22.596	-51.18793	-74.44494	17.53	2.4	136	0.231	791.5	403.2	646.9
2019	9	5	19	30	57.519	-50.92151	-73.58575	5.47	2.4	82	0.123	427.7	560.8	1492.9
2019	9	5	21	3	15.075	-50.91085	-73.59144	2.65	2.5	73	0.213	340.0	441.9	707.0
2019	9	5	22	14	25.456	-50.91840	-73.59396	3.01	2.4	74	0.267	365.0	464.3	814.8
2019	9	6	0	5	0.146	-50.91844	-73.58620	3.17	2.6	74	0.209	350.3	437.8	1040.2
2019	9	6	0	52	34.707	-50.92453	-73.59695	4.81	2.3	74	0.212	408.5	508.4	1094.0
2019	9	6	1	44	16.827	-50.92396	-73.58772	5.31	2.3	74	0.354	434.4	533.6	1173.4
2019	9	6	2	42	5.456	-50.92439	-73.58287	11.07	2.3	82	0.336	434.6	564.4	1462.6
2019	9	6	3	35	10.994	-50.93601	-73.59127	9.26	2.4	75	0.460	382.6	447.3	1037.7
2019	9	6	4	16	6.173	-50.91251	-73.58758	2.97	2.3	73	0.340	466.7	693.5	1185.5
2019	9	6	4	36	47.608	-50.92007	-73.58913	3.40	2.4	74	0.219	365.9	495.5	1234.9
2019	9	6	5	39	16.714	-50.92806	-73.58583	5.43	2.3	79	0.263	469.4	585.9	1427.5
2019	9	6	5	51	27.024	-50.91884	-73.58814	3.21	2.5	74	0.211	337.1	488.2	971.0
2019	9	6	6	43	13.672	-50.91839	-73.59590	2.06	2.5	74	0.286	347.9	448.4	586.7
2019	9	6	7	18	47.852	-50.92211	-73.58915	6.00	2.3	74	0.218	401.5	482.1	1215.0
2019	9	6	7	47	43.440	-50.91720	-73.58909	2.99	2.5	74	0.219	339.5	456.0	764.6
2019	9	6	8	46	32.430	-50.91841	-73.59299	2.25	2.4	74	0.223	328.1	410.6	579.0
2019	9	6	9	10	52.474	-50.92108	-73.59060	6.23	2.3	74	0.273	426.9	579.6	1379.0
2019	9	6	9	50	56.330	-51.02745	-72.06677	13.01	2.5	61	0.507	374.1	310.5	540.8
2019	9	6	10	0	57.763	-50.91965	-73.59009	3.05	2.5	74	0.224	351.7	409.6	781.6
2019	9	6	11	22	31.225	-50.91559	-73.58422	3.85	2.5	74	0.259	376.4	495.3	1124.5
2019	9	6	12	42	8.406	-50.92865	-75.76677	38.47	2.3	250	0.183	1160.6	681.0	3834.3
2019	9	6	12	56	59.959	-50.91477	-73.58421	4.79	2.7	74	0.332	369.3	469.3	1046.0
2019	9	6	13	51	34.703	-50.92276	-73.58285	5.99	2.3	82	0.205	469.4	670.4	1381.7
2019	9	6	14	8	33.188	-50.91928	-73.58232	7.90	2.4	74	0.425	353.7	390.1	1183.4
2019	9	6	15	12	28.817	-50.92064	-73.59739	3.00	2.5	72	0.259	360.2	398.4	627.3
2019	9	6	17	26	23.080	-50.91885	-73.58717	2.98	2.4	82	0.186	371.3	482.9	1139.7
2019	9	6	18	58	43.024	-50.91638	-73.59005	2.99	2.6	74	0.242	340.6	409.2	790.0
2019	9	6	21	5	54.175	-50.91843	-73.58814	3.95	2.5	74	0.224	340.7	388.0	886.9
2019	9	6	22	3	10.242	-53.49040	-71.79349	19.01	3.0	202	1.203	741.6	144.2	932.6
2019	9	6	23	20	5.246	-50.91760	-73.59201	2.70	2.5	74	0.214	352.8	423.0	771.2

ORIGIN TIME (UTC)						Latitude	Longitude	Depth	M_L	GAP	RMS	X error	Y error	Z error
yyyy	mm	dd	h	m	seconds	[°]	[°]	[Km]		[°]		[m]	[m]	[m]
2019	9	6	23	40	30.431	-50.92637	-73.59552	5.78	2.2	82	0.190	602.0	763.0	1718.3
2019	9	7	0	30	44.715	-50.91925	-73.58815	5.18	2.5	74	0.300	349.9	428.8	1195.0
2019	9	7	1	1	19.157	-50.93608	-73.57768	9.01	2.2	73	0.312	407.4	459.0	884.3
2019	9	7	1	49	9.077	-50.92646	-73.57804	7.65	2.3	74	0.458	459.8	597.1	1383.7
2019	9	7	2	9	25.184	-50.91640	-73.58520	3.62	2.4	74	0.230	344.3	432.5	1074.9
2019	9	7	3	23	43.141	-50.94527	-73.58022	6.01	2.1	148	0.411	713.5	1326.1	1547.1
2019	9	7	3	41	3.654	-50.92151	-73.58575	4.45	2.5	74	0.285	348.2	417.3	1207.6
2019	9	7	4	42	2.576	-50.92478	-73.58773	4.33	2.5	74	0.326	360.3	437.2	1060.8
2019	9	7	5	23	7.535	-50.92149	-73.58963	5.58	2.2	74	0.328	456.2	474.8	1012.2
2019	9	7	5	43	7.384	-50.92400	-73.57996	5.74	2.1	95	0.166	392.4	547.8	1244.7
2019	9	7	6	35	24.589	-50.92312	-73.59159	3.36	2.5	74	0.316	348.4	458.0	1030.1
2019	9	7	7	24	37.538	-50.92495	-73.59404	3.72	2.1	74	0.268	393.9	496.5	963.7
2019	9	7	7	53	23.030	-50.92065	-73.59545	5.47	2.2	74	0.208	426.1	557.8	1402.5
2019	9	7	8	25	3.756	-50.92601	-73.58678	4.59	2.4	74	0.288	352.7	420.3	1243.3
2019	9	7	9	11	32.379	-50.91683	-73.58132	5.22	2.1	74	0.322	444.7	496.3	1178.1
2019	9	7	9	23	19.372	-50.91783	-73.58667	2.87	2.2	163	0.102	643.1	744.3	1253.7
2019	9	7	10	3	13.409	-50.93069	-73.59218	3.64	2.2	75	0.176	498.9	563.2	1187.8
2019	9	7	10	19	47.892	-50.89485	-73.55873	0.67	2.2	73	0.654	408.1	462.8	509.8
2019	9	7	11	13	42.787	-50.92541	-73.58337	5.32	2.4	74	0.241	358.4	395.5	1025.3
2019	9	7	12	28	1.652	-50.91086	-73.58950	5.97	2.5	73	0.336	380.9	461.2	842.3
2019	9	7	12	41	54.856	-51.02447	-72.05126	14.56	2.5	60	0.495	458.4	399.9	603.6
2019	9	7	13	26	4.754	-50.85997	-74.73535	17.19	2.1	151	0.261	507.9	435.3	645.0
2019	9	7	13	46	35.938	-50.91967	-73.58718	4.03	2.5	74	0.239	346.8	400.4	932.0
2019	9	7	14	44	8.422	-50.92130	-73.58720	4.40	2.4	74	0.304	391.4	486.6	1049.5
2019	9	7	16	28	15.798	-50.92332	-73.59208	4.58	2.5	74	0.256	366.1	414.7	959.8
2019	9	7	17	41	24.308	-50.92457	-73.58724	5.30	2.9	72	0.445	365.9	415.1	931.6
2019	9	7	18	39	12.114	-50.92007	-73.58913	5.20	2.5	74	0.170	445.2	499.8	1327.9
2019	9	7	20	3	1.938	-50.92397	-73.58578	6.72	2.4	74	0.118	380.0	466.6	1186.4
2019	9	7	21	49	4.298	-50.91557	-73.58907	3.21	2.5	74	0.222	357.3	488.0	905.5
2019	9	7	22	56	47.726	-50.92332	-73.59305	5.22	2.5	74	0.191	376.9	495.7	1109.7
2019	9	8	0	58	37.084	-51.32929	-72.44359	8.44	2.6	70	0.436	368.4	274.9	1152.1
2019	9	8	1	42	2.793	-50.93421	-73.58300	10.13	2.4	73	0.678	364.9	422.2	775.8
2019	9	8	3	34	16.063	-50.91316	-73.21924	6.00	2.4	154	0.376	448.5	744.6	829.5
2019	9	8	4	40	39.280	-50.90897	-73.59966	2.60	2.6	73	0.224	376.9	515.6	896.0
2019	9	8	6	43	3.487	-50.92208	-73.59498	4.15	2.6	74	0.244	340.1	416.8	1009.5
2019	9	8	7	24	50.090	-50.92516	-73.59259	5.17	2.4	82	0.158	602.2	778.7	2042.6
2019	9	8	8	14	57.382	-49.87322	-73.43243	1.60	2.6	118	0.388	466.3	800.5	722.7
2019	9	8	8	31	47.486	-50.88989	-71.95698	11.69	2.3	54	0.516	445.7	393.9	1098.0
2019	9	8	8	41	5.070	-50.92703	-73.58728	7.62	2.6	74	0.263	388.7	442.5	1660.6
2019	9	8	8	45	4.589	-50.88673	-71.96966	11.00	2.7	54	0.522	355.9	319.9	890.1
2019	9	8	9	46	57.777	-50.92128	-73.59206	2.99	2.8	74	0.274	399.0	436.9	772.1
2019	9	8	11	48	30.649	-50.91519	-73.58324	5.51	2.7	74	0.318	349.5	419.5	925.6
2019	9	8	13	13	31.358	-50.93024	-73.59897	5.98	2.7	75	0.235	383.5	465.3	1167.5
2019	9	8	14	30	35.012	-50.91847	-73.58134	6.00	2.7	74	0.274	388.7	462.3	791.0
2019	9	8	15	55	42.083	-50.91927	-73.58427	5.98	2.6	74	0.312	367.6	420.7	830.0
2019	9	8	17	11	3.526	-50.92323	-73.61053	5.98	2.6	74	0.395	383.6	501.3	805.0
2019	9	8	18	57	56.651	-50.92500	-73.58434	6.00	2.6	82	0.387	386.3	478.2	787.8

ORIGIN TIME (UTC)						Latitude	Longitude	Depth	M_L	GAP	RMS	X error	Y error	Z error
yyyy	mm	dd	h	m	seconds	[°]	[°]	[Km]		[°]		[m]	[m]	[m]
2019	9	8	20	12	14.382	-50.91414	-73.58760	3.24	2.6	72	0.325	368.6	440.2	1011.9
2019	9	8	21	16	28.776	-50.92799	-73.59942	1.99	2.7	74	0.602	384.7	493.7	428.2
2019	9	8	22	46	14.279	-49.83637	-73.38228	6.00	2.5	149	0.963	464.5	845.0	614.6
2019	9	8	23	1	21.748	-50.91804	-73.58425	3.33	2.6	74	0.281	365.6	433.4	832.6
2019	9	9	0	11	45.581	-50.92834	-73.56981	9.26	2.4	75	0.571	340.4	435.5	1076.8
2019	9	9	1	2	34.755	-50.91673	-73.60171	4.89	2.5	74	0.261	385.4	463.3	954.5
2019	9	9	2	29	25.259	-50.51132	-72.58703	6.00	3.2	78	1.307	444.2	407.7	421.0
2019	9	9	2	52	43.086	-50.92131	-73.58623	5.98	2.7	74	0.147	405.9	476.4	1199.7
2019	9	9	5	51	27.539	-50.92083	-73.59885	4.56	2.6	74	0.245	347.9	430.6	1063.0
2019	9	9	6	24	27.096	-50.92502	-73.58045	9.01	2.4	79	0.644	487.6	573.2	1120.1
2019	9	9	6	55	45.733	-50.92661	-73.58824	4.85	3.0	74	0.274	351.1	484.9	1679.6
2019	9	9	7	49	35.857	-50.91901	-73.59543	3.36	2.5	82	0.309	457.6	575.5	1061.3
2019	9	9	8	40	22.474	-50.92069	-73.58768	3.71	2.6	74	0.192	346.3	416.3	1075.9
2019	9	9	9	40	16.806	-50.92224	-73.60323	3.00	2.6	74	0.341	352.5	414.9	600.1
2019	9	9	11	1	0.261	-50.92172	-73.58624	4.58	2.7	74	0.144	348.4	432.9	1001.8
2019	9	9	11	58	34.981	-50.55288	-72.69912	6.00	2.6	53	0.554	365.1	370.4	333.1
2019	9	9	12	34	20.472	-50.92559	-73.58774	6.01	2.8	74	0.415	376.6	428.5	924.9
2019	9	9	14	19	46.931	-50.91767	-73.57648	3.97	2.9	75	0.311	418.6	414.6	811.6
2019	9	9	17	0	52.414	-50.91847	-73.58134	6.00	2.6	82	0.247	391.1	493.5	887.6
2019	9	9	18	50	55.566	-50.91884	-73.58911	2.94	2.6	82	0.187	371.8	508.0	838.8
2019	9	9	20	25	47.814	-50.92274	-73.58674	3.26	2.7	74	0.257	371.2	502.7	1114.6
2019	9	9	21	41	37.398	-50.92294	-73.58625	6.61	2.7	74	0.281	340.2	432.1	1259.4
2019	9	9	23	21	41.352	-50.92007	-73.58913	3.62	2.8	74	0.220	372.6	439.3	1049.2
2019	9	10	0	39	45.627	-50.92050	-73.58331	4.42	2.7	74	0.215	350.0	417.9	1157.6
2019	9	10	1	46	16.725	-50.92128	-73.59206	3.85	2.8	74	0.252	352.4	452.7	1305.8
2019	9	10	2	15	30.542	-50.93540	-73.58981	9.02	2.6	75	0.342	538.4	660.0	1483.4
2019	9	10	2	53	8.407	-50.92007	-73.58719	3.87	2.7	72	0.247	367.1	422.7	942.5
2019	9	10	3	44	26.906	-50.91180	-73.60552	0.49	2.7	81	0.535	394.1	584.9	813.2
2019	9	10	4	41	47.856	-50.92520	-73.58482	4.55	2.6	82	0.175	436.3	552.5	1283.9
2019	9	10	5	51	24.349	-50.91762	-73.58716	3.01	2.9	74	0.258	362.5	456.4	902.6
2019	9	10	6	11	42.780	-50.92065	-73.59545	4.45	2.6	82	0.200	494.9	634.8	1676.4
2019	9	10	8	7	9.379	-50.92399	-73.58190	8.20	2.7	74	0.460	336.3	424.6	1262.0
2019	9	10	8	45	7.329	-50.91910	-73.57795	3.00	2.6	74	0.322	453.2	531.8	910.6
2019	9	10	9	48	15.560	-50.91437	-73.58323	3.40	2.8	74	0.244	340.6	388.6	761.1
2019	9	10	10	31	51.386	-51.44616	-74.56404	23.35	2.6	157	0.665	720.7	437.3	712.6
2019	9	10	12	23	38.496	-50.91187	-73.59194	2.45	2.8	73	0.207	390.3	591.6	1001.9
2019	9	10	13	24	42.849	-50.92132	-73.58332	6.00	2.6	74	0.181	382.3	525.2	996.7
2019	9	10	15	17	42.702	-50.91329	-73.59341	1.29	2.8	73	0.126	387.2	535.1	866.0
2019	9	10	16	11	25.439	-50.91583	-73.57791	5.58	2.6	74	0.215	367.7	439.3	940.7
2019	9	10	17	54	42.173	-50.91275	-73.58030	5.73	2.7	74	0.351	387.1	455.0	833.8
2019	9	10	18	56	37.057	-50.91684	-73.58035	6.00	2.5	74	0.285	389.4	595.4	892.1
2019	9	10	20	53	57.053	-50.92210	-73.59110	6.59	2.9	74	0.250	370.6	442.2	1078.6
2019	9	10	22	44	4.028	-50.93042	-73.56304	11.00	2.7	75	0.552	420.8	482.3	816.3
2019	9	10	23	25	15.887	-50.92926	-73.59070	5.37	2.8	75	0.268	484.3	616.7	1607.5
2019	9	11	0	23	33.807	-50.92334	-73.58917	4.24	2.8	74	0.180	399.2	471.3	1189.4
2019	9	11	2	19	30.604	-50.92418	-73.58336	6.80	2.6	82	0.150	405.3	532.4	1466.6
2019	9	11	4	51	49.152	-50.95757	-73.78537	29.20	2.2	90	0.979	712.7	708.2	980.5

ORIGIN TIME (UTC)						Latitude	Longitude	Depth	M_L	GAP	RMS	X error	Y error	Z error
yyyy	mm	dd	h	m	seconds	[°]	[°]	[Km]		[°]		[m]	[m]	[m]
2019	9	11	6	50	49.394	-50.92295	-73.58528	4.75	2.8	75	0.122	401.2	473.4	1557.4
2019	9	11	8	22	16.244	-50.91905	-73.58766	2.18	2.8	82	0.101	519.4	693.7	2015.9
2019	9	11	10	58	38.274	-50.92399	-73.58190	3.08	2.8	74	0.404	479.8	504.7	967.8
2019	9	11	14	11	44.856	-50.91990	-73.58185	8.86	2.9	74	0.373	448.9	540.9	1508.6
2019	9	11	15	31	28.156	-50.92305	-73.60519	3.90	2.8	74	0.225	520.7	541.9	1590.2
2019	9	11	18	46	56.581	-50.92437	-73.58676	5.13	2.8	82	0.194	406.1	527.2	1463.8
2019	9	11	21	30	30.992	-50.92137	-73.57264	10.69	3.0	74	0.597	385.7	491.6	1135.7
2019	9	11	22	55	21.686	-50.92625	-73.57853	7.66	2.9	74	0.236	380.8	456.4	1400.3
2019	9	11	23	45	25.369	-50.93113	-73.62471	4.72	3.0	74	0.300	430.3	520.2	2070.3
2019	9	12	0	42	54.994	-50.94553	-73.64773	2.29	3.0	126	0.417	658.8	826.5	772.3
2019	9	12	2	1	45.847	-50.93031	-73.58635	8.01	2.9	73	0.671	446.9	499.5	1450.1
2019	9	12	3	24	30.257	-50.93032	-73.58440	10.01	3.0	75	0.389	351.7	420.5	798.6
2019	9	12	5	42	35.766	-50.92821	-73.59603	5.16	3.1	74	0.190	367.8	462.3	1063.8
2019	9	12	6	42	24.612	-50.92007	-73.58913	6.00	2.9	74	0.255	373.1	452.0	1051.6
2019	9	12	8	0	40.428	-50.92942	-73.59993	5.32	2.8	74	0.297	422.5	488.9	1458.8
2019	9	12	8	45	8.174	-50.92171	-73.58721	4.30	3.0	74	0.202	342.6	422.7	1294.4
2019	9	12	10	31	25.808	-50.90937	-73.60064	2.99	3.1	73	0.395	384.7	443.7	623.6
2019	9	12	11	38	55.650	-50.92250	-73.59304	4.15	3.0	74	0.427	365.0	455.6	1090.3
2019	9	12	12	50	57.015	-50.92226	-73.59935	4.76	2.9	74	0.236	541.8	669.7	1779.3
2019	9	12	13	11	8.791	-50.92132	-73.58332	6.00	3.0	72	0.166	353.5	441.9	818.0
2019	9	12	14	11	22.064	-50.92258	-73.57654	8.54	3.0	74	0.548	382.4	439.5	1096.9
2019	9	12	14	58	36.759	-50.92064	-73.59739	5.97	2.8	82	0.213	443.4	559.7	1379.8
2019	9	12	15	51	28.427	-50.91970	-73.57942	6.00	2.9	74	0.247	391.4	442.0	784.4
2019	9	12	17	14	27.376	-50.92735	-73.60378	4.52	3.1	74	0.216	361.6	428.5	960.3
2019	9	12	18	44	42.296	-50.92229	-73.59353	4.22	2.9	74	0.159	374.9	473.0	1151.5
2019	9	12	19	44	45.811	-50.93055	-73.57810	9.18	3.2	93	0.456	514.0	648.4	1135.3
2019	9	12	20	26	29.848	-50.92007	-73.58816	4.73	2.9	74	0.248	356.5	424.7	1013.4
2019	9	12	22	48	29.027	-50.91659	-73.58957	3.08	3.0	74	0.271	380.3	511.6	785.4
2019	9	12	23	48	2.058	-50.92253	-73.58722	4.23	2.8	74	0.143	398.6	477.7	1217.0
2019	9	13	0	23	9.219	-50.92499	-73.58628	5.10	2.8	74	0.125	409.2	563.6	1421.9
2019	9	13	1	56	20.173	-50.92375	-73.58820	4.09	3.0	74	0.215	379.6	523.9	1257.4
2019	9	13	1	57	51.689	-52.46208	-71.42707	33.99	3.5	100	0.821	470.3	503.1	516.4
2019	9	13	3	19	1.428	-50.91554	-73.59490	2.74	2.9	74	0.237	341.3	398.5	642.0
2019	9	13	3	56	5.260	-50.63609	-74.40865	18.89	2.6	111	0.320	408.0	252.6	470.9
2019	9	13	4	24	14.422	-50.92335	-73.58626	4.83	2.8	74	0.163	328.8	377.2	904.5
2019	9	13	5	10	0.737	-50.92416	-73.58918	4.62	2.8	82	0.118	397.0	546.8	1340.2
2019	9	13	5	56	34.199	-50.92044	-73.59593	4.13	2.8	74	0.265	351.4	448.8	1033.1
2019	9	13	6	19	48.619	-50.91741	-73.58764	8.24	2.7	74	0.303	458.6	584.3	1847.0
2019	9	13	7	36	25.734	-50.91719	-73.59200	2.98	2.9	74	0.190	343.5	438.3	838.7
2019	9	13	8	10	14.045	-50.91574	-73.59538	4.37	2.8	81	0.194	529.4	761.9	1954.3
2019	9	13	8	44	35.745	-50.92116	-73.61438	1.00	2.8	74	0.365	346.6	438.1	641.1
2019	9	13	9	18	33.652	-50.92274	-73.58674	4.90	2.7	82	0.136	412.6	546.0	1613.9
2019	9	13	9	58	25.963	-50.92070	-73.58574	4.61	2.9	72	0.242	363.6	492.3	1145.3
2019	9	13	10	43	26.831	-50.92090	-73.58526	5.01	2.7	74	0.188	346.4	483.9	1175.1
2019	9	13	11	37	54.464	-50.93033	-73.58149	6.71	2.8	75	0.215	386.5	495.8	1136.8
2019	9	13	12	35	15.632	-50.92150	-73.58769	5.07	2.7	82	0.121	455.1	538.9	1599.8
2019	9	13	13	42	43.498	-50.91887	-73.58232	6.00	2.9	74	0.266	374.3	449.8	764.8

ORIGIN TIME (UTC)						Latitude	Longitude	Depth	M_L	GAP	RMS	X error	Y error	Z error
yyyy	mm	dd	h	m	seconds	[°]	[°]	[Km]		[°]		[m]	[m]	[m]
2019	9	13	14	58	23.298	-50.92335	-73.58723	4.69	2.9	74	0.127	349.2	441.3	981.8
2019	9	13	15	49	21.054	-50.92413	-73.59501	4.26	2.8	74	0.261	423.2	513.2	1147.3
2019	9	13	18	17	59.993	-50.91927	-73.58427	5.92	2.7	74	0.275	355.3	396.7	794.6
2019	9	13	19	23	1.080	-50.92975	-73.57420	5.74	2.5	75	0.195	399.5	509.0	1135.7
2019	9	13	19	49	58.521	-50.92274	-73.58674	9.43	2.6	142	0.423	629.9	893.7	1624.5
2019	9	13	20	16	37.467	-50.91188	-73.58903	6.00	2.8	72	0.505	406.0	561.1	737.1
2019	9	13	21	32	53.376	-50.92167	-73.59497	6.14	2.6	82	0.242	391.0	492.3	1269.2
2019	9	13	22	38	44.611	-50.92150	-73.58769	5.58	2.7	74	0.135	364.2	497.3	1105.4
2019	9	13	23	10	40.319	-50.91946	-73.58669	5.60	2.6	141	0.117	546.1	783.2	1683.3
2019	9	14	0	9	5.061	-50.91921	-73.59688	2.58	2.7	74	0.182	357.0	461.7	771.8
2019	9	14	1	9	30.838	-50.97280	-73.59563	6.00	2.7	86	0.616	344.1	485.4	1464.9
2019	9	14	2	45	18.579	-50.92067	-73.59156	9.45	2.9	95	0.211	568.1	652.6	1949.7
2019	9	14	3	56	42.856	-50.92252	-73.58819	6.00	2.7	74	0.224	392.1	476.5	1004.0
2019	9	14	5	12	19.201	-50.92310	-73.59548	4.68	2.7	74	0.277	358.1	475.4	1125.0
2019	9	14	6	7	58.223	-50.91966	-73.58815	4.48	2.6	74	0.180	401.8	480.7	1141.4
2019	9	14	9	58	57.734	-50.91798	-73.59784	4.56	2.6	82	0.298	398.1	608.6	1036.1
2019	9	14	10	57	25.497	-50.91602	-73.58034	6.00	2.6	74	0.262	369.1	504.0	876.2
2019	9	14	11	42	43.019	-50.91887	-73.44205	4.06	3.1	176	0.628	1036.2	761.5	1197.0
2019	9	14	12	55	12.695	-50.92095	-73.57652	6.53	2.8	74	0.319	374.9	472.7	1056.3
2019	9	14	14	14	29.563	-50.91107	-73.54680	5.97	2.8	81	0.389	751.4	750.8	1937.9
2019	9	14	15	54	8.878	-50.92637	-73.55523	6.20	2.8	82	0.453	338.5	493.6	877.4
2019	9	14	16	39	42.772	-50.91674	-73.59976	6.00	2.8	82	0.346	560.3	600.6	1065.5
2019	9	14	17	56	5.113	-50.93029	-73.59023	6.00	2.8	75	0.370	392.6	439.8	876.3
2019	9	14	20	30	0.359	-50.92831	-73.57661	10.53	2.7	75	0.544	420.1	521.9	956.1
2019	9	14	21	48	34.983	-50.92561	-73.58386	6.72	2.7	74	0.136	450.5	504.4	1428.5
2019	9	14	22	45	20.073	-50.90063	-73.54716	6.00	2.6	135	0.436	377.5	537.0	799.0
2019	9	15	0	11	1.264	-50.91680	-73.58715	4.42	2.6	74	0.240	348.1	406.1	908.9
2019	9	15	1	47	19.531	-50.92042	-73.59981	2.86	2.9	74	0.506	517.9	636.5	1013.2
2019	9	15	2	50	5.253	-50.91355	-73.58322	3.44	2.8	74	0.238	363.9	435.3	758.1
2019	9	15	6	46	43.992	-50.91802	-73.59007	3.68	3.1	74	0.276	354.1	442.2	912.5
2019	9	15	8	4	45.837	-50.92133	-73.58235	5.89	3.1	82	0.156	369.8	434.1	1013.0
2019	9	15	10	35	21.501	-50.92128	-73.59206	3.58	3.0	74	0.260	405.2	474.2	921.1
2019	9	15	11	42	30.117	-50.92460	-73.58142	6.06	3.0	82	0.344	362.9	447.5	1020.4
2019	9	15	15	39	13.830	-50.91969	-73.58233	5.98	3.0	82	0.302	398.8	501.2	1032.8
2019	9	15	17	11	14.296	-50.92316	-73.58383	5.11	2.8	82	0.132	495.1	561.8	1326.5
2019	9	15	17	53	45.096	-51.83177	-75.38699	26.58	3.9	255	0.368	3787.9	3432.9	3192.0
2019	9	15	18	4	29.016	-50.92565	-73.57609	8.98	3.4	82	0.200	664.6	678.4	1964.2
2019	9	15	21	21	5.475	-50.92296	-73.58237	8.31	2.9	53	0.286	457.0	467.3	1391.0
2019	9	15	22	20	10.493	-50.92312	-73.59159	5.11	2.8	54	0.107	433.6	467.5	1337.0
2019	9	16	0	9	45.723	-50.90819	-73.59189	6.00	2.8	99	0.431	463.6	651.1	1044.0
2019	9	16	3	43	33.188	-50.90968	-73.53756	4.56	2.9	60	0.437	499.3	433.9	858.4
2019	9	16	5	10	57.854	-50.92542	-73.62075	8.08	2.9	76	0.343	564.5	606.3	1679.8
2019	9	16	7	34	56.097	-50.41500	-74.77859	29.21	2.7	110	0.206	414.9	406.9	843.9
2019	9	16	15	8	17.421	-50.90798	-73.55016	6.00	3.0	81	0.463	512.8	491.4	1092.9
2019	9	16	16	35	12.531	-50.91563	-73.57548	5.98	2.9	54	0.334	533.4	492.0	1058.7
2019	9	16	17	27	25.870	-50.91538	-73.58470	3.14	2.9	54	0.524	465.9	527.2	1209.4
2019	9	16	19	16	51.267	-50.92010	-73.58233	3.56	2.7	75	0.088	540.4	549.5	1438.2

ORIGIN TIME (UTC)						Latitude	Longitude	Depth	M_L	GAP	RMS	X error	Y error	Z error
yyyy	mm	dd	h	m	seconds	[°]	[°]	[Km]		[°]		[m]	[m]	[m]
2019	9	16	20	46	38.056	-50.92376	-73.58626	5.98	2.8	53	0.139	461.7	506.6	1174.8
2019	9	16	21	40	50.212	-50.89479	-73.52914	1.75	3.0	97	0.591	897.5	1155.5	2879.5
2019	9	16	22	53	45.679	-50.93253	-73.79757	14.76	2.6	67	0.813	969.7	784.4	2112.4
2019	9	17	1	8	12.738	-50.93053	-73.58198	7.18	2.7	96	0.191	481.4	689.1	1670.9
2019	9	17	2	45	3.356	-50.92741	-73.59213	6.00	2.8	53	0.389	414.3	507.3	980.4
2019	9	17	3	56	48.828	-50.91678	-73.59103	3.31	2.9	76	0.259	393.9	463.6	879.4
2019	9	17	5	44	30.042	-50.91799	-73.59590	3.50	2.8	54	0.387	369.3	442.5	730.0
2019	9	17	7	34	41.721	-50.92152	-73.58381	9.76	3.0	54	0.360	439.2	488.5	1400.2
2019	9	17	8	44	11.417	-50.92047	-73.59010	3.81	2.9	54	0.264	395.2	438.4	948.1
2019	9	17	11	49	13.035	-50.91887	-73.58329	5.49	3.0	54	0.220	380.3	418.3	1356.7
2019	9	17	14	34	15.746	-50.92314	-73.58771	5.07	2.9	67	0.124	447.9	475.9	1431.0
2019	9	17	15	35	1.912	-50.92624	-73.58241	10.16	2.9	61	0.751	574.4	541.5	1010.7
2019	9	17	16	28	54.861	-50.92455	-73.59113	8.99	2.9	59	0.330	453.4	519.0	1314.1
2019	9	17	18	25	3.152	-50.91592	-73.60072	3.76	2.8	58	0.358	546.8	551.3	1147.1
2019	9	17	20	56	50.864	-50.92971	-73.62226	8.25	2.7	54	0.556	505.6	535.9	1796.7
2019	9	17	22	26	53.838	-50.93210	-73.59559	9.06	3.0	65	0.441	632.8	606.2	1533.6
2019	9	18	3	54	12.647	-50.91728	-73.61288	1.40	2.6	108	0.206	852.1	911.0	1171.4
2019	9	18	7	38	23.103	-50.90218	-73.56658	6.00	3.0	73	0.494	354.0	348.6	463.7
2019	9	18	8	30	35.632	-50.91885	-73.58717	3.70	2.8	82	0.129	377.1	429.8	861.8
2019	9	18	10	40	24.734	-50.92560	-73.58580	3.59	2.8	82	0.192	488.3	644.8	1754.0
2019	9	18	12	8	9.359	-50.92965	-73.59556	3.82	2.9	83	0.186	483.7	577.6	1645.2
2019	9	18	14	42	12.632	-50.92048	-73.58816	3.80	3.1	54	0.165	417.9	472.7	1169.9
2019	9	18	16	13	4.456	-50.92297	-73.58043	11.08	3.0	53	0.451	480.5	551.6	1065.8
2019	9	18	17	12	11.750	-50.92298	-73.57849	9.28	3.2	53	0.289	400.0	431.7	943.5
2019	9	18	18	31	51.303	-52.80852	-73.43262	1.83	3.8	236	0.574	877.4	1427.7	896.6
2019	9	18	19	12	17.340	-50.92232	-73.58770	4.33	3.1	54	0.118	497.2	534.8	1417.4
2019	9	19	0	44	23.467	-50.92702	-73.58825	7.99	3.1	59	0.557	433.7	410.7	1870.3
2019	9	19	2	12	33.568	-50.92394	-73.59160	4.65	3.3	54	0.171	426.0	467.3	1143.4
2019	9	19	3	33	54.267	-50.92801	-73.59554	5.31	3.3	102	0.215	642.8	523.9	1212.5
2019	9	19	4	29	48.426	-50.91724	-73.58230	5.98	3.1	76	0.314	427.9	486.1	1200.9
2019	9	19	9	39	35.120	-50.91854	-73.56678	9.71	2.9	75	0.583	410.3	542.0	965.0
2019	9	19	12	37	0.653	-50.56703	-74.40177	28.27	3.2	106	0.261	471.8	315.1	678.9
2019	9	20	9	39	8.943	-50.71325	-72.23056	10.16	3.5	49	0.524	390.5	377.9	705.5
2019	9	20	15	34	17.781	-52.54921	-71.29463	39.68	3.9	107	0.715	1174.7	1094.9	2082.7
2019	9	20	22	37	31.337	-50.91936	-73.60611	5.37	3.4	72	0.627	442.6	563.3	1357.8
2019	9	21	4	11	39.752	-50.91108	-73.58707	6.00	3.0	73	0.457	456.3	577.5	1103.0
2019	9	21	10	53	11.643	-50.90656	-73.59090	6.00	3.0	119	0.397	445.6	530.5	1151.2
2019	9	21	16	11	12.465	-50.92232	-73.58770	4.37	3.1	116	0.093	632.4	709.1	1974.2
2019	9	21	17	11	38.494	-50.89894	-73.60002	1.73	3.1	96	0.232	620.6	998.6	1382.7
2019	9	21	23	51	39.184	-50.89152	-73.57034	6.00	3.0	71	0.671	370.1	424.9	407.6
2019	9	22	0	57	32.341	-50.93731	-73.57575	9.71	2.8	83	0.545	422.8	550.8	827.5
2019	9	22	5	34	25.540	-50.92892	-73.57807	3.00	2.9	60	0.321	412.3	437.7	761.2
2019	9	22	8	37	8.666	-50.92000	-73.60272	8.66	2.8	76	0.329	402.2	477.4	1417.8
2019	9	22	9	40	14.254	-50.89445	-73.55776	16.00	3.0	115	0.291	456.6	773.8	767.6
2019	9	22	10	49	38.375	-50.92807	-73.58389	4.49	2.9	75	0.132	511.2	681.6	1919.4
2019	9	22	13	2	54.877	-50.92089	-73.58817	11.18	3.1	53	0.600	512.8	521.0	1207.0
2019	9	22	14	7	12.437	-51.01678	-73.91186	3.00	3.3	150	0.482	1419.5	1641.6	2006.6

ORIGIN TIME (UTC)						Latitude	Longitude	Depth	M_L	GAP	RMS	X error	Y error	Z error
yyyy	mm	dd	h	m	seconds	[°]	[°]	[Km]		[°]		[m]	[m]	[m]
2019	9	22	16	6	9.530	-50.92235	-73.58188	4.14	3.2	100	0.173	559.4	632.3	1455.1
2019	9	22	17	9	17.195	-50.92152	-73.58381	3.55	3.2	100	0.232	563.3	545.3	1815.2
2019	9	22	21	54	22.241	-50.91880	-73.59591	5.67	3.0	54	0.213	480.5	509.5	1217.1
2019	9	22	23	11	46.201	-50.92193	-73.58478	5.02	2.8	59	0.160	438.3	513.3	1507.7
2019	9	23	0	38	6.424	-50.92251	-73.59013	5.96	2.8	76	0.106	430.3	497.6	1195.8
2019	9	23	2	30	8.994	-50.92213	-73.58430	6.00	2.9	54	0.177	383.8	435.0	1095.1
2019	9	23	3	48	9.202	-50.91270	-73.58904	2.74	2.7	54	0.337	403.9	484.6	961.9
2019	9	23	4	39	1.935	-50.92475	-73.59356	3.20	2.8	54	0.176	424.1	441.8	860.6
2019	9	23	5	43	17.649	-50.92334	-73.58820	7.12	3.0	75	0.277	415.0	463.6	1412.7
2019	9	23	7	15	31.197	-50.91987	-73.58767	4.22	2.7	76	0.172	410.4	498.8	1615.2
2019	9	23	10	7	59.148	-50.91965	-73.59107	3.13	2.9	54	0.235	373.4	425.1	988.8
2019	9	23	11	9	58.995	-50.91473	-73.59294	5.32	2.6	54	0.168	419.1	514.7	1407.7
2019	9	23	12	49	32.682	-50.90704	-73.57538	6.00	2.7	76	0.406	421.5	510.3	738.7
2019	9	23	14	29	13.047	-50.92996	-73.57372	10.87	2.8	74	0.874	383.5	517.3	943.0
2019	9	23	16	3	47.523	-50.91970	-73.58136	6.00	2.7	54	0.334	405.4	459.3	829.9
2019	9	23	16	45	58.228	-50.92253	-73.58625	3.89	2.7	95	0.191	470.4	571.6	1217.3
2019	9	23	17	29	39.370	-50.91934	-73.60999	2.71	2.6	95	0.265	633.2	698.1	1628.9
2019	9	23	18	49	21.833	-50.91492	-73.59537	2.11	2.8	95	0.171	598.4	647.0	1584.7
2019	9	23	23	17	14.514	-50.92231	-73.58964	4.29	2.6	54	0.179	462.3	475.1	1523.9
2019	9	24	0	36	26.835	-50.92193	-73.58478	5.80	2.8	54	0.146	423.0	450.3	1159.2
2019	9	24	2	14	3.596	-50.91987	-73.58767	4.02	2.5	67	0.158	548.2	627.2	1679.5
2019	9	24	4	29	46.379	-50.92315	-73.58577	5.74	2.7	100	0.181	495.5	583.7	1352.5
2019	9	24	9	25	12.155	-50.91034	-73.57057	1.73	2.7	54	0.455	404.0	445.3	560.3
2019	9	24	10	11	54.631	-50.91906	-73.58572	5.43	2.9	100	0.135	544.3	692.2	1536.8
2019	9	24	15	7	30.033	-50.91423	-73.57013	6.01	3.0	76	0.316	601.1	569.1	1250.5
2019	9	24	20	45	18.937	-50.91519	-73.58324	6.00	2.7	68	0.365	565.5	558.9	1126.8
2019	9	25	2	56	51.113	-50.92460	-73.58142	6.84	2.8	53	0.166	395.6	480.7	1280.6
2019	9	25	4	29	58.428	-50.91848	-73.57940	4.99	2.9	54	0.173	461.5	546.6	1349.4
2019	9	25	6	18	10.361	-50.92251	-73.59110	5.57	2.8	67	0.230	447.8	500.2	1379.1
2019	9	25	7	14	4.635	-50.91975	-73.61097	6.32	2.8	65	0.409	435.1	453.4	1224.9
2019	9	25	10	43	36.716	-50.92151	-73.58575	5.27	2.8	54	0.138	460.8	544.1	1365.9
2019	9	25	22	53	20.205	-50.91565	-73.57160	6.35	3.0	54	0.415	487.6	507.1	1151.9
2019	9	26	0	10	47.544	-50.92334	-73.58820	4.26	3.1	59	0.193	424.9	486.9	1201.6
2019	9	26	1	57	15.669	-50.93405	-73.52959	3.90	3.4	54	0.582	597.1	596.5	1040.6
2019	9	26	4	24	48.907	-50.92213	-73.58430	6.00	3.2	59	0.168	414.1	485.8	1078.7
2019	9	26	6	29	49.391	-52.40914	-74.14394	14.82	3.7	267	0.741	1510.1	2424.5	1986.0
2019	9	26	7	5	30.404	-50.91981	-73.59932	3.90	3.0	88	0.200	487.5	619.3	1352.8
2019	9	26	8	16	19.367	-50.91908	-73.58184	4.84	3.1	54	0.209	470.2	569.3	1233.3
2019	9	26	9	19	45.825	-50.92088	-73.58914	3.66	3.1	54	0.189	411.2	471.0	1041.5
2019	9	26	11	35	51.013	-50.92336	-73.58432	6.41	3.1	53	0.239	428.6	472.7	1231.2
2019	9	26	12	40	25.503	-50.92396	-73.58772	4.96	3.2	53	0.160	489.1	507.5	1412.0
2019	9	26	14	8	37.882	-50.91675	-73.59685	2.86	3.2	54	0.181	414.6	512.3	926.2
2019	9	26	15	13	30.536	-50.91801	-73.59104	5.08	3.2	54	0.128	428.5	487.0	1413.5
2019	9	26	16	24	19.342	-50.92373	-73.59306	6.00	2.9	54	0.286	422.7	481.5	987.3
2019	9	26	18	39	12.502	-50.91765	-73.58133	5.92	3.3	54	0.308	366.9	461.8	993.5
2019	9	26	19	55	27.567	-50.92212	-73.58818	6.00	3.2	59	0.354	450.5	471.8	829.8
2019	9	26	21	2	10.051	-50.91986	-73.58961	5.19	3.0	54	0.133	490.0	587.8	1397.3

ORIGIN TIME (UTC)						Latitude	Longitude	Depth	M_L	GAP	RMS	X error	Y error	Z error
yyyy	mm	dd	h	m	seconds	[°]	[°]	[Km]		[°]		[m]	[m]	[m]
2019	9	26	22	18	55.651	-50.92172	-73.58624	5.34	3.1	54	0.204	387.2	459.7	933.0
2019	9	26	22	50	58.216	-50.91744	-73.58182	5.00	3.1	68	0.170	472.5	585.8	1682.7
2019	9	27	0	18	17.539	-50.92331	-73.59499	5.73	3.1	54	0.254	374.3	433.8	958.5
2019	9	27	1	6	57.783	-50.92989	-73.58731	5.75	3.1	53	0.260	383.3	472.0	817.2
2019	9	27	2	46	18.864	-50.92377	-73.58529	4.65	2.9	53	0.241	372.3	470.6	1061.8
2019	9	27	4	34	33.770	-50.91805	-73.58328	6.00	3.1	54	0.250	329.2	400.3	903.5
2019	9	27	6	12	42.811	-50.91917	-73.60465	3.68	3.3	54	0.256	417.0	403.1	1237.4
2019	9	27	8	40	11.480	-50.92088	-73.58914	4.17	3.1	54	0.243	358.1	412.6	1116.4
2019	9	27	9	45	58.551	-50.92433	-73.59452	5.99	3.1	57	0.165	419.9	523.5	1304.5
2019	9	27	11	3	44.571	-50.92213	-73.58624	4.89	3.1	54	0.257	359.3	390.1	1148.0
2019	9	27	12	24	35.893	-50.91887	-73.58329	6.00	3.2	54	0.285	386.1	431.4	850.6
2019	9	27	13	1	18.579	-50.91819	-73.59542	4.96	3.0	54	0.197	519.1	636.4	1638.2
2019	9	27	13	49	47.901	-50.92091	-73.58331	6.00	3.1	54	0.312	348.8	441.1	794.3
2019	9	27	14	37	0.866	-50.91845	-73.58425	5.98	3.2	54	0.207	429.0	583.5	1133.7
2019	9	27	15	30	40.007	-50.92609	-73.57124	9.82	3.1	53	0.746	370.2	406.3	775.8
2019	9	27	16	20	39.178	-50.92494	-73.59502	4.54	3.0	54	0.104	426.1	486.9	1358.8
2019	9	27	17	48	33.515	-50.92043	-73.59690	3.89	3.2	54	0.292	383.9	513.2	1292.8
2019	9	27	18	56	35.536	-50.91946	-73.58669	5.99	3.0	54	0.159	450.5	488.3	1242.2
2019	9	27	19	48	11.728	-50.91781	-73.59056	4.43	2.8	54	0.165	507.6	522.7	1405.1
2019	9	27	21	15	12.804	-50.91644	-73.57841	4.89	2.9	59	0.213	405.0	574.4	1322.7
2019	9	27	22	21	51.132	-50.92460	-73.58239	3.37	2.9	53	0.408	406.1	462.2	886.8
2019	9	27	23	31	38.271	-50.91725	-73.57939	5.96	2.8	76	0.288	433.6	519.1	1078.6
2019	9	28	1	10	12.602	-50.92255	-73.58334	6.00	2.8	53	0.151	391.6	447.6	971.7
2019	9	28	2	10	0.035	-50.92418	-73.58433	4.17	3.0	53	0.207	419.4	523.4	1420.5
2019	9	28	3	40	32.965	-50.91958	-73.60465	9.28	2.9	76	0.504	365.6	438.5	1083.5
2019	9	28	5	1	38.406	-50.92003	-73.59689	7.78	2.9	54	0.344	379.9	475.6	1607.7
2019	9	28	6	18	37.206	-50.90706	-73.57247	3.80	2.9	54	0.403	374.7	431.8	920.4
2019	9	28	6	51	44.415	-50.91902	-73.59348	8.32	2.8	54	0.313	436.4	595.6	1844.6
2019	9	28	7	42	28.419	-50.92047	-73.58913	3.80	3.0	57	0.221	361.2	480.9	1000.7
2019	9	28	9	12	19.314	-50.92083	-73.59885	2.92	2.8	54	0.246	376.9	479.4	882.3
2019	9	28	12	1	27.012	-50.91684	-73.57938	6.00	3.0	54	0.299	379.3	432.9	772.3
2019	9	28	17	33	17.617	-50.91560	-73.58228	5.49	3.0	54	0.352	381.5	430.1	1102.7
2019	9	28	20	18	21.759	-50.92169	-73.59109	6.00	2.9	54	0.168	391.7	437.4	947.8
2019	9	29	2	6	9.729	-50.92315	-73.58577	5.19	2.9	82	0.271	375.3	520.3	1577.6
2019	9	29	3	4	7.556	-50.91987	-73.58767	5.47	3.0	67	0.160	426.8	512.2	1164.3
2019	9	29	4	25	46.952	-50.92501	-73.58240	3.91	3.1	75	0.234	422.3	564.8	1048.8
2019	9	29	5	48	33.928	-50.92415	-73.59112	3.03	3.2	54	0.238	425.7	478.7	749.3
2019	9	29	7	34	32.757	-50.92256	-73.58139	6.00	3.1	67	0.118	395.4	440.6	1057.3
2019	9	29	8	30	18.548	-50.91825	-73.58377	5.23	2.8	58	0.177	518.8	598.6	1505.8
2019	9	29	8	48	39.232	-50.92332	-73.59305	4.36	3.2	54	0.194	390.0	445.0	1070.4
2019	9	29	10	35	21.155	-50.92193	-73.58478	4.39	3.1	53	0.363	375.1	462.9	1536.9
2019	9	29	11	38	53.114	-50.91802	-73.58910	6.00	3.0	54	0.363	409.4	456.1	730.7
2019	9	29	13	43	40.306	-50.91802	-73.58813	4.26	3.1	54	0.318	397.6	374.5	1395.6
2019	9	29	13	57	29.303	-50.93774	-75.72846	14.76	3.7	247	0.780	2150.9	880.2	1584.8
2019	9	29	15	14	11.573	-50.92009	-73.58428	6.00	3.1	54	0.226	390.4	420.6	762.8
2019	9	29	18	20	40.560	-50.91830	-73.57406	9.10	3.3	95	0.671	416.7	512.5	1088.7
2019	9	29	21	4	51.557	-50.91589	-73.60655	2.74	3.0	54	0.257	385.5	491.5	665.9

ORIGIN TIME (UTC)						Latitude	Longitude	Depth	M_L	GAP	RMS	X error	Y error	Z error
yyyy	mm	dd	h	m	seconds	[°]	[°]	[Km]		[°]		[m]	[m]	[m]
2019	9	30	1	59	50.743	-50.91594	-73.59587	4.60	3.1	54	0.277	435.5	487.7	1046.3
2019	9	30	4	39	13.090	-50.92128	-73.59206	3.89	3.0	54	0.223	350.7	391.6	827.3
2019	9	30	5	29	13.458	-50.91779	-73.59444	2.79	3.1	54	0.326	402.0	459.7	628.0
2019	9	30	8	27	47.199	-50.92007	-73.58719	3.21	3.1	54	0.216	354.1	378.5	799.5
2019	9	30	9	54	24.816	-50.92337	-73.58335	4.75	3.0	53	0.270	361.7	423.9	1258.2
2019	9	30	11	26	18.243	-50.91885	-73.58620	4.11	3.1	57	0.201	371.3	473.7	1117.6
2019	9	30	13	11	25.797	-51.98733	-74.07056	3.47	3.5	220	0.649	805.6	1464.6	1370.8
2019	9	30	14	40	20.013	-50.91905	-73.58766	4.72	2.9	82	0.287	431.2	496.8	1823.3
2019	9	30	16	48	9.094	-50.92213	-73.58527	6.78	3.0	74	0.219	415.7	492.6	1461.7
2019	9	30	18	5	9.332	-50.92490	-73.60375	4.17	2.9	82	0.305	479.3	548.4	1236.7
2019	9	30	19	6	17.131	-49.44876	-73.56424	3.00	3.6	186	0.362	539.9	1064.4	933.3
2019	9	30	20	3	31.202	-50.92292	-73.59014	5.77	2.9	54	0.254	398.2	407.9	946.5
2019	9	30	21	41	13.131	-50.92250	-73.59207	5.94	3.0	54	0.203	402.8	494.5	1069.0
2019	9	30	23	37	55.847	-50.92412	-73.59598	5.34	2.8	54	0.273	380.7	436.8	939.2
2019	10	1	2	15	44.921	-50.92008	-73.58525	4.65	2.7	74	0.231	333.5	396.1	988.4
2019	10	1	3	21	57.741	-50.92905	-73.59216	8.99	2.7	79	0.430	355.1	483.9	1462.3
2019	10	1	5	26	51.387	-50.92071	-73.58380	4.37	2.8	82	0.274	348.8	460.9	1120.4
2019	10	1	7	20	48.197	-50.94338	-73.58942	12.00	2.6	84	0.640	420.5	530.3	811.0
2019	10	1	8	3	9.301	-50.92764	-73.58680	10.37	2.6	79	0.479	455.6	608.8	1332.2
2019	10	1	8	50	44.282	-50.92249	-73.59498	3.40	2.7	82	0.264	343.2	466.5	824.6
2019	10	1	9	47	6.558	-50.92170	-73.58915	4.71	2.7	82	0.399	357.7	487.3	1016.8
2019	10	1	10	39	40.129	-50.92270	-73.59450	3.88	2.9	82	0.168	437.5	624.8	1595.2
2019	10	1	12	9	32.908	-50.92209	-73.59401	2.88	2.7	82	0.245	394.2	561.2	1138.3
2019	10	1	14	10	32.720	-50.91883	-73.59008	4.07	2.5	78	0.261	423.8	460.6	1095.0
2019	10	1	15	20	0.181	-50.91820	-73.59347	3.90	2.8	82	0.188	462.3	656.9	1471.8
2019	10	1	16	55	44.125	-50.92009	-73.58330	5.96	2.8	74	0.186	397.5	530.6	1168.2
2019	10	1	18	53	24.940	-50.92254	-73.58528	7.62	2.7	74	0.460	397.4	532.9	1061.2
2019	10	1	21	25	35.974	-50.92069	-73.58768	3.43	2.7	95	0.171	452.1	785.9	1525.4
2019	10	2	1	6	22.455	-50.92047	-73.59010	4.21	2.7	74	0.211	359.2	406.6	933.2
2019	10	2	1	55	27.333	-50.92861	-73.59895	6.24	2.6	82	0.280	422.2	521.9	1298.5
2019	10	2	3	24	53.763	-50.92090	-73.58623	4.50	2.6	82	0.230	351.5	475.7	1054.7
2019	10	2	4	4	28.846	-50.93619	-73.59564	10.00	2.4	83	0.328	498.4	752.6	1359.7
2019	10	2	5	15	13.214	-50.92047	-73.59010	3.62	2.6	78	0.310	340.4	433.5	890.9
2019	10	2	6	17	36.908	-50.91901	-73.59543	3.12	2.6	74	0.231	356.7	445.5	729.8
2019	10	2	6	53	36.411	-49.86871	-73.37779	6.00	2.8	143	0.822	417.1	567.3	422.4
2019	10	2	6	55	7.440	-52.77506	-73.26944	5.95	3.2	264	0.816	573.8	1195.3	1129.4
2019	10	2	7	6	46.457	-50.93152	-73.58927	8.03	2.9	83	0.269	384.8	488.7	1837.4
2019	10	2	8	26	46.902	-50.92294	-73.58625	5.16	2.7	74	0.253	361.2	492.9	1206.3
2019	10	2	9	7	10.077	-50.92069	-73.58768	3.43	2.6	74	0.137	452.4	572.0	1477.1
2019	10	2	9	53	21.824	-50.92414	-73.59306	5.06	2.5	82	0.240	371.6	553.6	1133.0
2019	10	2	10	6	45.847	-50.46815	-74.56856	30.31	2.2	106	0.646	423.6	377.9	561.8
2019	10	2	11	59	59.666	-50.92503	-73.57851	6.00	2.6	82	0.408	429.1	608.8	1133.0
2019	10	2	13	49	39.430	-50.92823	-73.59312	6.92	2.6	78	0.344	408.0	528.1	1052.9
2019	10	2	16	17	43.437	-50.89187	-73.58198	2.99	2.8	72	0.507	390.5	466.9	634.6
2019	10	2	18	59	43.024	-50.91015	-73.60841	2.92	2.8	81	0.324	520.1	589.8	827.7
2019	10	2	21	2	45.312	-50.44353	-72.62126	6.00	2.5	86	0.526	386.0	407.8	500.0
2019	10	2	21	26	26.047	-50.91738	-73.59346	3.51	2.6	141	0.176	466.1	749.3	1528.5

ORIGIN TIME (UTC)						Latitude	Longitude	Depth	M_L	GAP	RMS	X error	Y error	Z error
yyyy	mm	dd	h	m	seconds	[°]	[°]	[Km]		[°]		[m]	[m]	[m]
2019	10	2	22	54	36.137	-50.92290	-73.59499	4.42	2.7	82	0.159	430.8	547.2	1255.5
2019	10	2	23	57	32.248	-50.91736	-73.59735	3.71	2.5	82	0.282	463.4	676.9	1232.4
2019	10	3	2	1	37.664	-50.92049	-73.58525	4.46	2.5	82	0.159	383.4	623.3	1433.5
2019	10	3	4	13	21.892	-50.92130	-73.58817	4.44	2.8	74	0.266	354.0	477.3	1212.9
2019	10	3	6	21	50.860	-50.92172	-73.58624	5.36	2.9	74	0.252	356.8	443.8	1308.9
2019	10	3	8	27	29.924	-50.91562	-73.57840	5.83	2.4	74	0.299	368.3	408.0	944.4
2019	10	3	10	0	39.466	-50.92288	-73.59790	4.28	2.6	74	0.265	392.5	560.3	1738.7
2019	10	3	11	35	39.548	-50.93606	-73.58156	9.79	2.6	75	0.408	438.1	586.8	1086.5
2019	10	3	15	17	38.635	-50.91888	-73.58135	6.00	2.9	95	0.212	395.2	587.4	1215.8
2019	10	4	1	11	16.422	-50.92274	-73.58674	7.63	2.7	75	0.199	428.7	544.1	1696.1
2019	10	4	21	33	21.063	-50.93608	-73.57671	10.34	2.7	79	0.675	448.5	526.8	921.2
2019	10	4	22	42	25.343	-50.92151	-73.58575	6.64	2.5	94	0.419	449.3	581.7	1007.5
2019	10	4	23	47	10.730	-50.92272	-73.59062	3.41	2.9	82	0.158	458.0	697.5	1618.5
2019	10	5	0	51	41.584	-50.91802	-73.59007	3.83	2.8	82	0.168	399.0	565.7	1371.6
2019	10	5	2	23	55.397	-50.91884	-73.58911	5.01	3.0	74	0.254	384.2	473.7	1045.9
2019	10	5	4	16	42.630	-50.92416	-73.58918	3.15	2.8	74	0.338	411.2	468.6	797.3
2019	10	5	5	41	20.904	-50.92454	-73.59404	3.37	2.9	74	0.452	385.7	485.0	1625.5
2019	10	5	7	30	7.901	-50.92745	-73.58437	8.15	2.9	74	0.465	375.5	434.6	1749.2
2019	10	5	8	49	52.370	-50.92293	-73.58819	3.44	2.8	74	0.300	351.0	478.3	931.4
2019	10	5	10	46	23.312	-50.91884	-73.58814	3.39	2.8	74	0.261	358.8	530.6	884.2
2019	10	5	12	30	52.923	-50.93688	-73.58060	12.00	2.8	75	0.663	371.5	472.0	920.9
2019	10	5	14	20	42.821	-50.92214	-73.58236	5.98	2.7	82	0.217	396.5	510.3	1035.6
2019	10	5	15	51	0.812	-50.92597	-73.59454	4.66	2.7	82	0.154	589.8	629.2	1821.9
2019	10	5	18	42	53.764	-50.91576	-73.59150	3.28	2.8	95	0.173	505.5	765.7	1478.7
2019	10	5	20	34	27.002	-50.92254	-73.58431	9.71	2.8	74	0.420	412.4	512.2	2102.4
2019	10	5	23	34	5.172	-50.92276	-73.58285	5.37	2.8	82	0.215	378.6	553.5	1433.7
2019	10	6	1	2	7.248	-50.92826	-73.58632	8.99	2.7	74	0.398	399.6	506.8	1210.0
2019	10	6	4	36	16.536	-50.93194	-73.58734	7.60	2.9	75	0.396	397.7	514.1	1431.1
2019	10	6	6	10	11.058	-50.92132	-73.58429	3.54	2.8	82	0.286	366.9	544.2	920.8
2019	10	6	7	8	16.172	-50.92171	-73.58721	3.64	2.7	74	0.138	419.7	477.5	997.6
2019	10	6	8	27	7.385	-50.91884	-73.58911	3.01	2.8	74	0.304	387.7	539.6	905.6
2019	10	6	10	13	5.505	-50.92214	-73.58333	5.98	2.7	74	0.174	368.3	423.9	924.9
2019	10	6	11	37	40.941	-50.92866	-73.58827	5.16	2.8	82	0.247	370.0	519.0	1065.7
2019	10	6	12	37	26.936	-50.92804	-73.58972	6.56	2.8	82	0.248	513.6	603.0	1436.9
2019	10	6	14	0	47.975	-50.92393	-73.59355	4.72	2.7	82	0.164	428.3	643.5	1304.9
2019	10	6	16	1	5.534	-50.92151	-73.58575	5.39	2.7	82	0.248	391.7	503.1	956.5
2019	10	6	17	56	50.909	-50.92091	-73.58429	3.93	2.7	82	0.196	441.8	503.5	1290.9
2019	10	6	21	15	57.654	-50.92217	-73.57654	10.22	2.5	74	0.522	425.1	509.4	837.5
2019	10	6	22	32	47.558	-50.91905	-73.58766	5.70	2.5	82	0.254	502.3	586.8	1531.0
2019	10	7	0	13	3.403	-50.92086	-73.59399	5.53	2.8	59	0.285	409.6	495.4	1427.7
2019	10	7	1	36	58.587	-50.92170	-73.58915	5.05	2.7	54	0.218	416.7	447.9	1349.2
2019	10	7	3	39	21.563	-50.92230	-73.59158	4.65	2.6	76	0.150	446.3	570.1	1575.2
2019	10	7	5	3	4.677	-50.92375	-73.58918	5.49	2.8	59	0.168	447.3	444.9	1459.8
2019	10	7	6	31	20.792	-50.91968	-73.58524	4.24	3.0	54	0.201	445.8	507.8	1338.7
2019	10	7	7	58	22.916	-50.92149	-73.58963	6.01	2.6	54	0.268	437.7	533.8	1272.6
2019	10	7	9	16	15.780	-50.92313	-73.58965	4.02	2.8	75	0.227	680.4	635.3	1544.7
2019	10	7	22	11	17.923	-50.92640	-73.58969	8.36	3.1	82	0.221	470.1	620.2	1462.6

ORIGIN TIME (UTC)						Latitude	Longitude	Depth	M_L	GAP	RMS	X error	Y error	Z error
yyyy	mm	dd	h	m	seconds	[°]	[°]	[Km]		[°]		[m]	[m]	[m]
2019	10	8	8	32	24.733	-50.93362	-73.57862	10.01	2.9	79	0.634	422.9	538.1	1031.3
2019	10	8	11	27	26.206	-50.93401	-73.58154	9.26	2.9	83	0.357	401.1	540.1	947.3
2019	10	8	13	34	44.183	-50.91668	-73.57016	3.51	2.9	82	0.299	559.7	627.8	1788.7
2019	10	8	18	3	51.032	-50.93139	-73.57422	2.89	2.9	94	0.498	525.0	656.1	1329.9
2019	10	8	20	6	18.811	-50.92557	-73.59357	5.86	2.8	96	0.170	603.9	700.5	1545.5
2019	10	9	2	40	56.899	-50.92235	-73.58188	8.08	3.1	82	0.268	518.8	723.8	2346.6
2019	10	9	5	22	39.921	-51.76952	-75.50833	21.46	3.7	256	0.360	2505.8	2241.6	2240.3
2019	10	9	5	54	39.530	-50.91647	-73.57258	7.99	2.8	82	0.381	390.6	532.2	1184.5
2019	10	10	9	45	34.933	-50.92949	-73.58634	9.64	3.1	75	0.342	394.6	475.8	1006.1
2019	10	11	1	24	58.870	-50.92323	-73.57024	4.80	3.0	82	0.374	405.2	559.7	1913.9
2019	10	11	2	56	57.542	-50.91907	-73.58378	4.37	2.9	76	0.260	376.3	543.2	1610.2
2019	10	11	6	17	11.257	-52.46222	-71.45268	33.00	3.4	202	0.891	882.6	1346.4	827.7
2019	10	11	8	16	43.580	-52.28925	-71.51974	31.54	3.5	261	0.352	993.4	2018.1	911.1
2019	10	11	8	24	56.677	-50.93215	-73.58588	4.49	3.1	80	0.306	516.6	586.4	1534.1
2019	10	12	3	34	25.019	-51.79004	-73.46634	3.00	3.4	173	0.601	434.7	707.5	532.4
2019	10	12	6	7	50.700	-50.92326	-73.60373	3.70	3.0	82	0.224	506.1	588.6	1188.4
2019	10	12	9	19	49.480	-50.91391	-73.59293	3.09	3.0	81	0.294	421.3	560.1	951.5
2019	10	12	11	52	3.275	-50.92274	-73.58674	4.27	3.1	82	0.144	462.2	599.5	1750.7
2019	10	12	16	42	38.042	-51.72997	-74.05706	9.73	3.7	183	0.415	373.9	493.5	784.5
2019	10	12	21	11	10.089	-50.91419	-73.57789	8.00	3.2	81	0.495	463.5	554.1	1726.1
2019	10	13	2	49	33.943	-50.92148	-73.59157	4.72	2.8	82	0.178	504.3	607.3	1952.7
2019	10	13	4	31	46.618	-50.91952	-73.57505	5.91	3.0	82	0.315	476.3	520.9	1378.7
2019	10	13	5	52	37.277	-50.90982	-73.59191	6.00	2.8	81	0.384	455.9	460.8	1084.0
2019	10	13	8	9	21.804	-50.90699	-73.69814	14.02	2.8	95	0.397	603.0	731.8	1139.6
2019	10	13	10	18	33.820	-50.93567	-73.57767	10.06	2.8	83	0.604	440.0	535.0	1017.6
2019	10	13	11	32	19.965	-50.91760	-73.59104	3.44	3.0	82	0.279	450.6	513.1	1208.8
2019	10	13	13	24	43.015	-50.92318	-73.57995	6.01	3.0	82	0.298	368.9	485.9	1079.1
2019	10	13	14	33	43.605	-50.94205	-73.60883	10.67	2.8	83	0.711	397.2	423.7	916.6
2019	10	13	15	35	51.293	-50.92967	-73.59168	6.01	2.7	83	0.166	497.8	542.5	1417.6
2019	10	13	17	35	50.230	-50.91327	-73.55701	2.70	2.7	81	0.472	433.7	486.4	1074.6
2019	10	13	18	49	38.960	-50.92231	-73.58964	4.29	2.8	82	0.133	443.1	536.2	1551.8
2019	10	13	20	29	7.267	-50.93358	-73.58639	8.81	2.7	79	0.399	391.6	455.4	871.4
2019	10	13	21	37	33.510	-50.93562	-73.58641	8.99	2.6	75	0.599	363.5	436.7	933.4
2019	10	13	23	19	59.123	-50.91968	-73.58427	6.20	2.5	82	0.391	364.4	497.4	986.5
2019	10	14	0	19	42.077	-50.92457	-73.58724	3.33	2.4	74	0.324	380.5	446.5	722.8
2019	10	14	1	20	17.525	-50.92880	-73.60138	4.57	2.6	74	0.298	383.2	495.9	1126.9
2019	10	14	3	39	55.172	-50.92313	-73.58965	5.97	2.5	74	0.184	369.0	438.0	990.6
2019	10	14	5	42	15.245	-50.93550	-73.61069	6.00	2.8	78	0.654	401.4	520.5	823.4
2019	10	14	6	25	3.309	-50.91904	-73.58960	3.47	2.4	74	0.138	492.4	618.8	1757.4
2019	10	14	6	45	35.310	-50.92254	-73.58528	5.81	2.5	82	0.316	355.4	518.3	972.8
2019	10	14	7	30	25.635	-50.92806	-73.58583	7.85	2.4	74	0.386	364.3	420.0	1391.4
2019	10	14	7	34	26.579	-50.56957	-74.42883	20.63	2.2	107	0.377	363.8	287.6	755.3
2019	10	14	8	38	26.682	-50.92130	-73.58720	4.09	2.5	82	0.239	360.6	449.9	1072.9
2019	10	14	9	11	9.644	-50.91683	-73.58229	4.36	2.2	74	0.226	463.0	515.9	1262.8
2019	10	14	10	2	38.728	-50.91822	-73.58959	3.20	2.4	74	0.277	375.0	458.9	915.2
2019	10	14	11	21	31.398	-50.92665	-73.58047	6.00	2.4	95	0.350	377.4	516.8	874.1
2019	10	14	12	44	37.299	-50.92987	-73.59217	5.67	2.6	83	0.247	418.5	537.2	1199.2

ORIGIN TIME (UTC)						Latitude	Longitude	Depth	M_L	GAP	RMS	X error	Y error	Z error
yyyy	mm	dd	h	m	seconds	[°]	[°]	[Km]		[°]		[m]	[m]	[m]
2019	10	14	13	34	6.646	-50.92558	-73.58968	6.01	2.4	96	0.293	435.8	654.5	1228.9
2019	10	14	15	50	26.216	-50.91486	-73.56674	6.00	2.4	81	0.420	344.8	435.5	866.8
2019	10	14	17	3	32.802	-50.92272	-73.59062	3.96	2.4	74	0.240	518.3	555.1	1495.9
2019	10	14	19	0	22.877	-50.92542	-73.58143	5.30	2.4	95	0.185	392.4	555.9	1429.6
2019	10	14	20	52	51.229	-50.92743	-73.58825	5.98	2.5	82	0.206	384.0	472.4	969.5
2019	10	14	21	44	53.802	-50.92785	-73.58631	6.00	2.4	82	0.258	405.4	535.9	1103.0
2019	10	14	22	47	50.282	-50.92503	-73.57851	6.45	2.4	82	0.388	387.0	480.3	1028.1
2019	10	14	23	35	42.817	-50.92478	-73.58773	4.25	2.6	78	0.216	436.2	590.1	1602.0
2019	10	15	0	24	8.869	-50.92719	-73.59553	7.11	2.4	82	0.269	423.9	612.5	1514.7
2019	10	15	1	39	24.088	-50.91275	-73.58030	3.99	2.4	81	0.458	375.1	465.1	863.9
2019	10	15	3	27	20.725	-50.92087	-73.59205	3.80	2.4	82	0.230	374.4	469.2	1055.1
2019	10	15	4	23	33.554	-50.92639	-73.59164	7.46	2.5	82	0.167	451.6	624.8	1733.5
2019	10	15	6	0	2.374	-50.92478	-73.58773	4.61	2.5	74	0.252	353.5	460.9	1290.5
2019	10	15	6	59	11.603	-50.92702	-73.58922	6.24	2.4	82	0.273	373.2	489.8	1120.1
2019	10	15	7	54	11.883	-50.92125	-73.59691	3.01	2.5	74	0.259	391.1	506.5	918.0
2019	10	15	9	0	27.347	-50.92003	-73.59592	6.00	2.3	74	0.208	445.9	547.9	1029.1
2019	10	15	9	51	48.245	-50.92990	-73.58537	7.49	2.4	75	0.296	364.1	462.4	1508.9
2019	10	15	11	5	52.033	-50.92418	-73.58336	6.00	2.5	82	0.173	417.9	630.1	1108.9
2019	10	15	13	1	20.027	-50.92747	-73.58146	5.12	2.5	82	0.211	377.0	527.9	1263.8
2019	10	15	14	24	47.543	-50.92516	-73.59259	4.86	2.5	96	0.204	422.5	645.5	1366.0
2019	10	15	18	2	45.705	-50.92637	-73.59552	6.01	2.6	82	0.287	477.6	627.7	1250.8
2019	10	15	18	55	37.698	-50.92268	-73.59838	5.60	2.6	54	0.330	574.0	619.3	1651.3
2019	10	15	19	55	43.135	-50.92726	-73.58194	6.99	2.7	53	0.233	450.4	509.9	1366.7
2019	10	15	21	44	58.143	-50.92338	-73.58140	5.08	2.4	53	0.179	378.4	415.5	1064.2
2019	10	15	23	3	25.100	-50.92455	-73.59113	3.81	2.4	54	0.340	368.5	421.1	1026.3
2019	10	15	23	13	37.961	-50.43376	-74.42666	16.16	2.8	96	0.568	312.7	249.4	425.8
2019	10	16	0	42	4.080	-50.92636	-73.59746	6.52	2.5	54	0.362	412.0	543.2	1408.3
2019	10	16	2	46	42.082	-50.92210	-73.59110	3.01	2.5	54	0.266	409.4	491.3	898.4
2019	10	16	3	33	46.658	-50.91921	-73.59591	3.11	2.5	54	0.433	401.0	454.6	836.2
2019	10	16	5	10	33.896	-50.92539	-73.58725	5.44	2.5	53	0.154	378.6	425.9	1203.3
2019	10	16	6	1	53.790	-50.92579	-73.58920	4.89	2.4	53	0.259	368.7	434.4	974.9
2019	10	16	6	35	26.417	-50.92639	-73.59164	4.61	2.4	53	0.240	492.5	608.7	1331.4
2019	10	16	7	3	6.216	-50.92008	-73.58525	4.03	2.5	54	0.242	360.7	488.5	1191.6
2019	10	16	7	15	9.693	-50.92641	-73.58775	5.78	2.5	53	0.236	501.0	641.8	1399.5
2019	10	16	7	39	19.459	-50.92413	-73.59403	4.64	2.4	54	0.240	423.1	595.5	1239.9
2019	10	16	8	40	6.706	-50.92007	-73.58816	3.03	2.6	54	0.202	366.1	417.2	894.3
2019	10	16	9	12	6.632	-50.52966	-73.37293	17.03	2.4	101	0.889	744.7	1006.4	857.8
2019	10	16	9	23	7.990	-50.91820	-73.59347	3.00	2.4	54	0.373	398.1	513.7	776.2
2019	10	16	10	26	48.592	-50.92540	-73.58531	6.00	2.4	53	0.219	391.1	461.2	925.3
2019	10	16	11	3	31.792	-50.92703	-73.58728	5.83	2.5	53	0.206	415.8	551.5	1061.1
2019	10	16	12	10	44.282	-50.92234	-73.58382	5.31	2.6	53	0.213	504.3	538.1	1170.1
2019	10	16	14	1	33.923	-50.92147	-73.59352	4.68	2.8	54	0.323	417.4	556.2	1714.5
2019	10	16	15	41	57.667	-50.92175	-73.58041	4.93	2.6	53	0.221	431.2	454.8	1031.5
2019	10	16	17	47	26.982	-50.92924	-73.59459	5.52	2.6	53	0.213	489.7	568.3	1418.0
2019	10	16	19	30	41.427	-50.92252	-73.58819	4.77	2.6	54	0.263	466.6	525.5	1112.4
2019	10	16	23	32	3.536	-50.93435	-73.59611	9.73	2.7	53	0.604	446.2	504.9	865.2
2019	10	17	0	23	40.932	-50.91345	-73.60360	2.99	2.4	54	0.430	486.4	586.8	893.9

ORIGIN TIME (UTC)						Latitude	Longitude	Depth	M_L	GAP	RMS	X error	Y error	Z error
yyyy	mm	dd	h	m	seconds	[°]	[°]	[Km]		[°]		[m]	[m]	[m]
2019	10	17	1	13	34.286	-50.92395	-73.58966	4.29	2.5	54	0.125	489.1	616.5	1732.3
2019	10	17	2	57	30.689	-50.91970	-73.57942	6.00	2.7	54	0.279	361.3	405.2	911.1
2019	10	17	4	9	30.163	-50.92050	-73.58428	4.40	2.6	54	0.277	445.3	504.4	1354.0
2019	10	17	5	18	16.658	-50.92210	-73.59110	4.17	2.5	54	0.266	473.3	506.4	1343.8
2019	10	17	6	50	31.148	-50.91676	-73.59588	4.01	2.7	54	0.336	419.3	596.0	1108.5
2019	10	17	7	26	40.647	-50.91882	-73.59300	5.94	2.7	76	0.294	464.6	623.1	1087.7
2019	10	17	8	11	3.184	-50.92490	-73.60278	5.75	2.6	54	0.246	445.8	564.8	1249.4
2019	10	17	9	47	44.872	-50.92132	-73.58332	6.00	2.5	54	0.172	444.8	546.3	1305.1
2019	10	17	10	36	38.130	-50.92106	-73.59448	4.43	2.6	76	0.181	490.5	706.2	1564.6
2019	10	17	12	10	50.939	-50.92336	-73.58529	5.48	2.7	59	0.219	432.5	500.0	1260.8
2019	10	17	13	58	23.856	-50.92053	-73.57749	3.81	2.7	95	0.222	456.1	563.3	1340.5
2019	10	18	3	15	22.328	-50.92375	-73.58820	4.67	2.8	53	0.215	420.8	434.3	1086.8
2019	10	18	4	6	52.176	-50.90843	-75.07493	9.28	3.4	187	0.304	769.8	498.5	806.5
2019	10	18	4	15	46.210	-50.92312	-73.59159	4.45	2.9	76	0.146	456.7	541.1	1844.3
2019	10	18	4	20	21.488	-50.91139	-75.06923	8.21	3.3	186	0.456	797.5	529.9	917.6
2019	10	18	5	59	16.862	-50.92435	-73.59064	5.29	2.7	75	0.134	412.9	462.2	1064.4
2019	10	18	6	25	12.722	-51.69009	-72.89129	7.99	3.0	74	0.328	472.8	451.5	1090.0
2019	10	18	7	14	22.330	-50.92335	-73.58723	4.73	2.9	75	0.178	379.7	468.3	1167.6
2019	10	18	8	39	54.332	-50.92636	-73.59746	2.81	2.8	75	0.175	572.8	662.8	1361.5
2019	10	18	10	20	57.405	-50.92969	-73.58585	9.53	2.9	75	0.405	509.1	566.7	1661.5
2019	10	18	10	28	47.633	-50.55057	-74.15928	5.94	2.8	85	0.402	298.6	264.0	488.9
2019	10	18	11	26	54.457	-50.91599	-73.58617	4.62	2.7	54	0.211	467.3	534.0	1327.2
2019	10	21	9	49	57.790	-51.06987	-74.55911	15.83	3.1	145	0.378	537.2	332.0	576.6
2019	10	22	1	25	48.371	-51.29379	-75.50481	18.00	3.6	244	0.535	1210.5	758.8	1603.3
2019	10	22	10	15	43.961	-51.20033	-72.42171	13.37	3.0	66	0.363	375.9	324.1	871.8
2019	10	24	17	44	29.592	-52.41279	-71.36612	35.00	3.4	176	0.811	646.4	1072.6	689.6
2019	10	25	5	10	32.781	-50.38958	-72.39275	3.00	2.6	62	0.499	425.5	418.9	726.8
2019	10	25	9	39	53.056	-51.06986	-72.79634	10.22	3.0	74	0.337	408.2	348.3	1266.4
2019	10	25	17	36	31.579	-49.45360	-73.53747	8.99	3.0	185	0.495	494.6	749.6	829.1
2019	10	26	3	29	21.892	-49.96863	-72.53460	9.13	2.6	77	0.595	351.7	386.2	1159.9
2019	10	26	5	37	55.621	-50.92965	-73.59556	5.62	2.7	53	0.207	451.2	556.6	1430.9
2019	10	26	7	16	42.420	-50.92076	-73.61341	3.37	2.7	58	0.314	481.4	559.6	1217.8
2019	10	28	23	4	49.718	-50.92721	-73.59165	5.35	2.4	53	0.174	502.8	671.4	1638.6
2019	10	29	0	18	46.394	-50.63005	-74.40075	18.70	2.3	110	0.451	351.1	251.7	487.4
2019	10	29	2	8	40.831	-50.71289	-72.23830	10.98	2.7	49	0.607	312.0	311.0	542.1
2019	10	29	3	27	21.463	-50.92168	-73.59303	3.56	2.5	54	0.262	464.5	489.4	1174.7
2019	10	29	6	47	20.228	-50.92330	-73.59597	3.74	2.5	54	0.233	477.0	578.5	1255.1
2019	10	29	7	23	3.741	-50.92843	-73.59263	5.64	2.3	53	0.168	443.9	554.3	1409.8
2019	10	29	7	55	11.834	-50.91781	-73.59056	3.02	2.4	76	0.126	484.3	615.4	1178.1
2019	10	29	8	40	12.937	-50.92272	-73.59062	8.57	2.4	54	0.516	404.0	462.4	1259.8
2019	10	29	9	56	19.275	-50.91904	-73.58960	4.45	2.4	76	0.198	466.4	605.3	1292.6
2019	10	29	11	4	37.214	-51.11832	-74.77621	16.76	2.7	170	0.424	587.5	308.3	649.7
2019	10	30	11	13	49.722	-50.62375	-74.41407	20.01	2.5	111	0.274	402.5	317.0	717.9
2019	10	31	1	11	53.507	-50.62280	-74.35616	24.28	2.7	107	0.372	518.5	273.7	841.9
2019	10	31	12	5	6.091	-51.24930	-73.96778	14.54	3.1	90	0.358	353.4	291.5	722.8
2019	11	1	1	10	42.055	-52.01396	-74.27204	19.02	2.9	235	0.387	1461.8	1852.9	797.1
2019	11	1	2	39	19.751	-51.88010	-74.30048	19.91	3.0	218	0.507	722.3	725.7	713.1

ORIGIN TIME (UTC)						Latitude	Longitude	Depth	M_L	GAP	RMS	X error	Y error	Z error
yyyy	mm	dd	h	m	seconds	[°]	[°]	[Km]		[°]		[m]	[m]	[m]
2019	11	2	3	13	52.007	-51.71494	-74.63700	26.01	2.8	254	0.266	1941.5	1309.7	1113.8
2019	11	3	7	29	25.170	-50.63258	-74.39407	20.61	2.7	110	0.281	492.8	314.0	932.2
2019	11	4	0	10	44.046	-50.46343	-74.30449	18.56	2.8	94	0.277	595.6	372.9	589.1
2019	11	4	22	20	46.338	-51.84497	-74.31482	19.14	3.2	214	0.214	1624.9	1397.7	1085.4
2019	11	6	4	24	17.670	-51.11826	-74.71137	25.00	2.9	163	0.115	1096.7	520.7	1320.1
2019	11	9	1	59	15.885	-50.94405	-73.57923	13.73	2.5	114	0.732	583.5	844.1	1273.9
2019	11	9	3	28	46.217	-50.90843	-73.58364	5.82	2.3	77	0.426	584.9	696.3	1367.5
2019	11	9	7	8	24.783	-50.92556	-73.59551	4.49	2.3	75	0.148	464.2	567.3	1459.9
2019	11	9	8	24	2.596	-50.89995	-75.04544	16.24	2.3	183	0.317	640.8	507.5	1498.6
2019	11	9	20	47	23.223	-50.92308	-75.09063	7.85	2.6	189	0.486	673.0	471.8	1190.5
2019	11	9	22	5	51.231	-50.92231	-73.58964	4.06	2.0	116	0.131	633.4	767.1	2139.0
2019	11	9	23	33	28.122	-50.92638	-73.59358	3.86	2.1	115	0.121	689.1	931.0	1843.2
2019	11	10	4	53	14.951	-50.90067	-73.62091	0.79	2.3	117	0.593	626.4	801.9	836.6
2019	11	10	9	50	54.865	-50.92108	-73.59060	4.20	2.5	116	0.081	633.3	782.2	1663.0
2019	11	10	14	48	3.796	-50.91511	-73.55655	0.90	3.0	166	0.138	938.2	978.6	1891.6
2019	11	10	16	21	1.070	-53.16644	-72.48902	35.00	3.4	217	0.852	905.4	1917.6	3953.6
2019	11	11	4	3	44.702	-50.91777	-73.59832	2.71	2.1	116	0.090	739.6	838.6	1645.8
2019	11	11	4	8	38.267	-50.91704	-75.08550	10.29	2.3	188	0.098	661.6	454.6	1744.1
2019	11	11	5	0	51.927	-51.71138	-74.31835	16.18	2.6	182	0.514	712.7	633.8	742.0
2019	11	11	8	1	28.167	-51.26613	-73.32801	10.66	2.2	80	0.579	873.4	878.8	1686.9
2019	11	11	9	52	32.170	-51.61927	-73.86475	9.18	2.9	152	0.181	565.2	525.2	2387.5
2019	11	11	10	13	40.364	-51.62389	-73.87519	10.57	2.6	131	0.268	525.4	456.9	1667.1
2019	11	11	12	58	43.072	-50.91007	-73.58366	3.04	2.2	147	0.153	1003.6	680.0	1551.0
2019	11	11	16	15	39.152	-50.92395	-73.58966	6.01	2.1	115	0.224	616.5	675.2	1414.2
2019	11	11	18	13	54.626	-51.76751	-73.52297	5.30	2.7	134	0.478	477.4	518.0	698.3
2019	11	11	19	16	55.476	-50.91991	-73.57990	5.27	2.5	116	0.306	660.5	784.8	1661.7
2019	11	12	2	6	55.772	-50.92471	-73.60132	5.58	2.3	115	0.149	625.0	772.5	1492.8
2019	11	12	3	46	24.382	-50.92722	-73.58970	4.25	2.2	115	0.115	551.4	668.9	1504.8
2019	11	12	5	33	51.312	-50.91990	-73.58185	4.45	2.2	167	0.045	840.6	976.2	2174.1
2019	11	12	6	56	47.348	-50.91985	-73.59155	4.92	2.3	120	0.144	680.3	879.3	1690.4
2019	11	12	8	58	21.807	-50.91985	-73.59155	3.43	2.3	120	0.065	643.2	788.3	1798.3
2019	11	12	10	19	12.581	-50.92066	-73.59350	5.39	2.0	120	0.106	625.8	755.3	1678.1
2019	11	12	12	11	17.834	-50.91816	-73.60124	6.64	2.3	120	0.053	1014.6	775.9	2150.0
2019	11	12	13	25	23.836	-50.91823	-73.58765	3.90	2.3	167	0.087	713.3	883.1	1777.8
2019	11	12	14	40	12.495	-50.92305	-73.60519	3.63	2.2	161	0.135	1062.2	859.3	2149.7
2019	11	12	16	32	4.978	-50.92607	-73.57513	9.74	2.1	115	0.680	497.4	636.8	1123.4
2019	11	12	19	42	5.243	-50.92189	-73.59255	5.17	2.3	116	0.124	638.2	738.6	1740.0
2019	11	12	22	3	15.443	-50.92435	-73.59064	4.59	2.3	120	0.102	673.3	882.6	1748.4
2019	11	13	0	0	2.626	-50.91290	-73.59049	5.37	2.1	121	0.149	736.3	1063.5	1603.2
2019	11	13	0	49	51.250	-50.92315	-73.58577	4.65	2.3	166	0.069	570.1	911.1	1917.7
2019	11	13	2	19	58.342	-50.92476	-73.59162	5.97	2.4	119	0.068	516.8	844.2	2089.5
2019	11	13	7	57	37.236	-50.92313	-73.58965	5.27	2.5	120	0.136	619.4	779.5	1563.4
2019	11	13	9	53	2.905	-50.91749	-73.57211	11.29	2.6	116	0.718	610.5	823.2	1434.0
2019	11	13	11	43	24.506	-50.90577	-73.58507	14.01	2.4	122	0.343	392.2	694.0	898.4
2019	11	13	13	8	24.190	-50.92313	-73.58965	4.10	2.2	120	0.097	585.3	771.6	1963.6
2019	11	13	15	45	26.780	-50.91495	-73.58955	4.80	2.7	163	0.163	909.7	862.7	2096.6
2019	11	14	5	34	29.826	-50.62592	-74.38664	21.40	2.2	160	0.041	1752.4	554.7	2091.3

ORIGIN TIME (UTC)						Latitude	Longitude	Depth	M_L	GAP	RMS	X error	Y error	Z error
yyyy	mm	dd	h	m	seconds	[°]	[°]	[Km]		[°]		[m]	[m]	[m]
2019	11	15	3	42	57.373	-50.91625	-73.57501	11.62	2.7	116	0.658	780.8	890.7	1429.7
2019	11	15	5	2	15.132	-50.91793	-73.64395	4.02	2.8	115	0.706	753.3	1025.5	1078.3
2019	11	17	3	31	47.068	-51.38786	-72.50613	5.99	3.2	223	0.506	1198.1	738.7	1515.0
2019	11	17	19	30	58.833	-50.92251	-75.08818	10.18	3.0	189	0.179	592.1	432.2	1154.5
2019	11	18	0	56	5.713	-51.18631	-72.36086	1.17	3.3	189	0.568	993.8	824.6	958.0
2019	11	19	23	11	6.405	-50.16814	-75.97488	33.98	3.0	271	0.328	1252.3	883.3	1260.7